University of Sunderland

FlexiPill: 3D printed flexible dose combination

PhD researcher: Yasir Karkar

D.O.S: Dr Ahmed Faheem
Second supervisor: Amal Elkordy

Acknowledgement

First and foremost, I would like to express my deepest gratitude to my primary supervisor, **Dr Ahmed Faheem**, for his invaluable guidance, support, and encouragement throughout my PhD journey. His expertise and dedication have been instrumental in shaping the direction and quality of this research. I am also sincerely thankful to **Prof. Amal Ali Elkordy** for her thoughtful insights, constructive feedback, and unwavering support during this work. Your mentorship has been greatly appreciated.

To my beloved wife, **Dr Omnia Alhamadani**, words cannot express my gratitude for your steadfast support and belief in me. Your encouragement during the most challenging moments of this journey has been my greatest source of strength. You have been my rock, and I am forever grateful for your love and sacrifices.

I am also deeply indebted to **my parents**, whose continuous support, prayers, and unwavering belief in me have been a constant source of motivation. Thank you for always standing by me and cheering me on through every step of this journey.

Finally, I dedicate this work to my cherished children, **Yaseen and Gala**. My greatest wish is that, as you grow up, you will look back on this work with pride and know how much love and inspiration you bring to my life. Everything I do, I do with the hope of building a brighter future for you.

Abstract

The treatment of chronic conditions increasingly necessitates multidrug regimens targeting multiple pathological pathways. Although polypharmacy enhances therapeutic effectiveness, it often complicates medication adherence, dose optimisation, and treatment personalisation. Fixed-dose combinations (FDCs) were developed to simplify regimens by consolidating multiple drugs into a single dosage form, thus reducing pill burden and improving compliance. However, traditional FDCs offer limited flexibility for individualised dose adjustments, timing modifications, and the integration of pharmacogenomic data. As medicine advances toward precision and patient-centric care models, the rigidity of conventional dosage forms presents a growing limitation.

In response, this work presents the FlexiPill platform: a modular, 3D-printed oral dosage form that enables flexible, individualised polypharmacy. Using fused deposition modelling (FDM), drug-loaded thermoplastic filaments were extruded and printed into discrete modules, each engineered with a specific release profile. These modules can be physically combined into tailored polypills at or near the point of care, eliminating the need for reformulation and enabling rapid adaptation to patient-specific therapeutic requirements. This modular approach addresses the clinical need for personalisation while remaining compatible with pharmaceutical manufacturing and regulatory constraints.

Three case studies were undertaken to evaluate the platform's versatility. In the first, theophylline was selected to explore controlled release through modular formulation and a structured Design of Experiments (DoE), varying parameters such as drug loading, infill density, and immediate-to-sustained-release (IR-to-SR) ratios. The second study involved a personalised analgesic polypill combining paracetamol, ibuprofen, and caffeine, each embedded in tailored polymer matrices for distinct release profiles. The third case study extended the platform to gastroretentive delivery with a cardiovascular polypill comprising propranolol hydrochloride, enalapril maleate, and hydrochlorothiazide, targeting narrow absorption windows. Across all case studies, a consistent suite of analytical techniques was employed, including dissolution testing, thermal analysis (DSC, TGA), chemical analysis (FTIR), structural characterisation (SEM, XRD), and mechanical testing. Modified Principal Component Analysis (M-PCA) was applied to interpret dissolution profiles, while

Dynamic Vapour Sorption (DVS) assessed humidity-related stability and release performance.

The findings from all three case studies confirmed the functional robustness and adaptability of the FlexiPill platform. In the first case study, drug release profiles for theophylline were significantly influenced by both drug load and IR-to-SR ratios ($p < 0.05$). However, higher drug loads negatively affected filament viscosity, resulting in weight variation, poor print resolution, and formulation instability. In the second study, the analgesic polypill successfully combined paracetamol (55% w/w), ibuprofen, and caffeine—three APIs with divergent release and stability requirements—into a single dosage form. Paracetamol, embedded in a 1:1 blend of PVP K40 and Eudragit EPO, demonstrated rapid release under acidic conditions with over 85% release after one hour in acidic media, but less than 30% in alkaline conditions ($p = 0.00002$), confirming effective pH-dependent release and taste masking. Ibuprofen, incorporated into a gastro-resistant Eudragit L100-55 matrix, released less than 1% in acidic medium over 24 hours, with more than a tenfold increase in alkaline medium, confirming successful enteric protection. Caffeine, embedded in a fast-dissolving polyvinyl alcohol (PVA) matrix, exhibited rapid onset with 84% released within the first 30 minutes. The third case study demonstrated the platform's gastroretentive capabilities: propranolol was incorporated into a floating low-density printlet that maintained gastric retention for up to nine hours and released 96% of the drug within this period. Enalapril was printed at 150°C using a modified thermoplastic polymer matrix, maintaining chemical integrity despite its thermosensitive nature. Hydrochlorothiazide was delivered in an immediate-release matrix, achieving over 90% release within the first hour.

Collectively, this research establishes the FlexiPill platform as a versatile, scalable, and clinically relevant solution for personalised oral drug delivery. By enabling modular design, custom release control, and adaptable polypill assembly, the system offers a practical route toward integrating personalised medicine within existing pharmaceutical manufacturing frameworks. This approach holds promise for improving treatment adherence, safety, and therapeutic outcomes in complex disease management.

Research activity

The results of this work have been shared with the scientific community through several conferences and publications. The following is a list of these activities:

Publications

- Karkar, Yasir, Tanzeela Anis, Amal Ali Elkordy, and Ahmed M. Faheem. "Flexipill: A novel 3D printed flexible dose combination with a floating element." *European Journal of Pharmaceutics and Biopharmaceutics* (2025): 114736.
- Karkar, Yasir, Ihsan Amer, Amal Ali Elkordy, and Ahmed Faheem. "Flexipill: A novel 3D printed personalised analgesic polypill with diverse targeted drug release approaches." *Journal of drug delivery science and technology* 108 (2025): 106882.
- Karkar, Y., Faheem, A. and Elkordy, A., 2023. Three-dimensional printing of flexible polypill. *British Journal of Pharmacy*, *8*(2), pp.S1-S2.
- Karkar, Y., Elkordy, A. and Faheem, A., 2023. 3D printed flexible design for personalized drug release. *British Journal of Pharmacy*, *8*(2), pp.S1-S2.

Conference Presentations

- Speaker at the 1st Annual Postgraduate Conference, Sunderland, UK
- Poster Presentation at the Controlled Release Society Annual Meeting 2023, Las Vegas, USA
- Poster Presentation at the Academy of Pharmaceutical Science (APS), Reading, UK
- Poster Presentation at AAPS 2023 PHARMSCI 360 Annual Meeting, Orlando, FL, USA
- Poster Presentation at the Controlled Release Society Annual Meeting 2024, Bologna, Italy
- Speaker at the 2nd Annual Postgraduate Conference, Sunderland, UK (winner of the best presenter).

Novelty of the Work

- The work addresses polypharmacy issues in chronic disease management by developing a FlexiPill with two designs. This personalised 3D-printed flexible-dose drug combination is intended to be manufactured in a quality-controlled facility and assembled at the point of care to meet individual patient needs.
- The FlexiPill dosage form can control drug release by changing the ratio of immediate to sustained release units, as proven using the QbD methodology.

- A formulation of IR theophylline with three different concentrations of theophylline was printed successfully.

- Development and printing of Paracetamol formulation with Taste-masked, high drug load (55%) and printed at a low temperature of 100°C.

- Development and printing of ibuprofen formulation with Gastroprotective properties, limiting dissolution in acidic gastric media to <1% over 24 hours.

- Developing and printing propranolol HCl unit designed as a floating system, achieving 9-hour flotation and over 90% drug release.

- The development and printing of the enalapril maleate unit were formulated to prevent thermal degradation by printing at 150°C, below its degradation temperature, after multiple attempts by others that failed to do so.

Table of Contents

List of Tables

List of Figures

Chapter 1 : Introduction

This chapter explores the advantages of combination therapy over monotherapy, highlighting its role in improving clinical outcomes by targeting multiple disease pathways simultaneously. However, this led to an increase in the complexity of treatment regimens, which poses challenges in patient adherence, a critical factor for achieving optimal therapeutic outcomes. Fixed-dose combination (FDC) therapy, commonly referred to as a polypill, has emerged as a potential solution to adherence challenges by simplifying medication regimens and improving compliance. Nonetheless, FDCs lack the flexibility required for personalised medication, which has been gaining increasing interest in recent years. Additionally, they may lead to challenges in dose titration, increased risk of adverse drug interactions, and difficulty in identifying the specific agent responsible for side effects. Furthermore, FDCs can complicate treatment adjustments and are not suitable for patients requiring tailored therapy based on age, weight, organ function, or comorbid conditions. As a result, this created the need for flexible-dose combinations that can address the issue of polypharmacy and can be personalised according to patient needs. This gap in research will be the main subject of this thesis.

1.1 Combination Therapy Advantage in Chronic Disease

Treatment strategies for many chronic diseases, such as asthma, chronic pain, cardiovascular diseases, HIV, and malignant diseases, are moving toward combined therapy instead of monotherapy because of the benefits these strategies offer and their clinical outcomes (Garjon et al. 2020; Gandhi et al. 2023; Rajvanshi, Kumar, and Goyal 2024; Cohen, Vase, and Hooten 2021; Fisusi and Akala 2019). This section will attempt to shed light on some of these diseases, how they can benefit from combined therapy, and how that can be translated into clinical practice and outcomes.

For patients with HIV, over 60% of them are on combined antiviral therapy since these combinations block multiple stages of the viral replication cycle. Therefore, it has a significant advantage over single therapy in controlling replication, transmission and infection rate, which was reflected in the mortality and morbidity of HIV/AIDS patients (Weichseldorfer, Reitz, and Latinovic 2021).

In cancer patients, combined therapy can decrease side effects related to chemotherapy since combined therapy can target multiple pathways of cell proliferation and/or cell sustainment. As a result, these combined agents work synergistically or equitably; therefore, a lower therapeutic dose is required (Albain et al. 2008; Mokhtari et al. 2013). Moreover, some of these combinations may contain a protective agent that can protect normal proliferating cells from the toxic effects of the other agents (Blagosklonny 2005). Furthermore, combination therapy can prevent resistance that usually accompanies long treatment with nontherapeutic agents, which drive the malignant cells to find another salvage pathway (Khdair et al. 2010). For all these reasons, more than 5,000 clinical trials worldwide are being conducted to investigate new anticancer combinations (Boshuizen and Peeper 2020).

Moreover, Chronic pain affects one in three people. However, current painkillers have limited efficacy and dose-related side effects. Nevertheless, different painkillers can target many mechanisms for nociceptor transmission, leading to synergistic effects that provide better analgesia and fewer side effects than monotherapy (Gilron, Jensen, and Dickenson 2013). As a result, practitioners tend to rely on add-on analgesic agents when monotherapy shows moderate efficacy. Subsequently, more than half of patients with chronic pain use two medications or more (Berger et al. 2012).

Finally, cardiovascular diseases are one of the major causes of death and disability worldwide (Fuster et al. 2017). Multiple risk factors contribute to the prevalence of CVD; hence, primary and secondary prevention requires a combination of antiplatelet, cholesterol-lowering agents and antihypertension to reduce this risk (Fuster et al. 2017; CVD 2014; Wilkins et al. 2024). In a recently published study conducted in the U.S. for 20 years, It was reported that 60% of the patients with heart disease use five drugs or more, compared to the group average, which was only 17% (X. Wang et al. 2023). This was the highest prevalence in all the tested groups. Polypharmacy is most prevalent in geriatric patients since the average patient over 65 takes more than eight tablets daily at different times (Rochon et al. 2021). In summary, there is a well-established advantage in the use of combination therapy in most chronic diseases, and that has been reflected in clinical practice. It is causing a massive burden on the healthcare system due to its effect on patients' adherence.

1.2 Importance of Adherence

However, although combined pharmacotherapy is essential, it can decrease patient adherence, especially in chronic diseases requiring lifelong treatment. This section will showcase how adhesion plays a critical role in the clinical success of treatment and how the number of medications taken during the day can affect that adhesion.

Adherence can be divided into three steps the patient needs to take to be considered adhering to the treatment: the initiation of the treatment, implementation of the prescribed dose regimen and persistence for the complete duration of the treatment (Menditto et al. 2020). Adhesion averages around 50% across different diseases, and this rate has not improved for over 40 years despite the constant efforts of health organisations worldwide (Nieuwlaat et al. 2014; José M Castellano et al. 2014). Therefore, patient not adhering to their treatment is a challenge facing the healthcare system worldwide (Egan and Philipson 2014). Non-adherence is directly linked to a high hospitalisation rate, decrease in productivity and death. As a result, its effect exceeds individual patient health and causes a tremendous burden on the healthcare system (Hugtenburg et al. 2013). Non-adherence is a multifactorial problem. The WHO classify those reasons into five categories: socioeconomic factors, factors related to the healthcare system, patient-related factors, condition-related factors and therapy-related factors (Menditto et al. 2020). Therapy-related factors include the complexity of treatment and the number of medications that must be taken during the day (Ho, Bryson, and Rumsfeld 2009; Jose M Castellano, Copeland-Halperin, and Fuster 2013; Ingersoll and Cohen 2008). For example, in patients with hypertension, adherence was found to be significantly higher among those taking two medications compared to those prescribed six or more, with the former being nearly twice as likely to adhere to their treatment regimen (Chapman et al. 2005). A similar trend was observed in patients with diabetes, where those receiving a once-daily insulin dose demonstrated a 78% compliance rate, compared to only 38% among those requiring insulin administration three times per day (Paes, Bakker, and Soe-Agnie 1997). Patient-related factors involve issues such as forgetfulness, awareness and beliefs. Finally, the asymptomatic nature of the disease can be an example of condition-related factors. Since many of these challenges are prevalent in chronic diseases, adherence becomes particularly difficult, especially among elderly patients (Yeaw et al. 2009).

In conclusion, combined therapy, which is becoming a necessity for chronic diseases, is leading to an increase in the complexity of the treatment and a decrease in patient adherence to it, which in turn can lead to treatment failure.

1.3 Polypill to Improve Adherence

Fixed dose combinations can improve patient adherence by reducing the number of tablets needed throughout the day. The use of polypill or fixed-dose combination goes back to the 1950s when the first antihypertensive FDC was introduced to improve efficacy and decrease the side effects (Wofford 1997). Since then, the combination has been used for acute conditions, like the common cold, and chronic diseases like hypertension (Wilkins et al. 2024). A polypill is a name used for tablet FDC, but in this context, they will be used interchangeably because other forms of combination, like inhalation, topical, or injectable, are out of the scope of this discussion. Polypill can target a single condition or a closely related group of conditions (Janczura, Sip, and Cielecka-Piontek 2022).

Many clinical studies have demonstrated the importance of FDC on patient adherence to their medication and the reflection of this adherence on the clinical outcome of the condition. The FOCUS (Fixed-Dose Combination Drug for Secondary Cardiovascular Prevention) study shows that over 9 months, patients who were given polypill instead of three separate tablets to reduce CV risk showed better adherence to the treatment than the control group (68% vs. 59%, $p = 0.049$) (José M Castellano et al. 2014). The UMPIRE Randomized Clinical Trial tested the effect of polypill compared to regular therapy in 2004 patients over 15 months. The FDC group shows significantly better adhesion to the treatment and better control of the CV risk factor (Thom et al. 2013). The CRUCIAL trial has investigated the effect of amlodipine/ atorvastatin FDC on coronary heart disease compared to usual care over 12 months. The single pill arm of the study shows better risk reduction and fewer incidents of side effects compared to regular care (Lopez et al. 2010). A similar result was observed in a clinical trial done on 120 HIV patients over 2 years. The tested group adhered better to the simplified FDC regimen (Langebeek et al. 2014). Other clinical trials and meta-analyses have reached the same conclusion in different disease groups, the conclusion being that

FDC can positively affect patient adhesion and, as a result, improve clinical outcomes (Baumgartner et al. 2020).

This improvement in adherence through the use of polypill is due to a decreased number of tablets taken throughout the day, simplifying the dose regimen even in cases where the frequency is the same as usual care (Webster, Castellano, and Onuma 2017) and reducing the cost of treatment compared to regular care (Wilkins et al. 2024). However, polypill makes treatment personalisation rather tricky because these fixed combinations are typically designed to address the needs of the general population.

1.4 Disadvantages of Polypill

Although polypills can improve adhesion, as has been demonstrated, they usually introduce a set of new problems. One of the most concerning challenges with FDC is the difficulty of titrating the dose to reach optimal therapy, especially in CVD and DM patients. The same challenge arises with antiretroviral combinations for HIV patients, where the dose must be based on patient weight. As a result, many prescribers became reluctant to use FDC for their patients (Webster et al. 2016; Roy, Naik, and Srinath Reddy 2017).

Additionally, recent advancements in pharmacogenomics and pharmacogenetics show that different individuals will respond to the same medication differently. Hence, the old way of one-size-fits-all that has been adopted by the pharmaceutical industry is about to change (BG et al. 2023; Vaz and Kumar 2021). Additionally, patient-centric designed medications have shown improvement in patient adherence (Menditto et al. 2020). Nevertheless, FDC is usually designed to be suitable for a large population and not for a specific small number of patients, therefore it lacks the flexibility that personalised medication needs (Wilkins et al. 2024). Additionally, the incident of adverse reaction to one of the components of the polypill can lead to the discontinuation of the rest of the component and/or decrease the persistence.

Finally, physical and chemical interactions between the different APIs within the pill, different formulation requirements due to differences in solubility and permeability of the APIs, and differences in processing requirements like hygroscopicity,

compressibility, and thermal sensitivity are all factors that complicate the formulation of a polypill (Wilkins et al. 2024).

1.5 Personalised Medicine

Personalised medicine is garnering increasing attention among researchers and clinicians alike. It aims to dispense the right drug with the correct dose at the right time for the right patient, moving away from the current one-size-fits-all approach. Tailoring treatment to a patient's unique characteristics, such as genetics, lifestyle, and environment, offers a more effective alternative to trial-and-error prescribing and, as a result, improves clinical outcomes, boosts patient adherence, and reduces costs (Mathur and Sutton 2017).

The concept of personalised medicine is not a new concept. It can be dated back to Hippocrates 2400 years ago (Abrahams and Silver 2010). However, technologies that could enable personalised medicine have been developing fast in recent years. Among these enabling advancements are advancements in diagnostics and biomarkers (Ahmed et al. 2014), Artificial Intelligence and Machine Learning (Gifari, Samodro, and Kurniawan 2021) and 3D printing (Alzoubi, Aljabali, and Tambuwala 2023). However, all these technologies have their limitation that needs to be addressed before a broader adaptation of personalised medication becomes a reality.

This work aims to enhance the use of 3D printing to deliver personalised polypills. The next chapter will explore one of the most widely adopted 3D printing technologies, fuse deposition modelling (FDM), and highlight its capabilities and limitations.

1.7 Conclusion

In conclusion, combined therapy is becoming a clinical necessity in managing chronic disease. However, this approach presents challenges, as increasing the number of medications patients need to take daily can significantly impact adherence, particularly for long-term or lifelong treatment regimens. Polypill can offer a solution for this problem but introduces a new set of complications, such as difficulty with dose titration, personalisation, discontinuation, and others.

As a result, the need for dosage forms that can offer more flexible and personalised dose combinations instead of the fixed-dose combination has emerged. Figure 1.1 presents a flowchart illustrating the gap in the current approach to addressing the polypharmacy issue, along with the proposed solution.

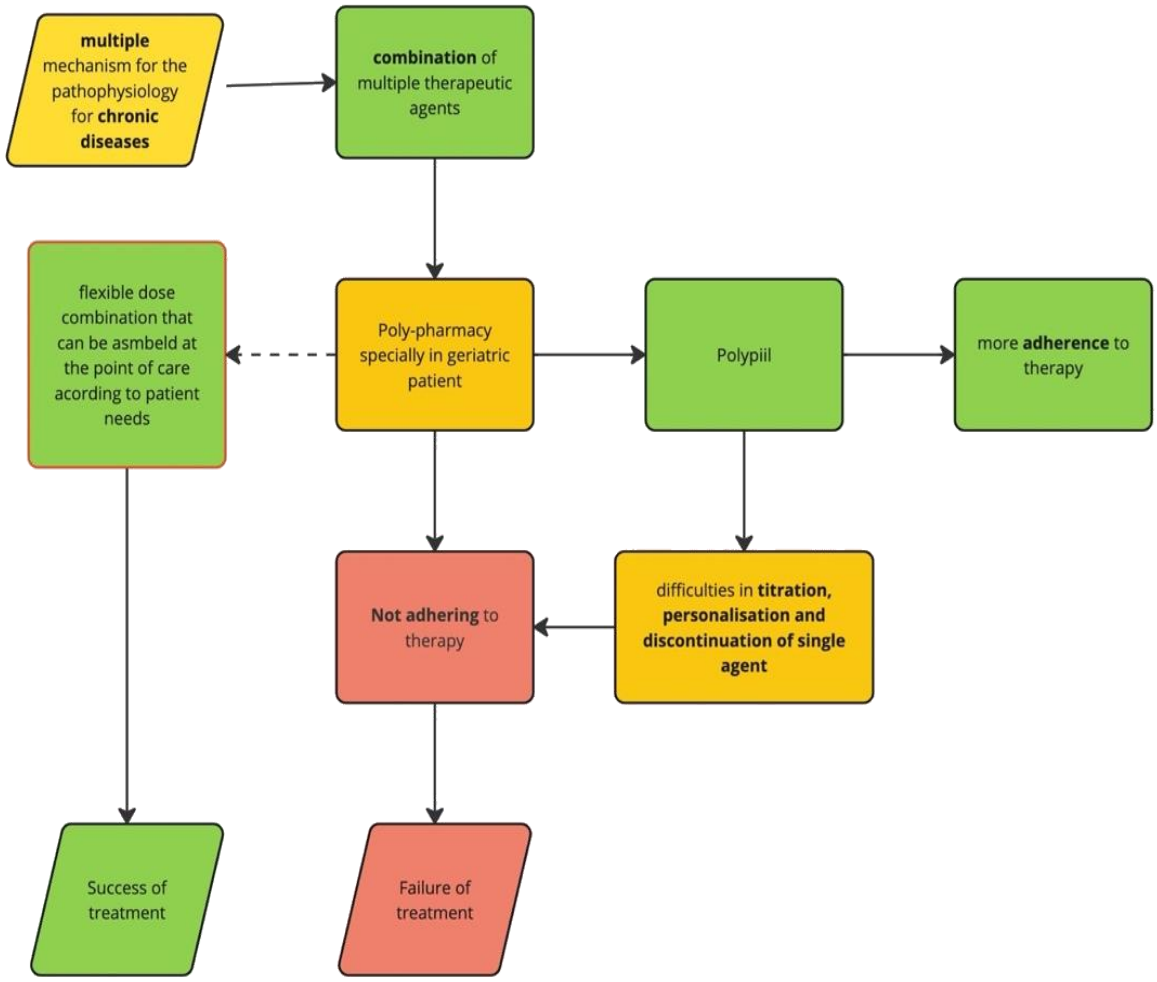

Figure 1.1 A flow chart showing the current gap in treatment and the proposed solution. (constructed by the author)

Chapter 2 : Literature Review

2.1. Introduction

Three-dimensional printing (3DP) is an additive manufacturing process for fabricating 3D objects, where the structure is designed using computer-aided design (CAD) software. This design guides the printing process, which involves vertically adding material layer by layer until a 3D object is formed. 3DP was introduced in the early 1980s by Charles Hull, who patented stereolithography (SLA), which uses UV light to solidify a resin bed (Tan, Maniruzzaman, and Nokhodchi 2018). Around the same time, other researchers at MIT introduced inkjet 3DP. Subsequently, by the late 1980s, Scott Crump patented the first fused deposition modelling (FDM) (L.K. Prasad and Smyth 2016; Dumpa et al. 2021; Kalaskar and Serra 2017), and after that, other 3DP technologies followed suit. Initially, the aim was to produce prototypes in a fast and cost-effective way. Since then, this technology has drawn the attention of many industrial sectors, such as automotive, aerospace and others (Park et al. 2019).

In pharmaceutical research, the technology of 3DP was employed to fabricate various drug delivery systems, such as implants (Nagarajan et al. 2018), microneedles (Economidou and Douroumis 2021), topical drug delivery (Goyanes, Det-Amornrat, et al. 2016) and oral dosage forms. This work will review the work done with oral dosage forms exclusively. The oral dosage form is the most prescribed and dispensed pharmaceutical form since it is easy to self-administrate and can provide a precise and safe dose. However, Since the invention of compression tabletting in 1834 (Araújo et al. 2019), there have been no new developments in the method of tabletting. However, tabletting by compression has its limitations such as the need for multiple steps, and a variety of excipients are needed to improve powder qualities such as flowability and compressibility. Moreover, additional steps such as coating may be necessary to control drug release or improve patient compliance (Gorkem Buyukgoz et al. 2022). Finally, there are few opportunities to modify the geometry and internal structure of a tablet for functional purposes. On the other hand, the advantages of an oral formulation produced by 3DP (printlet) are the possibility of personalising the formulation to patient needs. Moreover, drug release in the printlet can be controlled

without the need for extra steps by; either the geometry of the printlet which can be very intricate in 3DP, the percentage of the drug loaded in the printlet or the polymer used for printing (Araújo et al. 2019). Lastly, 3DP can improve drug load and decrease the number of excipients needed for tabletting (Melocchi et al. 2021).

Therefore, by the middle of the 1990s, 3DP found its way into pharmaceutical science and since then it has been gaining more and more interest from researchers in the field (Dumpa et al. 2021; Park et al. 2019; Trenfield et al. 2019; Cailleaux et al. 2020; Melocchi, Uboldi, Cerea, et al. 2020). This interest was magnified by the release of the first FDA-approved tablet, Spritam^{Ò} in late 2015, containing levetiracetam for the treatment of epilepsy in children (Jacob et al. 2016). Hence, a search in ScienceDirect for the phrase “3D printing in medicine” shows that more than 9,500 research articles have been published in the last 10 years with more than 50% of them in the last three years which reflects the growing interest in the subject in recent years. Figure 2.1 shows the number of published articles over the past ten years.

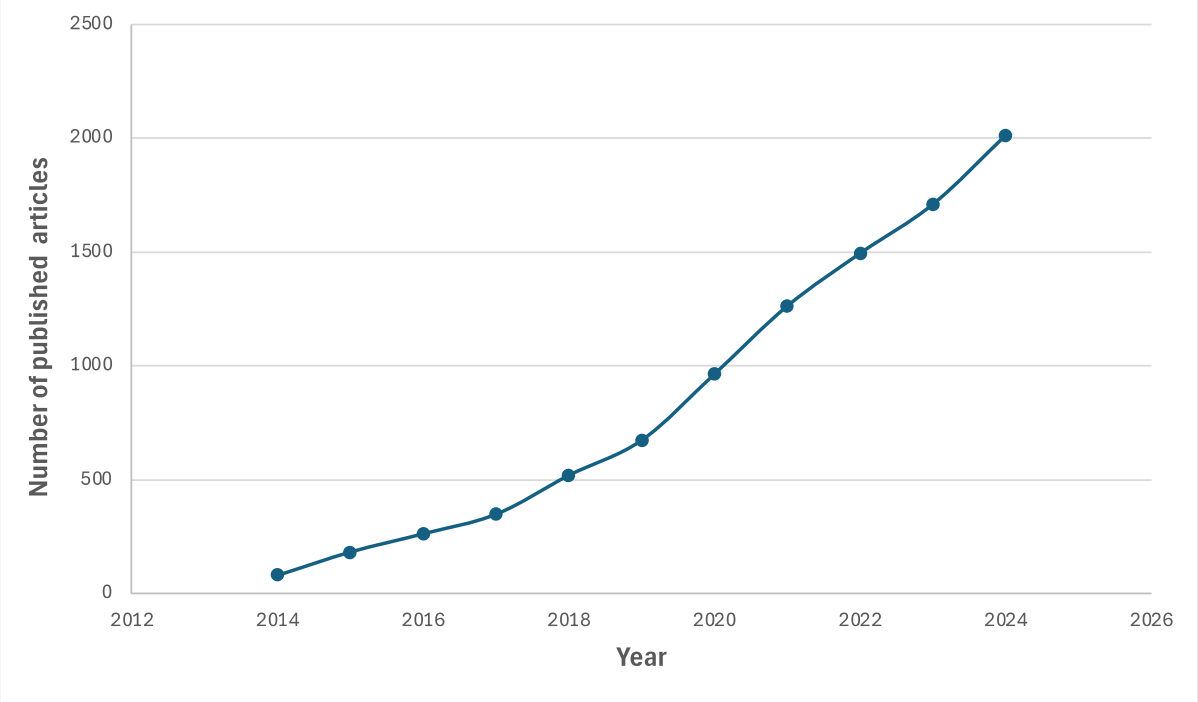

Figure 2.1 Number of publications in ScienceDirect from 2014 to 2024. (constructed by the author)

As has been mentioned previously, there are different 3DP technologies but all work according to one of these three general principles; extrusion, liquid solidification and powder solidification (Jamróz, Szafraniec, et al. 2018). Extrusion-based 3DP can be subdivided according to the nature of the material being printed and the method of

extrusion to melt extrusions like FDM or semisolid extrusion like pressure-assisted microsyringing (PAM). In FDM, a thermoplastic polymer extruded from a heated nozzle into a heated printing stage the polymer can be fed as filament and called fused filament fabrication (FFF) or as powder or granules like in direct powder extrusion (DPE) (Goyanes et al. 2019; Mendibil et al. 2021).

Lastly, FDM is the most studied printing method in the pharmaceutical field because of its low cost, simple equipment, ease of producing dosages with complex geometry (Okwuosa et al. 2016) , and less friable end product compared to powder bed printers (L.K. Prasad and Smyth 2016). Hence, this work will focus on advances made using FDM to produce oral dosage forms, the barriers this technique still faces, and ways to address them.

2. 2. Advantages That Fused Deposition Modelling (FDM) Offers to Oral Dosage Form

Since its introduction to pharmaceutical formulation, FDM has shown its potential in many applications. In this section, we will present the most investigated applications and what advantages FDM adds over the traditional tabletting method. Figure 2.2 presents the main application reported in the literature so far for FDM and some of the barriers that face this technology.

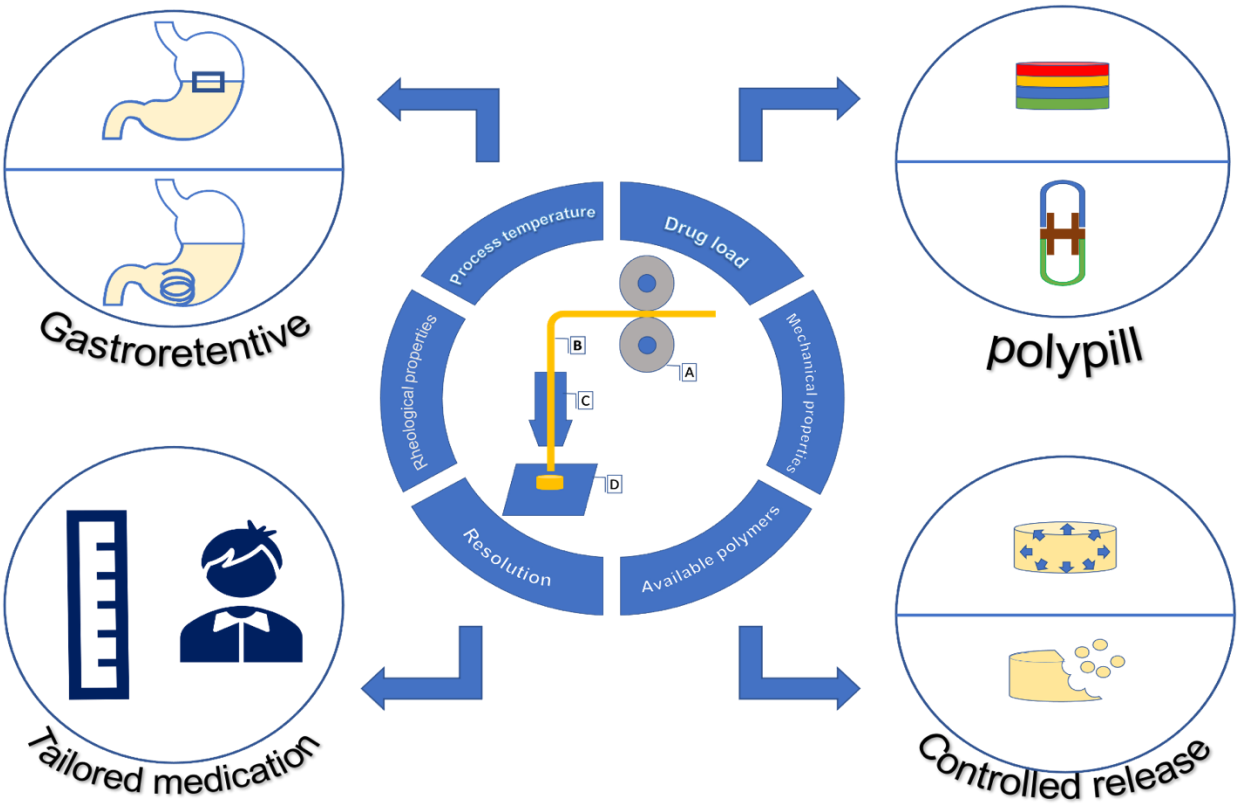

Figure 2.2 Graphical representation of the pharmaceutical application of FDM and the formulation barriers that it faces. (A= feeding gears, B= feedstock filament, C= heated nozzle, D= building platform). (constructed by the author)

2.2.1 Flexible Dose Combinations

As mentioned in the previous chapter, fixed-dose combinations (FDCs) are formulations that contain two or more active pharmaceutical ingredients (APIs) in a single dosage form. Their primary aim is to enhance patient adherence to complex medication regimens, particularly in chronic diseases (Baumgartner et al. 2020).

FDC can improve adhesion, which is necessary for treatment success, especially in patients with chronic disease who are on multiple medications throughout the day. Nonetheless, HCPs are sometimes reluctant to prescribe polypills due to the difficulty of personalising and titrating the dose (Webster et al. 2016; Roy, Naik, and Srinath Reddy 2017). This has been reinforced with increased evidence of the importance of personalised medication. Therefore, the old tendency to prescribe one-size-fits-all, adopted by the pharmaceutical industry, has changed (BG et al. 2023; Vaz and Kumar

2021). Additionally, patient-centric designed medications have shown improvement in patient adherence (Menditto et al. 2020).

This created the need for a more flexible dose combination that can be personalised to each patient's needs. Therefore, in recent years, there have been few publications utilising FDM to fabricate a polypill that can be printed and personalised at the point of care to meet the needs of individual patients. The main attempts to use FDM to print a polypill with more than one active ingredient will be presented and their objective will be discussed in this section. One of the first attempts to utilize an FDM printer to fabricate a tablet with more than one component was a multilayer tablet and a tablet within a tablet containing paracetamol and caffeine was fabricated. Although this study was not aimed to reveal the potential of flexible-dose polypill, however, it reflected the possibility of controlling drug release by changing the design (Goyanes, Wang, et al. 2015). Thereafter, multiple attempts followed suit, one of which was the printing of a bilayer tablet containing drugs that have different daily regimens (Gioumouxouzis et al. 2018). The printlet contained 2 mg of glimepiride in polyvinyl alcohol (PVA) for immediate release and 500mg metformin in a combination of Eudragit RL PO and polylactic acid (PLA) for sustained release. The drug release was controlled not by the design but by the polymer used in the formulation and the author highlighted the possibility of dose titration.

Moreover, another attempt at fabricating multiple drug combinations was in the form of a bilayer tablet that contained indomethacin in sustained and extended-release formulation and nifedipine as an immediate-release formulation (Althobaiti et al. 2022). Once more, the main objective of this work was to present the possibility of combination with different release profiles. Furthermore, a research group prepared a two-layer printlet that contains isoniazid in hydroxypropyl cellulose (HPC) and rifampicin in hydroxypropyl methylcellulose acetate succinate (HPMCAS) (Tabriz et al. 2021). This bilayer printlet was successful in separating these two anti-TB medications physically and in the release profile to prevent drug-drug interaction and degradation of rifampicin. In addition, the group was successful in controlling drug release by varying the infill density and the number of covering layers. The objective of the work was to demonstrate the capability of FDM to produce FDC.

Thereafter, a uni-matrix multilayer printlet for the treatment of cardiovascular disease (B.C. Pereira et al. 2019) was produced using PVA as a polymer and sorbitol and water as a plasticiser and temporary plasticiser, respectively. The API release from the matrix

was dependent on the solubility of each API and its layer position in the printlet. In this work, the possibility of dose titration and patient-centric polypill was demonstrated.
Moreover, in another effort to produce two layers of hydrochlorothiazide and enalapril tablets. The author's objective was to reveal the possibility of controlling.
APIs dose through control of the layer thickness to produce a dose-flexible polypill (Sadia, Isreb, et al. 2018). The thickness of the hydrochlorothiazide layer was either 0.8 mm or 1.6 mm, corresponding to doses of 12.5 mg or 25 mg, respectively. The thickness of the enalapril layer was either 1.1 mm or 2.2 mm, providing doses of 10 mg or 20 mg. Furthermore, another endeavour at producing polypill where drug dose can be controlled took the shape of a compressed tablet inside a printed shell. The printing was done in two steps, with the compressed tablet loaded between those steps the authors used amlodipine and atorvastatin as the model APIs and PVA as the printing polymer. Drug dose and release were controlled through the infill density of the print and drug load in the filament (Alzahrani et al. 2022). Additionally, a polypill containing melatonin and caffeine was printed into two compartments that can be assembled after printing. Caffeine was placed in a placebo compartment to delay its release while a doughnut-shaped melatonin printlet was attached to the top of this compartment. While melatonin release was immediate, caffeine release was controlled through wall thickness and the type of polymer within the formulation (Tabriz et al. 2023).
Furthermore, most of the previous attempts toward dynamic dose combination were utilizing two APIs. However, a recent work investigated the printing of layered polypills for metabolic syndrome containing nifedipine, simvastatin, and gliclazide. Although dose titration was not demonstrated in this work, the author emphasized the importance of dose personalisation and the ability to achieve it by adjusting the number of layers for each drug (Anaya et al. 2023).
Additionally, other 3D printing techniques were used to produce polypills. However, the polypill produced by FDM had relatively better resolution and more structural integrity compared to polypills produced by PAM (Khaled et al. 2015a, 2015b). Additionally, there was no interaction or cross-over between the layers when printing layered polypill with FDM, in contrast to polypill printed using SLA (Robles-Martinez et al. 2019). Moreover, printing polypill with FDM is much simpler since PAM requires an extra drying step, and SLA needs a modification in the method and interruption of the process to change the resin bed. Lastly, it is worth mentioning that others have (Maroni

et al. 2017) prepared a capsular device with two compartments that can be loaded with two different APIs. Although this device requires a loading step, these compartments can have different wall thicknesses and different materials controlling the release from each compartment separately. Table 2.1 lists some of the attempts made in recent years to formulate polypill using FDM.

In this section, researchers have shown that FDM can be used to fabricate polypills that will not only improve patient compliance but can also present different release profiles, flexible dosing on demand and prevent physical and chemical incompatibilities. Although there has been a significant increase in research on FDM in pharmaceutical studies, the amount of work on personalised polypills remains limited.

Table 2.1 Application of FDM in the production of polypills. NM=polymers are printed separately and are not a mixture, M= mixture.

Polymer	API	Extrusion temp.	Printing Temp	Application	REF.
PVA	lisinopril, Indapamide, Rosuvastatin and Amlodipine	90	150	IR Polypill	(B.C. Pereira et al. 2019)
Eudragit® RL PO, PVA (NM)	Glipizide, Metformin	140, 190	170. 205	Layered tablet	(Gioumouxouzis et al. 2018)
HPC, HPMCAS (NM)	Isoniazid & Rifampicin	160, 150	130,170	Dual tablet	(Tabriz et al. 2021)
Eudragit E PO	Hydrochlorothiazide, Enalapril	100	135	Flexible dose polypill	(Sadia, Isreb, et al. 2018)
PVA	Amlodipine, Atorvastatin	180	180-187	Core-shell design	(Alzahrani et al. 2022)
HPC, HPMCAS	Melatonin, Caffeine	140-160	150-170	LEGO-like design	(Tabriz et al. 2023)
HPMC, HPC, PEO	Indomethacin, Nifedipine	140, 180	200, 250	Layered tablet	(Althobaiti et al. 2022)
HPMCAS, HPC, PEG (M)	nifedipine, simvastatin, gliclazide	160, 135 ,145	160, 140, 155	Layered tablet	(Anaya et al. 2023)

HPMC, Kollicoat® IR, HPMCAS, and PEG. (NM)	-	165	180	Two compartments capsule	(Maroni et al. 2017)

2.2.2 Gastroretentive Tablet

A gastroretentive tablet is a tablet designed to remain in the gastric medium for an extended period. This can be achieved by either adhesion to the gastric wall, expansion beyond the pyloric sphincter of the stomach, through a magnetic system, sinking due to high density or floating above the gastric media due to low density (Fu et al. 2018; Ilyés et al. 2019). However, buoyancy and size expansion have the least interference with gastric physiological processes (Reddy Dumpa, Bandari, and A Repka 2020) and have proven their effectiveness in clinical settings (Lamichhane et al. 2019). Gastroretention aims to improve dissolution for basic molecules, retain medication that acts locally in the stomach, improve stability for molecules unstable in the intestinal medium (Chen et al. 2020) , or improve absorption for molecules that have a narrow absorption window in the upper parts of the gastrointestinal tract (GIT) (Fu et al. 2018).

A floating tablet (FT), prepared by conventional method, is either effervescent-based or made from gel-forming polymers. Both require complex manufacturing steps and multiple excipients. Additionally, a floating tablet that is prepared conventionally has limitations like food interaction and the lag time needed to initiate the floatation reaction, which puts it at risk of being cleared from the stomach before floatation commences (Ilyés et al. 2019). Due to FDM's capability to print hollow or partially hollow structures with air pockets, the resulting printlets can float immediately without delay. However, it is essential to use a polymer that remains stable in gastric fluid, as erosion could allow the gastric medium to penetrate, reducing the printlet's floatation time. Additionally, adjusting the wall thickness is crucial to prevent media penetration and enhance the printlet's hardness. Increasing wall thickness without expanding the overall volume decreases the internal void space, reducing the likelihood of floatation. Moreover, thicker walls may hinder or slow the release of the active pharmaceutical ingredient (API) to an undesirable level. While increasing the infill density improves drug loading and strengthens the printlet, it also raises the printlet's density, negatively

impacting its ability to float. Therefore, while floating printlets offer advantages over traditional approaches, their fabrication is a complex process that requires carefully balancing multiple factors (Mora-Castaño, Domínguez-Robles, et al. 2024).

The attempt to produce a floating oral dosage form using FDM can be divided into two types; a floating device that can be loaded with a compressed tablet to help it float, or a printlet with low density that contains the API within its formulation.

Firstly, the attempts to use the design flexibility of FDM to print flotation devices that can float a compressed tablet loaded inside the device will be discussed. One such attempt was preparing four different devices that can hold a riboflavin compressed tablet and make it float. All the designs had an air-filled chamber and a screen to allow the dissolution medium to come in contact with the compressed tablet (Fu et al. 2018). The devices were printed using commercially available PLA filaments at a printing temperature of 195 °C. In this study, the floating tablet prepared by 3DP has a very slow release of the API in acidic media making a device loaded with a compressed tablet the better choice. Although these floating devices can convert any compressed tablet into a floating tablet, it requires an assembling step. Another design was a floatation device consisting of three compartments two enclosed with air pockets and one with a screen for drug release to which the compressed tablet is loaded (Shin et al. 2019). Acyclovir was used as the model drug and the floatation device was retained *in vivo* test for more than 12 hr which improved the bioavailability of acyclovir. Moreover, other researchers were successful in preparing a floatation device using PVA and acrylonitrile butadiene styrene (ABS) (Huanbutta and Sangnim 2019). The device contained an air pocket at the top and a drug release orifice at the bottom and held a directly compressed metronidazole tablet. The size of the air pocket and orifice controlled the drug release. All the designs were able to float for 4 hr in an *in vitro* dissolution study and only the device with the large air pocket did not experience lag time in the dynamic dissolution apparatus.

Lastly, another floating design was a floating pulsated release shell that holds theophylline compressed tablet for 6 hr (Reddy Dumpa, Bandari, and A Repka 2020). The author added 0.5 % ethyl cellulose (EC) to HPC to add lag time for drug release by preventing fast media penetration into the shell and releasing the API. The shell was able to float for 6 hr, had no flotation lag time and re-float after mechanical submersion in the dissolution media. However, these devices require a step to load

the tablet into them, and tablet size which is determined by the total size of the device plus the tablet, governs the suitability for easy swallowing.

As a result, direct printing of hollow tablets containing the API can overcome these disadvantages. A sustained-release floating tablet using FDM 3D printing was first investigated by Chai et.al in 2017 (Chai et al. 2017). Domperidone was used as the model API because it can benefit from being formulated as a floating tablet since it is a basic drug with low bioavailability and a short half-life which mandates a three-time regimen. The printlet was printed using HPC as a hollow structure (0% infill) with two shells and a low density of 0.77 g/cm^3 which allowed it to float. The gastroretentive tablet of domperidone increased its bioavailability and reduced the frequency of its administration. The study concluded that a change in the number of tablet wall layers did not affect the buoyancy but affected drug release. The same result was observed when another group of researchers attempted to print theophylline floating tablet using HPC as the matrix polymer (Giri et al. 2020). In this work, the infill density determined the floatation time as well.

However, in another work, a floating tablet was fabricated using FDM. The filaments compassion was a combination of HPC and polyvinyl pyrrolidone (PVP) as polymers and itraconazole as the model API (Kimura et al. 2019). The group was able to control the release of itraconazole by adjusting the shell thickness. The resulting printlet was able to float for 9 hr and maintain a zero-order release for 12 hr. In this study, wall thickness affected both drug release and buoyancy. This resulted from using PVP in addition to HPC, which acted as a solubility enhancer that accelerates the penetration of the dissolution media through thinner walls. Therefore, the polymer's solubility can affect floating time this was confirmed by a group of researchers who fabricated an ellipsoid floating tablet using PVA-loaded filament with 10% propranolol (Chen et al. 2020). The *in vitro* floating time was around 2 hr, which is relatively shorter than other reported works. This was attributed to the fast erosion of PVA in gastric media. Increasing the infill percentage resulted in harder printlets, with less weight variation, slower drug release and shorter floating time.

Nevertheless, the hollow structures of such a design result in difficulties in printing due to the bowing of the top layers and weak mechanical properties of the printlet. Hence, the addition of a low-density infill can add structural support to the design. However, this will increase the density of the printlet and affect floating. Ultimately, wall thickness could affect floating time only if the polymer used has some water solubility which can

allow gastric media to breach the walls and sink the tablet, in this case, the wall thickness will be a limiting factor.

One other factor that could affect the floatation time is the design of the tablet. In a recent study, a team of researchers demonstrated the effect of three designs for verapamil floating tablets on the floatation time. The tablet was formulated with a 1:1 ratio of HPMC and Soluplus® as the main polymer. The three designs were cylinder, capsule and hemisphere with either 0 or 15% infill density. The flotation time was greatly influenced by the design, with the cylindrical tablet showing the longest flotation time, followed by the capsule, and finally, the hemisphere having the shortest flotation time. This effect was caused by faster media breach to the centre of the designs with curve walls since curve walls have less contact area between the printing layers (Qian et al. 2022).

Additionally, High drug loading is required in hollow tablets to deliver the required dose without an over-increase in the size of the tablet. As a result, a floating pregabalin tablet (Lamichhane et al. 2019) was printed using formulation filaments with 40 % HPMCAS, 10% polyethylene glycol (PEG) 400 and 50% API. The design had a closed bottom and a partially open top with 25% infill. Drug release by diffusion and polymer erosion followed zero-order kinetics. Moreover, other researchers tried to investigate the effect of drug load on the buoyancy. A metformin floating tablet with HPMC as the main polymer was formulated with varying drug loads from 10 to 50%. Although drug load affected drug release from the tablet, it did not affect the density and the buoyancy of the tablet (Mora-Castaño, Millán-Jiménez, and Caraballo 2023). On the other hand, a floating tablet containing 20% carvedilol was prepared by adding Eudragit RS PO to HPMC to investigate the effect of Eudragit RS PO on HPMC mechanical and rheological properties and improving gastric resistance (Ilyés et al. 2019). Floating was achieved by decreasing the printlet density through infill reduction to 20%. The printing was carried on using 180 °C to improve printing speed and welding of printed layers. The printlet was successful in maintaining floatation and releasing carvedilol for 24 hr. Therefore, to personalise floating tablets, an understanding of the effects of design and printing parameters must be established beforehand to decrease formulation time. As a result, researchers have attempted to use the design of experiments to establish the correlation between design and printing parameters on one hand and floatation force and dissolution rate on the other. The floating tablets with cinnarizine as the model drug and HPC and Kollidon as the carrier polymers. Hence, Floatation time was

controlled from 6 hours to more than 12 hours by adjusting the printing parameters and the design due to the significant correlation between these parameters and the flotation force (Vo et al. 2020).

On the other hand, there have been some attempts to merge the polypill concept with floatation to form a floatation mini tablet with floating properties. One such attempt was the preparation of floating polypill minitablets containing levodopa, benserazide and pramipexole for the treatment of Parkinson's disease. In their design, the minitablet floated without incorporating hollow space to decrease the density but depended on the low density of the polymer Ethylene-vinyl acetate (EVA). However, floatation was tested in 300ml of 0.1 N HCl acid with no rotation to simulate the gastric environment (Windolf et al. 2022). Moreover, another group of researchers printed a floating torus mini tablet containing propranolol, hydrochlorothiazide and diltiazem. The mini-tablet was formulated using HPMC as the main polymer with the intent to load four of them inside a size 0 capsule. The floatation of these mini tablets was tested in a 3D-printed stomach model for 2 hours (Zgouro et al. 2024). While this design provided a floating drug combination, it lacks the dosing flexibility typically expected from 3D-printed polypill, as all the APIs are included in the same formulation, allowing minimal room for dose adjustment. In conclusion, FDM can prepare a floating device or floating tablet simply and without the need for special equipment or material. Additionally, the floating printlet will have no lag time for floatation and will not be affected by food. The floating time can be controlled through adjustment of the design of the print, the type of the polymer, wall thickness and/or infill density.

Furthermore, gastric retention can be achieved through the expansion of the delivery system. To achieve this, the oral dosage form should be small enough to be swallowed and once in the stomach, expand to size with at least two dimensions greater than 13 mm, this will prevent its emptying through the pylorus. Moreover, the expanded structure should not prevent gastric emptying and should be cleared from the stomach before the next dose arrives to prevent drug accumulation.

Recently, a team of researchers took advantage of PVA's shape memory property. The group printed the polymer loaded with allopurinol into the expanded shape and then by increasing the temperature above Tg of the polymer they were able to program it into a swallowable shape (Melocchi et al. 2019). After swallowing the dosage form, the polymer will expand at body temperature to its original shape which will lead to retention in the stomach. Table 2.2 summarizes some of the attempts done in recent

years to 3DP gastroretentive tablets using FDM. Figure 2.3 represents the type of gastroretentive device and tablet prepared by FDM.

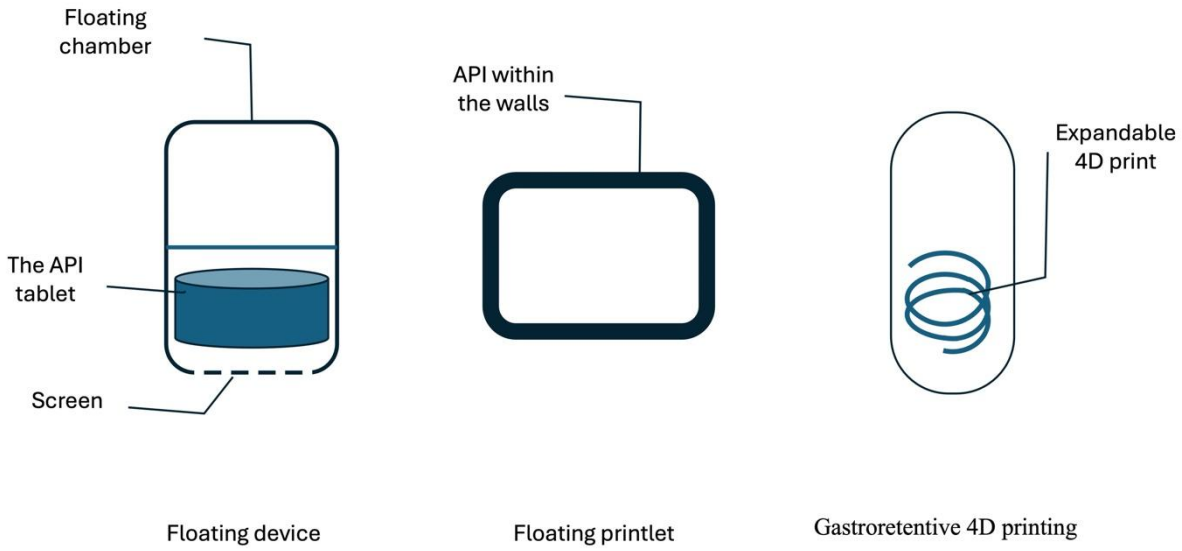

Figure 2.3 The three types of gastroretentive are prepared by 3D printing. (constructed by the author)

Table 2.2 Application of FDM in the production of gastroretentive dosage form.

Polymer	**API**	**E. Temp. (°C)**	**P. Temp (°C)**	**Dosage form**	**FT (Hours)**	**Reference:**
Hydroxypropyl cellulose (HPC) EXF	Domperidone	150°C	210°C	Sustained release (SR) floating tablets	10	(Chai et al. 2017)
PLA filament	Riboflavin (compressed tablet)	-	195°C	Floating device	>72	(Fu et al. 2018)
HPMCAS	Pregabalin	125°C	180°C	Sustained release (SR) floating tablets	24	(Lamichhane et al. 2019)
Modified HPMC and Eudragit RSPO (M)	Carvedilol	110°C	180°C	Floating Tablet	16-24	(Ilyés et al. 2019)

HPC & PVP(M)	Itraconazole	135°C	185°C	floating and zero-order sustained-release	9	(Kimura et al. 2019)
PLA filament	Acyclovir (compressed tablet)	-	210°C	Floating device	>12	(Shin et al. 2019)
PVA, ABS (NM)	Metronidazole (compressed tablet)	-	210,270°C	Floating device	>4	(Huanbutta and Sangnim 2019)
PVA	Allopurinol	170,175,200°C	200,230°C	Gastroretentive 4D printing	NA	(Melocchi et al. 2019)
PVA	Propranolol	142°C	185°C	Floating Tablet	2	(Chen et al. 2020)
HPC, EC (M)	Theophylline (compressed tablet)	165°C	190°C	Floating device	6	(Reddy Dumpa, Bandari, and A Repka 2020)
Kollidon VA64, HPC	Cinnarizine	130°C	165°C	Zero-order floating tablet	12	(Vo et al. 2020)
HPC	Theophylline	150°C	210°C	Floating tablet	>10	(Giri et al. 2020)
EVA, PVP-VA(M)	Levodopa, benserazide and pramipexole	100°C	220°C	Polypill minitablets	-	(Windolf et al. 2022)
HPMC, Soluplus®	Verapamil	115°C	195°C	Sustained-release gastric-floating tablet	4-6	(Qian et al. 2022)
HPMC, PEG	Metformin	150°C	200°C	Floating tablet	>8	(Mora-Castaño, Millán-Jiménez, and Caraballo 2023)
HPMC 4 M, PEG	Diltiazem hydrochlorothiazide propranolol	175°C	190°C	Torus-shaped floating polypill	2	(Zgouro et al. 2024)

HPMC	Felodipine	150°C	200°C	Controlled release floating tablet	>8	(Mora-Castaño, Millán-Jiménez, et al. 2024)
NM=polymers are printed separately and are not a mixture, M= mixture.						

2.2.3 Controlling Drug Release

One of the major advantages of FDM is its ability to control drug release in a variety of ways without the need for special equipment or extra steps. Drug release from polymer matrix is usually achieved throw one of three major mechanisms: polymer erosion (e.g., PLA, Soluplus, and PVA), diffusion (e.g., Eudragit RS and RL) and/or swelling (e.g., HPMC). What determines which of these mechanisms is the predominant one is the polymer's solubility in the dissolution media and the permeability of the API (S.K. Patel et al. 2021; S. Wang, Liu, et al. 2020).

In case diffusion was the predominant mechanism of release, the release profile would be fast at first due to the release of API being close to the surface of the printlet. However, as the release progresses, it will gradually decrease due to an increase in the distance that the API needs to travel from the core of the printlet to the surface. Diffusion is affected by the geometry of the printlet, composition of the printlet and temperature (Borandeh et al. 2021). On the other hand, polymer erosion can be either surface erosion or bulk erosion depending on the permeability of the dissolution media. Once more, the geometry of the printlet can result in either zero-order release in the case of a flat eroding printlet or gradually decreasing release as the surface area is decreased in the case of a sphere or cylinder printlet (Cossé et al. 2017; Borandeh et al. 2021).

Lastly, in some systems the API will be entrapped by the polymer chains, however, upon exposure to water and depending on the hydrophilicity of the polymers, they tend to swell (Nashed, Lam, and Nokhodchi 2021) as a result of the hydration of the polymer chains, which leads to their disentanglement and increase in the void space within the polymer and its transition from a glassy state to elastic state. After that, the polymer either erodes (Melocchi et al. 2015) or the API diffuses from it through the channels that form during swelling (Borandeh et al. 2021). Therefore, understanding these

mechanisms can help formulators control the release of the API from 3D printed dosage form through multiple strategies that are discussed below. Figure 2.4 represents the main mechanisms for drug release from FDM printed tablets.

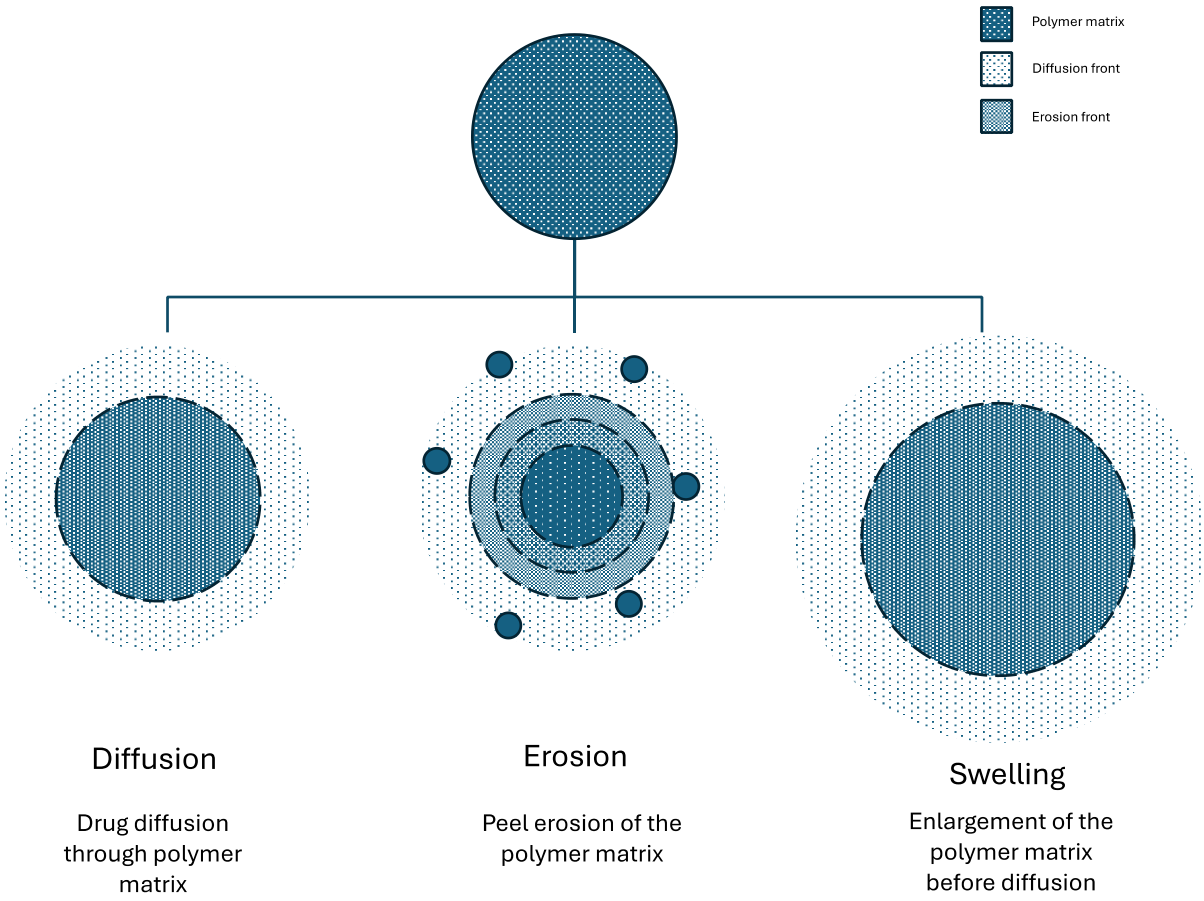

Figure 2.4 The major drug release mechanism from the polymeric matrix. (constructed by the author)

2.2.3.1 Composition (Polymers and Excipients)

The type of polymer used in printing will control the mechanism by which the drug will be released. As a result, polymer selection can be a critical step in determining the mode of release. For instance, drug release from different pharmaceutical-grade polymers was evaluated (Melocchi et al. 2016) by preparing multiple disks with different polymer matrices and furosemide as the model API. The disks prepared by FDM with polyethylene oxide (PEO) and Kollicot IR release the API immediately. However, the HPMC disk took some time before releasing the API this lag time is

attributed to the time it takes the polymer to swell and erode, and it depends on the thickness of the polymer layer. Moreover, other polymers like; HPMCAS and Eudragit L were only soluble in basic media and insoluble in gastric media giving them enteric release properties. Furthermore, EC and Eudragit RL disks were insoluble, and drug release was governed by diffusion through channels in the polymer, which can provide prolonged drug release. In another instant, different grades of the same polymer had different release profiles. The release of paracetamol was modified using different grades of HPMCAS; LG, MG and HG (Goyanes et al. 2017). Paracetamol release was prolonged release for all three grades. Nonetheless, the release was faster from LG and MG grades compared to HG because they had lower pH thresholds. Moreover, Eudragit EPO and Soluplus were used separately to print two printlets of felodipine. The resulting printlet had different dissolution rates and different disintegration mechanisms, bulk disintegration for the Eudragit EPO and peeling for Soluplus (Alhijjaj, Belton, and Qi 2016). This work shows that polymer selection will not only affect the dissolution mechanism but the disintegration mechanism as well. Furthermore, other researchers added another polymer to the blend as a release modifier. Hence, the release of ibuprofen from EC was improved by adding release modifiers such as; HPMC and PVA (Yang et al. 2018). The improvement was directly related to the concentration of the release modifier. Another group adopted the same approach (Shi et al. 2021). Where they used different release modifiers to control the release of Ibuprofen from the EC printlet. Moreover, other components of the polymer matrix, like plasticisers, can affect drug release depending on their hydrophilicity and level of interaction with the polymer (Nashed, Lam, and Nokhodchi 2021; Obeid, Madžarević, and Ibrić 2021).

Lastly, it has been demonstrated that the co-extrusion of an immediate-release polymer with the insoluble polymer can serve to control the release from the immediate-release polymer. For instance, Kollicot IR filament loaded with aripiprazole and commercially available PLA filament were co-extruded to formulate a sustain-release from the printlet (Jamróz, Kurek, et al. 2018). The PLA decreases the surface area of the soluble polymer exposed to the dissolution medium.

In summary, these studies demonstrate that drug release from an FDM printlet can be effectively regulated by modifying the polymer type and/or grade, as well as by incorporating release modifiers or other excipients into the formulation.

2.2.3.2 Drug Load

An increase in the amount of an API loaded within a printlet will increase its release because of an increase in the amount available for dissolution media. This was investigated in prior work, where it showed that increasing drug content from 16% to 24% was directly related to the amount of drug released after 24 hours (Yang et al. 2018). Moreover, another group of researchers prepared a tablet within a tablet containing glipizide (Q. Li et al. 2017). The outermost layer contained 2.2% to release the API in a sustained manner, while the inner layer contained 4.8% drug load to give faster drug release. As a result, by using different drug loading in the external and internal layers, the drug release profile was controlled.

2.2.3.3 Infill Density

In 2017, a research group reported that infill density has an inverse relationship with drug release (Goyanes et al. 2017). The group recorded an increase in API release when infill density reduced from 100% to 20%. Moreover, others have fabricated a 10% loaded haloperidol printlet and were able to change drug release from 120 minutes to 45 minutes by decreasing the infill density from 100% to 60%, respectively (Solanki et al. 2018). This increase in dissolution is rationalized by an increase in the porosity of the low infill printlet which will lead to an increase in the surface area exposed to the dissolution medium. Additionally, the same results were produced when a group of researchers decreased the infill density of their PVP printlet from 100% to 50%, as pantoprazole release was shortened from 10 min to 3 min (Kempin et al. 2018). Additionally, in another publication decreasing the infill density from 80% to 50% had a significant effect on increasing the Cinnarizine release from floating tablets (Vo et al. 2020).

However, it has been reported that an increase in the infill density from 15% to 25% increases the dissolution rate as a result of an increase in the surface area exposed to dissolution media (Yang et al. 2018). In summary, decreasing the infill density from 100% will increase porosity and facilitate dissolution media penetration. However, at very low infill density, a further decrease in the density will have minimal effect on

porosity but a high impact on contact surface area which will lead to a decrease in the release. Therefore, as infill density can be easily controlled in FDM through computer software, the formulator can control drug release through this property easily. Figure 2.5 represents a diagram representation of the relation between infill density and drug release.

Finally, the infill pattern can also affect the release of API from the printlet. A recent publication found that the release of Amlodipine from a PVA printlet increased when the infill pattern was in a zigzag shape compared to cubic, tri-hexagon and concentric patterns (Obeid, Madžarević, and Ibrić 2021).

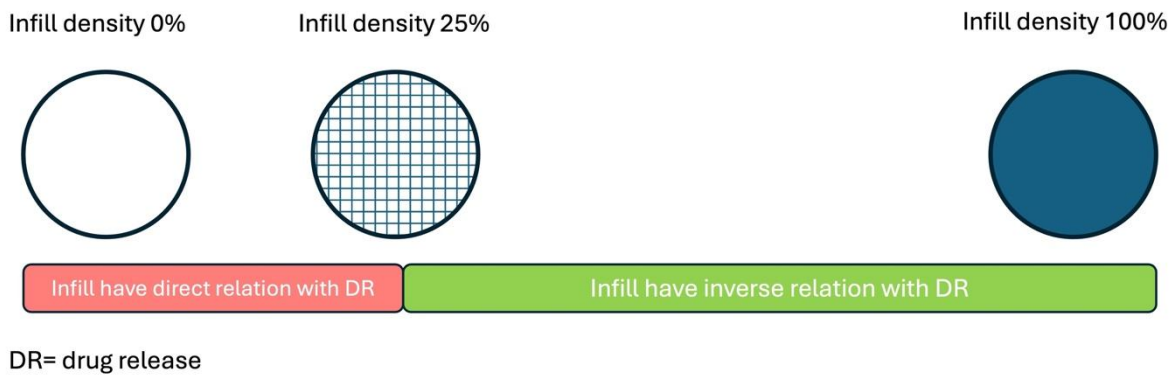

Figure 2.5 A diagram representation of the relation between infill density and drug release at different infill ranges. (constructed by the author)

2.2.3.4 Printlet Size and Walls Thickness

Since smaller printlets will have a higher surface area-to-mass ratio, it has been reported that an increase in drug release can be achieved by decreasing the size of the printlet (Palekar et al. 2019). However, a recent publication revealed that decreasing the size of the printlet prepared from PCL and different forms of Dexamethasone had no effect on the release profile and only decreased the dose (dos Santos et al. 2023). This resulted from using a water-insoluble polymer which made diffusion the dominant method for drug release and decreased erosion profoundly. Furthermore, this method to control drug release is governed by drug load and the dose required to be delivered.

Moreover, an increase in the thickness of the walls in case of infill less than 100% will decrease the chance of dissolution media penetration to the printlet core and,

therefore, reduce the drug release rate (Lamichhane et al. 2019; J. Zhang et al. 2017; Yang et al. 2018; Obeid, Madžarević, and Ibrić 2021; Vo et al. 2020; Tabriz et al. 2023).

2.2.3.5 The Design

Controlling the printlet design, which can be controlled easily in FDM, is another way to control drug release. In a study conducted in 2015, PVA filaments loaded with paracetamol (Goyanes, Martinez, et al. 2015) were used to print five geometrically different tablets (pyramid, cube, sphere, torus and cylinder). Drug release through these printlets was governed by the surface area to volume ratio, not by surface area alone. Pyramids achieved 90% release after only 2 hr and the slowest were spheres and cylinders which needed 12 hr to achieve 90% release. Moreover, it was reported that four designs with swellable HPMC had different release rates depending on their surface area-to-volume ratio. However, the gride design with and without a cap had the same drug release due to a thin cap and similar internal structure (E. Prasad et al. 2019). This indicates that surface area to volume ratio is a determinate factor for drug release regardless of the mechanism.

Furthermore, a radiator-like novel design was printed using different molecular weight PEO and loaded with theophylline (Isreb et al. 2019). The purpose of the design is to increase the surface area to the mass ratio which will improve API release. The group printed four printlets with the same surface area to mass ratio but a different spacing between the radiator plates (0.5, 1, 1.5 1 and 2 mm). All printlet had the same accelerated drug release except the 0.5 mm spaced design which was slower. The swelling mechanism of PEO release in the desolation media led to adhesion between the adjacent plates that resulted in a decrease in the surface area. The study confirms the capability of FDM to control drug release by adjusting the surface area to mass ratio.

However, in another publication, printlets were prepared using HPC SSL as the polymer and theophylline as the model API (Arafat, Wojsz, et al. 2018). The printlet was designed with 8 gaps between 9 block units (Gaplets) connected by three bridges. In these gaplets, drug release was directly related to the size of the gaps although the surface area to mass ratio was close. This was attributed to the effect of gap size on the disintegration and dissolution mechanisms. In another study, a printlet was

designed to contain channels of 0.6 mm in width and pass through the tablet in either a longitudinal or transfer direction (Sadia, Arafat, et al. 2018). Once more here, the surface area to mass ratio was equal but the shorter transfer channels resulted in faster drug release as a result of better dissolution media flow through these channels. Furthermore, a dual nozzle printer was used to fabricate different designs of printlets (Tagami et al. 2018). Alternating between drug-loaded PVA and either water-soluble blank PVA or water-insoluble PLA, drug dissolution was controlled by controlling the exposed surface area of the tablet.

Moreover, a group of researchers were able to fabricate a shell device that can contain different dosage forms in its core. This design can provide for the API in the core with taste masking, delayed release and/or improved bioavailability by avoiding the harsh environment in the stomach. HPC was used for the shell, and paracetamol (the model drug) was loaded into the core using four different formulations: solution, hydrogel, compressed tablet, and printlet. Drug release was different depending on; the core formulation, the polymer used in the shell and the infill density for the core printlet (Z. Zhang et al. 2023). Figure 2.6 illustrates some of the recent attempts to use FDM design flexibility to control drug release. In conclusion, FDM has an outstanding design flexibility that can be explored even further to control drug release and can provide great flexibility to pharmaceutical formulators in drug release control and other applications.

A

(Goyanes, Martinez, et al. 2015)

B

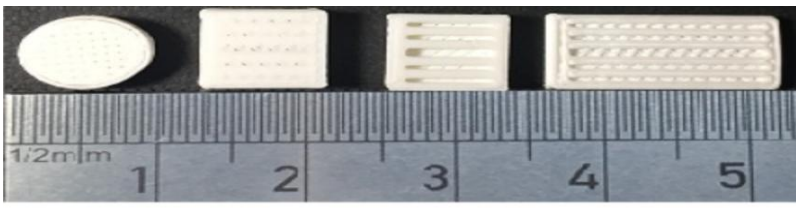

(E. Prasad et al. 2019)

C

(Isreb et al. 2019)

D

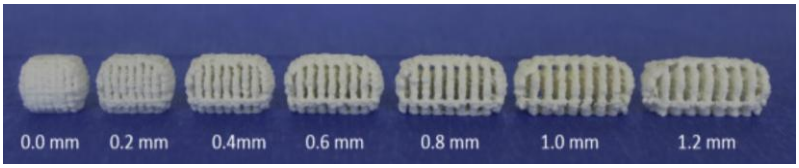

(Arafat, Wojsz, et al. 2018)

E

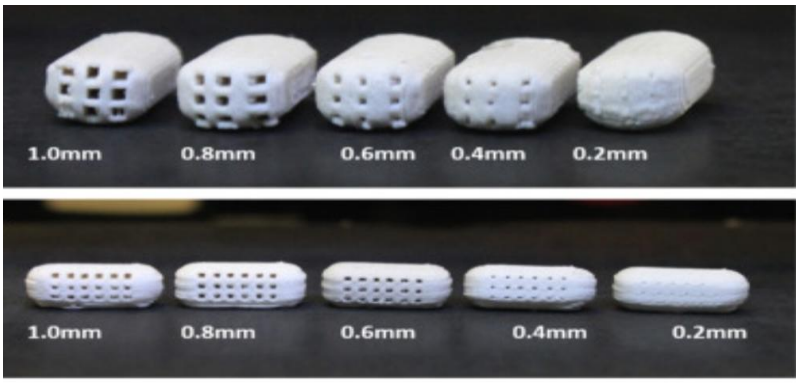

(Sadia, Arafat, et al. 2018)

F

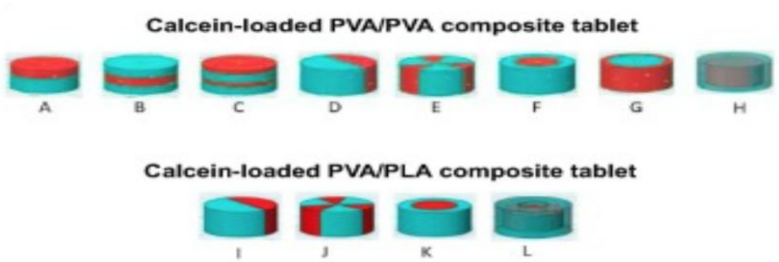

(Tagami et al. 2018)

Figure 2.6 The applications of FDM design flexibility to control drug release.

2.2.4 Extemporaneous Formulations:

In addition to the aforementioned advantage, FDM can reduce the equipment needed to manufacture different dosage forms or release profiles and pave the way for personalised medicine to become a reality. Personalised medication tailored to everyone's needs can enhance safety, efficacy, and patient compliance, as discussed in 1.5 Personalised Medicine. Nevertheless, the presence of a 3D printer in a pharmacy setting or hospital to produce personalised medication faces several barriers, one of which is the regulatory aspect of this practice. However, this technology can assist in the manufacturing of orphan medications aimed at treating rare diseases (Dumpa et al. 2021; Saydam et al. 2022). Due to the small number of patients affected by these conditions, there are limited incentives to produce treatments for them on a large scale, making the management of these diseases both inaccessible and costly.

Furthermore, FDM's design flexibility can improve compliance with paediatric dosage forms by printing them with shapes and figures that are appealing to children (Scoutaris, Ross, and Douroumis 2018; H. Wang, Dumpa, et al. 2020). Lastly, it has been demonstrated that printing mini tablets using FDM can provide a great solution to dose titration for paediatric patients. The printlets had better content uniformity and precise dosage than the traditional method of splitting adult-size tablets (Gorkem Buyukgoz et al. 2022).

2.3. Challenges That Face FDM

This section will discuss the main formulation barriers that stand in the way of the FDM, along with the attempts that have been made in the literature to address them. There are other process challenges, like lack of regulation, slow printing speed and safety (Nashed, Lam, and Nokhodchi 2021; Parulski et al. 2021) will not be discussed in this work.

2.3.1. Drug Load

Apart from 3D-printed devices designed to hold pre-prepared dosage forms, other 3D-printed dosage forms require the API to be incorporated directly into the printer's feed ink. There are three methods for incorporating API into the fed filament for FDM; impregnation of the drug into the filament or the printlet through diffusion by soaking in a solution of the API (Saviano et al. 2022; Verano Naranjo et al. 2021), hot melt extrusion (HME) (Tan, Maniruzzaman, and Nokhodchi 2018) and casting them in a rubber tube (Korte and Quodbach 2018). Although multiple attempts have been employed to improve drug loading by microwaves-assisted impregnation or soaking in a supercritical fluid (Saviano et al. 2022; Kukkonen, Ervasti, and Laitinen 2022; Rosales et al. 2021), HME is still considered to be the best method since a higher drug loading can be achieved, it avoids the use of an organic solvent, which may cause degradation and/or toxicity problems, and it is suitable for continuous manufacturing. However, drug loading in HME depends on the polymer and API used and the desired end product (Verstraete et al. 2018). If the extruded material is desired to be amorphous solid dispersion, the drug load is governed by the solubility of the API in the polymer (Aho et al. 2019). However, if the presence of the API in a crystalline form is acceptable, drug load is restricted by its effect on the mechanical properties of the filament and its printability (Than and Titapiwatanakun 2021).

Additionally, if the API is miscible with the polymer, a high drug load can affect the printability of the filament due plasticizing effect (Gottschalk et al. 2021). Therefore, drug loading was an area of interest for the research. Some of the most notable works were methacrylate polymers loaded with 50% theophylline (Pietrzak, Isreb, and Alhnan 2015) and thermoplastic polyurethane (TPU) filaments have been reported to achieve 60% metformin and theophylline drug load (Verstraete et al. 2018). Nonetheless, sometimes for certain APIs or certain diseases, a higher drug load may be needed (Than and Titapiwatanakun 2021). Therefore, drug load remains a limitation that needs to be tackled further.

Additionally, the loading efficiency may sometimes be as low as 70%, perhaps due to longer exposure to high temperatures (Sadia et al. 2016) or due to adhesion to the wall of the HM extruder (Borandeh et al. 2021; Q. Li et al. 2017; Boetker et al. 2016; Tabriz et al. 2021). However recently, it has been demonstrated that using fine particle

size PVA powder improves API adhesion and loading efficiency (Saviano et al. 2019). Moreover, the extrudability and printability of the filament improved with finer particle size.

As a result of low drug loading and low efficiency of some extruded formulations, the resulting printlet will be bound to have a high volume to deliver the required dose, rendering it hard to swallow especially in the case of polypills and floating tablets (Azad et al. 2020).

2.3.2. Printability of The Filament

During FDM, the printing head melts part of the filament. Mechanical gears push the molten polymer through the nozzle by using the unmolten filament as a piston. Therefore, for the filaments produced by HME to be suitable for FDM, they have to be stiff enough to prevent entanglement in the printer gears but not brittle and break due to the pressure imposed by the gears (Dumpa et al. 2021). The mechanical properties of the filament are not affected only by the polymer used but by all the formulation components. Miscible components will soften the filament while immiscible components will make them brittle (G.G. Pereira et al. 2020). Therefore, many publications aimed to find measurable parameters for the mechanical properties of the filament from the mechanical response curve such as Young's modulus (YM), deformation, breaking force and breaking distance to predict the printability of the filaments produced by HME and compare it to the commercially available filament. Figure 2.7 illustrates a typical stress-strain curve of filament under deformation and some of the parameters used to predict printability.

Young's modulus (YM) can be calculated from the slope of the linear part in the elastic region where deformation is reversible and Hooke's law can be applied, to the stress-strain curve. YM demonstrated the strong predictive power of the printability of the filament (Aho et al. 2019). Young modulus or stiffness constant is equal to the load imposed on the filament in one direction divided by the maximum deformation which results from this load before breakage. A high-value YM indicates that the filament can withstand great load with minimum deformation before it breaks. However, a low value of this modulus reflects that the filament is either brittle and breaks with minimum force or so soft that it deforms greatly with minimum force. In either of these cases, the

filaments are deemed unsuitable for printing. Thereby, the printability of the filament can be forecasted using the value of YM (Tan, Maniruzzaman, and Nokhodchi 2020; Borujeni et al. 2020; H. Wang, Dumpa, et al. 2020). Researchers tested filament extruded from HPC and found that filament with a stiffness constant (YM) of less than 40 g/mm^3 cannot be printed (H. Wang, Dumpa, et al. 2020; Z. Zhang et al. 2023).

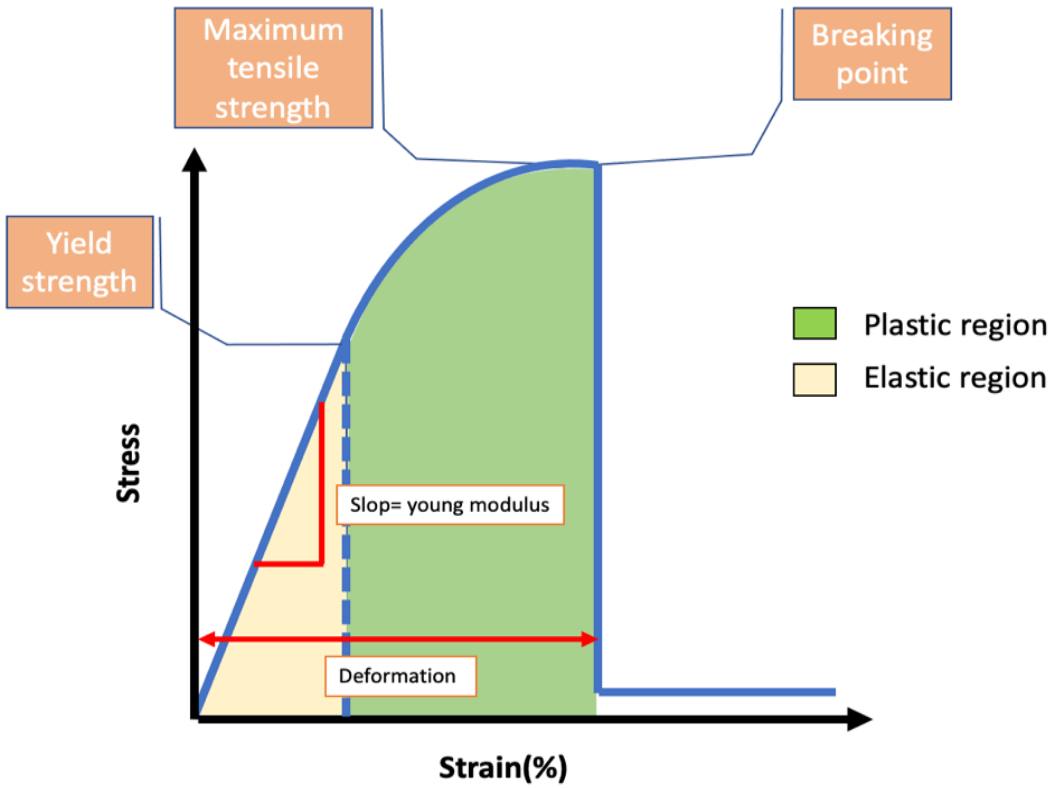

Figure 2.7 Parameter that can be measured from the stress-strain curve to predict the printability of the filament. (constructed by the author)

On the other hand, the test method to measure deformation is still under investigation. Therefore, in a study with different combinations of HPMC, EC with either HPC EF, HPC LF, Soluplus or Eudragit L100 was used to form a controlled release paracetamol printlet by Zhang et. al (J. Zhang et al. 2017). The author investigated the filament printability before printing using the three-point bending test and he deducted that for the filament to be printable it must withstand the stress of more than 2900 g/mm^2 and deformation of more than 1 mm. his method was carried out by multiple researchers as standard to test for filament printability (Repka-Zhang method) (Dumpa et al. 2021). However, when a group of researchers prepared and printed loratadine immediate-release tablets, the 3-point bending test was not a precise predictor of the printability

of the filament prepared with polyethylene oxide or hydroxypropyl cellulose (Omari et al. 2022).

Furthermore, the mechanical properties of filaments are direction-dependent since the chains of the polymer are rearranging in the direction of extrusion during HME. Therefore, the mechanical property must be tested in the cross and longitudinal direction (Korte and Quodbach 2018). Hence, the tensile strength test was used to predict the printability of PEG filaments, and it has been revealed that low molecular weight PEG produces a more brittle filament that breaks at low tensile force (Isreb et al. 2019). Additionally, texture testing with axial compression was used to measure the flexibility profile of multiple filaments, and afterwards, the printability of those filaments was tested using an FDM printer (Nasereddin et al. 2018). Subsequently, comparison of the flexibility profiles with those of commercially available filaments revealed that all printable filaments exhibited a mean statistical correlation above 0.5, while all unprintable filaments showed a mean correlation below 0.5. Additionally, the author was able to categorize the filament using principal component analysis of three components into three clusters: printable, can be printed by adding a plasticiser and unprintable cluster.

Moreover, a group of researchers used indomethacin as a model drug to print 32 filaments and compared three different methods to test the printability of the filament: the three-point brittleness test, resistant test and stiffness test. Then, it was concluded that the toughness of 80 g/mm^2 measured with stiffness test has more predictive power than the other two (Xu et al. 2020). However, because there are different models of FDM printers, different test conditions and different formulations, it is hard to standardize a test method to predict the printability of the filament (Dumpa et al. 2021; Gottschalk et al. 2021). Lastly, micro and nanoindentation of the filament were also used to predict the mechanical property and printability of filaments, where the depth of a sharp nano-indenter was recorded as a function of the force applied (Gioumouxouzis et al. 2018). A group of researchers used this method to study the effect of drug load on printability along with the 3-point bend test and the tensile test. All three methods showed that a high drug load of 40% had better mechanical properties and, as a result, predicted the printability (Fina et al. 2020). Figure 2.8 A illustrates some of these measurement techniques.

Nevertheless, a more challenging task than predicting the printability of filaments is the production of printable filaments with HME. HME for years has been developed to

produce brittle filaments that can be easily broken down and compressed into tablets. Hence, the main challenge is to produce filaments with mechanical properties that can result in successful printing. Therefore, researchers attempted to improve the mechanical properties of the filament by adjusting the formulation, such as adding plasticizers to brittle filament (Z. Zhang et al. 2023; Yang et al. 2021) or adding another polymer to enhance stiffness (Vo et al. 2020; Shi et al. 2021; Yang et al. 2021). Additionally, the effect of filler, high melting API and high strength polymer on the mechanical properties of an over-plasticized polymer was investigated. It was found that all three strategies can adjust printability (Yang et al. 2021). This reflects that mechanical properties and printability are affected by immense variables, and it is not as simple as adding a plasticiser to the formulation.

Therefore, others tried improving the feeding method without adjusting the formulation. One such attempt was to connect the drug-loaded filament to the end of commercially available PLA, which is known for its printability (Kempin et al. 2018). However, this practice can provide a solution for small batches only. Similarly, another research group (Gottschalk et al., 2021) tested a novel feeding method using three different polymers -Kollidon VA64, Soluplus, and Eudragit EPO- known for their brittleness. The method involved extending the feeding path and attaching a segment of filament with favorable mechanical properties to the end of the brittle filament intended for printing. Although the filaments were loaded with 40% Ketoconazole, which resulted in increased brittleness, the new feeding approach successfully enabled their use in 3D printing (Gottschalk et al. 2021). However, this method can prevent filament breakage resulting from bending but not from an axial force. Moreover, the extrusion of a filament within a filament was tested with two different polymers (Ai et al. 2021). The mechanical properties of the resulting filaments were independent of the polymer used for the core of the filament. This can be used to improve the mechanical properties of the core filament by using a polymer known for its acceptable mechanical properties in the outer layer of the filament. However, to achieve this, both polymers' layers must have the same viscosity of the melt and shear thinning at the printing temperature to be extruded simultaneously; otherwise, the printer nozzle will be clogged. Figure 2.8 B illustrates some of these attempts to improve the printability of the filament that is otherwise considered unprintable.

Finally, the diameter of the filament must be in a range that suits the commercially available printers' heads (1.7 mm- 2.8 mm). The diameter of the filament also must be

uniform throughout the length of the filament, any inconsistency can result in great weight variation or, worse, failure to print (Lamichhane et al. 2019). Extrusion temperature, screw speed and Feeding rate in HME can change the diameter of the filament (Korte and Quodbach 2018; Than and Titapiwatanakun 2021). Lubricants are used in HME when the diameter of the extruded filament is not constant to decrease the fraction which results in the variation (G.G. Pereira et al. 2020). Moreover, extrusion swell (die swell) is an occurrence that usually accompanies the extrusion of a polymer, but it can be controlled by a large length-to-diameter ratio die, installing a calibrator or pulling of the filaments upon exiting the die (Aho et al. 2019). Moreover, the uniformity of the filament diameter can be improved by adding a melt pump before the die or a conveyor belt after it (Parulski et al. 2021). In conclusion, the mechanical properties and the diameter of the filaments are very critical properties for successful printing and need to be controlled and monitored closely to negate any problem that can cause failure in the printing process.

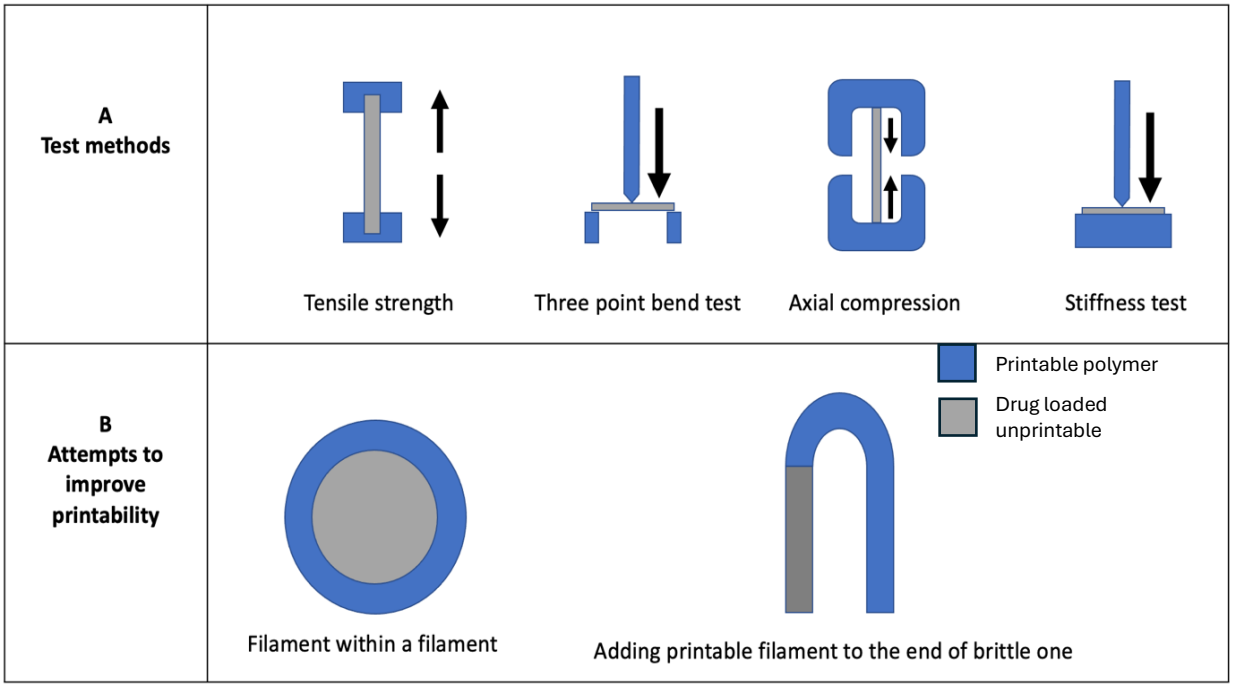

Figure 2.8 Illustrates some of the test methods used to predict printability (A), and the feeding method used to improve printability (B). (constructed by the author)

2.3.3. Rheological Properties of The Melt

Polymers are viscoelastic materials that have both viscous liquid-like properties and elastic solid-like properties, depending on the time and scale of applied deformation (G.G. Pereira et al. 2020; Kalaskar and Serra 2017). Viscoelasticity is best expressed by the dynamic modulus, which consists of two parts: the storage modulus (elasticity) and the loss modulus (viscosity). Having a high storage elasticity, the polymer will be hard to extrude and clog the printing head and having a very low loss modulus, the polymer will flow like liquid, and the printlet will not hold shape (Azad et al. 2020). Hence, understanding the properties of the polymer (or polymer mix) is important to determine the process and formulation parameters (Kalaskar and Serra 2017; Azad et al. 2020; Elbadawi 2019).

Therefore, multiple rheological properties can predict the behaviours of polymers during extrusion and printing. Viscosity is the most important rheological property because it can predict the process temperature and torque required for the extrusion and printing of a polymer mix(Azad et al. 2020). However, measuring the rotational steady state shear viscosity for a polymer with high viscosity usually led to sample rupture and flow disturbance. As a result, to avoid wasting samples when using a capillary rheometer, researchers have been using an oscillating shear rheometer and applying the Cox-Merz rule (Aho et al. 2019). Nevertheless, the empirical relation between the oscillating shear viscosity and steady rotational share viscosity is negated at high drug content. Additionally, the Cox-Merz can only predict the viscosity up to 700 second^{-1}, while the shear during printing through the narrow nozzle can reach thousands (Boetker et al. 2016). Additionally, FDM is based on high processing temperatures that push most filaments within their shear-thinning region, making the shear rate a critical parameter in determining viscosity. Nevertheless, it was found that the viscosity of the melt should be between 14,000 Pa.S and 1000 Pa.S at 0.1 Sec^{-1} angular frequency to ensure consistent flowability and prevent nozzle blockage during HME (Verstraete et al. 2018; Than and Titapiwatanakun 2021). However, it has been reported that a viscosity lower than 8000 Pa.S is needed (Than and Titapiwatanakun 2021; Isreb et al. 2019) for optimal filament printing. In contrast, others have reported successful printing for PLA and biobased poly (butylene) succinate in a viscosity range of 1000 Pa.S to 100 Pa.S at 100 Hz frequency (Qahtani et al. 2019). Hence, there is

no real defined range for printing viscosity. In addition, viscosity not merely affects the printing process but can also affect the release profile of the resulting printlet (Azad et al. 2020), as a release from a highly viscous polymer is slower than from a less viscous one.

Moreover, the viscosity of the melt depends on the printing temperature, printing speed and the nature of the filament (polymer, excipient, API and API solid-state) used. Therefore, viscosity can be adjusted by mixing with another polymer. This was reported in a recent publication (Boetker et al. 2016) where the researchers added 20% HPMC to PLA filament; the viscosity of the mixture was higher than pure PLA. Moreover, others (Than and Titapiwatanakun 2021) were able to improve the melt viscosity of Kollidon and Eudragit EPO by adding HPC. Furthermore, PEG (Alhijjaj, Belton, and Qi 2016) was used to lower the melt viscosity of Eudragit and Soluplus. Another approach was to adjust viscosity by adding thermostable filler (Sadia et al. 2016) such as tricalcium phosphate, which was added to improve the viscosity of Eudragit EPO. Moreover, since viscosity has an inverse relationship with the printing temperature (Yang et al. 2018; Pietrzak, Isreb, and Alhnan 2015; Elbadawi 2019), adding a plasticiser can decrease viscosity and/or shear thinning (Elbadawi 2019; Aho et al. 2019). Nevertheless, it can lead to soft unprintable filament, as mentioned in the previous section. Lastly, drug loading and the crystal status of API in the polymer matrix can influence the viscosity of the melt (Aho et al. 2019). In conclusion, although viscosity is a critical rheological parameter, it is hard to adjust, its value is difficult to define for FDM, and there is no optimal method to measure it.

On the other hand, the melting index (MI), which is the ability of the melted polymer to flow, can provide a piece of important information on the printability of the filament. Low MI reflects the hardness by which the polymer will flow from the nozzle, which may lead to nozzle blockage. However, a very high MI means that the polymer will flow as a droplet from the nozzle, which will also lead to print failure (Genina et al. 2016). It was found that 1 g/min. flow is required for the successful printing of many polymers (Caillleaux et al. 2020). However, MI does not reflect the effect of the shear rate on the viscosity of the melt (Aho et al. 2019). Lastly, thixotropicity is the measurement of the time required for a polymer to retain its viscosity after a shear-thinning, which makes it an important property to study in FDM (Azad et al. 2020).

In conclusion, multiple rheological properties need to be studied to select the most appropriate formulation for successful printing. Each of these properties gives partial

information on the rheological behaviour of the polymer during extrusion and printing. However, studying these behaviours of a polymer melt can aid in predicting the printability, the resolution of the printlet and drug release from the printlet.

2.3.4. High Processing Temperature

Although, the high process temperature can be considered an advantage with FDM since it prevents microbial contamination, improves polymer-drug interaction and negates the need for solvent, which reduces processing time and cost (Melocchi et al. 2021). Nevertheless, high temperature is considered the most important limitation in FDM because it has limited this technology to thermostable APIs. It was also noted that the temperature needed for printing is higher than the extrusion temperature. This was rationalized by the brief heating time in the printing head compared to the longer heating time in the extruder and the narrow diameter nozzle of the printer compared to the extruder, which requires a further decrease in viscosity (Oladeji et al. 2022). A higher temperature is needed during printing to reach the required viscosity of the polymer to be printable. Moreover, the sheer force that is applied during extrusion can decrease the required temperature to extrude (Than and Titapiwatanakun 2021).
Therefore, to lower the processing temperature, the glass transitional temperature (Tg) of the polymer must be lowered since extrusion is usually carried 20-40° C above its Tg (Nashed, Lam, and Nokhodchi 2021). This can be done using plasticisers miscible with the main polymer since they will increase the intermolecular space between the polymer chains, increasing the freedom of motion and reducing the temperature needed to soften the polymer. Different plasticisers have been reported in the literature, such as triethyl citrate (TEC) (Sadia, Arafat, et al. 2018; Arafat, Qinna, et al. 2018), PEG (Isreb et al. 2019), Tween 80 (Alhijjaj, Belton, and Qi 2016), Kolliphor TPGS (Ilyés et al. 2019), etc. However, excessive use of a plasticiser may lead to a soft unprintable filament and affect the stability of solid dispersion due to increased freedom of motion (Gottschalk et al. 2021). In addition, decreasing the Tg of the polymer may lead to the printlet being deliquescent after printing, affecting its integrity. As a result, researchers have tried using water as a temporary plasticiser (B.C. Pereira et al. 2019) , decreasing the processing temperature of PVA from 200° C (Goyanes, Kobayashi, et al. 2016) to 150° C. Nonetheless, this method adds an extra drying step

that will increase the processing time and is only suitable for certain polymers. On the other hand, it was found that using a polymer in which the API is miscible can decrease the processing temperature and act as a plasticiser (Y. Li et al. 2014). Hence, the acid-base super solubilisation technique was used to improve the miscibility of haloperidol with polymer Kollidon® VA64 (Nirali G. Patel and Serajuddin 2023) or a polymer mix of Kollidon® VA64 and HPMC (Nirali G Patel and Serajuddin 2021), by adding a weak acid (malic or glutaric acid, respectively) the miscibility of haloperidol with polymers increases which in turn led to a decrease in the required extrusion and printing temperature. This improvement in miscibility also improved the printability of Kollidon filament, drug load and drug release.

Nevertheless, the most promising attempts to lower printing temperature were using polymers or polymer mix with low (Tg). One such attempt was in 2016, where a group of researchers (Okwuosa et al. 2016) used two APIs (theophylline and dipyridamole) to print an immediate-release tablet using PVP as the polymer, TEC as a plasticiser and talc powder as a lubricant. The temperature needed to print was 110° C, which was enough to prevent any thermal degradation of the ingredient. PVP is a hygroscopic material, and it was found, during differential scanning colourimetry (DSC) analysis, that the water content reduces the Tg of the polymer acting as a plasticiser, as mentioned previously.

In addition, the two APIs (theophylline and dipyridamole) interacted with the polymer, which also resulted in lowering the Tg of PVP. Additionally, polycaprolactone (PCL) (Alhijjaj et al. 2019) was reported to be printable at 70° C. Nevertheless, printing at this temperature was only possible at a low printing speed (30 mm/s), and the resolution of the film produced was not adequate. Therefore, acetylsalicylic acid (ASA) incorporated filament was printed at a higher temperature (100°-120° C). Same result with PCL was documented by Aho et al. (Aho et al. 2019), where PCL was loaded with indomethacin and printed at 100° C into a disk printlet. Moreover, Kollidon® VA64 (PVP+VA) alone or in combination with Kollidon® 12PF (Kollamaram et al. 2018) was extruded with Ramipril or 4-aminosalicylic acid (4-ASA) to produce filaments that can be printed at a temperature as low as 90° C, which prevented the thermal degradation of these APIs. Kollidon® 12PF could not be used alone because the resulting filaments were so brittle. In this study, two types of plasticisers were used: PEG 1500 and mannitol.

Lastly, researchers (Kempin et al. 2018) were able to print used pantoprazole, which is a thermolabile drug, as an immediate-release tablet using five different polymers: PEG 6000, PEG 20000, PVP K12, Kollidon® VA64 (PVP+VA) and poloxamer 407. However, the lowest printing temperature (54° C) was achieved using PEG 6000.
On the other hand, the possibility (Goyanes et al. 2019) of one-step printing by an innovative single-screw direct powder printer was demonstrated recently. The printlet produced of itraconazole using different grades of HPC (UL, SSL, SL and L) was printed under a printing temperature of 170 ° C, compared to previous work with HPC where PEG was used as plasticiser and the printing temperature was 180 °C (Melocchi et al. 2016). The scope of this work was not to improve processing temperature, but we can see how this new design can bridge the gap between extrusion temperature and printing temperature. Finally, it must be mentioned that FDM can be used to print a structure that can be impregnated with API later, avoiding the thermolabile drug's degradation (Melocchi, Uboldi, Maroni, et al. 2020). However, this adds an impregnation step, which will increase the processing time, and the drug load is mostly inefficient.

2.3.5. Resolution of The Print

One of FDM's major advantages is its ability to produce complex designs that conventional compression tabletting cannot. However, the printing resolution is considered a significant limitation, especially when the design details have a functional role (Melocchi, Uboldi, Maroni, et al. 2020). In addition, the laminar finish of FDM can affect patient compliance, so improving print resolution is a major challenge with FDM. Nevertheless, the resolution of the printlet can be improved by decreasing the layer height and increasing the number of layers to a certain extent (Pietrzak, Isreb, and Alhnan 2015). However, this will lead to an increase in the printing time and may lead to a problem with fast layer cooling (Melocchi et al. 2016). Furthermore, decreasing the orifice size of the printing head can aid in improving resolution at the expense of increasing the printing time and risk of clogging the nozzle. Therefore, the resolution of the printlet fabricated through FDM resolution can be hundreds of micrometres (Azad et al. 2020)in size. However, for details smaller than hundreds of micrometres, resolution is considered poor; this has been addressed by adding an etching step after

the fabrication of microneedles (Luzuriaga et al. 2018). The resulting microneedles, which were produced from PLA, ranged in length from 200 mm to 2.5 mm and had adequate mechanical strength.

2.3.6. Limited Number of Available Polymers

In order for a polymer to be used in FDM, it must be thermoplastic, which means it will soften when subjected to heat above its Tg. In addition, to incorporate FDM to print oral dosage form, the polymer must be Non-toxic and biocompatible. Furthermore, as mentioned earlier, the rheological properties of the polymer melt should be suited for FDM.

All these restrictions add to the scarcity of a suitable polymer. Therefore, the list of polymers used for FDM in pharmaceutical formulation is limited (Aho et al. 2019; Yang et al. 2018). EC, HPC, HPMC, Eudragit®, PCL, PLA, PVA and Soluplus® are among the most researched polymers in the FDM (Azad et al. 2020). Therefore, Many researchers have employed polymer mixing to enhance filament properties (Borujeni et al. 2020; Alhijjaj, Belton, and Qi 2016; J. Zhang et al. 2017; Boetker et al. 2016; Tan, Maniruzzaman, and Nokhodchi 2020; Reddy Dumpa, Bandari, and A Repka 2020). Moreover, other researchers have tried to mitigate this challenge by introducing new materials to 3DP, such as plant protein (Rowat, Legge, and Moresoli 2021; Chaunier et al. 2018) and lipid-based material (Vithani et al. 2019). Table 2.3 presents several documented attempts in the literature utilising various polymer formulations to print oral dosage forms, along with their extrusion and printing temperatures.

Table 2.3 Polymer API formulation for FDM is reported in the literature. NM = polymers printed separately and not a mixture; M = polymers mixed.

Polymer used	API used	Extrusion temperature	Printing temperature	Reference
PEG 6K	Pantoprazole	48	54	Kempin 2018a (Kempin et al. 2018)
PEG 20000		50	60	
Poloxamer 407		43	60	
PVP K12		51	79	

Kollidon® VA64(PVP+VA)		56	85	
Kollidon® VA64(PVP+VA) + Kollidon® 12PF	Ramipril or 4-ASA	70	90	Kollamaram 2018 (Kollamaram et al. 2018)
Poly(E-caprolactone) (PCL)	Indomethacin	100	100	Aho 2019 (Aho et al. 2019)
PCL	Dexamethasone	90	85,105, 110	Santos 2023 (dos Santos et al. 2023)
PCL	ASA	100	100-120	Alhijjaj 2019 (Alhijjaj et al. 2019)
Poly lactic-co-glycolic acid (PLGA)	mAb	90	105	Carlier 2021 (Carlier et al. 2021)
Polyvinyl pyrrolidone (PVP)	Theophylline or Dipyridamole	90	110	Okwuosa 2016 (Okwuosa et al. 2016)
Kollidon® VA64(PVP+VA), malic acid	Haloperidol	100, 120	100, 125	Patel 2023 (Nirali G. Patel and Serajuddin 2023)
Kollidon®VA64(PVP+VA), HPMC, glutaric acid.	Haloperidol	115	120	Patel 2021 (Nirali G Patel and Serajuddin 2021)

Eudragit E PO	5-aminosalicylic acid–5-ASA, captopril, prednisolone or theophylline	100	135	Sadia 2016 (Sadia et al. 2016)
Eudragit E PO	Warfarin	100	135	Arafat 2018a (Arafat, Qinna, et al. 2018)
Eudragit E PO	Hydrochlorothiazide	100	135	Sadia 2018 (Sadia, Arafat, et al. 2018)
PEO 200K, 300K, 600K	Theophylline	65,70, 80	105, 110, 145	Isreb 2019 (Isreb et al. 2019)
Kollidon® VA64 (PVP+VA), PCL (M)	Caffeine	140	150	Fuenmayor 2018 (Fuenmayor et al. 2018)
PEG +PEO, Eudragit® E PO or Soluplus®. (M)	Felodipine	100, 120, 130	150	Alhijjaj 2016 (Alhijjaj, Belton, and Qi 2016)
Soluplus®, Kollidon® VA64 and Eudragit® E PO	Ketoconazole	180	140-160	Gottschalk 2021 (Gottschalk et al. 2021)
EVA*	Indomethacin	105	165	Genina 2016 (Genina et al. 2016)

HPMCAS	Indomethacin	140	165	Scoutaris 2018 (Scoutaris, Ross, and Douroumis 2018)
Polycaprolactone, PEG 200, 4000 and 8000 g/mol	Ciprofloxacin	-	170	Elbadawi 2019 (Elbadawi 2019)
HPC UL, SSl, SL or L	Itraconazole	-	170	Goyanes 2019 (Goyanes et al. 2019)
HPMCAS	Hydrochlorothiazide	165	170	Oladeji 2022 (Oladeji et al. 2022)
HPC, PEO	Paracetamol	110, 120	170	Fina 2020 (Fina et al. 2020)
Eudragit RS, RL, E and HPC	Theophylline	130	140-170	Pietrzak 2015(Pietrzak, Isreb, and Alhnan 2015)
Ethylcellulose	Ibuprofen	120	178	Yang 2018 (Yang et al. 2018)
EC, Eudragit, Kollidon, PVA, PEG 6K, Soluplus (M)	Ibuprofen	100	178	Shi 2021(Shi et al. 2021)
HPC	Acetaminophen	165	180	Melocchi 2015

				(Melocchi et al. 2015)
HPMC 15 LV	Diltiazem HCl and Diazepam	135	180	Kadry 2018 (Kadry et al. 2018)
Eudragit RL	Theophylline	140-180	180	Korte and Quodbach 2018 (Korte and Quodbach 2018)
Thermoplastic polyurethanes (TPU)	Theophylline or Metformin	150	180	Verstraete 2018 (Verstraete et al. 2018)
EC, HPC (M)	Carbamazepine	105-125	187	Borujeni 2020 (Borujeni et al. 2020)
PEO, PVA (NM)	Ibuprofen	60, 90	165,190	Ehtezaz 2018 (Ehtezazi et al. 2018)
HPC-SSL	Theophylline	120	190	Arafat 2018b (Arafat, Wojsz, et al. 2018)
PLA, PVA (NM)	Calcian	210	190	Tagami 2018 (Tagami et al. 2018)
HPMCAS LG, MG, HG	Paracetamol	110	190	Goyanes 2017 (Goyanes et al. 2017)

HPC, Eudragit RL PO, PEG(M)	Theophylline	110	195	Tan 2020 (Tan, Maniruzzaman, and Nokhodchi 2020)
Polyvinyl alcohol (PVA)	Glipizide	180	195	Li 2017 (Q. Li et al. 2017)
PVA	Ciprofloxacin	160-175	195	Saviano 2019 (Saviano et al. 2019)
PLA, HPMC (Metolose®) (M)	Nitrofurantoin	180	200	Boetker 2016 (Boetker et al. 2016)
HPC, Kollidon or Eudragit EPO (M)	Theophylline	135-160	200	Than 2021 (Than and Titapiwatanakun 2021)
PVA	Metformin	170	200	Nukala 2019 (Nukala et al. 2019)
HPMC E5, EC N14 (M)	Paracetamol	180	200	Zhang 2017 (J. Zhang et al. 2017)
HPMC E5, HPC EF (M)		180	200	
HPMC E5, HPC LF (M)		180	200	
HPMC E5, Soluplus (M)		180	200	

HPMC E5, Eudragit L100 (M)		180	200	
EC N14, Eudragit L100 (M)		160	200	
PVA	Paracetamol or caffeine	180	200	Goyanes 2016 (Goyanes, Kobayashi, et al. 2016)
Kollicoat IR (PVALcohole + PEG)	Aripiprazole	150	210	Jamroz 2017 (Jamróz et al. 2017)
Kollidon® VA64(PVP+VA), Kollicoat® IR, HPMC, HPMCAS	Haloperidol	150	210	Solanki 2018 (Solanki et al. 2018)
PEO N80, HPC EF(NM)	Loratadine	110	220	Omari 2022 (Omari et al. 2022)
PEO, Kollicot IR	Furosemide	65, 160	160, 180	Melocchi 2016 (Melocchi et al. 2016)
Eudragit L, HPMCAS		160, 180	160, 200	
EC, Eudragit RL		160, 120	200, 160	
HPC, HPMC, PVAlcohole, Soluplus®		160, 190, 120	200, 225, 200	
PVP, methacrylic acid	Budesonide, theophylline, and diclofenac	90,125	110,185	Okwuosa 2017 (Okwuosa et al. 2017)

2.4. Conclusion

This Chapter investigates the very promising 3D printing technique (FDM). This method has gained considerable interest in recent years due to its simple and affordable equipment, its appropriateness for pharmaceutical polymers, its unique capacity to create hollow structures, and the favourable mechanical properties of its final product. Consequently, in recent years, researchers have sought to investigate the use of FDM to produce polypills with layers containing different APIs, fabricate a gastroretentive drug delivery system, control drug release, and discuss the potential for producing personalised medication. However, FDM still faces several formulation challenges before becoming an established manufacturing technique in the pharmaceutical industry. Some of these challenges include dependence on high process temperatures, limited drug loading and loading efficiency, difficulty in producing filaments with suitable mechanical properties, challenges in defining the process viscosity range, the limited variety of suitable polymers, and resolution that is less than ideal.

Many researchers have applied different techniques to solve these challenges. From adding excipients like plasticisers to using polymer mix or simply reducing the particle size. However, these challenges are interrelated and attempting to solve one can introduce a problem with the others which complicates the process further. Hence, further study into these challenges is needed.

Chapter 3 : Methodology

3.1 Materials

Theophylline anhydrous, PEG 4000, Triethyl citrate (TEC), Talc, Polyvinylpyrrolidone 40,000 M.W (PVP 40K), Polyethylene oxide 200,000 g/mole (PEO), and polyethylene glycol 6000 g/mole (PEG 6000), paracetamol, ibuprofen, caffeine and ethyl cellulose were purchased from Sigma Aldrich (Gillingham, UK). Eudragit RL PO and Eudragit EPO were donated by Evonik Industries (Darmstadt, Germany). Scotch blue painter's tape 50 mm was supplied by 3 M (Bracknell, UK).
Additionally, propranolol (PR) was purchased from Thermo Fisher Scientific (Waltham, MA, USA). While enalapril maleate (EM) and hydrochlorothiazide were ordered from Molekula Ltd (Darlington, UK).

3.2 Methods

3.2.1 HCP survey

The survey consisted of four close-ended questions and one open-ended question. The first two questions were targeted to recognise if the issue of polypharmacy did exist in their practice and whether a fixed-dose combination is used to solve this issue. The third question was open-ended. It was designed to explore what refrains HCPs from prescribing polypills in those patients with polypharmacy. Lastly, the last two questions were to evaluate the importance of personalised medication in general and personalised polypill specifically. Table 3.1 lists the survey question and their response format.

Table 3.1The survey questions and their response format.

Survey questions	Response Format
What is the approximate percentage of your patients who are on more than one medication?	Five choices with 20% increment
How often do you prescribe fixed dose combinations (a pill that contain more than one medication) to these patients?	A scale from 1= never to 5= very often
In those patients with multiple mediation regimens, would you sometimes prefer **not to** prescribe fixed dose combinations? And why?	Open-ended question
How important is personalised medication (medication that is designed to meet individual needs) to your patients?	A scale from 1=not important to 5= very important
Would a personalised polypill be useful to your patients?	Three choices: Yes, No and maybe

3.2.2 Filament Preparation

To incorporate the active pharmaceutical component into the thermoplastic polymer and prepare the feedstock filament required for FDM a single screw extruder was used. The material was mixed using a mortar and pestle for 10-15 minutes and then extruded using a single screw extruder (Noztec Pro hot melt extruder, Noztec, Shoreham-by-Sea, UK) with nozzle diameter 1.75 mm and screw speed 15 rpm. A

Figure 3.1 Filament preparation steps from mixing to extrusion and printing. (constructed by the author)

rubber tube was used to guide the extruded filament. The bulling effect of gravity helped to ensure a consistent pull on the filament and, as a result, a consistent diameter. The filaments were then kept in a desiccator containing silica until printing. Figure 3.1 illustrates the steps taken for filament preparation.

3.2.3 Filament Tensile Strength

To predict the printability of the extruded filament and to test the effect of the formulation on the printability, tensile strength test was performed. The filaments' mechanical strength was tested using (a universal uniaxial testing machine Zwick/Roell Z010). The diameter of the filament was measured using Clarke 4500360 Cm145 Digital Vernier Calliper. The filaments were cut into 50 mm in length and placed in the anti-slip fixture. The pulling deformation rate was 20 mm/minute, and the data was collected every 50 milliseconds. All measurements were done in triplicate. Figure 3.2 demonstrates the specification of the tensile test for the filament and the instrument used.

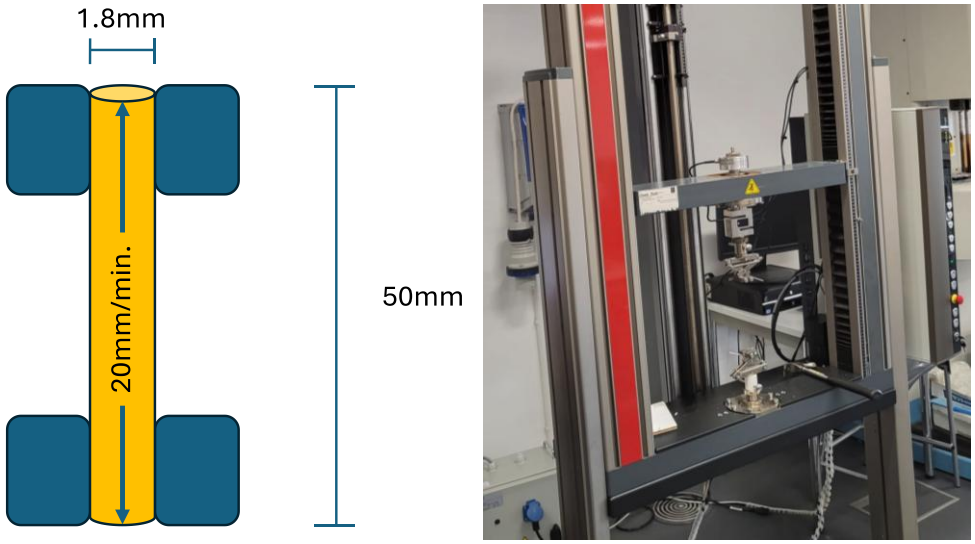

Figure 3.2 Tensile strength test for filaments. (constructed by the author)

3.2.4 Design and Printing

The FlexiPill was designed using Autodesk® Tinkercad™, a free online 3D modelling tool (Autodesk, CA, USA), and exported as an STL file for use with the printer's slicing software. The Flexipill disc dimensions (all four units) are 5mm in height and 7.5mm in radius joint size 2 mm, while the second design consists of stacked frustums. Each frustum was 5 mm in height, 3.75 mm base radius and 2.5 mm top radius. However, the bottom frustum had a closed base to enclose empty chamber in the middle, and the other had an open base to the space in the middle to facilitate joining of the units. Figure 3.3 present the two FlexiPill designs.

Then, the design was printed with a MakerBot replicator + (Makerbot Industries, LLC., USA) with a 0.4 mm nozzle, 90 mm/s print speed and 0.2 mm layer hight. A heated building platform system from (IDE Vesterling, Germany) was fixed to the printer. The temperature of the heated platform was set between 40-60ºC, to further enhance the adhesion of the printed tablet and for easy detachment from the building platform, blue scotch tape was laid down on top of the building platform.

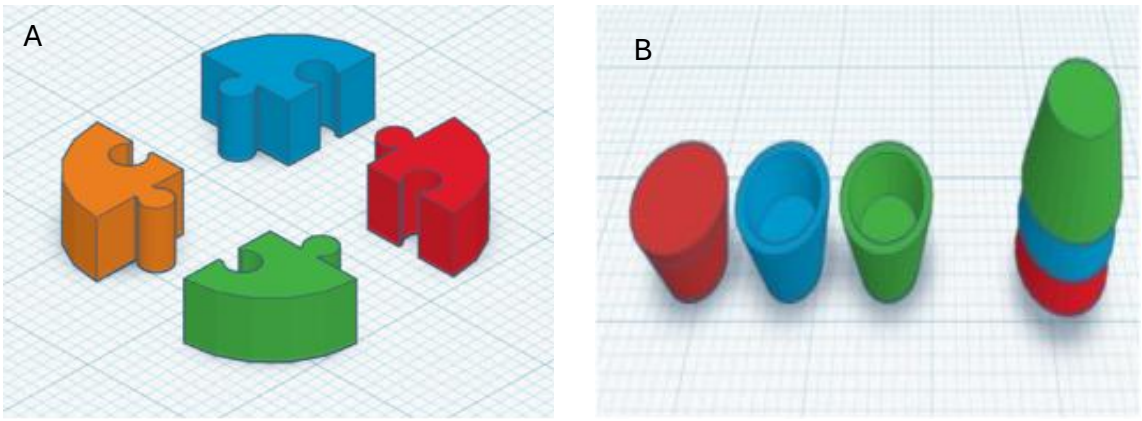

Figure 3.3 The two design iteration of the FlexiPill, (A) disc design and (B) frustum design.

3.2.5 Rheological Properties

Complex viscosity was measured using a Kinexus rheometer from Malvern (Malvern Instruments, Worcestershire, UK) with 25mm/ 65mm upper/lower smooth parallel plates. The formulations were pressed to 25 mm disc after extrusion and 1mm thickness. In Chapter Four, the formulations were assessed at the extrusion and printing temperature using a temperature sweep from 150º-50º C with a cooling rate of 5ºC/minute and a normal force of 0.1 N and a gap between 0.1-5 mm. The frequency

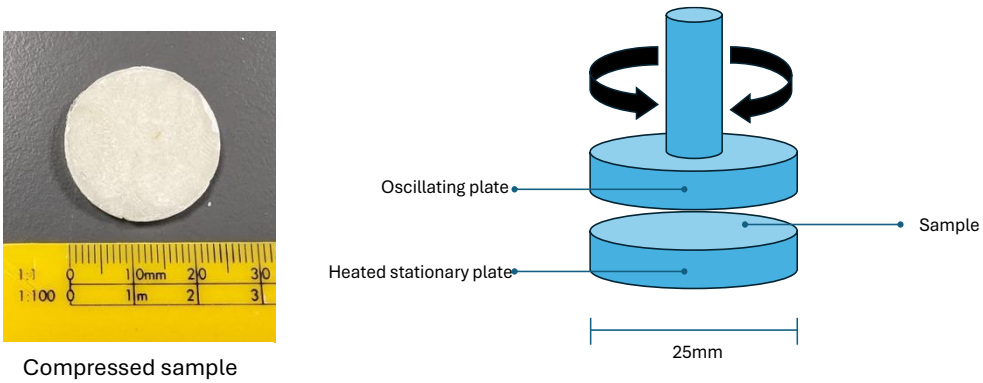

Figure 3.4 Rheological properties method for measurements. (constructed by the author)

and the shear strain were set at 1 Hz and 1%, respectively, to keep the measurement within the viscoelastic region. The samples were loaded at 100°C with an initial gap of 1 mm discs. A frequency sweep was performed from 100 to 0.1 Hz and 1% shear strain for chapters five and six. The temperature was set to 150°C during screening, while the printing temperature for each formulation was used to evaluate the viscosity at the print. Figure 3.4 illustrates the rheological testing method.

3.2.6 Scanning Electron Microscope

A scanning electron microscope (SEM) (Hitachi S300N electron microscope, Hitachi, UK) was used to examine the surface morphology of tablets and the filaments and the printed layer uniformity. The samples were placed on aluminium stubs 25 mm in diameter with carbon double adhesive. Then, it was coated with a gold-palladium coat in an argon atmosphere at about 10 pascals for 1 minute, to improve conductivity and image resolution. The scanning electron microscope was set to 20 KV.

3.2.7 Fourier Transform Infrared

Fourier transform infrared (FT-IR) analysis was performed post-printing to evaluate potential interactions between the active pharmaceutical ingredients (APIs) and the polymeric matrices, as well as to detect any polymorphic transformations.
Spectrum BX FTIR Spectrophotometer (Perkin–Elmer, Cambridge, UK) was used to analyse the formulations' Infrared spectra. The frequency range was 4000–800 cm^{-1} at 2.0 cm^{-1} resolution, and 32 scans were performed. Happ-Genzel was used as an apodization function.

3.2.8 Thermal Analysis

Thermal analysis was performed using differential scanning calorimetry (DSC) with (TA instruments Q1000) and Alodine hermetic pans. Heat/cool/heat circle was conducted at a 5° C/min heating rate and a 10° C/min cooling rate. The starting

temperature was set to 0 °C, while the end temperature varied according to the degradation temperatures of the APIs and excipients, as determined by thermogravimetric analysis (TGA). The end temperatures for each API were as follows: theophylline – 274 °C, caffeine – 270 °C, ibuprofen – 250 °C, paracetamol – 180 °C, propranolol and enalapril – 200 °C, and hydrochlorothiazide – 250 °C. Nitrogen purge rate was set at 50 ml/min and the sample weight was in the range of 5-10mg.
Thermal gravimetric analysis (TGA) was performed using a METTLER Thermal Analyzer (Mettler Instrumente AG, Greifensee, Zurich). A 100 microlitre pan with no lid was used with a heating ramp from 25^{o} C to 600^{o} C at a heating rate of 10^{o} C /minute.

3.2.9 Powder X-ray Diffraction

The diffraction pattern needed to be taken to determine the API's crystallinity in the final printed product. Samples were printed into 25mm discs, and physical mixtures of the powder formulations were used as controls. The sample was mounted into the sample holder using Putty, and the control powder was placed on a 16 mm sample holder.
The diffraction parameters were: soller slit = 0.02 rad, Ni Kβ filter, 2θ range: 5–30 °, step size was 0.0334 °, scan speed was 0.03 °/s.

3.2.10 Dynamic Vapour Sorption

The gravimetric analysis for dynamic vapour sorption of the paracetamol formulation was performed using the DVS Advantage 1 instrument (Surface Measurement Systems UK Ltd., London, UK) equipped with an ultra-microbalance exhibiting a mass resolution of 0.1 µg. The extruded and control formulation without Eudragit EPO were milled and placed in an aluminium pan. The sample temperature was fixed at 25^{o} C and was exposed to a cycle of relative humidity from 0% to 90% and to 0% again. Each step lasted until the mass change rate was less than 0.005%/minute.

3.2.11 Drug Content

The FlexiPill units were milled using a mortar and pestle to measure the drug content. A finite amount of the milled unit was then weighed and placed in the corresponding solvent. The following solvents were used: distilled water for theophylline, paracetamol, caffeine, propranolol, and enalapril; acetonitrile for ibuprofen; and methanol for hydrochlorothiazide. Then, 2 ml was transferred to HPLC vials and measured using the method described in 3.2.12 Chromatography.

3.2.12 Dissolution Test

The dissolution test was performed using USP dissolution apparatus II (Erweka GmbH, Germany) with rotating paddles the rotation speed was 72 rpm in Chapters 4 and 5 and was increased to 100 rpm in Chapter 6 to simulate more vigorous conditions to test the floatation. The temperature was set to 37 ± 0.5 °C and the dissolution media were either 1000 mL 0.1 M Hydrochloric acid HCl pH 1.5 or phosphate buffer with pH 7.2. Samples were collected at (15,30,60,120, 180, 360, 540, 720 and 1440 minutes) using 10 ml syringes and filtered using 0.2 micrometre PTFE syringe filters into 2 ml tented HPLC vials.

3.2.13 Chromatography

High-performance liquid chromatography (HPLC) was employed to quantitatively determine the amount of each active pharmaceutical ingredient (API) in both the drug content analysis and the dissolution test. The HPLC system used was an Agilent 1290 infinity HPLC system coupled with a G4212A diode array detector (DAD) (Agilent Technologies, Inc., Santa Rosa, CA). The stationary phase was a reversed-phase C-18 (100x4.6 mm) and pore size 2.5 mm, for chapters 5 and 6, and Luna 3 µm Phenyl-Hexyl (100x4.6 mm) column, for chapter 7. The mobile phase used was a gradient mixture of acetonitrile with 0.1% phosphoric acid, D.W. with 0.1% phosphoric acid for chapters 5 and 6, and D.W. containing 0.1% phosphoric acid and methanol for chapter 7. The gradient tables for both methods. The flow rates were 1.2 mL/min, for Chapters

5 and 6, and 0.4 mL/min, for Chapter 6. The detection wavelengths were set to 273 nm, in Chapter 5, 220 nm, in Chapter 6, and 210 and 280 nm, in Chapter 7. The run time was 10, 7 and 15 minutes, for chapters 5, 6 and 7, respectively. Seven calibration graphs for each of the APIs were constructed with 21 points and used to calculate the amount of the drugs in the drug content and dissolution experiments. Table 3.2 summarizes the chromatography methods used in the contribution chapters.

Table 3.2 The chromatography methods used in the three contribution chapters evaluate API concentration in the drug content and dissolution test.

	Chapter 5	**Chapter 6**	**Chapter 7**
Stationary phase	Reversed phase C-18 (100x4.6 mm) and pore size 2.5 mm	Reversed phase C-18 (100x4.6 mm) and pore size 2.5 mm	Luna 3 µm Phenyl-Hexyl (100x4.6 mm) column
Mobile phase	Acetonitrile with 0.1% phosphoric acid and D.W. with 0.1% phosphoric acid	Acetonitrile with 0.1% phosphoric acid and D.W. with 0.1% phosphoric acid	Methanol and D.W. containing 0.1% phosphoric acid.
Gradient sequence	Minute 0-1: 10% O + 90% A Minute 7: 90% O + 10% A Minute 7.1: 10% O + 90% A Minute 10: 10% O + 90% A	Minute 0-1: 10% O + 90% A Minute 5: 90% O + 10% A Minute 5.1: 10% O + 90% A Minute 7: 10% O + 90% A	Minute 0-3: 20% O + 80% A Minute 10: 55% O + 45% A Minute10.1: 20% O + 80% A Minute15: 20% O + 80% A
APIs	Theophylline	Paracetamol, Ibuprofen and caffeine	Propranolol, enalapril and hydrochlorothiazide.
Flow rates	1.2 mL/min	1.2 mL/min	0.4 mL/min
Detection wavelengths	273 nm	220 nm	210 and 280 nm

For Chapter 7, the same method was used for liquid chromatography-mass spectrometer (LC-MS) with one modification: the phosphoric acid in the aqueous part of the mobile phase (solution A) was replaced with formic acid. Agilent single quad detector (Agilent Technologies, Inc., Santa Rosa, CA) was used.

Chromatographic method validation was carried out in accordance with ICH Q2(R1) (Guideline 2022) to confirm the reliability and accuracy of the HPLC methods employed throughout this study. The validation focused on evaluating linearity, limit of quantification (LOQ), and reproducibility for each of the active pharmaceutical ingredients analysed.

Linearity was determined by constructing calibration curves for each drug across a range of concentrations relevant to their expected content in the formulations. For theophylline, an eleven-point calibration curve was prepared, ranging from 250 micrograms per litre to 500 milligrams per litre, yielding a correlation coefficient (R^2) of 0.9977. Paracetamol was assessed over a seven-point range from 25 to 300 milligrams per litre, resulting in an R^2 value of 0.9992.

Caffeine was evaluated using a seven-point calibration curve from 5 to 60 milligrams per litre, with an R^2 of 0.9997. Similarly, ibuprofen showed excellent linearity across a range of 20 to 240 milligrams per litre, with an R^2 of 0.9999. Propranolol hydrochloride, enalapril maleate, and hydrochlorothiazide were each evaluated using six-point calibration curves covering 2 to 50 milligrams per litre, all of which produced R^2 values of 0.9999. These results confirm strong linearity across all tested concentration ranges, with all methods achieving correlation coefficients near or above the accepted threshold of 0.999.

The limit of quantification (LOQ) for each API was determined based on either the signal-to-noise ratio approach or by calculating the standard deviation of the response and the slope of the calibration curve. The LOQ values obtained for theophylline, paracetamol, caffeine, ibuprofen, propranolol hydrochloride, enalapril maleate, and hydrochlorothiazide were found to be (Theophylline =250 microgram/L, Paracetamol= 2 mg/L, Ibuprofen= 10mg/L, Caffeine= 10mg/L, Propranolol= 0.5 mg/L, Enalapril= 2mg/L and HCT= 250 microgram/L). These values indicate that the methods were

capable of detecting and quantifying low concentrations with acceptable accuracy and precision.

Reproducibility was assessed through intra-day and inter-day precision studies, using replicate injections of standard solutions at varying concentration levels. For each API, the relative standard deviation (RSD) was calculated to evaluate variability in peak area responses. The RSD values for all tested APIs were within the acceptable limit of <2%, confirming the repeatability and robustness of the developed methods under the specified analytical conditions.

These validated HPLC methods provided accurate, precise, and reliable quantification of drug content and dissolution profiles across all case studies. Each method was optimised not only for its analytical performance but also to ensure efficient runtime and separation, facilitating the analysis of multi-component polypills under complex formulation conditions.

3.2.14 Statistical Analysis

In chapter four, A Box–Behnken design was selected as the experimental design model due to its efficiency in estimating second-order (quadratic) models with a reduced number of experimental runs compared to a full factorial design. The experimental design included three independent variables: infill density, drug concentration, and the ratio of immediate-release (IR) to sustained-release (SR) units. Each variable was studied at three levels (low, medium, and high). The methodology involves fitting a second-order polynomial equation to the data and conducting statistical analyses such as regression modelling and analysis of variance (ANOVA) to determine the significance of individual factors and their interactions. Response surface method (RSM) also facilitates the generation of contour plots and three-dimensional surface response graphs, which are valuable for visualising factor-response relationships and identifying potential optimal design regions.

The average release of each run was calculated to reflect the level of drug release. However, the modified principal component analysis was adopted to assign value to the shape of the drug release curve (Y. Wang et al. 2016). Equation 3.1 was used to

construct a residual matrix (RM) where the shape effect is isolated. This matrix was studied using PCA to find the eigenvalues using SPSS software. Three eigenvalues had over 90% cumulative variance. Afterwards, using the design of the experiment software Stat-Ease 360, the effect of the three experiment variables on the level and shape was studied.

$$RMrt = (Xt - X) - (Xra - X) - (Xta - X)$$ ----------(Equation 3.1)

Where RMrt is the residual matrix point at run (r) and time (t), Xt is the release at time t, X is the total average release, Xra is the run average release, and Xta is the time point average release.

3.2.15 Kinetic model fitting

Microsoft Excel was used to solve for the least Residual Sum of Squares (RSS) between the prediction model and the release data to fit drug release to a kinetic model. The data point used was before the plateau was reached. Afterwards, the correlation coefficient (R^2) between the prediction and release data was calculated. Thereafter, the Akaike Information Criterion (AIC) were computed for each model using the RSS, with the equation:

AIC= n ln (RSS/n) +2k----------(Equation 3.2)

Where n is the number of data points used, K is the number of model parameters and RSS is the Residual Sum of Squares.

Chapter 4 Evaluating Feasibility

To evaluate the feasibility of implementing a personalised polypill solution such as FlexiPill in real-world healthcare settings, a targeted survey was conducted involving healthcare professionals (HCPs), particularly general practitioners (GPs) both within and outside the United Kingdom. These practitioners often serve as the first point of contact for patients with chronic diseases and are frequently responsible for managing complex polypharmacy cases. The survey aimed to assess current prescribing practices, attitudes towards fixed-dose combinations (FDCs), and openness to personalised medication approaches.

The survey comprised four close-ended questions and one open-ended question. The initial questions evaluated the prevalence of polypharmacy in clinical practice and the frequency of FDC use. Subsequent questions assessed perceived barriers to prescribing polypills, the importance of personalised medicine, and the potential utility of a personalised polypill. The findings revealed that over 57% of respondents estimated that more than 60% of their patients were on multiple medications, with one-third estimating this number to exceed 80%. However, despite this high prevalence, more than half of the respondents reported that they rarely or never prescribed polypills.

When asked to elaborate, participants cited dose inflexibility, risk of adverse reactions, and the lack of specific combinations as key barriers to FDC use. This reluctance highlights a mismatch between clinical needs and currently available pharmaceutical solutions. Figure 4.1 and Figure 4.2 represent HCPs' responses to the first two survey questions related to polypharmacy and polypills.

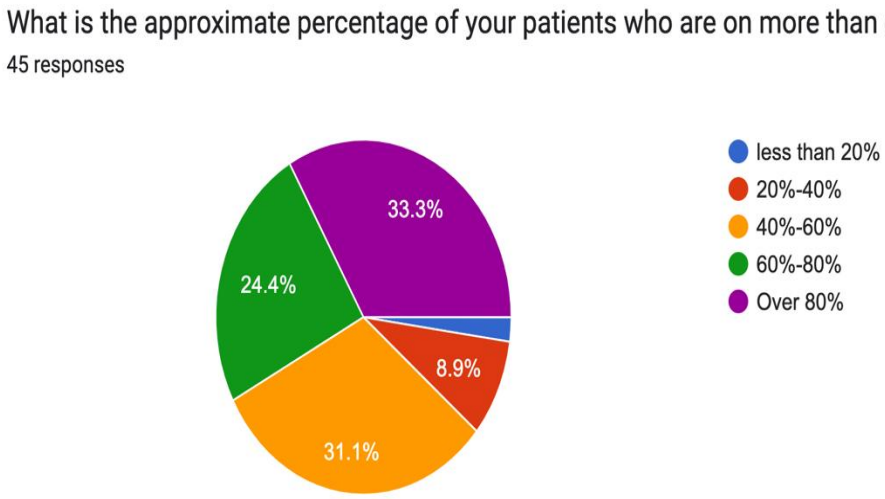

Figure 4.1 HCPs estimation of the percentage of patients with polypharmacy. (constructed by the author)

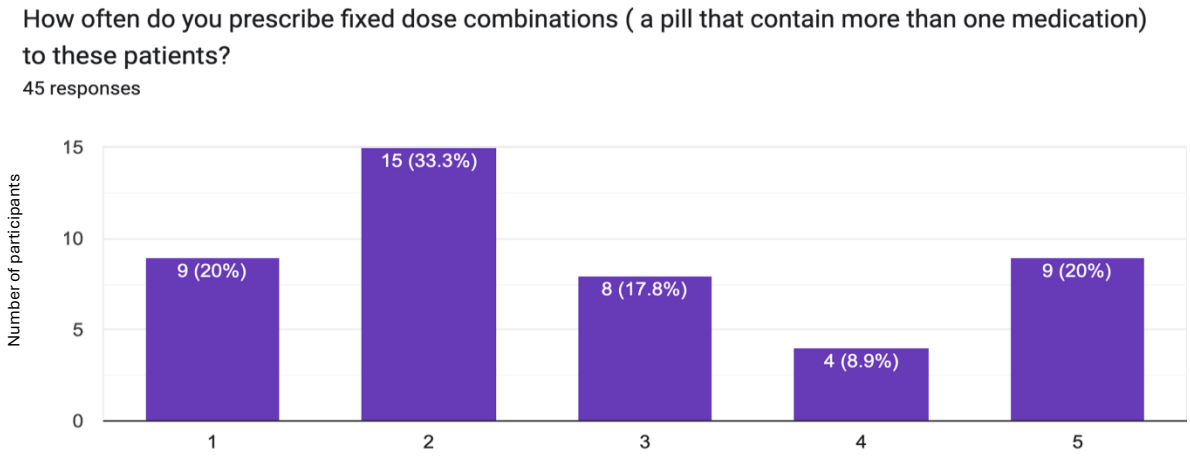

Figure 4.2 The tendency of HCPs to prescribe polypills survey (x-axis scale 1= not often to 5 very often). (constructed by the author)

On the other hand, when the participants were asked about personalised medication, over 75% considered it important or very important to their patients. On the other hand, regarding a personalised polypill, 58.7% regard it as a helpful dosage form that can help their patient, 37% of them were on the fence, and only 4.3% think that this is not useful. This can further explain why HCPs are reluctant to use polypills since they find personalisation and ease of dose titration to be more of a priority than solving the polypharmacy issue. Figure 4.3 and Figure 4.4 show HCPs' responses to the

importance of personalised medication and the usefulness of personalised polypills, respectively.

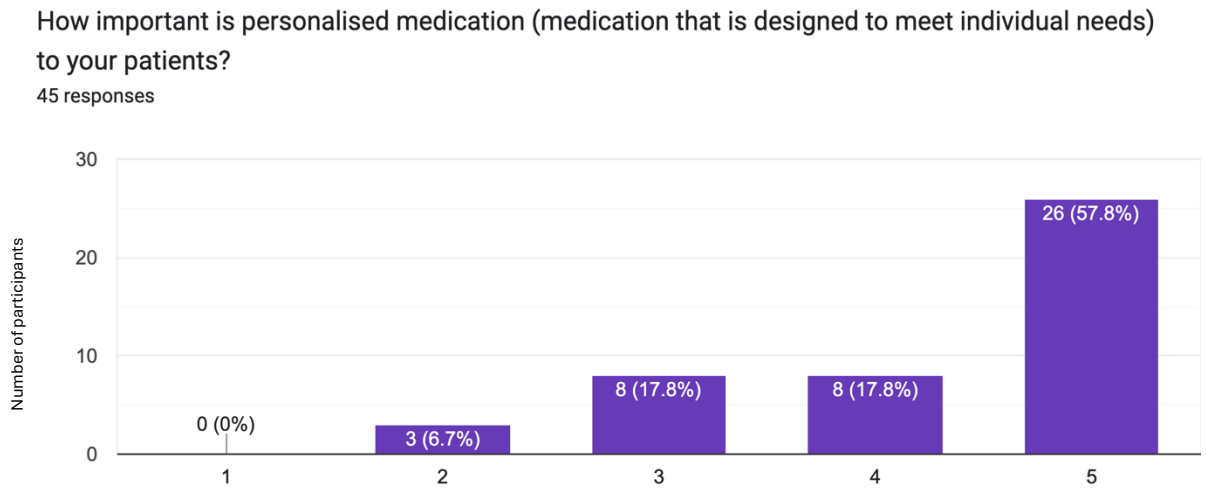

Figure 4.3 The importance of personalised medication according to the HCPs participating in the survey (x-axis scale 1= not important to 5 very important). (constructed by the author)

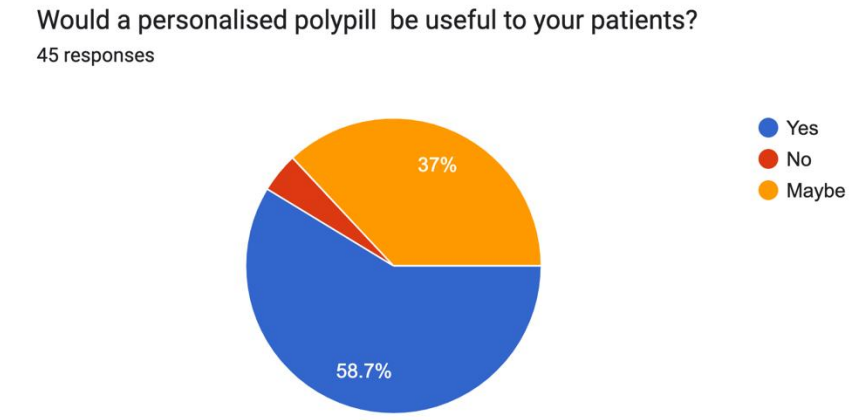

Figure 4.4 The usefulness of flexible-dose combination to the HCPs' patients. (constructed by the author)

The FlexiPill concept addresses this gap by separating drug fabrication from final dose assembly. Drug-containing units would be manufactured in quality-controlled, GMP-compliant facilities and later assembled at the point of care into a modular polypill tailored to individual patients. This approach mitigates regulatory concerns associated with point-of-care 3D printing while retaining the benefits of customisation. It mirrors the structure used in existing modular delivery systems and aligns with recent

regulatory trends that favour hybrid models combining industrial quality assurance with clinical adaptability. This architecture presents a scalable and safe framework that may prove more acceptable to regulatory agencies such as the FDA and MHRA compared to direct clinical printing.

In terms of real-world application, FlexiPill could be implemented in several healthcare settings. In community pharmacies, pharmacists could assemble patient-specific polypills during consultations based on current prescriptions. In clinical trial settings, FlexiPill allows for rapid prototyping of study arms requiring different drug release profiles. The system also suits home-based chronic disease management, particularly for elderly or poly medicated patients who struggle with complex regimens.

Economic feasibility is equally critical. While 3D printing entails specific capital and material costs, these may be offset by reduced pill burden, lower packaging and dispensing overheads, and better therapeutic outcomes through improved adherence. Inventory management could be simplified through modular stocking of standardised units, and waste reduced by tailoring quantities per patient.

Finally, the perspectives of patients and pharmacists will be crucial for successful adoption. Patients stand to benefit from reduced cognitive and logistical burden, especially in long-term therapy contexts. Pharmacists, meanwhile, would require appropriate training and procedural integration to support FlexiPill assembly within their existing workflows. Further feasibility studies should include user-focused trials to assess patient acceptability and operational assessments in pilot healthcare settings.

In summary, the FlexiPill system presents a feasible, innovative approach that combines the simplicity of FDCs with the flexibility of personalised medicine. By leveraging pharmaceutical 3D printing, it offers a modular, scalable, and clinically meaningful solution to the persistent challenges of polypharmacy, with strong potential for regulatory compliance, cost-effectiveness, and wide-ranging implementation in healthcare practice.

Chapter 5 : FlexiPill to Personalise Drug Release of Theophylline

5.1 Introduction

The current paradigm for drug therapy is one size fits all. As a result, healthcare professionals are administrating the same drug to different patients at the same dose and frequency and expecting the same response. However, as it has been discussed in 1.5 Personalised Medicine, recent advancements in the field of pharmacogenetics and pharmacogenomics revealed the shortcomings of this paradigm because it can lead to undermedication or overdose (Vaz and Kumar 2021; Singh 2020), which will lead to ineffective treatment and side effects, respectively. Personalised medication that can deliver the right drug at the right time and dose will improve efficacy and safety. Additionally, personalised medication can improve patient compliance and decrease the cost of treatment (Sadia, Isreb, et al. 2018). Dosage form personalisation can include tailoring the dose, drug release, drug combination or even just the shape to improve patient compliance. Dose adjustment at the point of care is particularly difficult with solid dosage forms because it usually involves splitting or grinding the tablet, which can result in inaccurate dosing due to human error and/or destroy the certain functionality of the dosage form, such as coating (Verrue et al. 2011; Espinosa et al. 2023). Many emerging technologies in the pharmaceutical field have the potential to make personalised medication a reality; one of these technologies is 3D printing. A great bulk of work has been done in recent years to explore the application of three-dimensional printing (3DP) to formulate personalised medication because of its capacity to formulate one-off batches for each individual need (Seoane-Viaño et al. 2021). As mentioned previously, this work will focus on fused deposition modelling (FDM), an extrusion-based 3DP technique and the most studied technique due to its low operation cost and ease of use (Dumpa et al. 2021). FDM involve the use of a heated nozzle to extrude a thermoplastic polymer into a building platform. As discussed previously in 2.2.3 Controlling Drug Release, many researchers have demonstrated the ability of FDM to control drug release by controlling formulation (Melocchi et al. 2016; Goyanes et al. 2017; Shi et al. 2021), drug load (Yang et al.

2018), infill density (Kempin et al. 2018; Solanki et al. 2018) and other design factors (Goyanes, Martinez, et al. 2015; Isreb et al. 2019; Tagami et al. 2018). However, all these publications were intended to control the release during formulation or at the printing stage. This requires the printing to be carried out at the point of care for each patient to personalise the release for them. Nevertheless, having a 3D printer in a pharmacy setting or a hospital to print personalised medication has many barriers to overcome, one of which is the regulatory aspect of this practice (Beitler et al. 2022). Quality control of the printed medicines at the point of care is a cumbersome task that requires the regulation of the printer, printing ink and the printer operator.

Finally, theophylline is a bronchodilator used in asthma and obstructive pulmonary diseases. Theophylline has a low therapeutic index and needs close monitoring and precise dosing. Therefore, personalisation can be of great importance because it can help control the drug release within this window, resulting in more effective and safe treatment. In this work, the aim was to investigate the possibility of using the design flexibility that comes with FDM to print a novel tablet in which the release of the API can be personalised to meet patient needs. The design suggested can be produced in an industrial, quality-controlled setting and assembled according to patient needs in clinical settings after printing. This design can also improve shelf life, save time and decrease the cost of personalised medication.

5.2 Results and Discussion

5.2.1 Tablet Design and Formulation

The formulation was prepared by mixing all components in a mortar and pestle and then extruded using a single screw hot melt extruder the filament is then used to print the design immediately to decrease the effect of storage on the filaments. The design consists of 4 units that interlock like a jigsaw puzzle, forming a disc tablet. Although, the tablet size is still within the accepted limits for a tablet to be ingested, which is 17mm in diameter (FDA. 2022). This work can be considered as a proof of concept for a more potent drug where the tablet can be even smaller. The new flexible design can provide controlled drug release by controlling the release from each of the four units in the design and using a different configuration of the units. Two types of units were

prepared: one for immediate release and another for sustained release. For the IR formulation, PVP was used as the thermoplastic matrix polymer due to its water solubility, which makes it a sensible candidate for immediate release. However, PVP on its own has poor flow through the printer nozzle and can't form a structurally sound print; therefore, the thermostable filler talc was used (Okwuosa et al. 2016). Moreover, TEC was used as a plasticiser to improve filament flexibility and decrease the printing temperature of the formulation. For the SR formulation, E RL PO was used as the polymer matrix. E RLPO is composed of ethyl acrylate, methyl acrylate and less than 10% methacrylic acid ester with quaternary ammonium groups, making it water insoluble and quaternary ammonium groups give it its swelling and permeability properties, which will enable sustained release of the drug by diffusion (Korte and Quodbach 2018; Dos Santos et al. 2021). Additionally, PEG 4K was used as a plasticiser with no solid fill. The SR formulation drug load and infill density were kept constant, while the immediate release formulation drug load and infill density were adjusted to three levels according to the experimental design. Additionally, only one unit of the SR formulation was used in each tablet while using one, two or three units of the IR one. Figure 5.1 shows the FlexiPill design and the FlexiPill after printing.

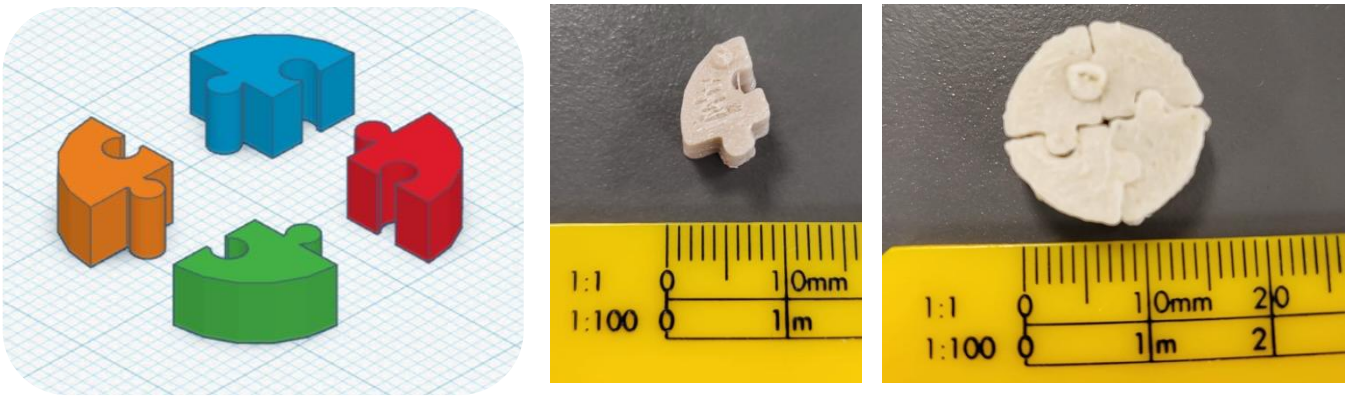

Figure 5.1 FlexiPill design (left), printed SR-Theo unite (middle) and assembled FlexiPill (right).

Table 5.1 Formulations and their respective compositions.

Formulation	PVP 40K	Eudragit RLPO	Theophylline	TEC	Talc	PEG 4K
Placebo	50%			12.5%	37.5%	
IR-Theo 10%	50%		10%	12.5%	27.5%	

IR-Theo 15%	50%		15%	12.5%	22.5%	
IR-Theo 20%	50%		20%	12.5%	17.5%	
SR-Theo		50%	40%			10%
IR= immediate release, SR= sustained release, Theo= theophylline						

5.2.2 Experimental Design

Quality by design (QbD) is a method for understanding which input variable has a greater effect on the outcome of a particular process. Experimental design (DoE), an aspect of QbD, is a systematic approach to creating a series of experiments based on statistical principles that help determine the relationships between input and output variables (Fukuda et al. 2018). In this work, DoE will be used to determine which variable in the Flexipill will have the greatest effect on the theophylline drug release.

Therefore, in the experimental design, three variables- drug load, infill density in the IR units, and the number of IR units- were chosen to study their effect on drug release in the FlexiPill design. These factorial variables represent three stages of 3D tablet printing: pre-extrusion, pre-printing and post-printing stages. Personalisation can be easier to carry out if done at a later stage of the process because it does not require a change in the formulation and/or the printing settings. However, all previous attempt to personalise medication using 3D printing was performed at the formulation or pre-printing stages (Sadia, Isreb, et al. 2018).

Therefore, three formulations were prepared for the IR units with 10, 15 and 20% drug load of theophylline, in addition to the SR formulation and placebo formulation. Table 5.1 summarizes the four theophylline formulations and the placebo one.

The box–Behnken design (BBD), a three-level design used to study the surface response of the three independent variables, was used. BBD avoids using the extreme levels (the corners) to decrease the number of experiments compared to a full factorial design, saving time and cost. The centre point, where all the variables are at a medium level, is repeated three times to improve precision. Figure 5.2 and Table 5.2 summarise the experimental design.

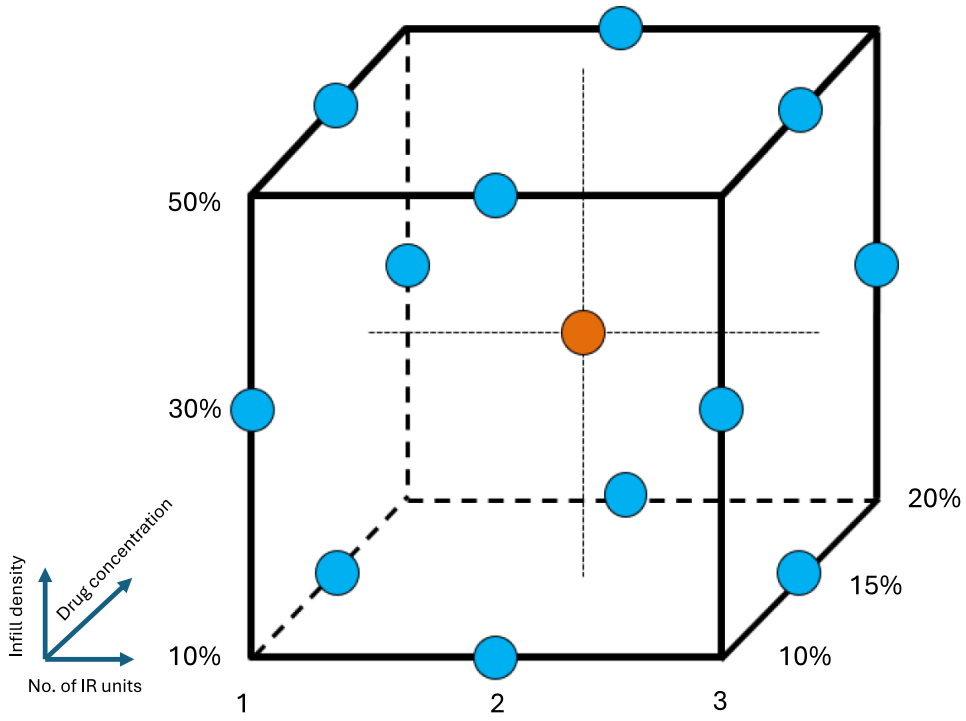

Figure 5.2 Experimental design (Box-Behnken) showing the three levels of the independent variables and the experimental runs. (constructed by the author)

Table 5.2 The experimental design runs and the level on the three variable for each run.

Run number	Infill (%)	API (%)	NO. of IR Units in the Flexipill
1	50%	20%	2
2	10%	20%	2
3	50%	10%	2
4	10%	10%	2
5	50%	15%	3
6	10%	15%	3
7	50%	15%	1
8	10%	15%	1
9	30%	20%	3
10	30%	10%	3
11	30%	20%	1
12	30%	10%	1
13	30%	15%	2
14	30%	15%	2
15	30%	15%	2

This chapter will not investigate the SR formulation further since it was adapted from the literature (Korte and Quodbach 2018). Instead, the focus will be on the effect of different drug contents on the IR formulation and the experimental design.

5.2.3 Filament Mechanical Properties

Thereafter, the effect of drug load on the mechanical properties of the extruded filaments was studied through tensile strength. Although, there was no significant difference (p-value>0.5 in one way ANOVA) in the maximum stress at the breaking point between the three formulations, the elongation (maximum strain) was higher in the formulation with a high drug load (9%, 9.8% and 12.2% for Theo 10%, Theo 15% and Theo 20%, respectively). Additionally, young modulus decreased as the concentration increase (Theo 10%=2.12 Pa, Theo 15%= 2.03 Pa and Theo 20%= 1.56 Pa), indicating that an increase in the concentration of theophylline increases the elasticity of the filaments. This can be attributed to the plasticisation effect of theophylline on the PVP. Figure 5.3 represents the strain against stress graph for the three formulations.

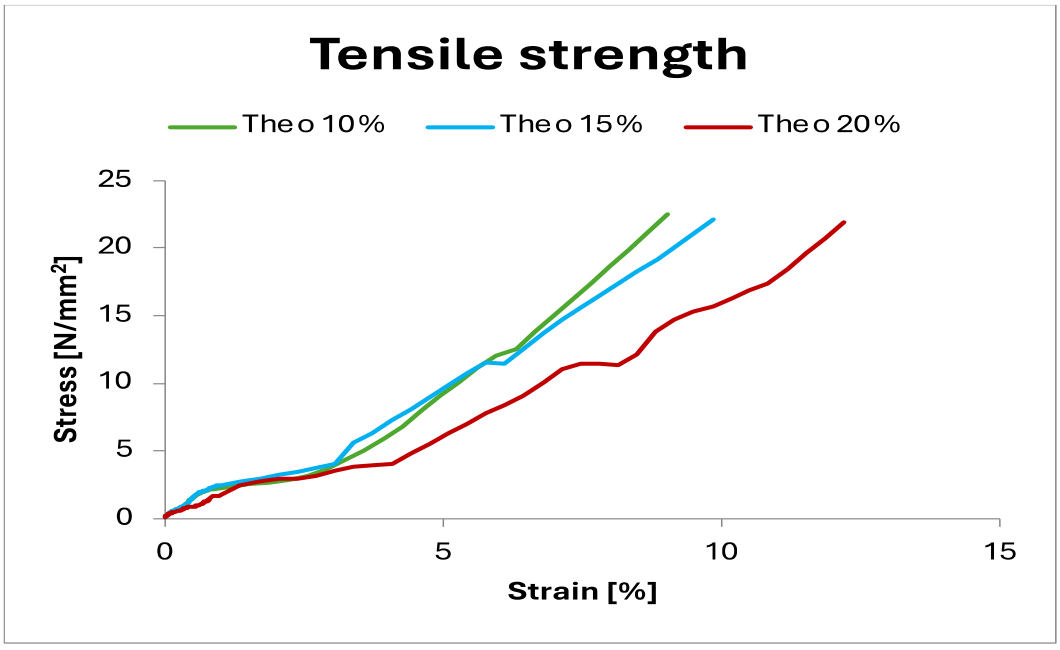

Figure 5.3 Stress against strain curve for tensile strength of the extruded filaments.

5.2.4 Printing

The units were printed at temperatures approximately 40 °C higher than their respective extrusion temperatures, as noted in Chapter 2, as a result of the longer heating duration and the additional shear stress encountered during the extrusion process. An exception was the sustained-release (SR) unit, which required an even higher printing temperature to ensure proper material flow and print quality. Weight variation was minimal at low drug concentrations (±3.34 mg); however, at higher drug concentrations, the standard deviation increased in Theo 15% and Theo 20% to ± 16.5 and 16.9 mg, respectively, indicating inconsistent extrusion from the printing head with these formulations. Despite this, drug content uniformity was maintained across all formulations, indicating that the extrusion and printing did not alter the concentration of the API because of adhesion to the walls and/or degradation. At the printing stage, each of the IR formulations was printed at three infill densities, 10, 30 and 50%, to serve as the second variable in the experimental design. However, the SR formulation was only printed at 50% infill density. The adhesion of the printlet to the building platform was poor at the start. Thus. A heated platform at 40ºC and masking tape on top of the platform were used to improve adhesion and facilitate the removal of the units from the printer. Table 5.3 provides a summary of the units' weight variation, drug content, as well as extrusion and printing temperatures.

Table 5.3 Summary of units' weight and drug content for the formulations and their extrusion and printing temperature (n=3).

	Average Units Weight (mg)	**Standard Deviation (mg)**	**Drug content (%)**	**Standard Deviation (%)**	**Extrusion temperature (°C)**	**Printing temperature (°C)**
IR-Theo 10%	231.5	3.34	100.93%	1.03%	80°C	120º C
IR-Theo 15%	250.53	16.5	97.11%	0.08%	80°C	120º C
IR-Theo 20%	236.97	16.9	98.87%	1.06%	80°C	120º C
SR-Theo	239.7	2.3	102.12%	0.78%	125°C	180º C
Placebo	235.7	4.1	-	-	100ºC	140º C
IR= immediate release, SR= sustained release, Theo= theophylline						

5.2.5 Rheological Study

To evaluate the impact of drug content on the viscosity of the IR formulation and gain insights into the extrusion and printing processes, the complex viscosity was analysed during a temperature sweep. The complex component of the shear viscosity measurement shows that as the concentration of the drug increases, the complex viscosity decreases significantly at both the extrusion and printing temperature, see p-values in Figure 5.4. However, in the post hoc analysis, when the least significant difference (LSD) was tested, the decrease was significant between all pairs apart from the 15% and 20% drug load, where the difference in viscosity was statistically insignificant. This reflects the plasticization effect of theophylline on the PVP 40K, which is a concentration related to a certain concentration, after which it becomes less significant. Moreover, the temperature of the maximum loss tangent (tan δ), where the storage modulus equals the loss modulus, represents the transition point of the formulation from elastic to viscous behaviour (Achorn and Ferrillo 1994). This temperature typically occurs near the glass transition temperature (Tg) of the polymer. In the theophylline formulations, this transition temperature averaged 84.87°C, compared to 90.96°C observed in the placebo formulation. This confirms the formation of solid dispersion in the IR formulations, which requires less energy to transform into viscous behaviour than the pure PVP polymer. Finally, the temperature point at which the viscous modulus reaches its peak, which represents the maximum point of freedom of motion in the polymer mix (Xie et al. 2020), was also shifted from 81.38°C in the placebo formulation to 67.21°C. These shifts are another indication of an interaction between the polymer and the API since the interaction resulted in a decrease in the energy required to increase the mobility of the polymer chains. Figure 5.4 represents a comparison between the rheological properties of the IR formulations and the placebo formulation.

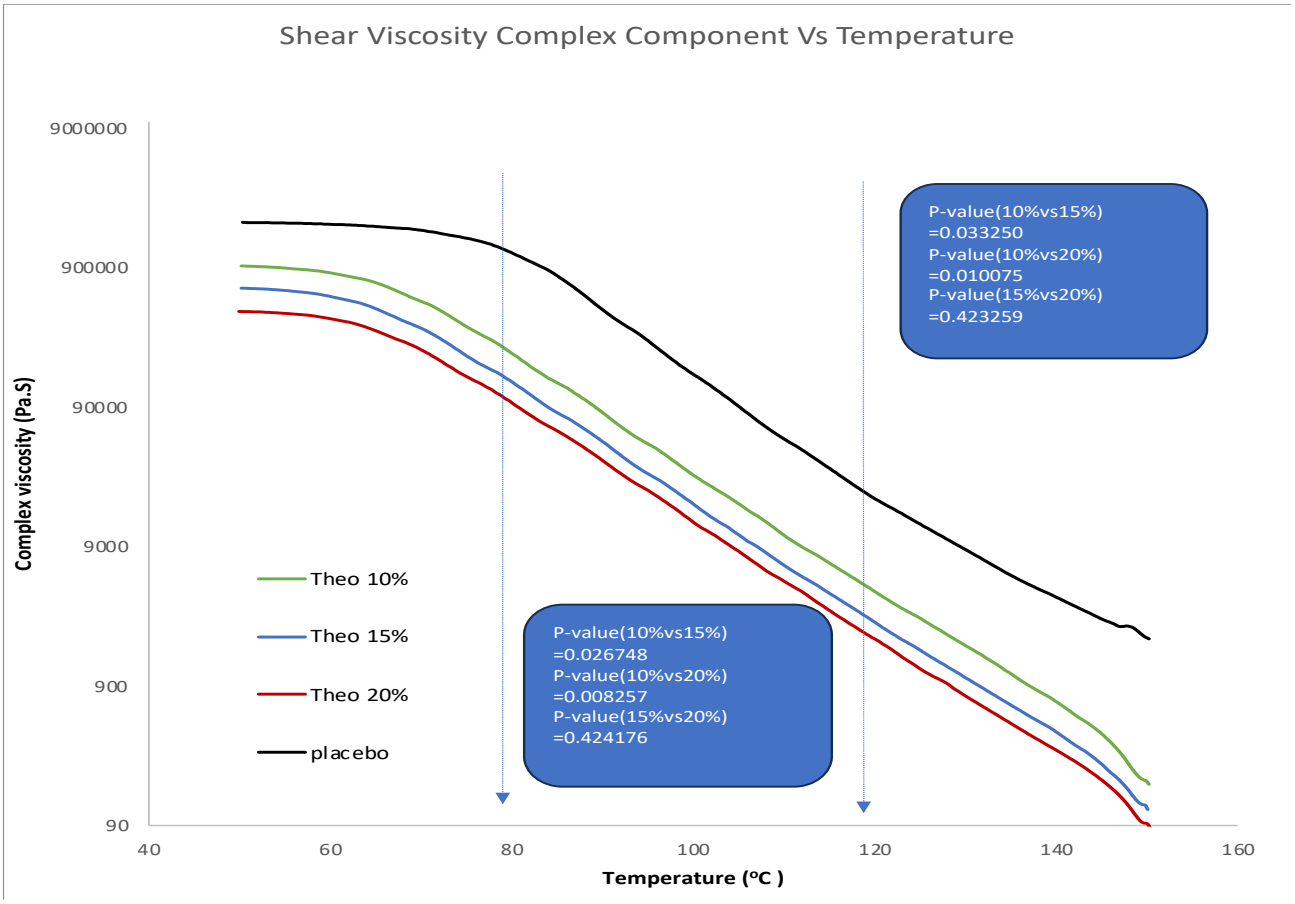

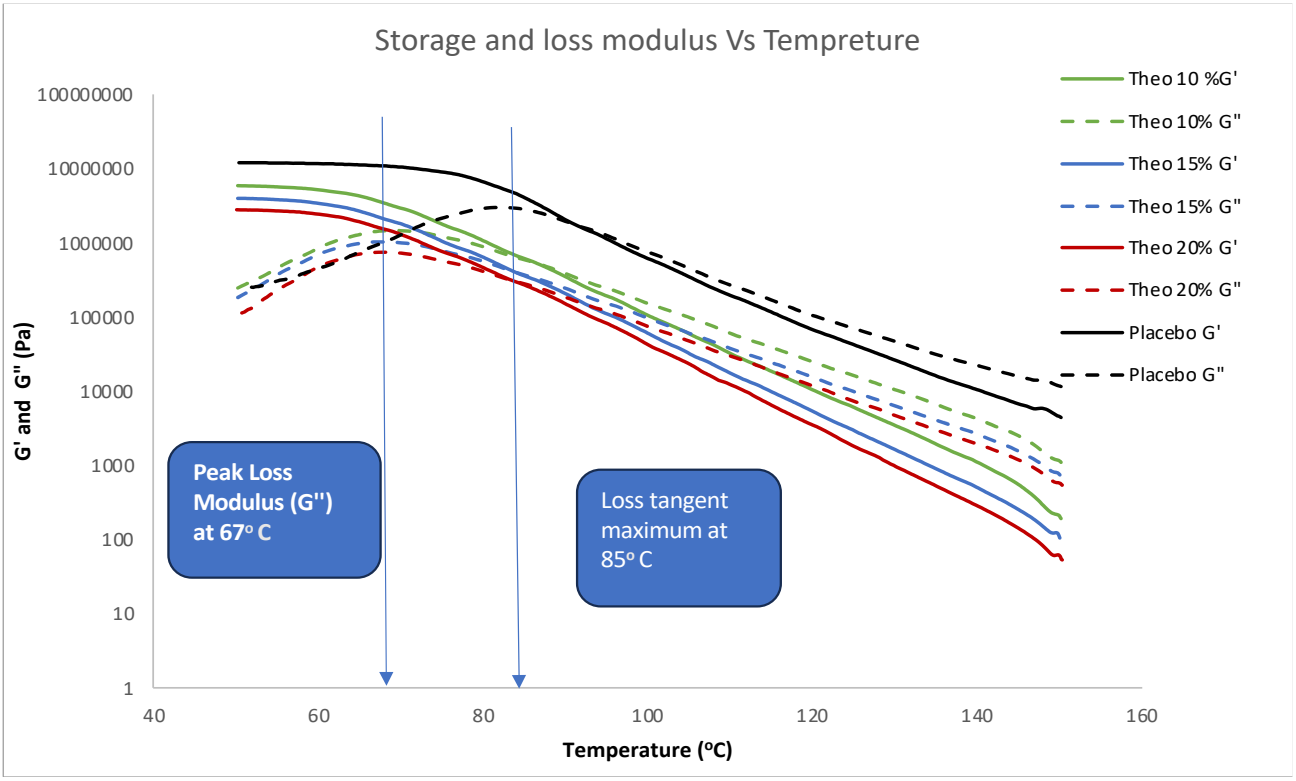

Figure 5.4 Complex Viscosity Vs. Temperature for the IR formulations with p-values at extrusion and printing temperature (top), Storage and loss modulus Vs. temperature (bottom)

5.2.6 Scanning Electron Microscopy

The SEM images for the filament show comparable surface morphology with a slight increase in the diameter in the filament with high concentration of theophylline due to die swell. However, the cross-section of the 20% theophylline filament appears more

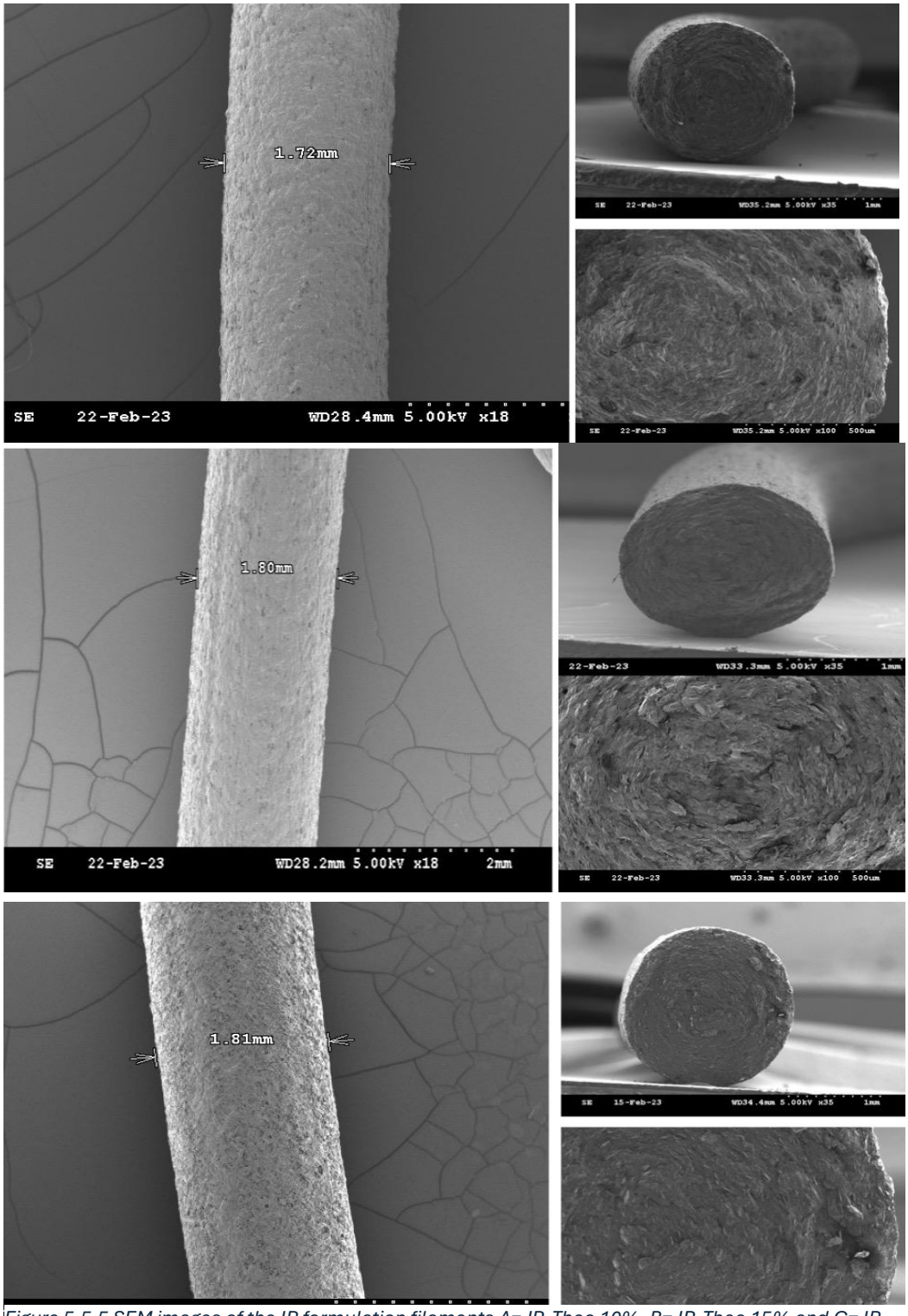

Figure 5.5.5 SEM images of the IR formulation filaments A= IR-Theo 10%, B= IR-Theo 15% and C= IR-Theo 20%. IR= immediate release, SR= sustained release, Theo= theophylline

heterogeneous, with larger agglomerates, which indicates incomplete miscibility of theophylline at high concentrations. Figure 5.5.5 shows the SEM images for the three filaments.

The effect on viscosity was reflected in the quality of the print. Hence, at a low concentration of 10% theophylline, the layer thickness was more uniform. However, as the concentration of theophylline increased to 15% and 20%, more discrepancies in the layer thickness could be seen in the SEM images. This was mainly due to higher viscosity at low drug load, which results in more uniform extrusion from the print head. Figure 5.5.6 presents electron microscope images of the immediate-release formulations and the effect of drug load on surface properties.

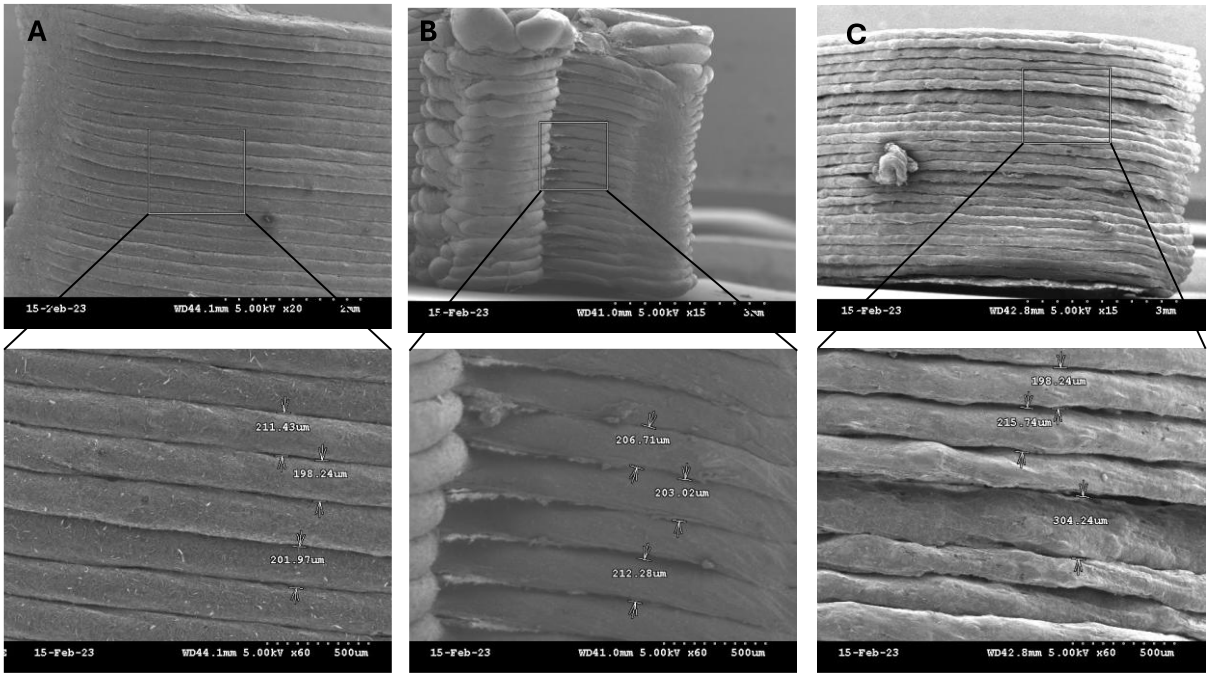

Figure 5.5.6 SEM image of the side of the printed Flexipill units 20X and 50X; A= IR-Theo 10%, B= IR-Theo 15% and C= IR-Theo 20%. IR= immediate release, SR= sustained release, Theo= theophylline

5.2.7 Fourier Transform Infrared Spectroscopy

FTIR spectrum of all three IR formulations showed the same peaks but with different intensities and when compared to the spectrum of reference theophylline some of the fingerprint peaks show either a red or blue shift reflecting the interaction between the theophylline and PVP 40K. The peak at 1558 cm^{-1} which corresponds to imino stretching vibration has shifted to 1566 cm^{-1} indicating the formation of hydrogen

bonds between theophylline and the polymer PVP 40K (PUTTIPIPATKHACHORN et al. 1990; Puttippipatkhachorn et al. 1990). No shift in the C-O stretching in the 1315 cm^{-1} was recorded. However, the band at 1701 cm^{-1} which corresponds to C=O stretching shifts to a higher frequency at 1712 cm^{-1}. Additionally, the band at 1666 cm^{-1} which corresponds to C=O amide stretching shifts to a lower frequency at 1662 cm^{-1} (Nafisi et al. 2003). Moreover, the band at 1419 cm^{-1} correspond to C=N stretching shifted to 1423 cm^{-1} in the formulations spectrums (Al-Salman et al. 2021). All this indicates the formation of H-bonds between the theophylline and the PVP 40K. Figure 5.7 represents the FTIR spectrum for the immediate release formulation compared to the spectrum of unprocessed theophylline.

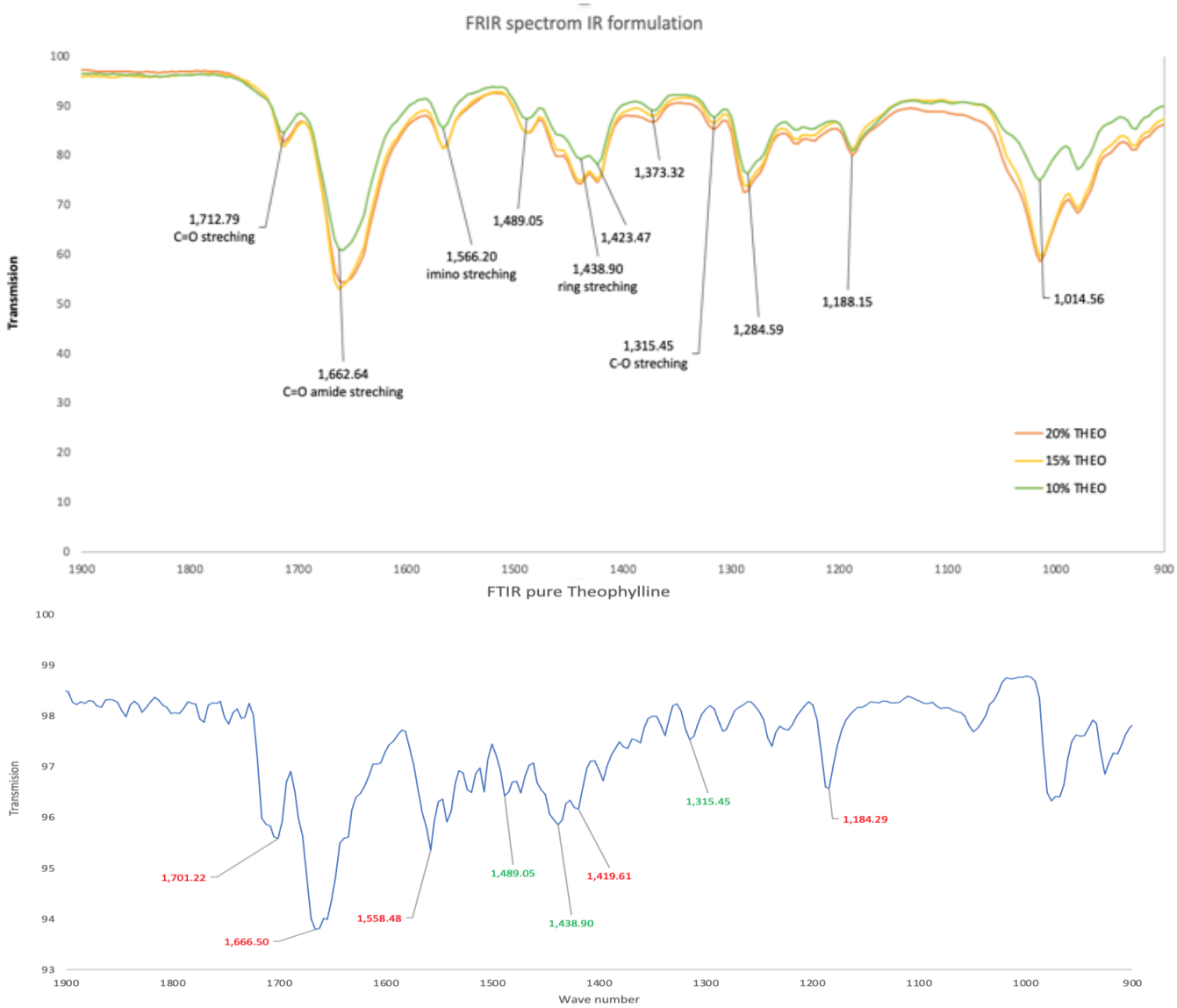

Figure 5.7 FTIR of the Immediate release formulation (top) and FTIR of theophylline (bottom).

5.2.8 Thermal Analysis

The DSC data for all formulations (IR, placebo and powder theophylline) are presented in Figure 5.8. Thermal analysis of these formulations shows no melt exothermic peak

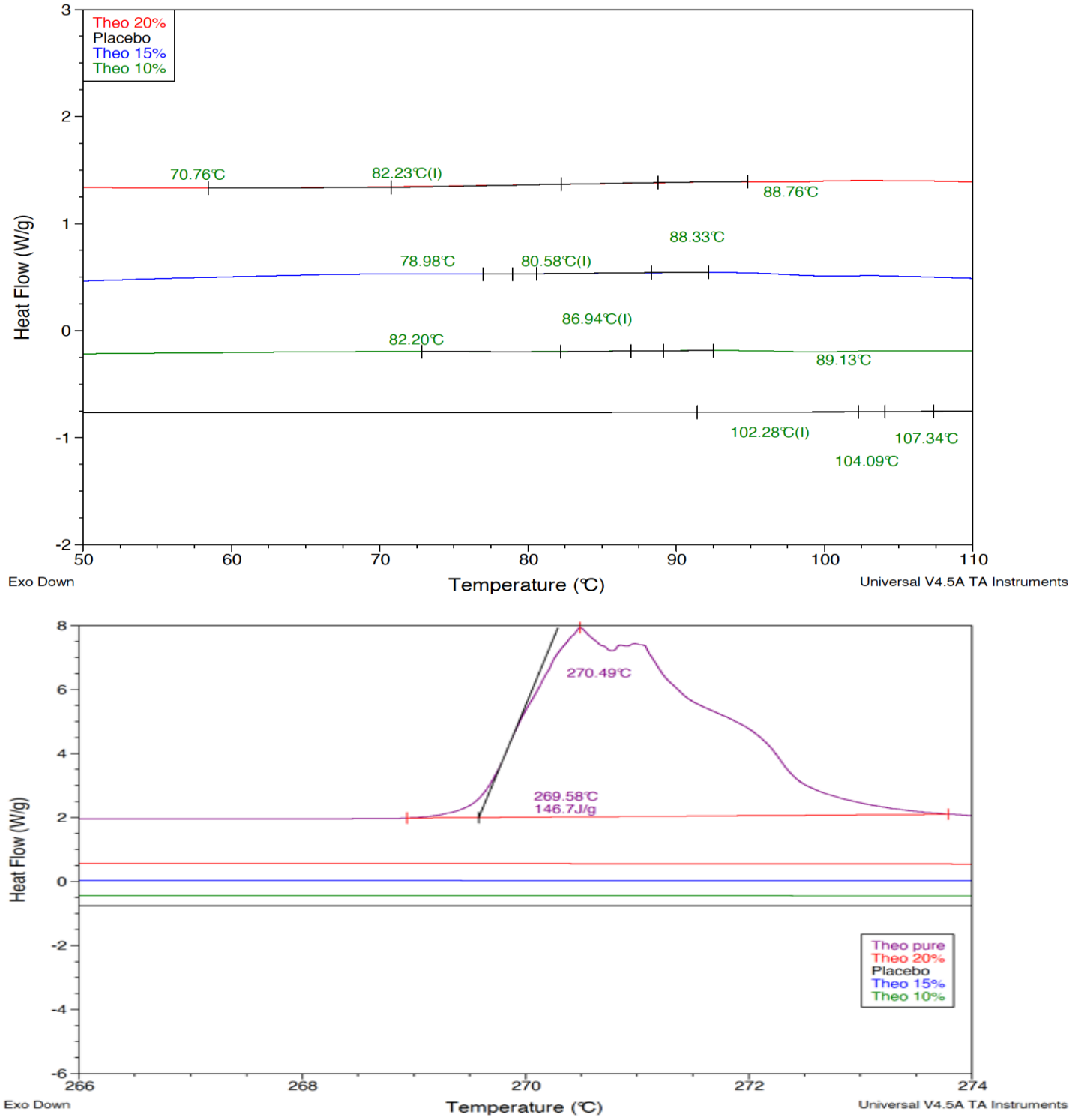

Figure 5.8 DSC of the IR- formulation and placebo showing the Tg (top) and DCS of the IR formulation, placebo and theophylline showing the melting point of theophylline (bottom) .

of theophylline at 270°C compared to pure theophylline. Additionally, all the

formulations had Tg at 84°C, apart from the placebo formulation, where the Tg was at 104°C. This suggests the formation of amorphous solid dispersion during hot melt extrusion and confirms the plasticisation effect of theophylline on the formulation, which decreased the viscosity (Crowley et al. 2007).

Thermal gravimetric analysis of PVP 40K shows a 10% decrease in weight around 100°C, representing moisture evaporation from the hygroscopic polymer although sample have been stored in a desiccator with silica gel until testing. However, this event shifts to 145° C in all formulations reflecting the entrapment of water molecules inside the solid dispersion matrix requiring more energy to evaporate (Fitriani, Haqi, and Zaini 2016). Theophylline and PVP 40K show the onset of the degradation around 250° C and 360° C, respectively. In the formulation, the same degradation events for theophylline and PVP 40K are present in addition to the event of TEC evaporation, which overlaps with the degradation of theophylline. However, the evaporation of TEC can be seen clearly in the placebo formulation as an 11% drop in weight at 295 ° C. Figure 5.9 represents the thermal gravimetric analysis of the three IR formulation, placebo formulation and their components.

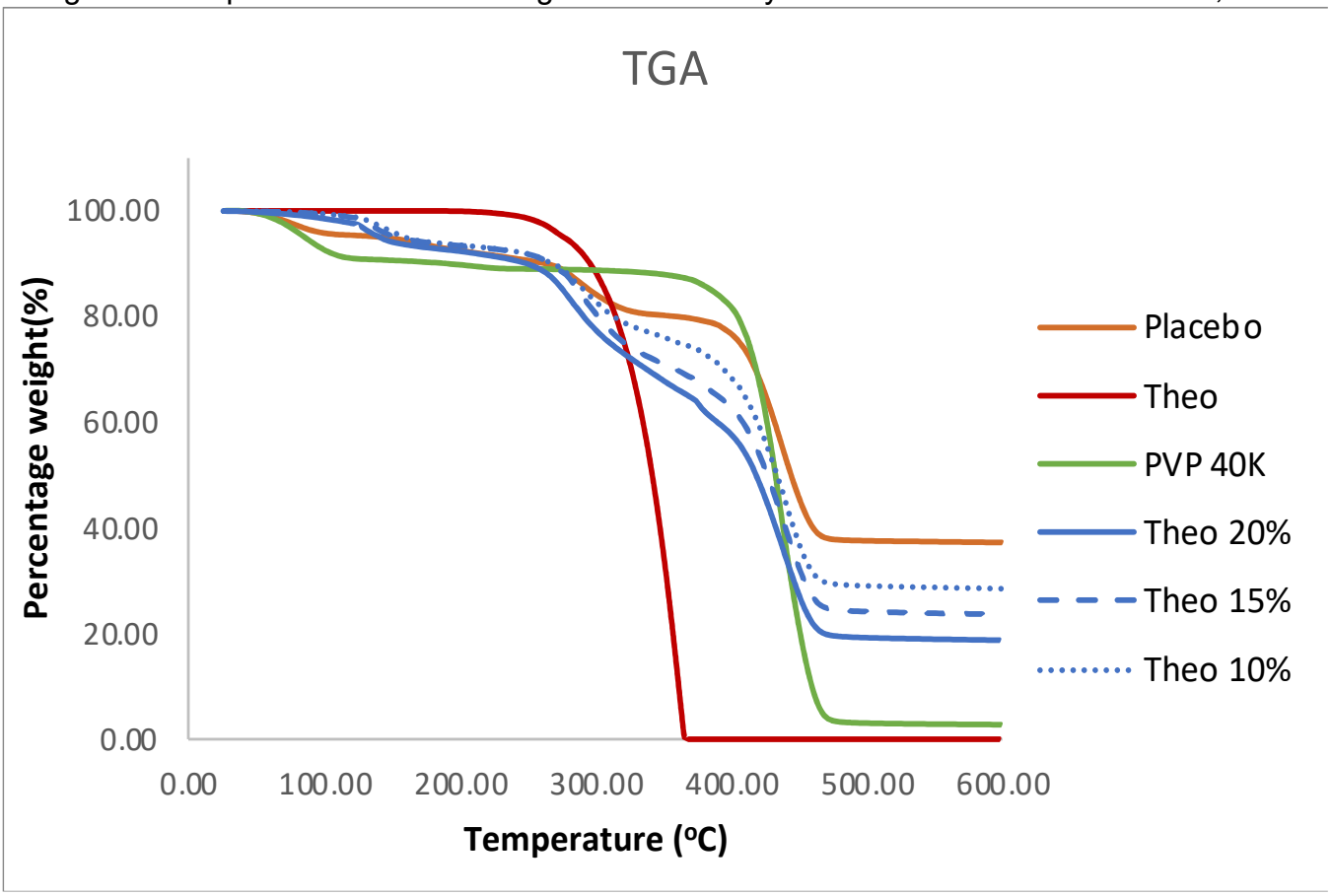

Figure 5.9 Thermal gravimetric analysis of the polymer, API and extruded filaments. IR= immediate release, SR= sustained release, Theo= theophylline.

5.2.9 Powder X-ray Diffraction

PXRD patterns confirm the formation of solid dispersion. Although in Theo 20% formulation, partial crystallinity of theophylline was detected in the PXRD pattern as the intensity peaks at 12.6, 24.1, 25.6 and 29.4° which correspond to theophylline crystalline form is present in the X-ray diffraction pattern for the formulation. The presence of theophylline crystals is the result of the high drug load in this formulation which either exceeded the miscibility of the API in the polymer or led to recrystallisation because of limited space in the polymer matrix for the API molecule due to high concentration. Talc remains crystallin in all the formulations hence the intensity peaks at 9.4, 18.9 and 28.5°. Figure 5.10 presents the X-ray diffraction pattern for the IR formulations and their components.

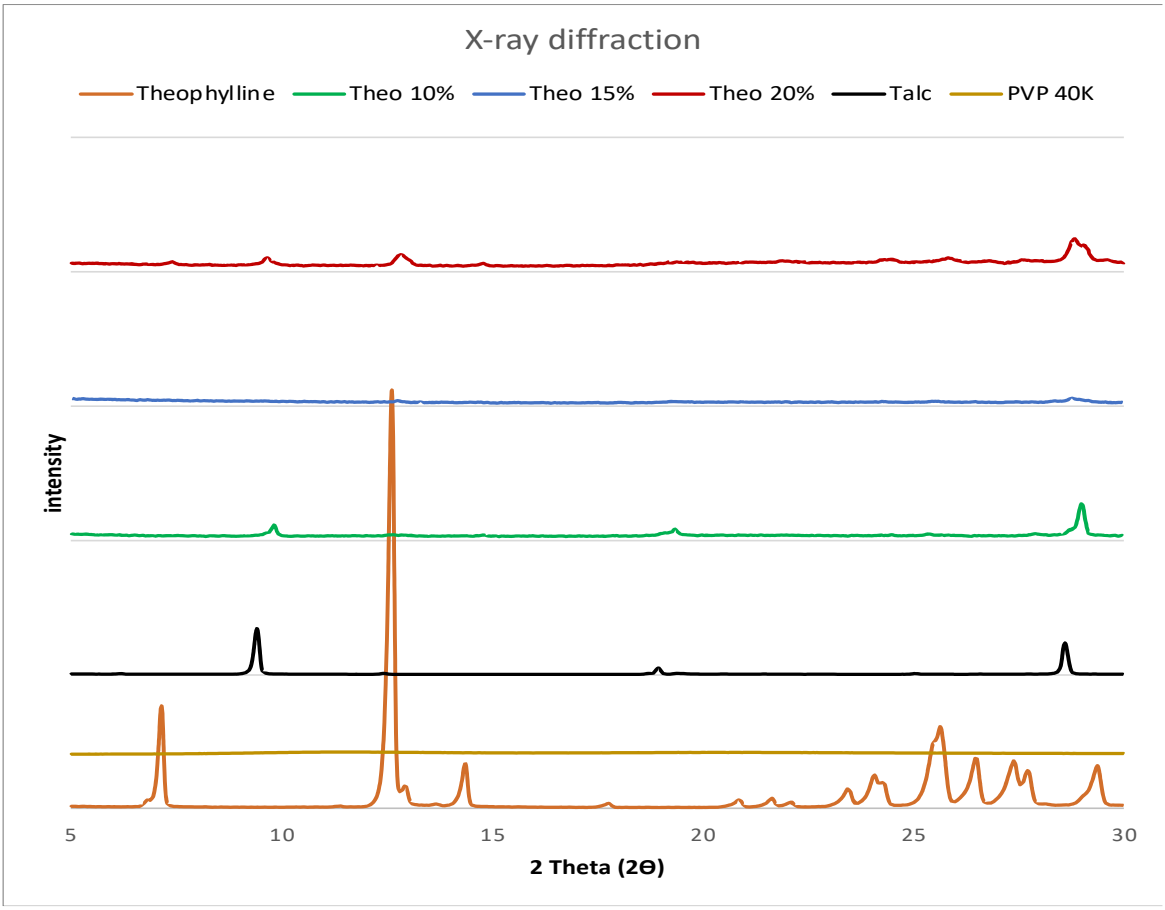

Figure 5.10 Powder X-ray diffraction of the IR formulations, API and Talc. IR= immediate release, SR= sustained release, Theo= theophylline.

5.2.10 Dissolution Test and Statistical Analysis

After the printing, the tablet units were assembled according to Box–Behnken design with the three variables mentioned in section 5.2.2 Experimental Design. Because of the effect of high drug load on the quality of print, the hinge had to be chiselled to facilitate assembly by removing imperfections in the joints. Thereafter, fifteen tablets were assembled (n=3) to run the dissolution test in 0.1 M HCl acid. Table 5.4 and Figure 5.11 show the dissolution release matrix and drug release curves for all the experimental design runs, respectively.

Table 5.4 Experimental drug release time matrix for the FlexiPill assembled tablet with the mean run release, the mean time release and the grand mean (n=3).

Run number /time (% release)	**15**	**30**	**60**	**120**	**180**	**360**	**540**	**720**	**1440**	**Average run release (level) (X_{ra})**
1	32.95	48.55	58.72	63.27	71.01	78.75	80.69	79.76	81.43	59.51
2	28.73	46.83	55.88	59.92	63.98	71.37	74.84	76.61	80.65	55.88
3	19.47	32.18	42.56	47.85	52.64	61.97	68.22	71.14	71.04	46.71
4	19.65	29.25	39.60	45.15	50.08	59.16	64.66	68.35	78.90	45.48
5	30.76	46.82	56.89	59.57	63.27	68.61	70.02	74.98	79.31	55.02
6	31.14	46.16	54.47	58.74	62.05	68.28	71.38	75.82	79.08	54.71
7	16.95	18.85	21.07	25.77	28.25	35.91	43.20	45.54	48.87	28.44
8	16.76	24.71	31.19	35.32	40.81	47.96	51.59	52.04	55.94	35.63
9	38.28	58.57	61.90	65.22	67.71	74.73	76.14	78.85	82.61	60.40
10	30.56	44.73	48.07	52.43	57.29	65.77	68.33	73.40	76.99	51.76
11	27.19	38.62	44.18	49.80	54.68	69.49	73.33	76.09	78.33	51.17
12	13.90	24.42	30.48	37.39	42.66	53.99	61.66	66.22	71.44	40.22
13	28.22	44.61	49.99	53.56	57.70	66.44	67.23	72.44	77.77	51.80
14	30.55	46.35	55.07	58.52	62.06	71.40	71.77	75.72	79.61	55.11

15	22.71	25.95	32.63	39.34	43.13	45.15	48.37	52.43	56.25	36.60
Average time point release (X_{ta})	25.85	38.44	45.51	50.12	54.49	62.60	66.10	69.29	73.21	48.56 (total average release) (X)

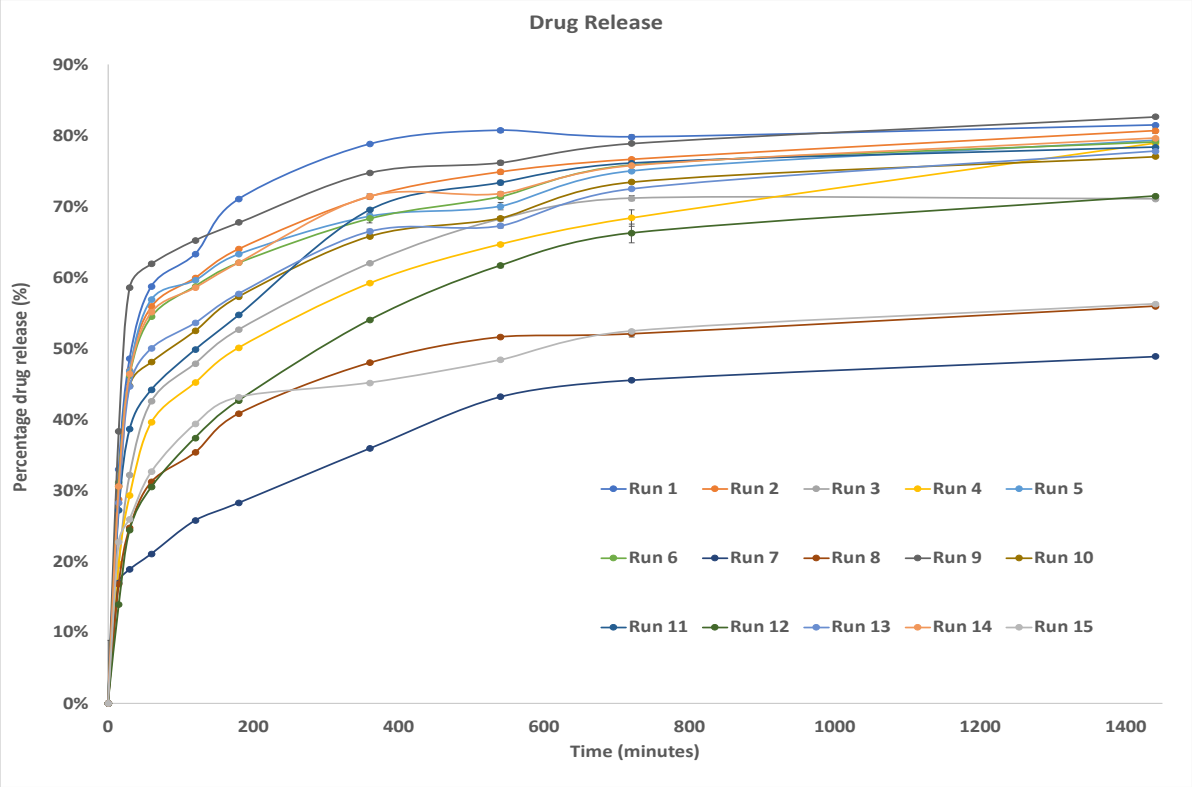

Figure 5.11 Dissolution curve for the 15 runs of the factorial design for the assembled FlexiPill tablets in 0.1 M HCl for 24 Hr.

During the dissolution test, the IR units dissolved completely after 2 Hours. However, the SR units released theophylline by diffusion through the polymer as a result the units remained intact after the 24-hour run. To compare the dissolution profile over a time curve for the design runs and to analyse the effect of the independent variables on drug release level-shape analysis using modified principal components analysis (M-PCA) was adopted. Although similarity factor f_2 is usually used to compare drug release profiles by many regulatory bodies, it could not be implicated here because it can't investigate a group of profiles with no obvious reference. Additionally, the similarity factor can't measure the degree of variability which is necessary in this case to analyse the effect of the design variables (Stevens et al. 2015). The level-shape

analysis looks at the drug release curve in terms of its level and shape separately. The level component can be calculated from the average release of the different time points. However, to separate the shape component from the effect of the level, a residual matrix was constructed by subtracting the grand mean (X), the raw (X_r) and the column mean (X_t) according to Equation 3.1. Table 5.5 represents the residual matrix.

Table 5.5 Modified residual matrix with level component removed.

Run	**15 min.**	**30 min.**	**60 min.**	**120 min.**	**180 min.**	**360 min.**	**540 min.**	**720 min.**	**1440 min.**
1	-3.86	-0.84	0.022	0.021	0.055	0.052	0.036	-0.48	-2.74%
2	-0.044	1.07	0.03	0.024	0.021	0.014	0.014	0.001	0.12
3	-0.045	-4.41	-0.011	-0.004	8.28E-05	0.012	0.039	3.70	-0.31
4	-0.031	-0.061	-0.028	-0.018	-0.013	-0.003	0.016	2.14	8.77
5	-0.015	0.019	0.049	0.029	0.023	-0.004	-0.025	-0.77	-0.37
6	-0.008	0.015	0.028	0.024	0.014	-0.004	-0.008	0.38	-0.29
7	0.112	0.005	-0.043	-0.042	-0.061	-0.065	-0.027	-3.63	-4.23
8	0.038	-0.008	-0.013	-0.018	-0.007	-0.017	-0.015	-4.32	-4.35
9	0.005	0.082	0.045	0.032	0.013	0.002	-0.017	-2.29	-2.44
10	0.015	0.03	-0.006	-0.008	-0.003	-0.0002	-0.009	0.91	0.58
11	-0.012	-0.024	-0.039	-0.029	-0.024	0.042	0.046	4.19	2.51
12	-0.036	-0.056	-0.066	-0.043	-0.034	-0.002	0.039	5.28	6.57
13	-0.008	0.029	0.012	0.002	-0.0002	0.006	-0.02	-0.09	1.32
14	-0.018	0.013	0.03	0.018	0.01	0.022	-0.008	-0.12	-0.15
15	0.088	-0.005	-0.009	0.011	0.006	-0.054	-0.057	-4.90	-5.00

Principal component analysis (PCA) is a statistical method for the dimensional reduction of large data sets into uncorrelated components. This method finds multiple directions that data follows (Eigenvectors) and how much each direction captures of the data (Eigenvalues) to understand the patterns that the data follows (Greenacre et al. 2022).

Therefore, PCA was performed on the residual matrix for the shape of curves. Three components were extracted that had accumulative eigenvalues of 90%. Therefore, only these shape components will be analysed further. Figure 5.12 and Table 5.6 represent the eigenvectors and their eigenvalues extracted from PCA.

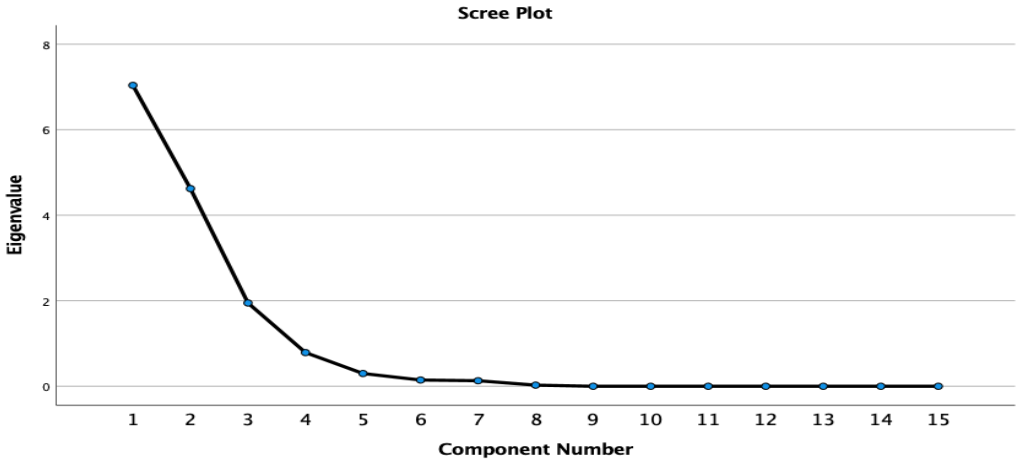

Figure 5.12 The sree plot of the extracted shape component using PCA.

Table 5.6 Eigenvalues of the components extracted from PCA .

Total Variance Explained

Component	Initial Eigenvalues			Extraction Sums of Squared Loadings			Rotation Sums of Squared Loadings		
	Total	% of Variance	Cumulative %	Total	% of Variance	Cumulative %	Total	% of Variance	Cumulative %
1	7.038	46.920	46.920	7.038	46.920	46.920	6.895	45.969	45.969
2	4.623	30.823	77.743	4.623	30.823	77.743	3.839	25.595	71.564
3	1.949	12.991	90.734	1.949	12.991	90.734	2.876	19.170	90.734
4	.788	5.253	95.987						
5	.299	1.991	97.978						
6	.146	.976	98.954						
7	.130	.866	99.820						
8	.027	.180	100.000						
9	9.302E-16	6.201E-15	100.000						
10	6.760E-16	4.507E-15	100.000						
11	3.534E-16	2.356E-15	100.000						
12	2.811E-16	1.874E-15	100.000						
13	1.299E-16	8.663E-16	100.000						
14	-1.919E-16	-1.279E-15	100.000						
15	-5.609E-16	-3.740E-15	100.000						

Extraction Method: Principal Component Analysis.

Nevertheless, only the first shape component was significantly affected by the design variables. Table 5.7 lists the experimental design with the level and shape components.

Thereafter, the surface response analysis was used to study the effect of drug load, infill density and number of IR units in the FlexiPill on the level and shape of the dissolution curve. Although more complicated than comparing similarity factors, this method considers the shape of the curve instead of just the level of the curve, since the shape of the curve can have clinical significance. The analysis showed that both drug load and the number of IR units have significant effects on both the level and the shape of the curve. Figure 5.13 A and B present the surface response graph for the shape and level of the dissolution release profile.

Table 5.7 Summary of the experiment design and level and shape variable calculated from M-PCA.

Run	Level	Shape 1	Shape 2	Shape 3
1	0.59	0.05	0.43	-0.34
2	0.56	0.17	0.52	-0.02
3	0.47	-0.30	0.30	-0.12
4	0.45	-0.35	0.12	0.18
5	0.55	0.49	0.21	0.00
6	0.55	0.45	0.22	0.03
7	0.28	-0.01	-0.28	-0.01
8	0.36	0.06	-0.30	-0.17
9	0.60	0.56	-0.04	0.07
10	0.52	0.12	-0.32	0.31
11	0.51	-0.46	0.07	0.04
12	0.40	-0.37	0.05	0.13
13	0.52	0.33	0.06	0.38
14	0.55	0.37	0.37	0.03
15	0.37	0.18	-0.27	-0.12

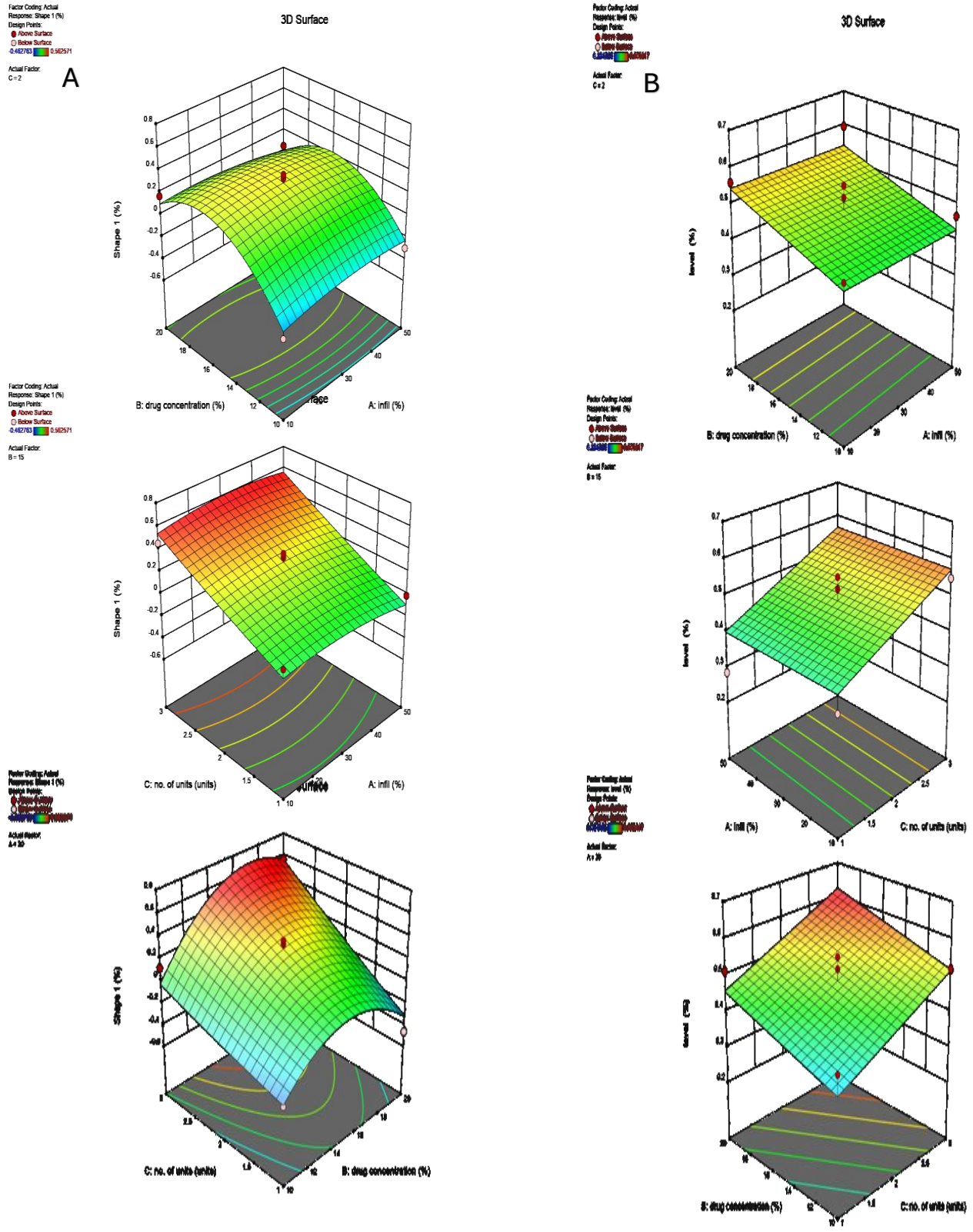

Figure 5.13 The curve shape(A) and level (B) response to the three design variables; infill, drug concentration and No. of IR units.

Increasing the drug load and the number of IR units will increase the percentage of the drug that is released immediately resulting in higher levels and low slope shapes. However, infill density had no significant effect on the dissolution curve. Although previous publications showed that drug release can be affected by infill density, as demonstrated in 2.2.3.3 Infill Density, in this work this was not the case. This can be the result of the high porosity of the printed structure which led to an insignificant effect of the infill on the porosity or the surface area. Using the experimental design, an equation was generated to predict the dissolution curve shape and level using drug load (formulation variable) and the number of IR units (post-printing variable). The square of the drug load also had a significant effect on the shape. Figure 5.14 and Table 5.8 shows the design prediction and the prediction equation, respectively.

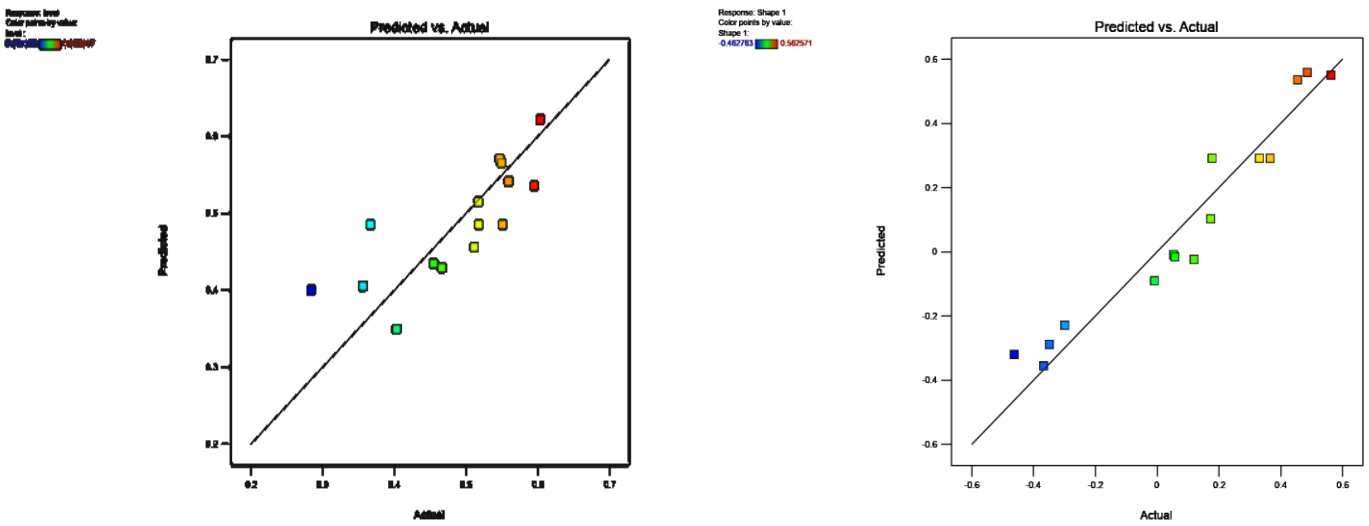

Figure 5.14 Design prediction Vs. actual experiments; level (left) and shape (right).

Table 5.8 Prediction equation and statistical significance of each term.

	Intercept	**Infill(A)**	**Conc. (B)**	**No. Units (C)**	**AB**	**AC**	**BC**	**A^2**	**B^2**	**C^2**
Level	0.485	-0.002	0.053	0.082						
p-values		0.907	**0.042**	**0.004**						
Shape 1	0.291	-0.012	0.152	0.300	-0.042	0.024	0.134	-0.056	-0.340	0.012
p-values		0.809	**0.029**	**0.002**	0.578	0.747	0.119	0.484	**0.006**	0.877

This work shows that the new FlexiPill design can be used to adjust drug release according to patient needs without the need to change the formulation or the print

settings. This can help move the personalisation of medication to the point of care while keeping the 3D printing in quality-controlled manufacturing sites. On the other hand, in this work, infill had no effect on the drug release, and drug load had a significant effect on drug release but led to a decrease in the viscosity of the polymer blend, which affected the quality of the print. The FlexiPill design has four units that can be IR, SR or placebo, leading to 81 possible configurations and 81 possible release profiles. Providing flexible control over drug release at the point of care.

5.3 Conclusion

In conclusion, personalised medicine is one of the most vital aspects in the development of the healthcare system that must be addressed. 3D printing can serve as an excellent facilitator for this process. However, a significant gap remains between the regulation and application of 3D printing at a clinical level. The FlexiPill design has the potential to bridge this gap and facilitate the transition of 3D printing to medication personalisation applications. Furthermore, the FlexiPill design can act as a substitute for compounding, which is time-consuming and prone to human error. In this chapter, the FlexiPill design effectively controlled the drug release of theophylline by altering the configuration of the units. This approach was also more efficient compared to traditional formulation and pre-printing methods for controlling drug release. It was observed that while infill had no significant effect on the outcomes, drug load significantly influenced dissolution, albeit at the expense of altering viscosity and print quality as a consequence.

Chapter 6 : FlexiPill as Personalised Analgesic Polypill

6.1 Introduction

As has been discussed in Chapter 1, polypharmacy refers to the prescribing of multiple medications to address specific health conditions, a common practice particularly in geriatric patients and those with chronic diseases. This arose from either the presence of concomitant conditions or the synergistic effects sought after by healthcare providers (Rochon et al. 2021). However, one of the major problems that faces polypharmacy is patient adherence to therapy, which can lead to high mortality in this group of patients in certain cases (Roshandel et al. 2019). Hence, to enhance patient adherence, the concept of a polypill has been proposed for individuals requiring polypharmacy, incorporating more than one active pharmaceutical ingredient (API) within a single pharmaceutical formulation. Moreover, combining multiple medications in the same oral dosage form can decrease the cost of packaging and transportation (Tan, Maniruzzaman, and Nokhodchi 2018). One of these chronic diseases that can benefit from polypharmacy and polypills is chronic pain. Chronic pain has a high prevalence in developing countries, amounting to 18% of the population (Sá et al. 2019). Chronic pain is also related to anxiety, depression, opioid abuse and overall poor quality of life (Gilron, Jensen, and Dickenson 2013). Therefore, it has been suggested that the optimal strategy to treat chronic pain is a combination of oral analgesics. Combining products featuring distinct mechanisms of action not only affords multimodal coverage across a diverse range of pain but also has the potential to elicit a synergistic effect. Moreover, from a safety standpoint, the utilization of lower doses of each constituent analgesic within the combination may result in a reduced incidence of individual adverse events (Raffa 2001). Additionally, a polypill can lead to the enhancement of patient adherence by minimizing the overall number of medications required for pain management.

However, the utilization of fixed-dose polypills will limit the number of cases where patients necessitate precisely identical combinations at exact dosages. Therefore, the current paradigm needs to change to a more flexible polypill that can be personalised

to each individual patient (Sadia, Isreb, et al. 2018). Additionally, the combined APIs may have different formulation requirements to ensure safety and efficacy, requiring multiple steps and complex manufacturing processes (McDonagh, Belton, and Qi 2023). The advent of three-dimensional (3D) printing stands out as a pivotal technology that holds promise for facilitating the transition towards more personalised polypill formulations. Numerous endeavours have been undertaken to leverage 3D printing for the customisation of a polypill (Robles-Martinez et al. 2019; Gioumouxouzis et al. 2018; Goh et al. 2021). These endeavours primarily focused on personalising polypills during the printing process, advocating for the conduction of printing procedures at the point of care. However, this practice cannot be expanded to include all the patients who need such personalisation due to regulatory concerns. This led to the need for other solutions that can bridge this gap between the wide application of personalised polypill and regulatory bodies. Moreover, among the various 3D printing techniques, fused filament fabrication (FDM) has gathered significant attention due to its simplicity and cost-effectiveness, as have been discussed in Chapter 2. Nevertheless, this method is not without its formulation constraints, including elevated printing temperatures, restricted drug loading capacities and limited resolution (Cailleaux et al. 2020). The high printing temperature needed for the thermoplastic polymer to be extruded out of the print head can result in API degradation. Researchers previously have attempted the use of plasticisers to lower printing temperature. Nonetheless, high use of plasticisers can render the filament soft and unprintable. Additionally, the optimal method for incorporating an active pharmaceutical ingredient (API) into filament entails hot melt extrusion (HME). However, even with this technique, there exists a limitation on drug load, necessitating the production of larger printlets to attain the requisite dosage. Therefore, there are two primary objectives for this chapter: firstly, to develop an analgesic polypill employing the FlexiPill design, wherein personalisation can be conducted after the printing phase through the assembly of printed units tailored to individual patient requirements. Secondly, the work seeks to address certain formulation challenges inherent in FDM, including concerns related to high printing temperatures and restricted drug loading capacities.

6.2 Result and Discussion

6.2.1 Filament Preparation

After mixing each formulation powder with a mortar and pestle, it was fed into the extruder. The extrusion temperature was determined by gradually raising the temperature with a 5^{o}C increase at a time until a constant flow of the filament was observed from the die. Thereafter, the temperature was adjusted to decrease die swell by decreasing the extrusion speed. Die swell usually occurs at high extrusion temperatures due to high extrusion speed, leading to an increase in the filament diameter, which renders the filament unprintable (Aho et al. 2019). Then, the printing was performed at a temperature higher than the extrusion temperature by 40^{o}C and adjusted to the lowest possible temperature. Unlike the previous chapter, printability was not assessed using tensile strength, as it proved to be a less reliable predictor than the actual performance observed during printing.

6.2.2 Design and Printing

The FlexiPill was designed to consist of four units joined by interlocking joints to form a single disc tablet. This facilitates the personalisation of medicines for each individual patient with ease through assembling the required units at the point of care of these units. The dimensions of the FlexiPill, after assembling the units, are 5 mm in height and 15 mm in diameter, remaining below the FDA's recommended upper limit of 17 mm in diameter for disc-shaped tablets (FDA. 2022). Figure 6.1 shows the design of the FlexiPill and FlexiPill after printing and assembly.

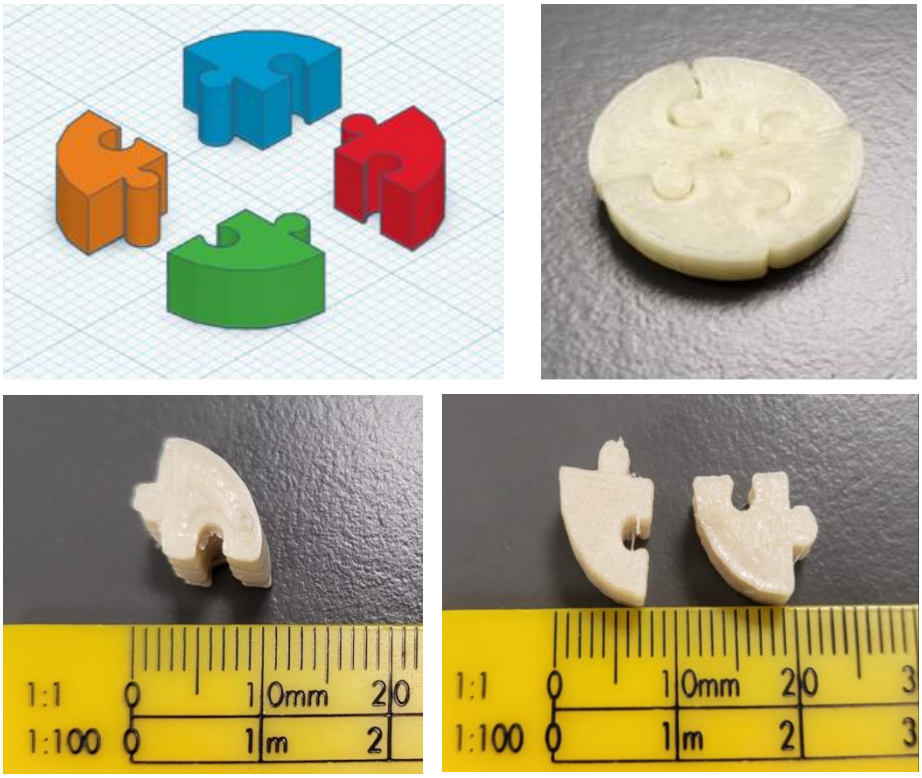

Figure 6.1 Shows the design of the Flexipill (top left), Flexipill after printing and assembly (top right), Ibu-F unit (bottom left) and Para-F and Caff-F units (bottom right).

To meet the drug release goals for each API, a different polymer blend was used in each formulation. In the formulation of paracetamol (Para-F), the objective was to achieve immediate release upon reaching the gastric fluid while keeping the release at a minimum in the oral cavity for taste masking. Therefore, polyvinylpyrrolidone (PVP) 40K was selected as the primary polymer for immediate release, as in the previous chapter. However, Eudragit EPO (E EPO), a cationic copolymer, is only soluble in media with a pH below 5, making it a rational candidate for taste masking due to its ability to reduce the dissolution rate in the alkaline environment of the mouth (Porfiryeva et al. 2019; C.N. Patra et al. 2017). Despite this advantage, E EPO is known for its brittleness, which poses challenges for filament production and 3D printing when used alone (Yang et al. 2021). Conversely, PVP 40K has a high glass transition temperature (Tg) of 93°C, necessitating elevated processing temperatures during both extrusion and printing (B.C. Pereira et al. 2019). E EPO, with a lower Tg of 48°C (C.N. Patra et al. 2017), can reduce the overall processing temperature when blended with PVP 40K. According to the Fox equation (Pochan, Beatty, and Pochan 1979), a 1:1 mixture of the two polymers should theoretically display a Tg of 63.3°C.

$1/Tg_{mixture} = W_1/Tg_1 + W_2/Tg_2$ ---------(Fox equation).

Where W_1 and W_2 are the weight fractions of the two polymers, $Tg_{mixture}$ is the glass transition temperatures of the polymer blend and Tg_1 and Tg_2 are the glass transition temperatures of the individual polymers. This strategy led to a significant decrease in the extrusion and printing temperature. Only a few previous attempts were able to print at a temperature of 100°C or lower (Kempin et al. 2018; Kollamaram et al. 2018). However, these attempts typically required high proportions of polymeric carriers to reduce the processing temperature, which in turn led to low drug loading. In contrast, the present study necessitated a relatively high drug load to deliver the therapeutic dose of paracetamol, presenting additional formulation challenges. Beyond that, PVP 40K is a hygroscopic polymer, and water acts as a plasticiser when absorbed into the formulation where PVP 40K is the main polymer (B.C. Pereira et al. 2019). This can lead to an increase in the mobility of the polymer chains and destabilisation of the formulation. Therefore, the incorporation of E EPO, a non-hygroscopic polymer, can offer a protective effect to the formulation. As a result, Para-F consisted of 55% paracetamol and equivalent amounts of PVP 40K, and E EPO and was printed at 100°C. In conclusion, compared to the IR formulation of theophylline in the previous chapter, the inclusion of E EPO led to a decrease in the printing temperature, improved drug loading, taste masking, and potentially enhanced the effectiveness stability, compared to the previous chapter where PVP alone was used.

For the ibuprofen formulation (Ibu-F), it has been previously demonstrated that ethyl cellulose (EC) can be the primary polymer used to print a sustained-release tablet using various release modifiers (Yang et al. 2018). Therefore, this work used ethyl cellulose as the main polymer, with ibuprofen and Eudragit L100-55 (E L100-55) as the release modifier.

E L100-55 is an anionic methacrylate copolymer that is insoluble at a pH lower than 5.5, a property that could be utilised in decreasing drug release in the gastric medium and achieving targeted drug release in the duodenum (C.N. Patra et al. 2017). Subsequently, PEG 4K was used as a channelling agent to improve drug release from the EC matrix.

Lastly, caffeine was formulated with only PVP 40K as the main polymer to give immediate release in both acidic and basic media. Table 6.1 lists the components of each formulation with its extrusion and printing temperature.

Table 6.1 Formulation contents with their extrusion and printing temperature.

Formulation	**PVP 40K**	**Eudragit EPO**	**Eudragit L100-55**	**Ethyl cellulose**	**PEG 4000**	**Triethyl citrate**	**Talc**	**API**	**Extrusion temperature**	**Printing temperature**
Para-F	20%	20%				5%		55%	63°C	100°C
Ibu-F			20%	55%	5%			20%	100°C	165°C
Caff-F	50%					12.5%	17.5%	20%	75°C	140°C
Para-F= paracetamol formulation; Ibu-f= ibuprofen formulation; Caff-f= caffeine formulation										

6.2.3 Scanning Electron Microscope

The printed units of the FlexiPill were scanned using SEM to check the morphology and the printing layers' uniformity. The Para-F images show the filament having a 2.13 mm diameter higher than the extruder die diameter. This was the result of the die swell that the filament encountered after leaving the die (Aho et al. 2019). The surface of the filament was generally smooth with some cavities that may have resulted from the diameter expansion after leaving the die. Moreover, the layers of the printed units were uniform with a mean height of 165 ± 2 mm, which is smaller than the layer height set by the printing software, 0.2 mm, indicating the shrinking of the printed layer during cooling after deposition. Figure 6.2 shows the SEM images for the filament and the printed unit of Para-F.

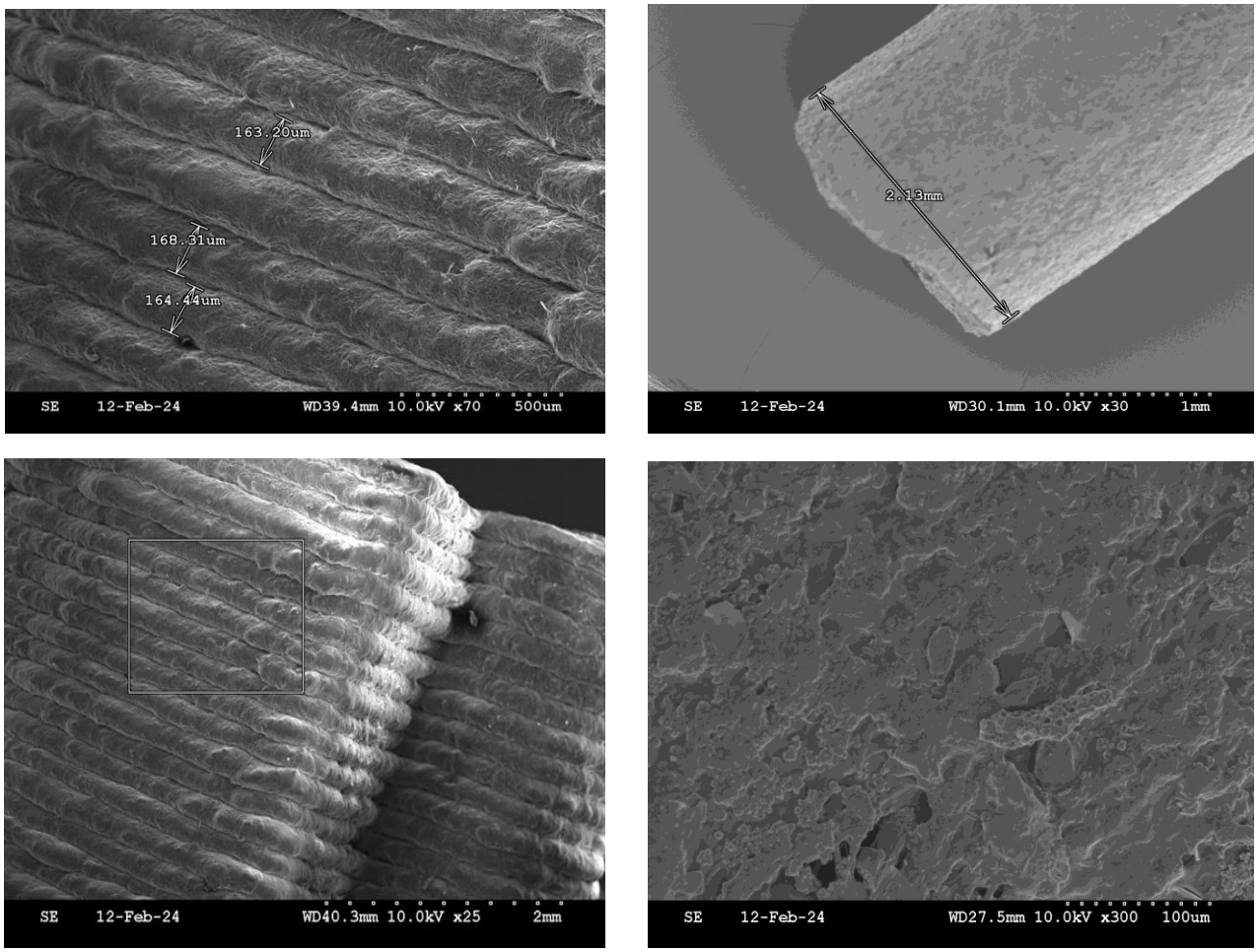

Figure 6.2 SEM images for the Para-F unit (left: top = x70 and bottom = x25 magnification) and filament (right: top = x30 and bottom = x300 magnification). Para-F = paracetamol formulation.

Moreover, Ibu-F had a rough surface and less die swell, but the printed layers were very irregular due to the formulation's low melt viscosity and low viscoelastic properties. These properties reduced the flow and surface irregularity. Figure 6.3 presents the Ibu-F printed unit and filament.

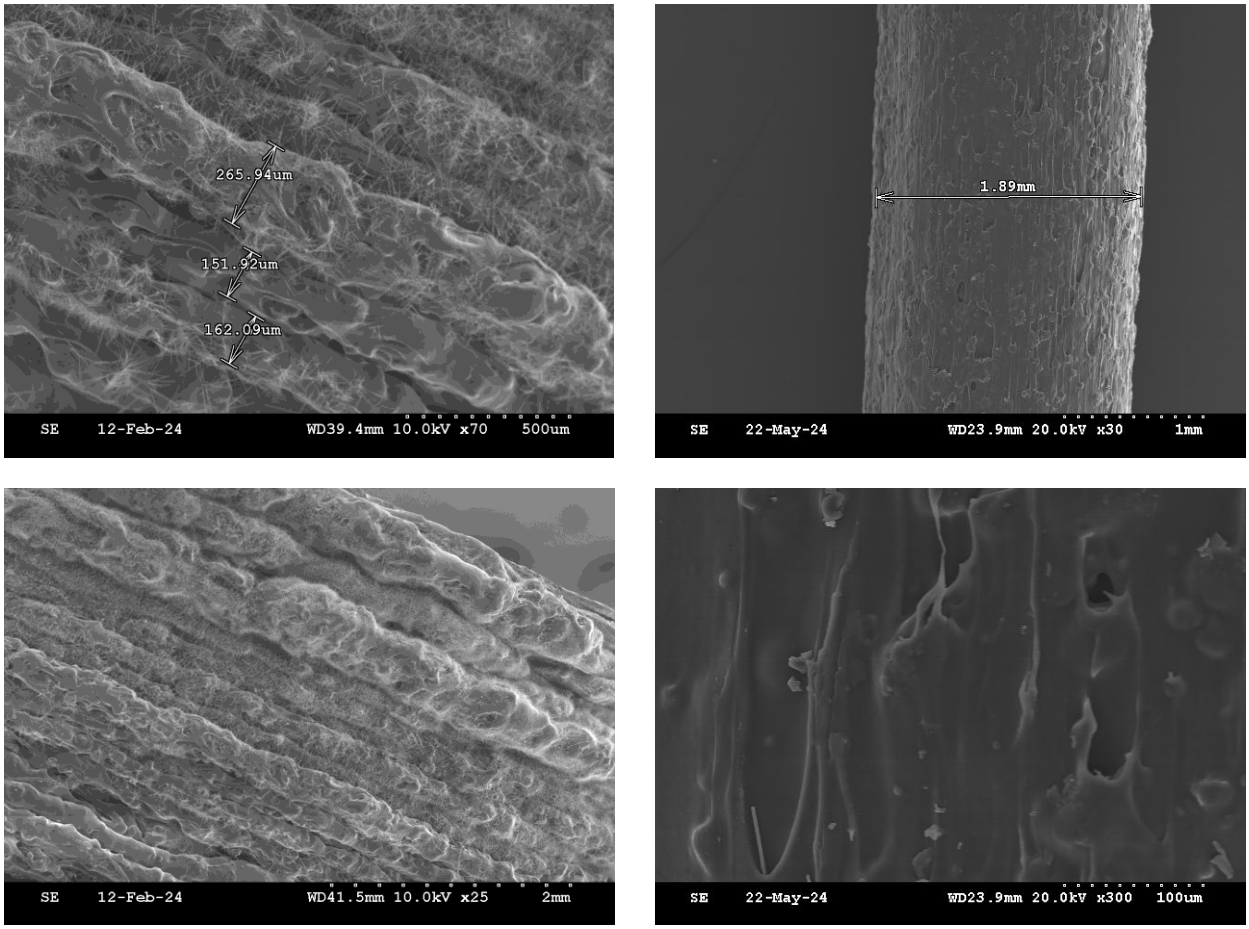

Figure 6.3 SEM images for the Ibu-F unit(left) and filament (right). *Ibu-f= ibuprofen formulation.*

Furthermore, the Caff-F filament exhibited a diameter of 1.96 mm because of the die swell. Additionally, the filament had a rough surface with more valleys arranged in the same direction of extrusion, and this could be attributed to the less viscoelastic formulation with a decreased flow that resulted in an irregular surface. Lastly, the Caff-F had thicker printing layers due to its low viscosity as well. Figure 6.4 presents the SEM images for the filament and the printed unit of Caff-F.

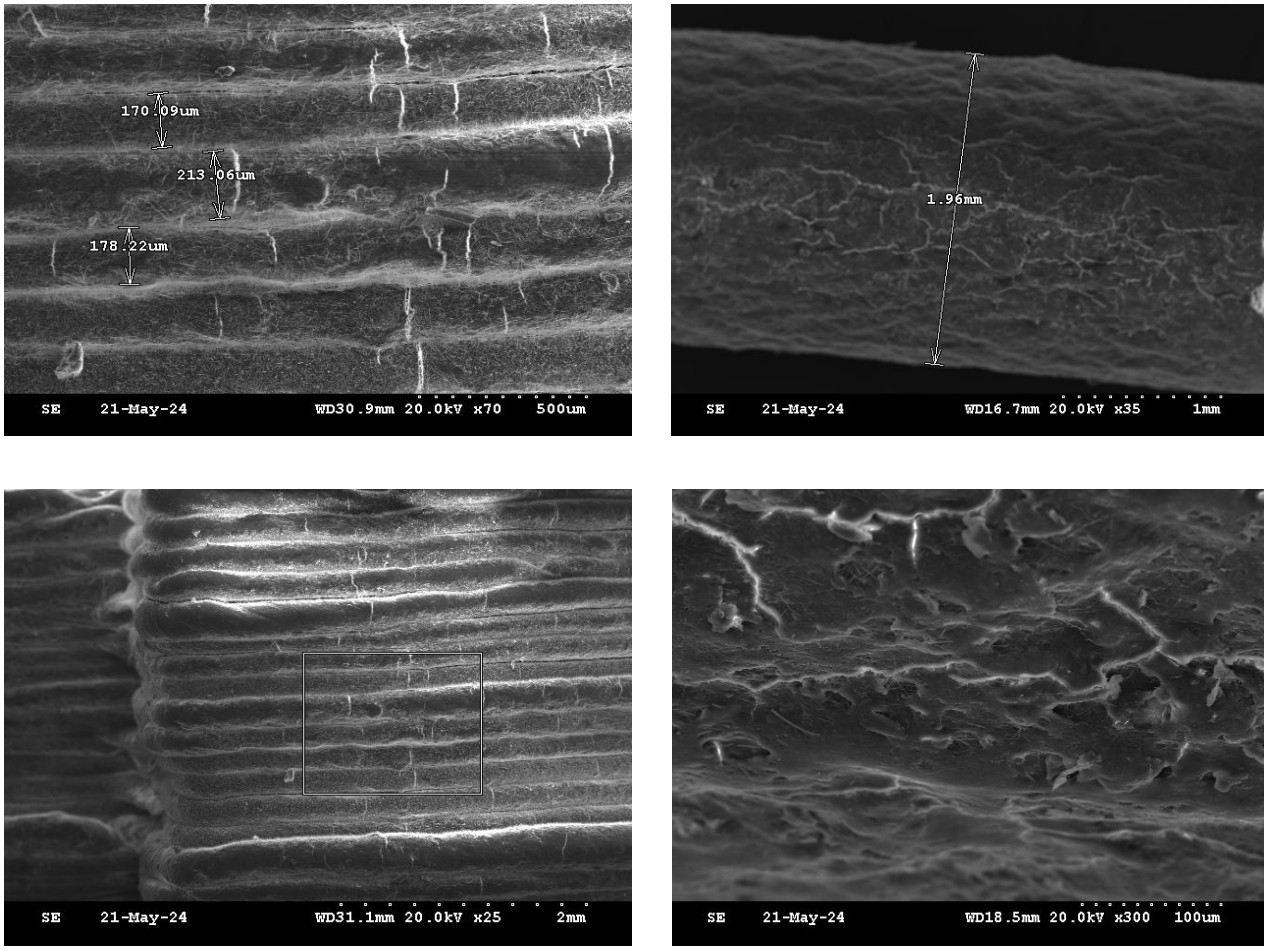

Figure 6.4 SEM images for the Caff-F unit(left) and filament (right). Caff-f= caffeine formulation

6.2.4 Thermal Analysis

Thermal analysis for the three formulations was performed to evaluate any interaction between the APIs and the polymer mix. Differential scanning colourimetry (DSC) confirmed that both ibuprofen and caffeine have formed an amorphous solid dispersion as indicated by the absence of the melting endothermic peaks at 78.23°C and 235.14°C, respectively. However, in the Para-F, the melting peak exhibited a decrease in intensity and a shift from 169°C to 154°C, indicating that paracetamol retained some crystallinity and did not shift completely into the amorphous state. However, a polymorphic change from the stable form I to the metastable form II of paracetamol have accrued to the part that did not form amorphous solid dispersion. Figure 6.5 presents DSC for all three formulations, each with the DCS of its pure API.

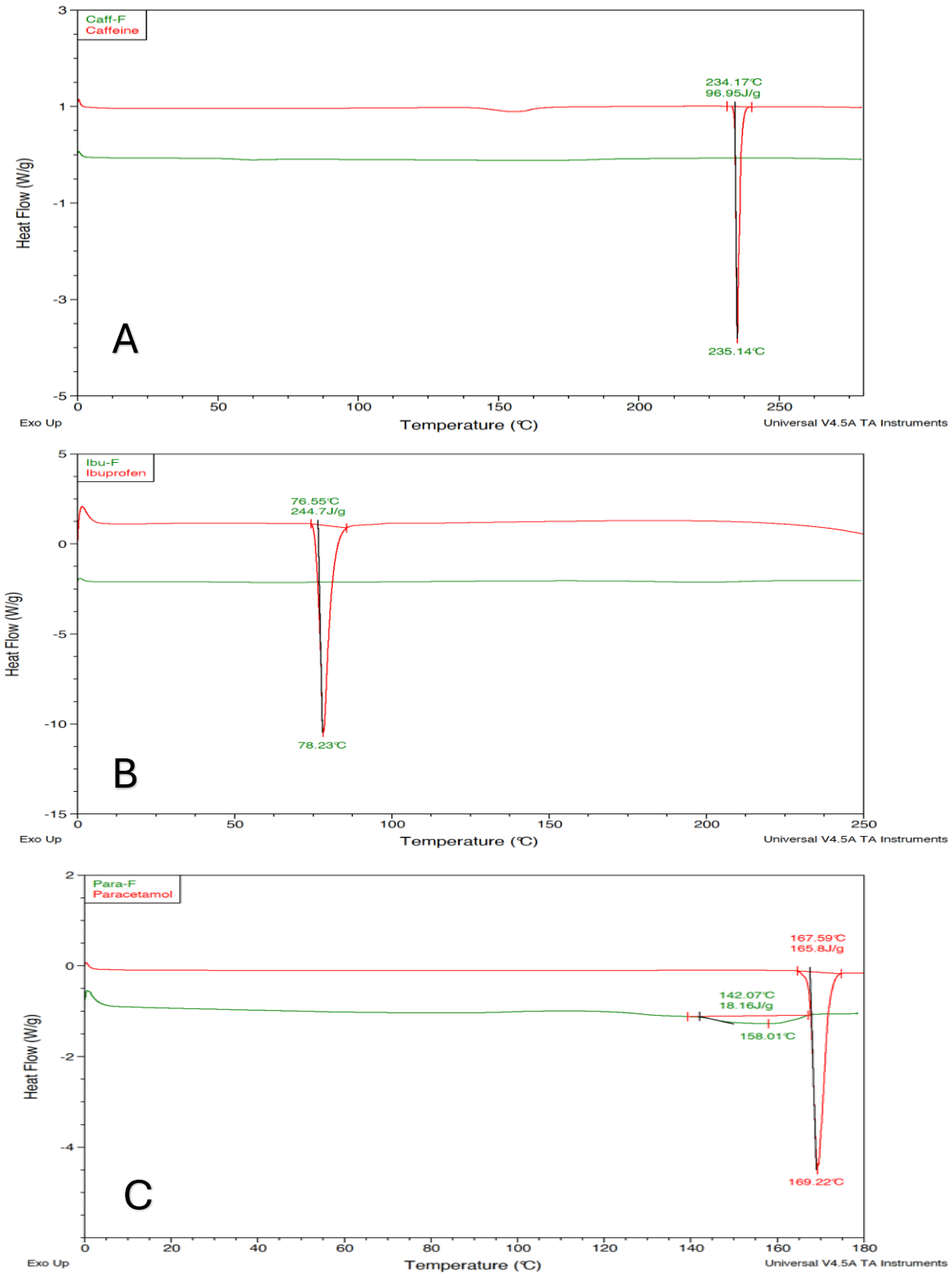

Figure 6.5 DSC for each of the formulations overlapped with the DSC of its pure API. (A) Caff-F, (B) Ibu-F and (C) Para-F. Para-F= paracetamol formulation; Ibu-f= ibuprofen formulation; Caff-f= caffeine formulation(n=3).

Thereafter, thermal gravimetric analysis (TGA) was performed to determine the thermal degradation of each of the components and the formulations. TGA for Eudragit E PO (E EPO) shows a decrease of less than 1% up to 200°C, reflecting the low moisture content of the pure polymer. The thermal degradation of E-EPO shows two

steps of degradation. The first step is between 242- 317°C, with a 25% decrease in weight, corresponding to removing the dimethylamino groups. The second step from 345°C to 448°C with a 68% decrease corresponds to the full decomposition of the polymer (Porfiryeva et al. 2019). PVP 40K thermal degradation starts with an 8% decrease in weight between 52-104°C, corresponding to moisture evaporation from the polymer. However, the main degradation event starts at 365°C. Paracetamol degradation start at 194°C. Finally, the degradation of the Para-F formulation shows two steps of degradation as well. However, the first degradation step starts at a lower temperature than that of E EPO, 194°C, due to the overlapping of paracetamol degradation with the removal of the dimethylamino groups from E EPO polymer and the second step corresponds to the second step of E EPO degradation and PVP 40K degradation. Figure 6.6 A shows the thermal gravimetric analysis of Para-F and its components.

Furthermore, the degradation of pure ibuprofen starts at 168°C and reaches the peak degradation rate at 256°C. EC degradation was initiated at 290°C and did not degrade completely at 600°C. E L100-55 and PEG 4000 both start their thermal degradation around 300°C. Therefore, the Ibu- F shows two steps of degradation; the first corresponds to the early degradation of Ibu, and the second indicates the degradation of the polymer's mixture. Figure 6.6 B presents the TGA for Ibu-F and its components. Lastly, the degradation of caffeine starts at 185°C and finishes at 288°C. However, Caff-F shows two thermal degradation steps; the first step, from 174.7°C to 336°C with a 33% decrease in weight, corresponds to the degradation of caffeine and the evaporation of TEC and a second between 388°C and 470°C with weight loss of 40% this corresponds to the degradation of PVP 40K and the 20% residual weight reflects the weight of talc powder in the formulation which only degrades at temperature higher than 600°C. Figure 6.6 C presents the TGA for Caff-F and its components.

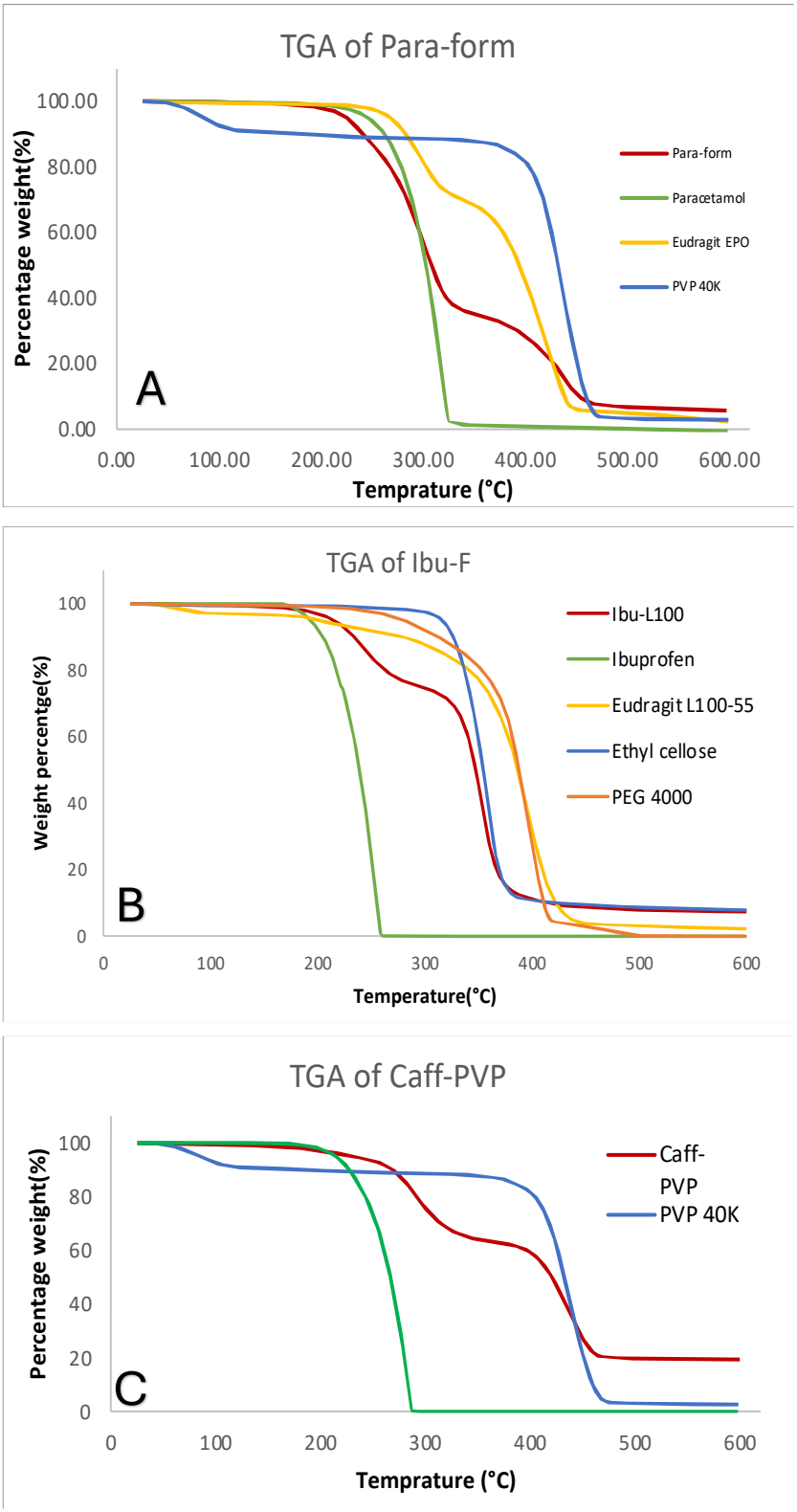

Figure 6.6 TGA for the three formulations and their components. (A) Para-F, (B) Ibu-F and (C) Caff-F. Para-F= paracetamol formulation; Ibu-f= ibuprofen formulation; Caff-f= caffeine formulation

6.2.5 Fourier Transform Infrared Spectroscopy

FTIR spectra were evaluated to confirm the DSC result of API-Polymer interaction and the polymorphic change in paracetamol. Paracetamol is known to have three polymorphs in addition to the amorphous form. Form I with monoclinic crystal lattice is the thermodynamically stable form. Both forms II and III have an orthorhombic lattice, but form II is metastable, and form III is only stable under certain conditions (Zimmermann and Baranović 2011; Al-Zoubi, Koundourellis, and Malamataris 2002). FTIR spectrum of paracetamol formulation shows many peak shifts compared to the powder mix indicating that extrusion and 3D printing led to interaction between the polymer mix and paracetamol. The peak at 1654.9 corresponding to stretching vibrations of C=O has shifted to 1651 cm^{-1}. Moreover, CH_3 deformation vibrations which is reflected as transmission peak at 1375 cm^{-1} shifted to 1370.2 cm^{-1}. Furthermore, the ratio between at 806 cm^{-1}, with represents intramolecular interaction of the monoclinic form, and the peak at 837 cm^{-1}, which appears in both forms, has decreased after extrusion and printing indicating a polymorphic change of form I monoclinic to form II orthorhombic during processing (Burgina et al. 2004; Sudha, Parimaladevi, and Srinivasan 2015). The results of FTIR with the result from DSC indicate that paracetamol has formed amorphous solid dispersion with the polymer mix partially, while the remaining crystal have gone through partial polymorphic transformation to the metastable orthorhombic form II. Figure 6.7A shows the FTIR spectrum for Para-F and its physical mixture.

The FTIR spectrum of the Ibu-F demonstrates a blue shift in the CH3 bound symmetrical stretch from 1377 CM^{-1} to 1373 CM^{-1} and a red shift in the asymmetrical stretching peaks from 2951 CM^{-1} to 2974 CM^{-1}. This reflects the nonpolar interaction between the CH_3 group in the ibuprofen and the ethyl ether group on the ethylcellulose polymer (Ramukutty and Ramachandran 2012). In addition, the very strong 1701 CM^{-}

[1] band representing C=O stretching also shifted to 1732. Therefore, the FTIR spectrum suggests the formation of solid dispersion. Figure 6.7B shows the FTIR spectrum for

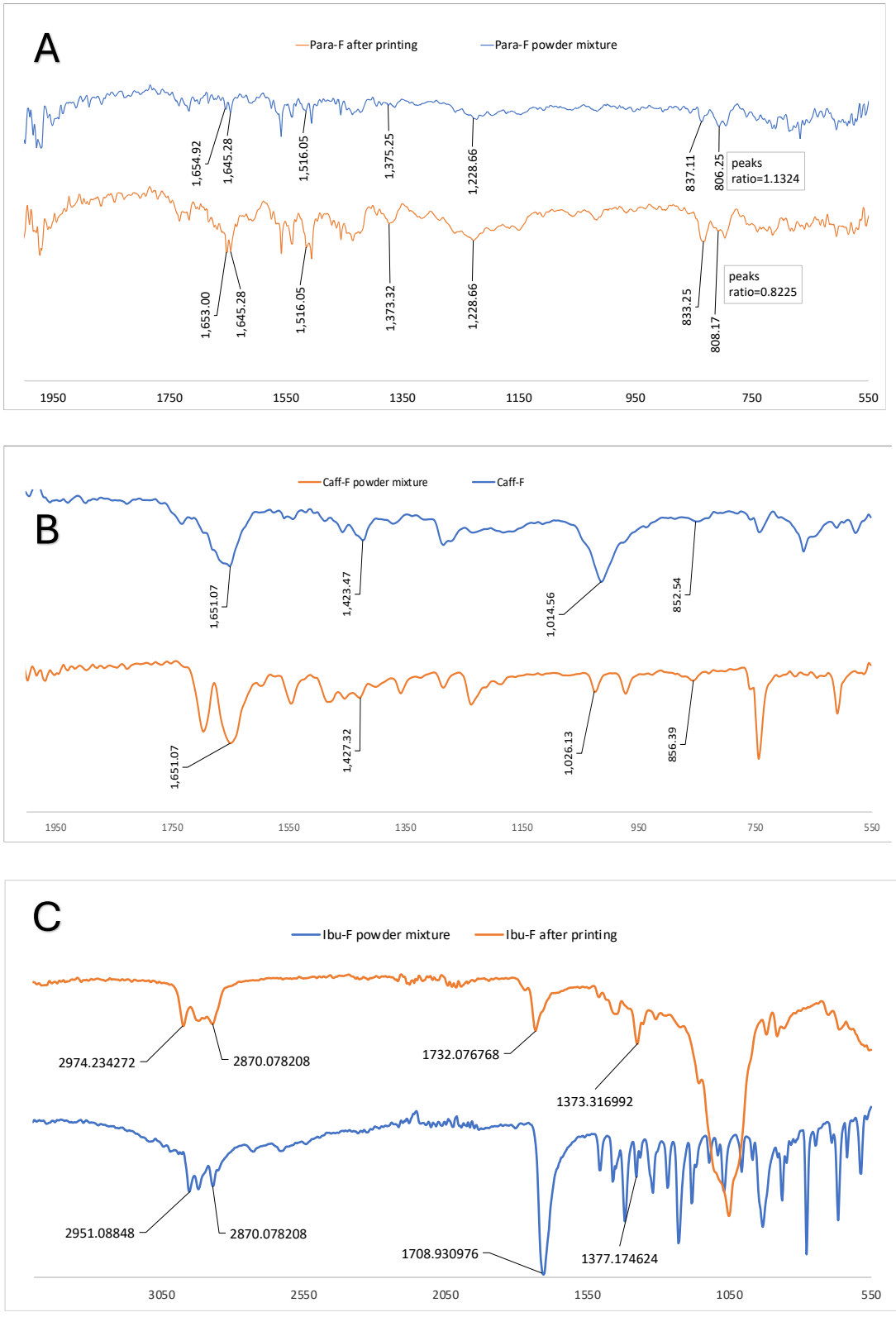

Figure 6.7 The FT-IR spectrum for the three formulations overlayed with the formulation physical mixture for each one. (A) Para-F, (B) Caff-F and (C) Ibu-F. Para-F= paracetamol formulation; Ibu-f= ibuprofen formulation; Caff-f= caffeine formulation.

Ibu-F and its physical mixture.

Subsequently, the FTIR spectrum for the Caff-F shows a shift in the peak at 1014.56 which corresponds to C=O stretching to 1,026.13. Additionally, the peaks at 852.54 and 1,423.47 which correspond to C-C stretching and C=C stretching, respectively, have also shifted in the formulation spectrum (Paradkar and Irudayaraj 2002). This confirms the result obtained from DSC regarding the formation of amorphous solid dispersion for this formulation as well. Figure 6.7C shows the FTIR spectrum for Caff-F and its physical mixture.

6.2.6 Dynamic Vapour Sorption

Dynamic vapour sorption (DVS) was performed to test the stability of the metastable form of paracetamol in the formulation. Instead of a 1:1 mixture of PVP 40K and E EPO, a control formulation with PVP 40K only was used. Para-F shows a mean maximum water vapour sorption of 10.09%, while the control formulation mean sorption was 15.6% with a significant difference between the two (P-value <0.05). This

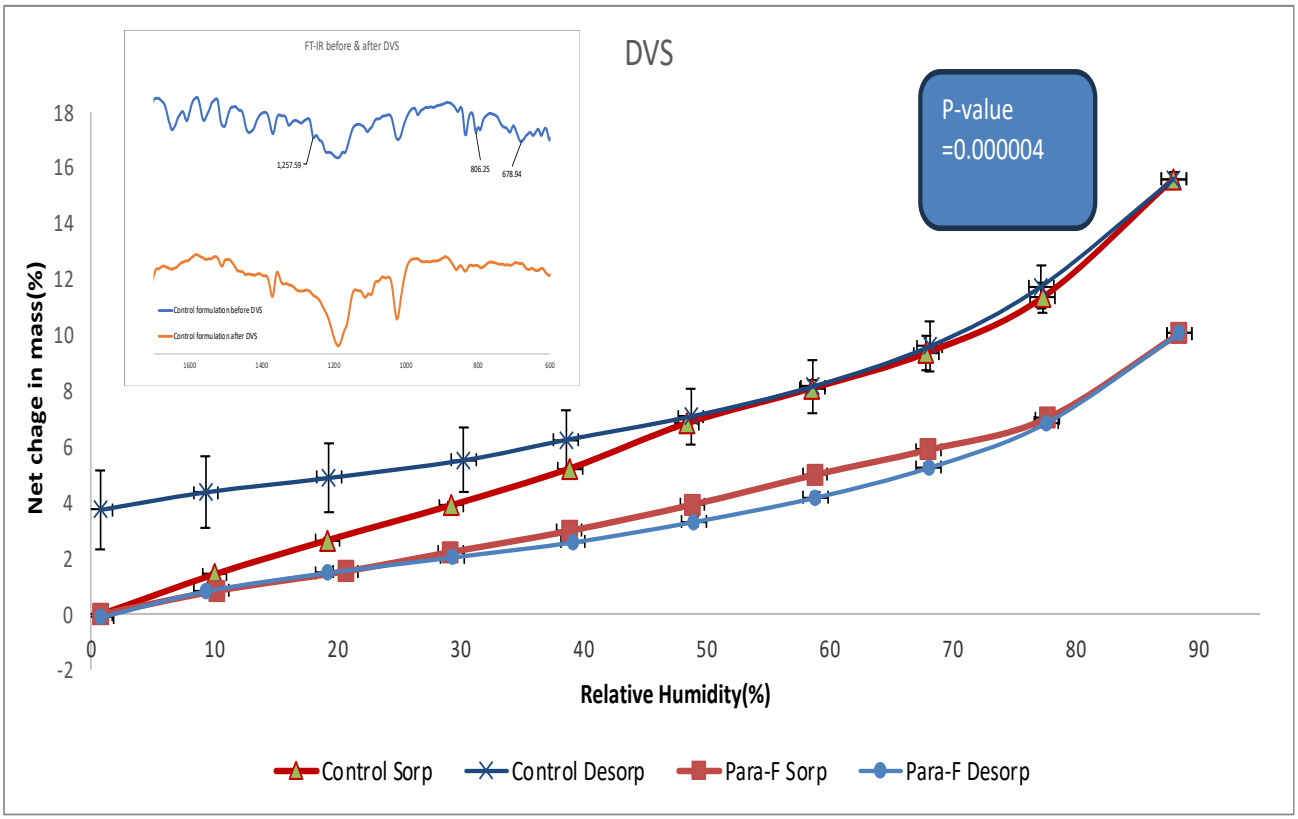

Figure 6.8 DVS Isotherm plot at 25° C for the Para-F and its control with the FTIR spectrum before and after the sorption-desorption cycle. Para-F= paracetamol formulation.

result reflects the effect of E EPO in decreasing the hygroscopicity of the formulation. Additionally, the control formulation had an open hysteresis indicating a major change in the formulation after the sorption-desorption cycle. FT-IR spectrum of the control formulation before DVS indicating the presence of form I of paracetamol. However, the FTIR spectrum for the control formulation after the DVS cycle reveals a shift to the stable form I by the disappearance of the characteristic peaks at 678.94, 806.25 and 1,257.59 which correspond to an extra inter or intra-molecular interaction within the monoclinic lattice of the stable form I (Al-Zoubi, Koundourellis, and Malamataris 2002). However, the FTIR for the Para-F before and after the DVS show no change, which indicates that form I of paracetamol is intact after the sorption-desorption cycle which is also evident by the close hysteresis in the DVS. These results prove that the incorporation of E EPO in the formulation not merely decreased the hygroscopicity of the formulation but also protected the API from polymorphic change under harsh conditions. Figure 6.8 presents the isotherm plot for the sorption desorption cycle for both Para-F and its control with the FTIR spectrum for control formulation before and after the cycle.

6.2.7 Rheology

The rheological properties of the formulations were tested to better understand the printing process and the reason behind the differences in printing resolution among the formulations. Therefore, the complex viscosity of the three formulations was measured while performing a frequency sweep at the printing temperature for each of the formulations to determine the viscoelastic response of the formulation. In response to increasing frequency, all three formulations exhibited shear-thinning behaviour, as indicated by their shear index (n) values which are less than 1. The shear index is a parameter derived from the power-law model that quantifies the flow behaviour of non-Newtonian fluids—values less than 1 indicate shear-thinning (pseudoplastic) behaviour, where viscosity decreases with increasing shear rate. Furthermore, all the formulations had shear viscosity lower than 1000 Pa. S at high frequencies which agrees with the viscosity limits set previously by Qahtani et. al for PLA printing (Qahtani et al. 2019). The complex viscosity of the formulations decreases in the order of Para-F > Caff-F > Ibu-F. This trend aligns with the layer consistency observed in the SEM images, indicating that the FDM printer requires higher viscosity formulations to

achieve more consistent layer deposition. Lastly, the viscous component of the shear modulus was higher than the elastic component at all test frequencies for all the formulations. This indicates that, at printing temperature, the formulations behave more like a liquid while flowing through the nozzle. Figure 6.9 presents viscosity complex components against frequency, shear modulus elastic and viscous components against frequency and the shear index.

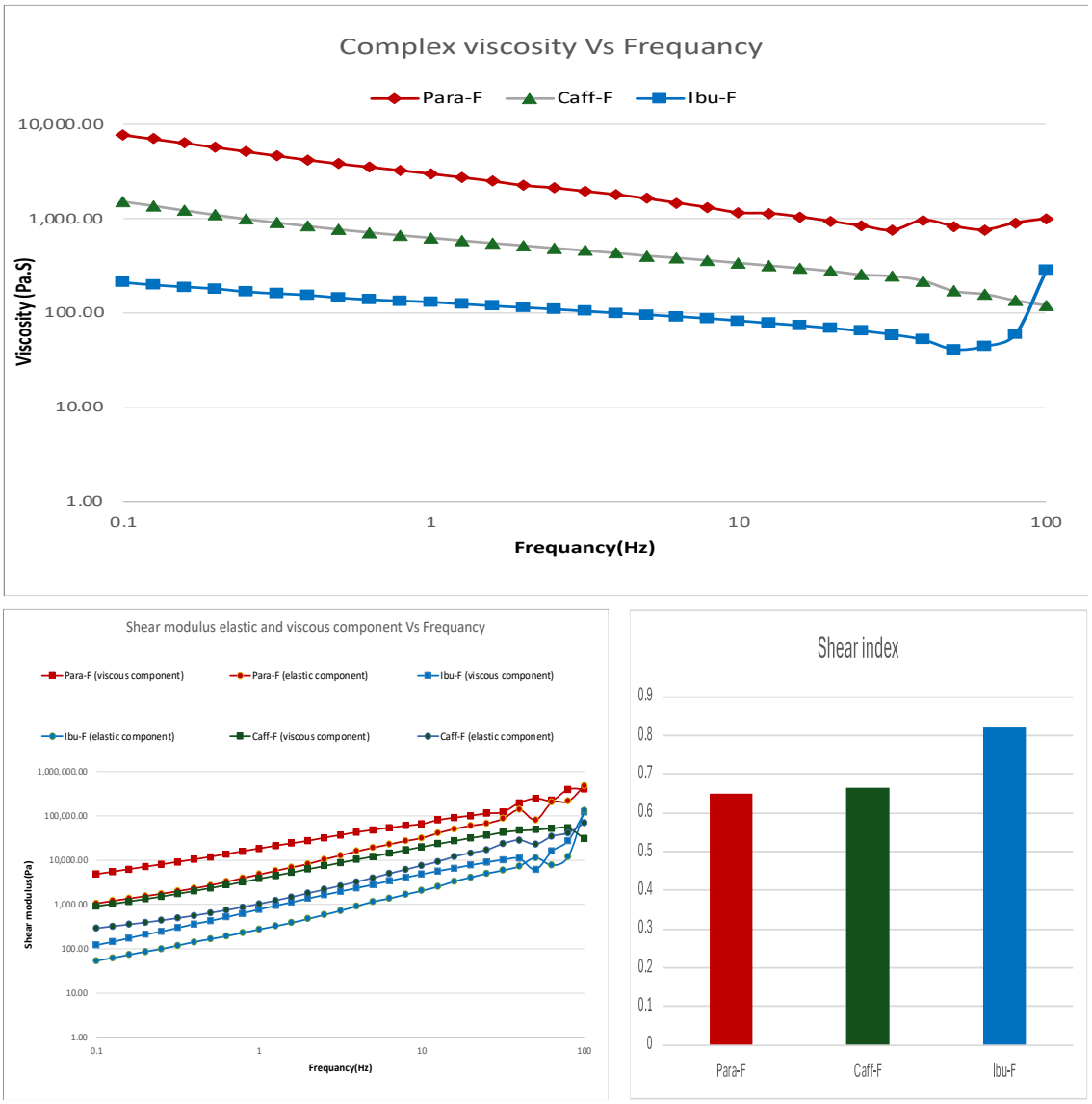

Figure 6.9 Viscosity complex component VS frequency(top), shear modulus elastic and viscous components Vs. frequency (bottom left) and the shear index (bottom right). Para-F= paracetamol formulation; Ibu-f= ibuprofen formulation; Caff-f= caffeine formulation.

6.2.8 Chromatography, Drug Content and Dissolution

Subsequently, an HPLC method was developed for concomitant evaluation of the three APIs. The HPLC method achieved adequate separation for the three APIs in the

tablet. The retention times for paracetamol, caffeine and ibuprofen were 1.9, 2.9 and 4.6, respectively. Figure 6.10 shows the chromatogram of the HPLC method and the three APIs retention peaks.

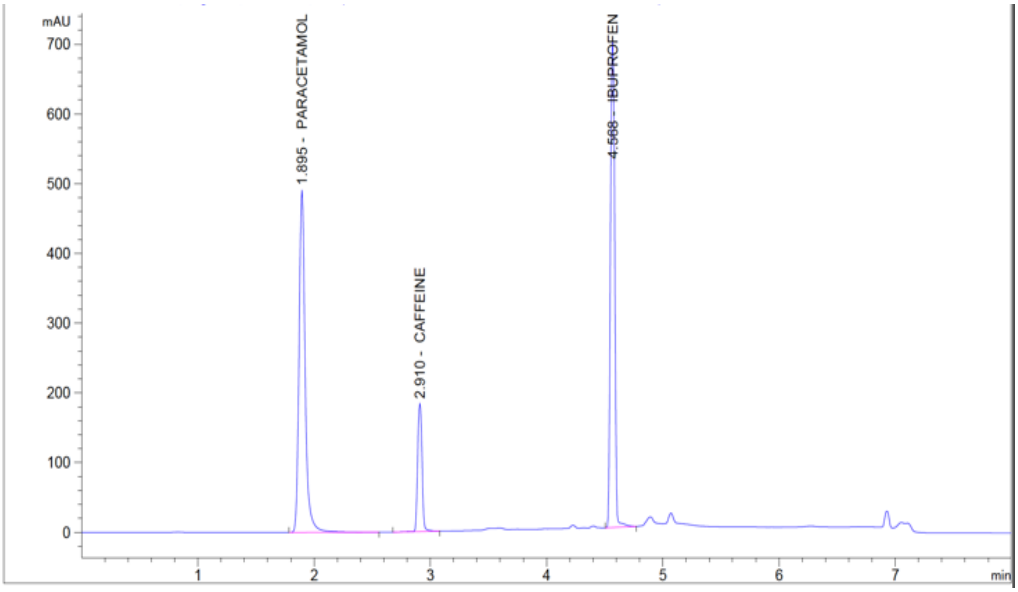

Figure 6.10 Chromatogram for the HPLC method showing the retention time for the three APIs.

Thereafter, drug content was above 95% for all formulations, with a low standard deviation. This decrease in drug content can be attributed to material loss during mixing and/or extrusion. Table 5.2 presents the unit's mean weight and the drug content in each of the printed units.

Table 6.2 Mean units' weight and drug content for the three formulations

	Mean unit weight(mg)	**SD (mg)**	**Mean drug content (%)**	**SD (%)**
Para-F	249.22	10.84	97.46%	0.74%
Ibu-F	232.77	5.84	95.92%	0.85%
Caff-F	274.58	14.71	95.24%	0.30%
Para-F= paracetamol formulation; Ibu-f= ibuprofen formulation; Caff-f= caffeine formulation.				

The polypill was assembled in three different configurations: 2:1:1, 1:2:1 and 1:1:2 of paracetamol, ibuprofen and caffeine units, respectively. The aim was to showcase the

ability of the FlexiPill to control dose with ease and to test the effect of change in dose on the rate of drug release. All three configurations of the FlexiPill were placed in both acidic and alkaline media to simulate the release in different regions of the gastrointestinal tract. Firstly, drug release of paracetamol from Para-F was significantly faster in the acidic medium (p-value=0.00002), with a mean release of over 85% after one hour in the acidic medium and less than 30% in the alkaline media. As a result, this formulation will mask the bitter test of paracetamol since the release will be slower inside the alkaline medium of the oral cavity. On the other hand, the Ibu-F shows a significant difference between the release in the acidic medium and that in the alkaline medium (p-value=0.000149). The release in the acidic medium after 24 hours was less than 1%, whereas the release was 10-fold higher in the alkaline medium. This significant difference in release can provide the desired gastroprotective effect required from the formulation. Moreover, due to the low percentage of the release modifier E L100-55, the drug release was not complete in 24 hours, therefore for future work higher percentage of the release modifier should be used to improve drug release (Yang et al. 2018). Furthermore, the release kinetics of the Ibu-F follows Higuchi's model which is typical of a fickian diffusion through insoluble matrix (Petropoulos, Papadokostaki, and Sanopoulou 2012). However, since drug release was low this kinetic study can only be described as initial and future work needs to confirm the result. Lastly, drug release from the immediate-release Caff-F in the acidic and the alkaline medium was similar with no significant difference (p-value= 0.632). The release flowed first-order release kinetics with over 84% release within the first 30 minutes. Finally, the change in API dose by increasing the number of units to two units did not affect the drug release in any of the formulations. Several drug release models were used in kinetic analysis. The zero-order model describes a constant drug release rate independent of drug concentration, making it suitable for controlled-release formulations. The first-order model, on the other hand, suggests that drug release depends on the remaining drug concentration, which is common in immediate-release formulations (Talevi and Ruiz 2021). Higuchi's model was included because it accounts for diffusion-controlled release from a porous matrix, often observed in a polymer matrix (Petropoulos, Papadokostaki, and Sanopoulou 2012). The Hopfenberg model is particularly useful for formulations where drug release is controlled by the erosion of a polymeric matrix. Lastly, the Korsmeyer-Peppas model was applied as a general

mathematical approach to describe drug release mechanisms, particularly when both diffusion and erosion contribute to the release process. The release exponent (n) obtained from this model provides insight into whether drug release follows Fickian diffusion, anomalous transport, or Case-II transport (swelling-controlled release) (Paarakh et al. 2018). If n < 0.45, it indicates Fickian diffusion, where drug release is primarily controlled by diffusion. When n falls between 0.45 and 0.89, it suggests anomalous transport, meaning the release mechanism involves a combination of diffusion and polymer relaxation. If n exceeds 0.89, it signifies Case-II transport, where drug release is dominated by polymer swelling and erosion.

For Para-F, the first-order model provided the best fit for drug release in an acidic medium (R^2=0.9997), indicating that the drug release was primarily concentration-dependent. The Higuchi model also showed a relatively high fit (R^2=0.9612), suggesting that some degree of diffusion contributed to the release. In the acidic, E EPO is soluble and therefore, erosion on the polymer contributed to the mechanism of drug release pealing erosion of the polymer matrix led to the first-order kinetics.

However, in an alkaline medium, the Korsmeyer-Peppas model provided the best fit (R^2=0.9977, n=0.4221), suggesting a combination of diffusion and erosion-controlled release (Fickian diffusion). The first-order model (R^2=0.9963) also demonstrated a strong fit, reinforcing the role of concentration-dependent release. The higher role of diffusion in this environment can be attributed to the insolubility of E EPO in the alkaline medium. Hence, the miscible API was released through diffusion.

For caffeine release in both acidic and alkaline conditions, the first-order model provided the best fit (R^2=0.9986 and R^2=0.8558, respectively), indicating that its release was mainly dependent on concentration. In the acidic medium, the Korsmeyer-Peppas model (R^2=0.8978, n=0.5018) also suggested that anomalous transport, involving both diffusion and erosion, played a role in caffeine release. In an alkaline medium, however, the Korsmeyer-Peppas model (R^2=0.8499, n=0.3071) indicated that Fickian diffusion was more dominant in this environment. Ibu-F model fitting was not investigated due to the low percentage of drug release, which limits the value of model fitting. Figure 6.11 and Table 5.3 present the release profile for the three printed units and their kinetic model, respectively.

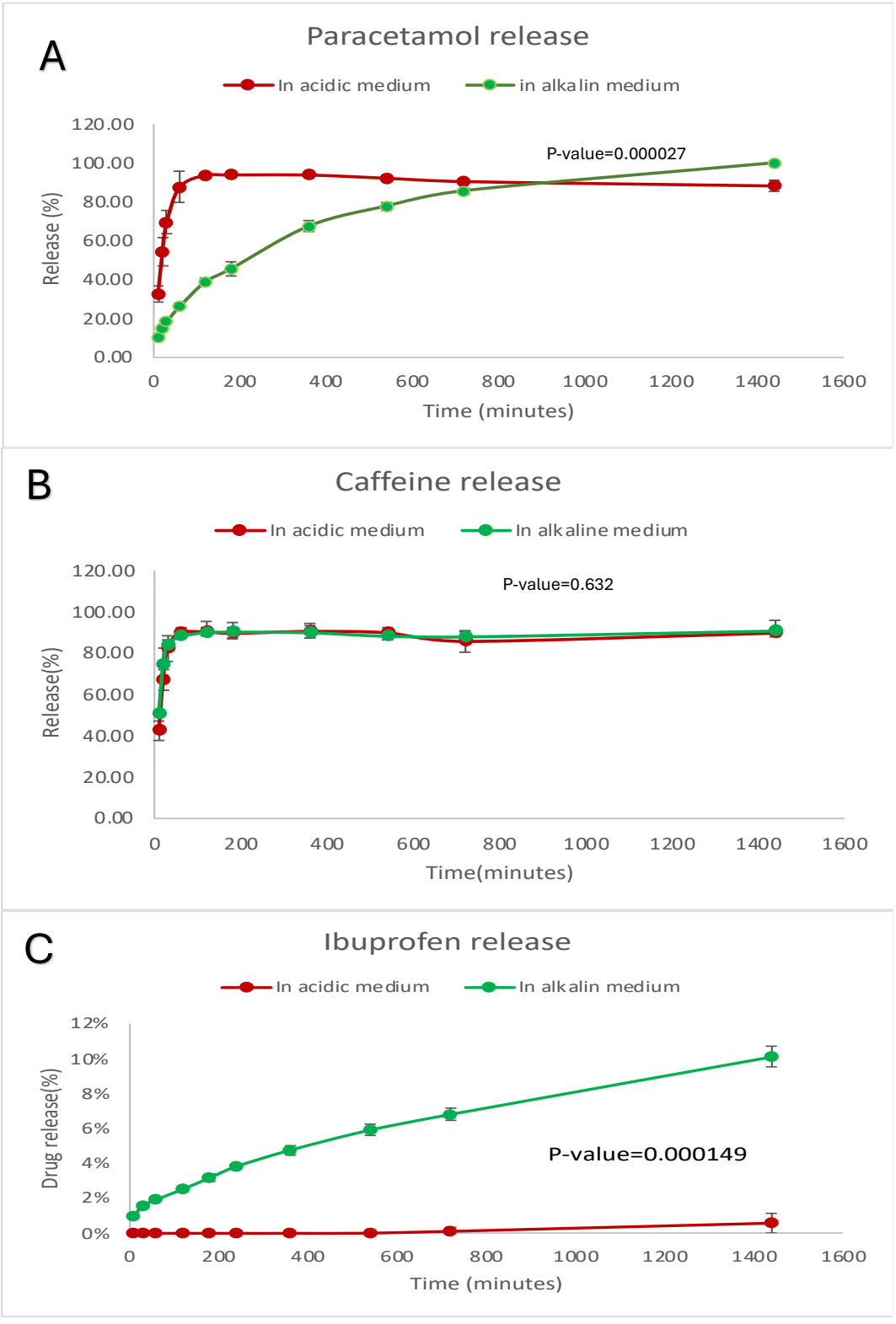

Figure 6.11 Dissolution drug release profile of Para-F (A), Caff-f (B) and Ibu-F (C). Para-F= paracetamol formulation; Ibu-f= ibuprofen formulation; Caff-f= caffeine formulation. Para-F= paracetamol formulation; Ibu-f= ibuprofen formulation; Caff-f= caffeine formulation.

Table 6.3 Kinetic drug release models fitting for the paracetamol, caffeine and ibuprofen units.

	Zero-order	First-order	Higuchi's model	Hopfenberg's model	Korsmeyer-Peppas model
Para-F release model regression in acid (R^2)	0.8975	**0.9997**	0.9612	0.8892	0.9621 (n= 0.5583)
Para-F release model regression in alkaline (R^2)	0.9279	0.9484	0.9943	0.9073	**0.9977 (n= 0.4221)**
Caff-F release model regression in acid(R^2)	0.7544	**0.9986**	0.855	0.7959	0.8978 (n= 0.5018)
Caff-F release model regression in alkaline (R^2)	0.6655	**0.8558**	0.7796	0.7346	0.8499 (n= 0.3071)

6.3 Conclusion

In this chapter, the successful utilisation of Fused Deposition Modelling (FDM) technology to produce a flexible dose combination system (the FlexiPill) specifically designed for pain management is demonstrated. The innovative design of the FlexiPill comprises four modular units that can be assembled at the point of care, facilitating personalised treatment without necessitating onsite 3D printing capabilities. The FlexiPill system is engineered to deliver multiple therapeutic agents, providing a flexible approach to drug titration and customisation based on individual patient needs. Each modular unit within the FlexiPill is capable of housing different therapeutic agents and can be formulated with distinct drug release profiles, tailored to the specific characteristics and formulation requirements of each drug.

Moreover, this work addresses common limitations associated with FDM technology, such as the high printing temperatures and low drug loading capacities. By employing a polymer mixture of PVP 40K and Eudragit EPO in a 1:1 ratio, the work achieved a significantly higher drug loading capacity of 55%, while also enabling printing at lower temperatures. This advancement in material selection not only enhances the drug load but also mitigates the challenges posed by high-temperature printing, thereby expanding the applicability of FDM technology in pharmaceutical manufacturing. This

research highlights the potential of FDM 3D printing to revolutionise personalised medicine by offering customisable, multi-drug delivery systems with adaptable release profiles, all while addressing the technological challenges traditionally associated with this manufacturing process.

Chapter 7 : FlexiPill as a flexible dose combination with a floating element

7.1 Introduction

Hypertension is one of the major risk factors for cardiovascular diseases (CV) and renal disease, affecting 25% of the population (Kearney et al. 2005). Although most clinical hypertension researches reflect the effect of antihypertension therapy in reducing CV events (G.S. Stergiou 2006). Nonetheless, many studies reported that less than 50% of the patients reach their systolic blood pressure goals (G. Stergiou et al. 2003; Amar et al. 2002; Mukete and Ferdinand 2016). This lack of control is often attributed to practitioners avoiding aggressive therapeutic strategies to manage hypertension (G.S. Stergiou 2006). However, other reviews suggest that systolic blood pressure control remains challenging, even in clinical trials where patient compliance and physician expertise are ensured (Mancia and Grassi 2002). Consequently, the recent guidelines recommendation was to start treatment with a combined antihypertensive agent (Williams et al. 2018; Unger et al. 2020). Additionally, the data available suggest that more than 70% of the patients with hypertension will eventually require at least two antihypertensive agents (Gradman et al. 2010; D. Smith et al. 2018; D.K. Smith, Lennon, and Carlsgaard 2020). Hypertension has a multifactorial pathophysiology; hence, a combination of more than one agent increases efficacy and decreases side effects (G.S. Stergiou 2006). Nevertheless, polypharmacy, especially in geriatric patients, can lead to a reduction in the adherence to the treatment and eventually its failure (Mukete and Ferdinand 2016; Yeaw et al. 2009). Therefore, a bulk of research has directed attention towards fixed-dose combinations (FDC) or polypills as the solution to improve adherence and reduce the cost of polypharmacy (de Cates et al. 2014; Wald et al. 2016; Group 2011), as have been discussed previously in 1.3 Polypill to Improve Adherence. An FDC is a single dosage form that contains more than one API, and it can be delivered as a capsule, injectable or tablet (polypill). Nevertheless, FDCs have many concerns such as; the difficulty of does titration of one of the components, difficulties in treatment discontinuation, possible physical and chemical interaction between the different APIs and different solubility

pharmacokinetics which leads to differences in formulation requirements for each component (Roy, Naik, and Srinath Reddy 2017). However, in recent years the advancements in 3D printing have encouraged many researchers to investigate the use of this technology to print polypills that can be customized according to patient needs at the point of care (Sadia, Isreb, et al. 2018; B.C. Pereira et al. 2019; Robles-Martinez et al. 2019; Khaled et al. 2015a). Pharmaceutical research introduced several technologies, but fused filament fabrication remains the most studied due to its simplicity and cost-effectiveness (Cailleaux et al. 2020).

However, 3D printing personalised pharmaceutical products at the point of care raises many regulatory concerns (BG et al. 2023). The current practice is to regulate personalised 3D-printed medication through guidance for extemporaneous preparation (Englezos et al. 2023). Nonetheless, this can only be done on a small scale. Consequently, to address the significant challenge of hypertension control, a personalised polypill that can be prepared and regulated within the framework of a large-scale industry is needed.

In this work, using fused filament fabrication (FFF), an attempt was made to formulate units that can be 3D printed and tested in a manufacturing site and thereafter can be personalised according to patient needs by assembling at the point of care into a polypill (FlexiPill). The design was composed of multiple frustums that can be stacked on top of each other. Three antihypertensive medications were used as the model APIs: propranolol, enalapril and hydrochlorothiazide. In addition to the synergistic benefit to hypertension of using more than a single agent, ACE inhibitors decrease the diabetogenic risk compared to monotherapy with HCT or propranolol alone (Cooper-DeHoff et al. 2013).

Each of these antihypertensive drugs has different formulation requirements. Propranolol has higher solubility in the acidic medium of the stomach and is subject to degradation in the alkaline medium of the small intestine (Chen et al. 2020). Therefore, propranolol bioavailability can be improved if formulated in gastroretentive formulation. Floating tablets are one of the well-known strategies for gastric retention. It has been demonstrated in previous research that FFF can offer a great advantage in formulating floating tablets with no lag time compared to the old traditional formulation technique of floating tablets (Ilyés et al. 2019; Lamichhane et al. 2019). On the other hand, enalapril is a thermolabile drug that degrades at a temperature of 160^{o} C (Hoffmann, Breitkreutz, and Quodbach 2022a) which makes processing with FFF rather

challenging. Finally, hydrochlorothiazide is a class II drug according to the (BCS) with low solubility and good permeability, Hence, its bioavailability can be improved if formulated into a solid dispersion in hydrophilic polymer (Ruponen, Rusanen, and Laitinen 2020).

The objectives of this study are twofold. First, to fabricate the FlexiPill design and demonstrate its efficacy in delivering drug combinations in a flexible manner that enables personalised therapy. Second, to address the formulation requirements of each active pharmaceutical ingredient (API) and enhance their delivery profiles.

7.2 Results and Discussion

7.2.1 Design and Formulation

In this chapter, two types of challenges were addressed: a design challenge and a formulation challenge. The design challenge involved creating a flexible dosage combination that could be easily assembled according to patient-specific needs while maintaining the overall size within acceptable limits and incorporating a functional floating unit. Compounding using 3D printing technology has gained interest in recent years due to its capability to automate the compounding process to produce personalised dosage forms. However, this has been raising regulatory concerns regarding the quality and safety of the final product (Melnyk and Oyewumi 2021; Beer et al. 2023). The FlexiPill design enables the flexibility to tailor the polypill's components and dosage directly at the point of care using pre-printed, quality-controlled units that can be assembled at the point of care, removing the need for on-site printing. This approach can help address regulatory concerns related to the quality and safety of the final product while also enabling broader personalisation, ultimately benefiting a greater number of patients than is currently possible. Secondly, a formulation challenge specific to each API will be discussed in detail later. From a design perspective, the FlexiPill with the staked frustums is designed in such a way that 2 mm of the bottom frustum goes inside the top one leaving 3 mm. As a result, each additional unit will add 3 mm to the total length of the FlexiPill after the initial 5 mm of the first frustum. Therefore, even a FlexiPill with 5 units will have a length of less than 2 cm and a diameter of 7.5 mm, which is smaller than a size 0 capsule,

making it easily swallowable. Patient compliance can be further improved by containing the FlexiPill in a capsule or adjusting the design to have smooth sides in the future.

Additionally, to ensure that the propranolol unit (PR-U) will float in the gastric juice its density must be lower than that of the gastric fluid. Therefore, the PR frustum was designed to have a closed base with a hollow centre while the other units are intended to sink after detachment from the PR frustum. The volume must be calculated to calculate the density of each frustum, and then the weight of each frustum must be divided by its volume.

From the formulation perspective, the floating frustum must release the API employing diffusion with no polymer erosion, since any erosion to the walls of the units can lead to the entry of the dissolution medium into the hollow centre which can result in the sinking of the unit. Hence, the PR unit was formulated with Eudragit RLPO (E RLPO) as the main polymer because of its pH-independent release of the API through swelling of the polymer and diffusion of the dissolution media (C.N. Patra et al. 2017). An additional contingency was drug load, which must be relatively high to achieve a 40mg dose per unit. This led to a unit with 155.4 cm^3 volume and a mean weight of 147.6 ±2.1 mg. As a result, the unit density was 0.95 cm^3/g which is lower than the gastric fluid density of 1.003 cm^3/g resulting in the flotation of the unit (Chen et al. 2020). Table 7.1 presents the frustums' mean weight, mean drug content, calculated volume and calculated density.

Table 7.1 Frustum units' weight, drug content, volume and density.

	Mean unit weight	**SD***	**Drug content**	**SD***	**Volume**	**Density**
EM-U*	136.9 mg	1 mg	102.88%	1.24%	93 mm^3	1.47 g/cm^3
HCT-U**	111.1 mg	3.8 mg	97.59%	4.21%	93 mm^3	1.19 g/cm^3
PR-U**	147.6 mg	2.1 mg	96.23%	3.05%	155.4 mm^3	0.95 g/cm^3
***SD= standard deviation, **EM-U= enalapril maleate unit, ***HCT= hydrochlorothiazide unit, ****PR-U= propranolol unit.**						

On the other hand, EM-U and HCT-U should have immediate release formulations with erosion of the units to disconnect from the PR floating unit. As a result, Eudragit EPO (E EPO) a cationic methacrylate polymer was chosen as the main polymer to

print these units since its immediate release of the API in the acidic medium has been established (Sadia et al. 2016). Additionally, enalapril has an additional challenge due to its thermolabile nature making the drug liable to degradation at the high temperature of the HME and FFF. Consequently, the enalapril formulation needs to be extruded and printed at low temperatures. Although E EPO has a Low Tg of 48^{o}C (C.N. Patra et al. 2017) and can be processed at a low temperature; it has been reported that filaments produced with E EPO are brittle, and multiple strategies have been suggested to improve its printability (Yang et al. 2021; Gottschalk et al. 2021). One of these effective strategies was the addition of a high molecular weight polymer as a flexibility modifier to improve its printability and decrease its brittleness. However, adding the high molecular weight polymer can increase the viscosity of the melt leading to the need for higher printing temperature. The effectiveness of this strategy was demonstrated by Than et. al, who used Hydroxypropyl cellulose-L (HPC-L) with a molecular weight of 140,000 g/mole as the flexibility modifier and the printing temperature had to be raised to 200^{o}C (Than and Titapiwatanakun 2021). Additionally, a different research group used polyethylene oxide (PEO) with a molecular weight of 100,000 g/mole to improve the flexibility of E EPO, but the filament had to be printed at 190^{o}C (Hoffmann, Breitkreutz, and Quodbach 2022a). Nonetheless, Alhijjaj et al. also used PEO 100K. They managed to decrease the printing temperature to 150^{o}C by adding polyethylene glycol (PEG) 4000, which was used to adjust the viscosity of the formulation (Alhijjaj, Belton, and Qi 2016). Therefore, in this work, PEO 200,000 g/mol was used as a flexibility modifier to improve filament printability but at low concertation and with the use of PEG 6000 as a viscosity modifier for the polymer blend and consequently the printing temperature.

7.2.2 Enalapril Formulation Screening

The screening was performed to determine the best percentage of PEO to E EPO. Thereafter, the complex viscosity of the polymer mix was measured, and the printability was evaluated using the printer. Talc was used for screening to decrease the waist of the APIs, and the concentration of talc was kept at 10% in all the screening formulations to decrease its effect on the mechanical properties of the filament. The PEO to PEG 6000 ratio was also kept constant at 1:1 this percentage was reported previously to be sufficient for the PEO plasticization (Isreb et al. 2019). In the first

screening formulation (F1) an equal percentage of each of the 3 polymers was used. However, the filament produced had a waxy texture and was very brittle. Hence, in the second formulation, TEC was used as a plasticiser and the percentage of E EPO: PEO: PEG was 2:1:1. The filament was printable, but due to high viscosity, it required a high printing temperature of 180^{o} C, and the tablet was very soft. Therefore, to reduce the viscosity, a lower concentration of PEO was used in the third screening formula and that resulted in a filament printable at a lower temperature of 165^{o} C. Table 7.2 presents the screening formulation, their printability and their processing temperature.

Table 7.2 Screening formulations and their printability, extrusion and printing temperature.

	Eudragit EPO	**TEC****	**PEO**	**PEG 6000**	**Talc**	**Printability**	**Extrusion temp.**	**Printing temp.**
*F 1**	30%	0%	30%	30%	10%	Brittle	70^{o}C	-
*F 2**	40.5%	4.5%	22.5%	22.5%	10%	Printable	80^{o} C	180^{o} C
*F 3**	54%	6%	15%	15%	10%	Printable	70^{o} C	165^{o} C
**F1, F2 and F3= formulation 1,2 and 3. ** TEC= triethyl citrate*								

The rheological test for the screening formulations was conducted at 150°C, the optimal printing temperature chosen to prevent enalapril degradation. The rheology test shows a direct relationship between the concentration of the high molecular weight polymer PEO and the shear viscosity. Therefore, as the concentration of PEO decreased from F1 to F3, the shear viscosity also decreased. Moreover, all three screening formulations show pseudoplastic behaviour. However, the slope of the complex viscosity-frequency graph also slightly decreases with the decrease in the concentration of PEO, which indicates that PEO has a marginally higher rate of thinning at this temperature compared to E EPO. Furthermore, Qahtani et. al mentioned that the viscosity of their formulation had to be lower than 1000 Pa. S to be printed with FFF. However, although the viscosities of both F2 and F3 were below the required threshold at 150^{o}C, a higher temperature was still required to print these formulations. Furthermore, a significant difference has been observed between the temperatures required for extrusion and printing, as printing demands lower viscosity compared to the relatively higher viscosity ranges needed for HME. Since thermo-

thinning depends on the formulation, this temperature gap can vary accordingly. Figure 7.1 presents the complex viscosity versus the frequency at 150° C.

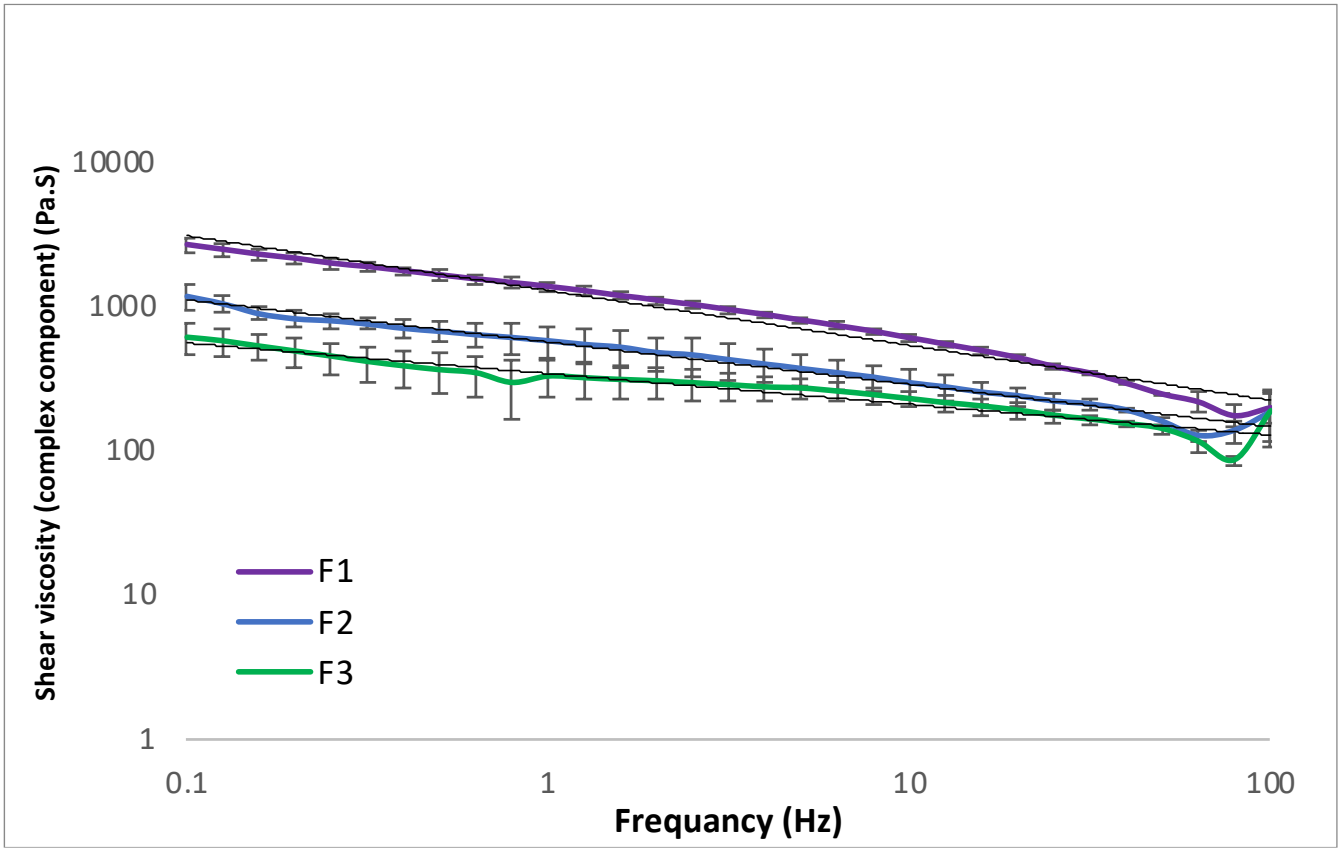

Figure 7.1 Complex viscosity versus frequency curve for the screening formulations. F1, F2 and F3 screening formulation (for composition refer to Table 7.2).

For the EM-F, a higher drug load and a lower printing temperature compared to F3 were necessary. Additionally, EM had a plasticising effect on the polymer mixture. Therefore, a higher percentage of talc powder was required to counteract this effect and improve the mechanical properties of the filament. As a result, the total amount of the polymers was reduced to 50% with a ratio of 6:1:1 of E EPO: PEO: PEG and the talc and EM formed the other 50%. Using inert fillers like talc, in concentrations between 37.5% to 50%, has proven effective in improving the mechanical properties of filaments and printlets made with E EPO (Yang et al. 2021). Consequently, talc was used in 35% of the total weight, which is close to 1:1 ratio with E EPO, to improve the mechanical integrity of the filament and the printed units. Furthermore, No TEC was used since the enalapril is miscible with E EPO and there is no need for extra plasticisation. Finally, the concentration of EM was 15% to achieve the dose of 20mg

per unit. Therefore, the printing temperature for EM-F was set to 150 °C, as required to remain below the degradation temperature of enalapril. Hydrochlorothiazide was formulated with E EPO as well. However, due to its high melting point and the presence of a high h concentration of talc, the polymer mobility was limited, which led to the improvement of the mechanical strength of the E EPO without the need for a flexibility modifier. This strategy, which was suggested by Yang et al., has proven effective in improving the printability of E EPO with inert filler and high melting API (Yang et al. 2021). Although the printing and extrusion temperatures were high, processing temperature was not a concern for this formulation as in with enalapril. Table 7.3 lists the final formulations for the three antihypertensive systems.

Table 7.3 The final formulation for the FlexiPill units.

	Eudragit EPO	**Eudragit RLPO**	**TEC**	**PEO**	**PEG 4000**	**PEG 6000**	**Talc**	**API**	**Extrusion temp.**	**Printing temp.**
*EM-F**	37.5%			6.25 %		6.25 %	35%	15%	70° C	150° C
*HCT-F***	46.75%		3.25 %				37.5%	12.5%	100° C	160° C
*PR-F****		60%			10%			30%	70° C	160° C
**EM-F= enalapril maleate formulation, **HCT-F= hydrochlorothiazide formulation, ***PR-F= propranolol formulation.*										

7.2.3 Three-dimensional (3D) printing

The infill densities of EM-U, HCT-U, and PR-U were set to 90%, 50%, and 20%, respectively, to align the amount of drug in each unit with the clinical required doses for all three antihypertensive agents. Consequently, the infill or the number of units used can be easily modified to personalise the dose, as proven in Chapter 4. Figure 7.2 presents the design of the FlexiPill units, the units after printing, and the floatation in 0.1 N HCl.

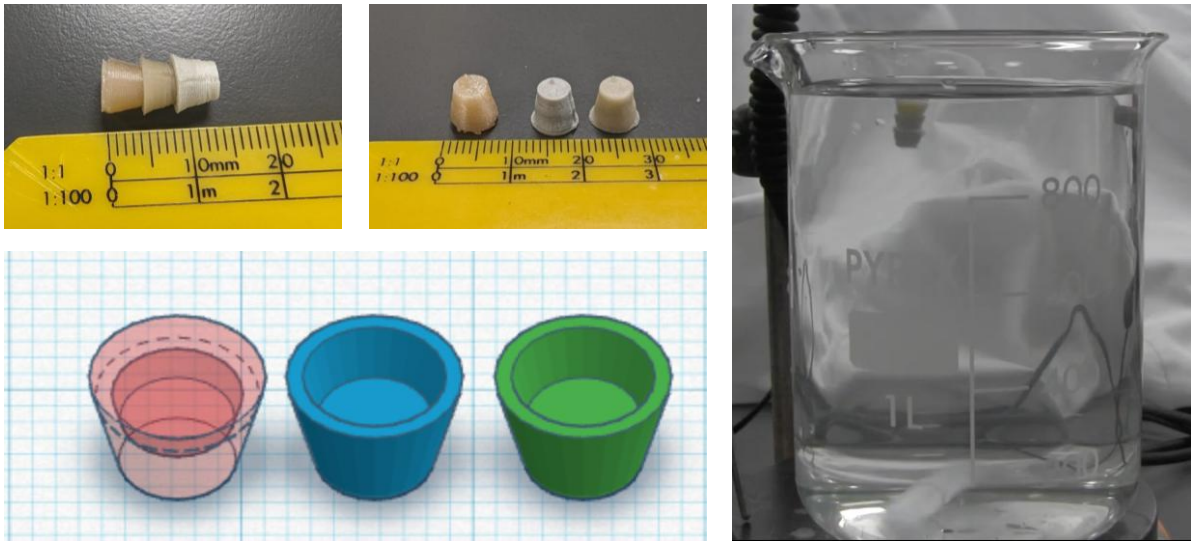

Figure 7.2 The design of the FlexiPill units (bottom left), the units after printing (top left) and the floatation in 0.1 N HCl (right side).

7.2.4 Scanning Electron Microscope

The SEM images of the filaments show that the PR-F filament has a smooth surface with some textural voids and inclusions. However, no propranolol crystals were observed. Moreover, the EM-F filament appeared smoother with no voids but some inclusions. Additionally, the filament cross-section spiral arrangement of the extruded material is more visible due to the presence of talc. Lastly, the HCT-F had much more surface texture and more visible pores. The cross-section once again shows the spiral arrangement of the extrudate due to the high percentage of talc. Figure 7.3 shows the SEM images of the three filaments prepared by HME.

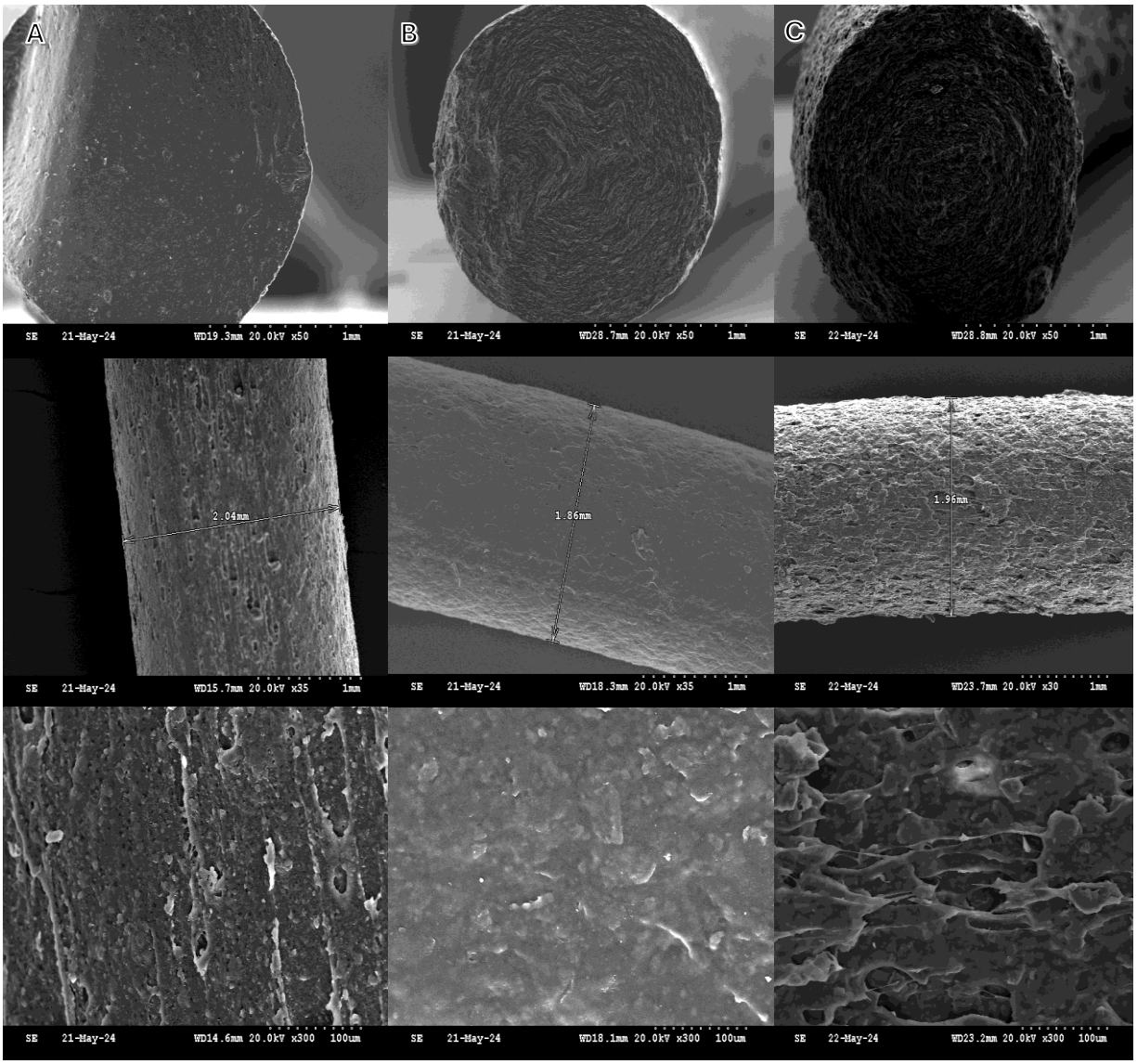

Figure 7.3 SEM images of the three filaments prepared by HME. (A) PR-F, (B) EM-F and (C) HCT-F. EM-F= enalapril maleate formulation, HCT-F= hydrochlorothiazide formulation, PR-F= propranolol formulation.

Figure 7.4 shows the SEM images of the printed units. Both PR-U and EM-U show acceptable layer adhesion, with no gaps and uniform layer thickness. However, the HCT-U had less layer uniformity, caused by high viscosity of the formulation leading to non-uniform material extrusion.

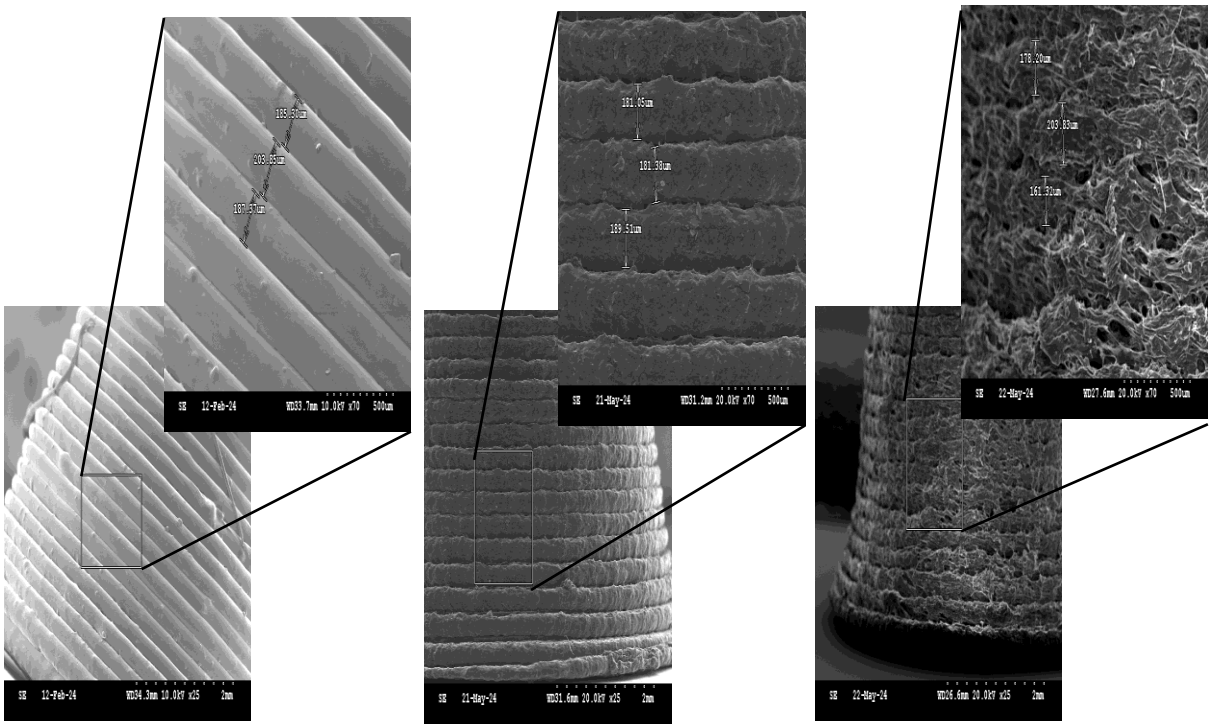

Figure 7.4 SEM for the printed units. (A) PR-U, (B) EM-U and (C) HCT-U. EM-F= enalapril maleate formulation, HCT-F= hydrochlorothiazide formulation, PR-F= propranolol formulation.

7.2.5 Thermal Analysis

Thereafter, thermogravimetric analysis (TGA) was performed on all three formulations to investigate the stability of the formulation under the processing temperature. TGA of pure EM shows two steps of decomposition the first step corresponds to a 24% decrease in weight between 156° C to 221° C and a peak in the derivatised thermalgravimetric (DTG) curve at 171° C and corresponds to the formation of diketopiperazine by intramolecular cyclisation after the removal of the water and the maleate molecules (de Souza et al. 2016). The second step is the result of the complete degradation of diketopiperazine which shows a peak degradation rate at 345° C. Additionally, E EPO also shows a two-step degradation, the first between 236° C and 331° C with a peak rate at 299° C. The weight lost in this step is 27.3% which corresponds to the removal of the dimethylamino groups from the polymer and the formation of six-membered cyclic anhydrides (Porfiryeva et al. 2019). The second step

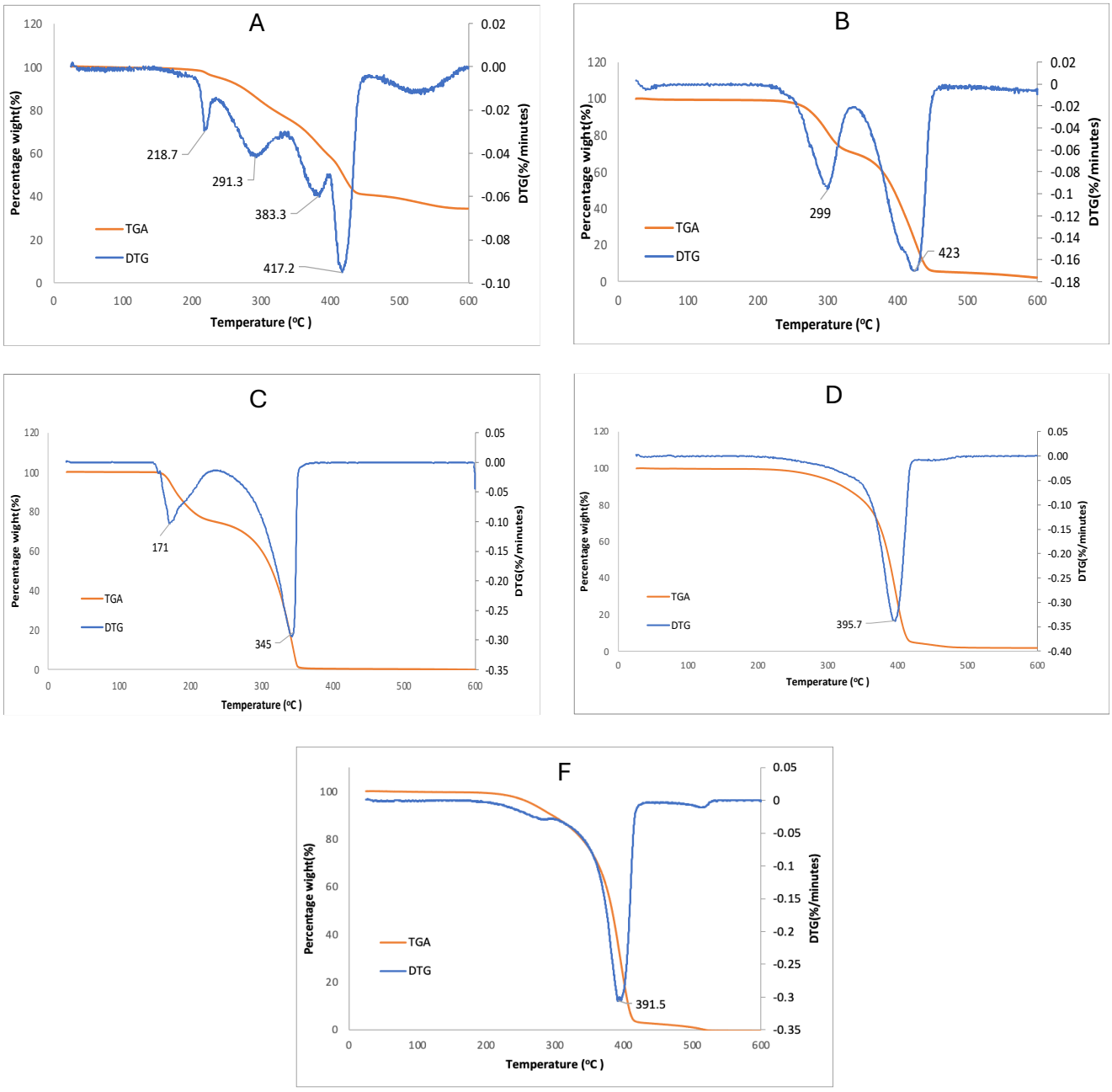

Figure 7.5 Thermal gravimetric analysis and differential thermogravimetry for; (A) EM-F, (B) Eudragit EPO, (C) Enalapril maleate, (D) PEO 200K, (E) PEG 6000. EM-F= enalapril maleate formulation.

corresponds to the complete degradation of the polymer and peaks at 423° C. PEO 200K and PEG 6000 both show one-step degradation that peaks around 395 ° C due to the similarity in the chemical structure. As a result, the DTG of the EM-F show four degradation steps the first is the formation of diketopiperazine from enalapril that peaks at 218.17° C, the second is a combination of the complete degradation of enalapril and the removal of the dimethylamino groups from the E EPO that peaks at 291.3° C, the third step is caused by the degradation of PEG 6000 and PEO 200K

peaking at 383.3° C and the fourth step is the complete degradation of E EPO peaking at 417.2° C. Figure 7.5 presents the TGA and DTG for EM-F and its components.

The PR-F degradation thermograph reveals two steps of degradation. The first starts at 210° C and peaks at 270° C with weight loss of 30% equivalent to propranolol concentration in the formulation. The second step peaks at 395°C and is caused by the degradation of both E RLPO and PEG 4000. Figure 7.6 presents the TGA and DTG for PR-F and its components.

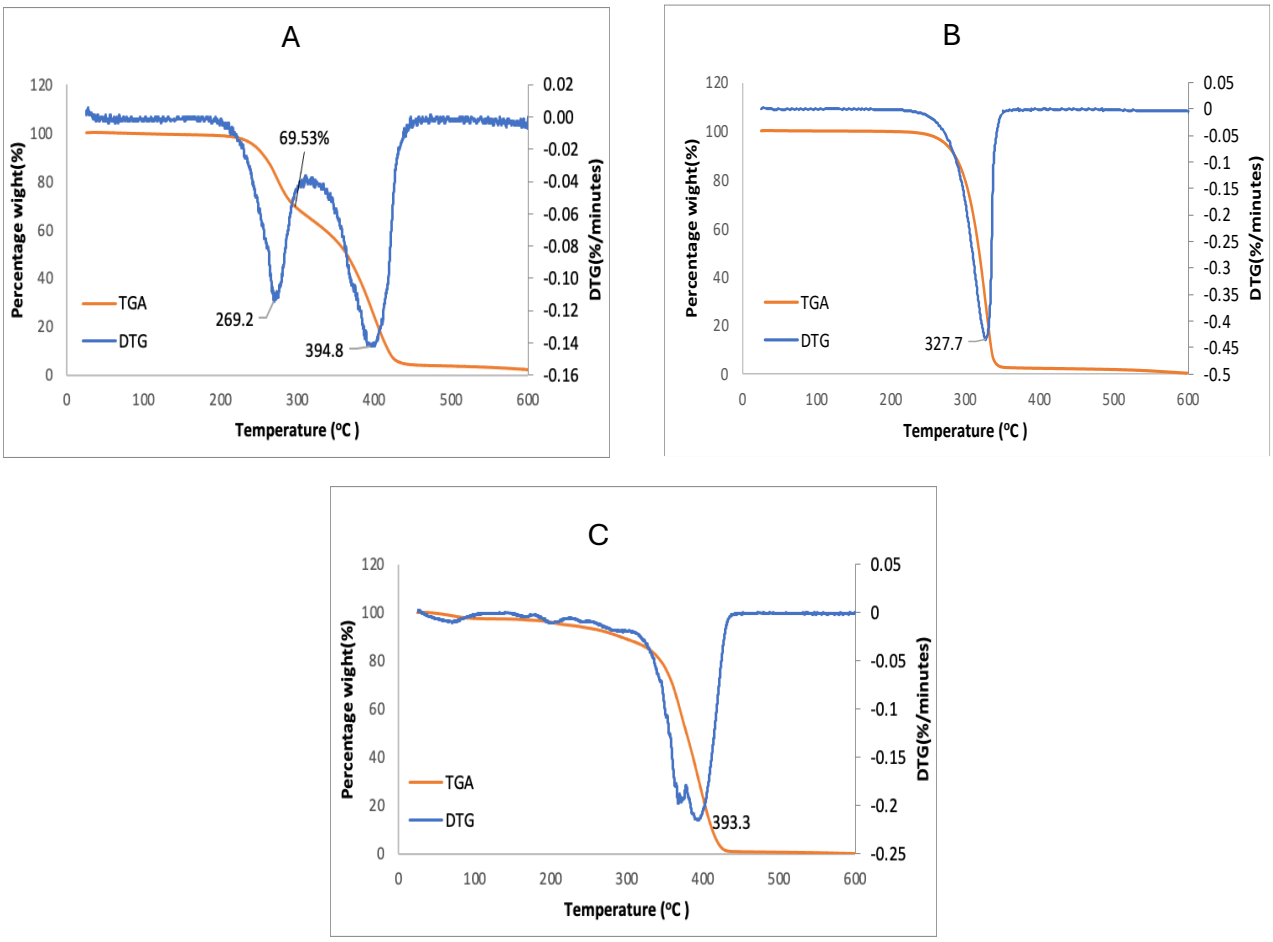

Figure 7.6 Thermal gravimetric analysis and differential thermogravimetry for; (A) PR-F, (B) Propranolol HCl and (C) Eudragit RL PO. PR-F= propranolol formulation.

The thermal degradation of the HCT-F is presented in two steps. The first, which peaks at 294° C, corresponds to both the degradation of HCT and the initial step of E EPO thermal degradation. The second step, which peaks at 425° C, is caused by the complete degradation of the polymer. Figure 7.7 presents the TGA and DTG for HCT-F and its components.

TGA for the three systems reveals that the formulations are stable under the extrusion and printing temperature since the degradation temperature of all the components is higher than that of the processing temperature.

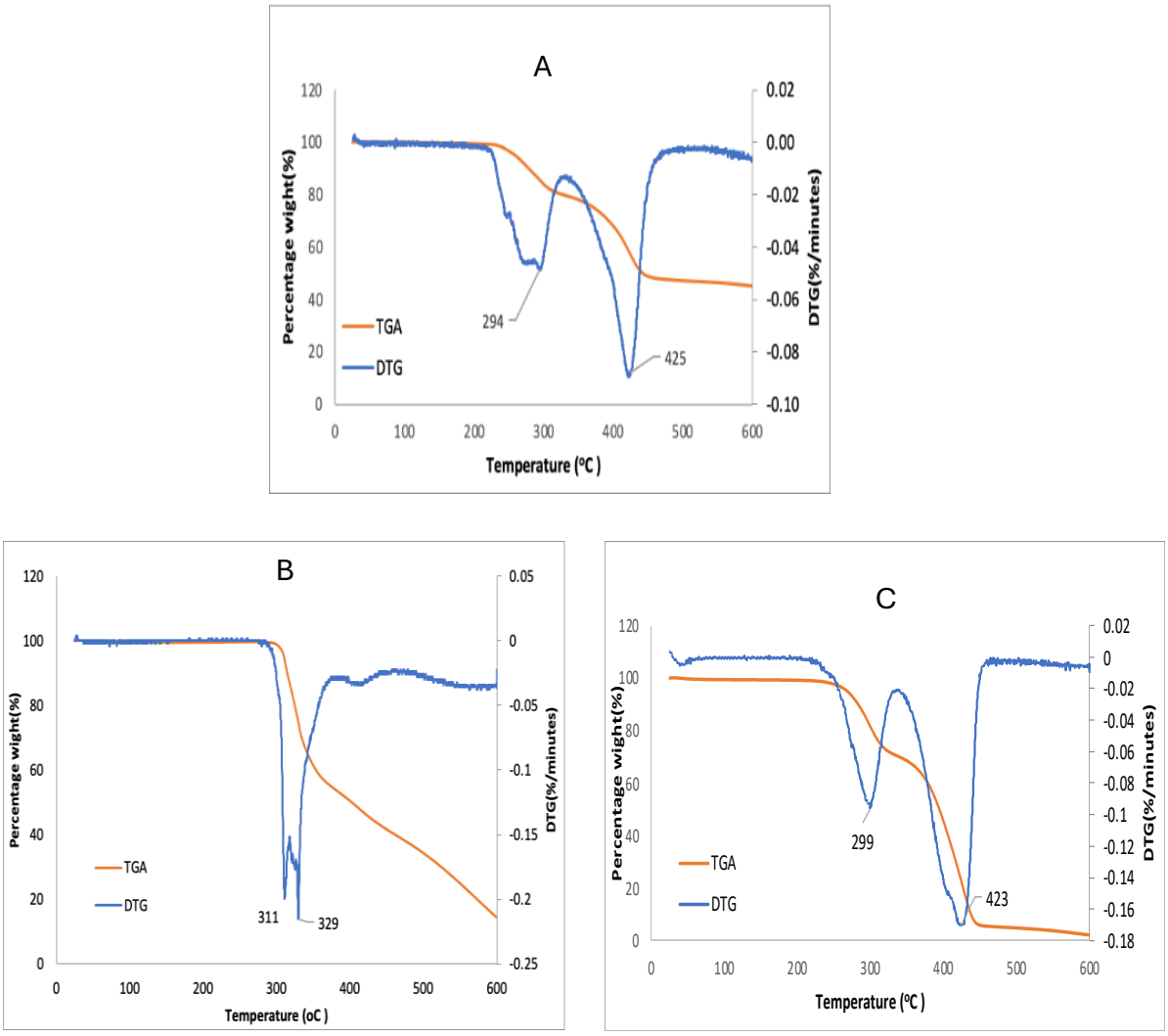

Figure 7.7 Thermal gravimetric analysis and differential thermogravimetry for; (A) HCT-F, (B) hydrochlorothiazide, and (C) Eudragit E PO. HCT-F= hydrochlorothiazide formulation.

In the DSC, enalapril shows two overlapping peaks. The first sharp peak at 149° C results from the melting of the enalapril crystals and a second broader peak at 160° C is caused by the degradation of enalapril (Hoffmann, Breitkreutz, and Quodbach 2022b). However, these peaks are not shown in the DSC of the EM-F printlet, indicating that EM has interacted with the polymer, forming an amorphous solid dispersion. The only endothermic peak present in the thermograph at 53.4°C is resulting from the melting of PEG 6000. Figure 7 .8 A shows the DSC of the EM-U and pure EM.

The DSC of powder propranolol has a sharp endothermic peak at 163.85^{o} C corresponding to the melting of propranolol. On the other hand, the PR-U thermograph shows an endothermic peak at 160^{o} C indicating that some of the 30% propranolol in the formulation is still in its crystalline state. Additionally, the other endothermic peak at 57^{o} C results from the melting of PEG 4000. Figure 7.8 B shows the DSC of the PR-U and PR.

Finally, DSC of HCT-F could not be used to show the presence of hydrochlorothiazide melting peak since degradation of the methacrylate polymer at 250^{o} C interfered with the melting signal of hydrochlorothiazide at 267^{o} C. Figure 7.8 C shows the DSC of the HCT-U and pure HCT.

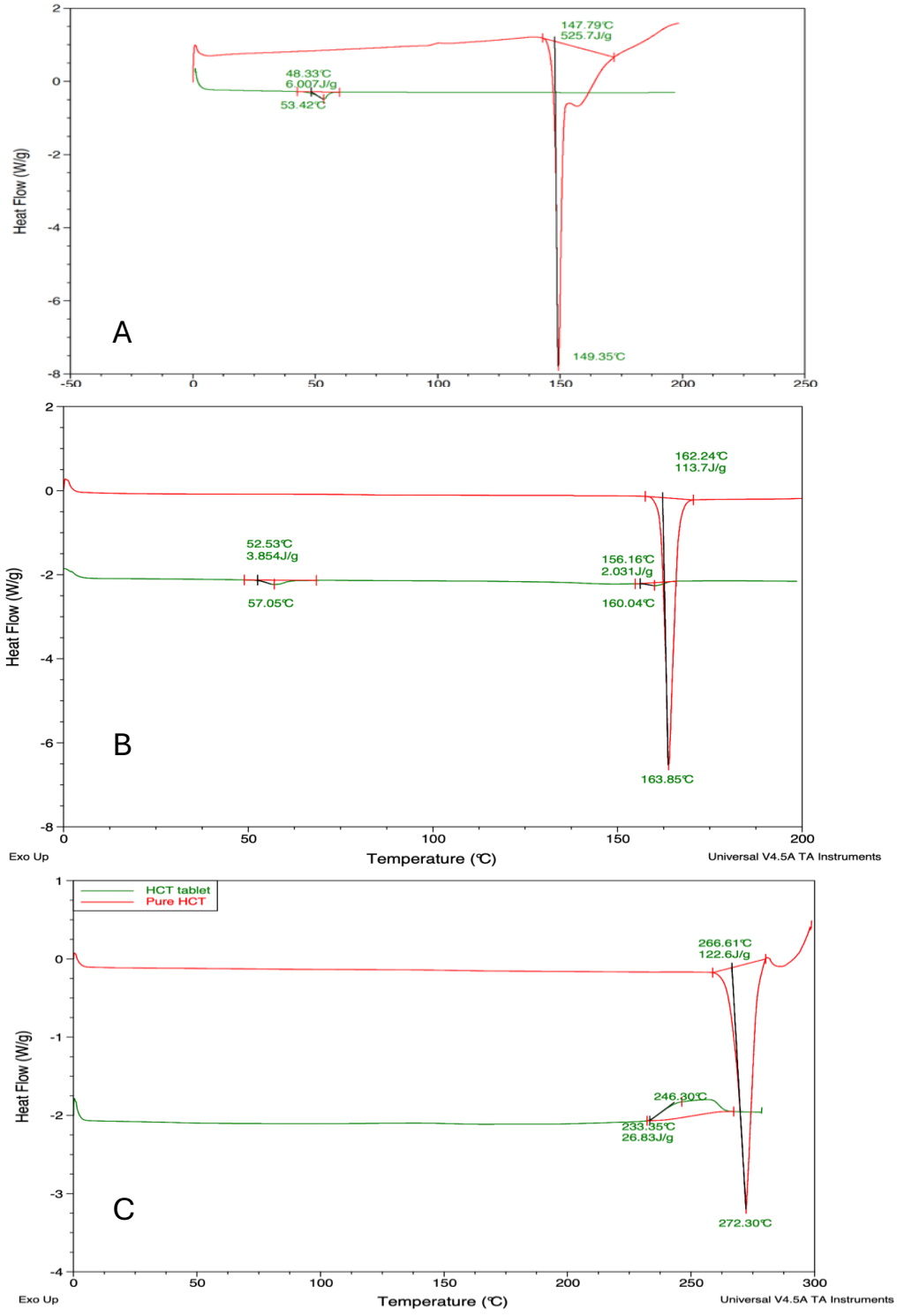

Figure 7.8 Differential scanning calorimetry for the printed units (green) and the pure APIs (red). (A) EM-F and enalapril, (B) PR-F and propranolol and (C) HCT-F and hydrochlorothiazide. EM-F= enalapril maleate formulation, HCT-F= hydrochlorothiazide formulation, PR-F= propranolol formulation.

7.2.6 Fourier Transform Infrared

Thereafter, the FTIR spectrum was investigated to find any interaction between the APIs and the polymers. If the formulation spectrum shows a shift or disappearance of the band from the API spectrum this is a sign of supramolecular interactions. In the EM spectrum, the peak at 3,211.48 cm^{-1} which corresponds to stretching vibrations of N-H disappears in the formulation spectrum. Additionally, the band at 2,980.02 cm^{-1} that is assigned to asymmetric CH_3 stretching vibration shifts to 2,970.38 cm^{-1}. Furthermore, the band at 1,749.44 cm^{-1} caused by the carbonyl stretching of ester disappeared and the carboxylic acid peak at 1,724.36 cm^{-1} shifted to 1,726.29 cm^{-1} in the formulation spectrum. The carbonyl stretching of the tertiary amide at 1,645.28 also shifts to 1,668.43 in the formulation (Lin et al. 2002). The FTIR spectrum confirms the finding of DSC and proves the complete miscibility of EM in the methyl acrylate polymer. Figure 7.9 A compares the FTIR spectrum for the EM printed units with the spectrum of pure EM.

In the spectrum of pure HCT, the asymmetric and symmetric vibrations of the sulphonyl groups are visible at 1,315.45 cm^{-1} and 1,147.65 cm^{-1}, respectively. Both bands decrease in intensity and shift to 1,319.31 cm^{-1} and 1,134.14 cm^{-1}, respectively (Ruponen, Rusanen, and Laitinen 2020). The NH stretching of the sulphonamide and amine groups, which appears at 3,356.14 cm^{-1}, 3,265.49 cm^{-1} and 3,169.04 cm^{-1}, its band does not shift but the band intensity decreases in the IR spectrum of the formulation. The CH2 stretching at 2,987.74 cm^{-1} and 2,900.94 cm^{-1} does not shift in

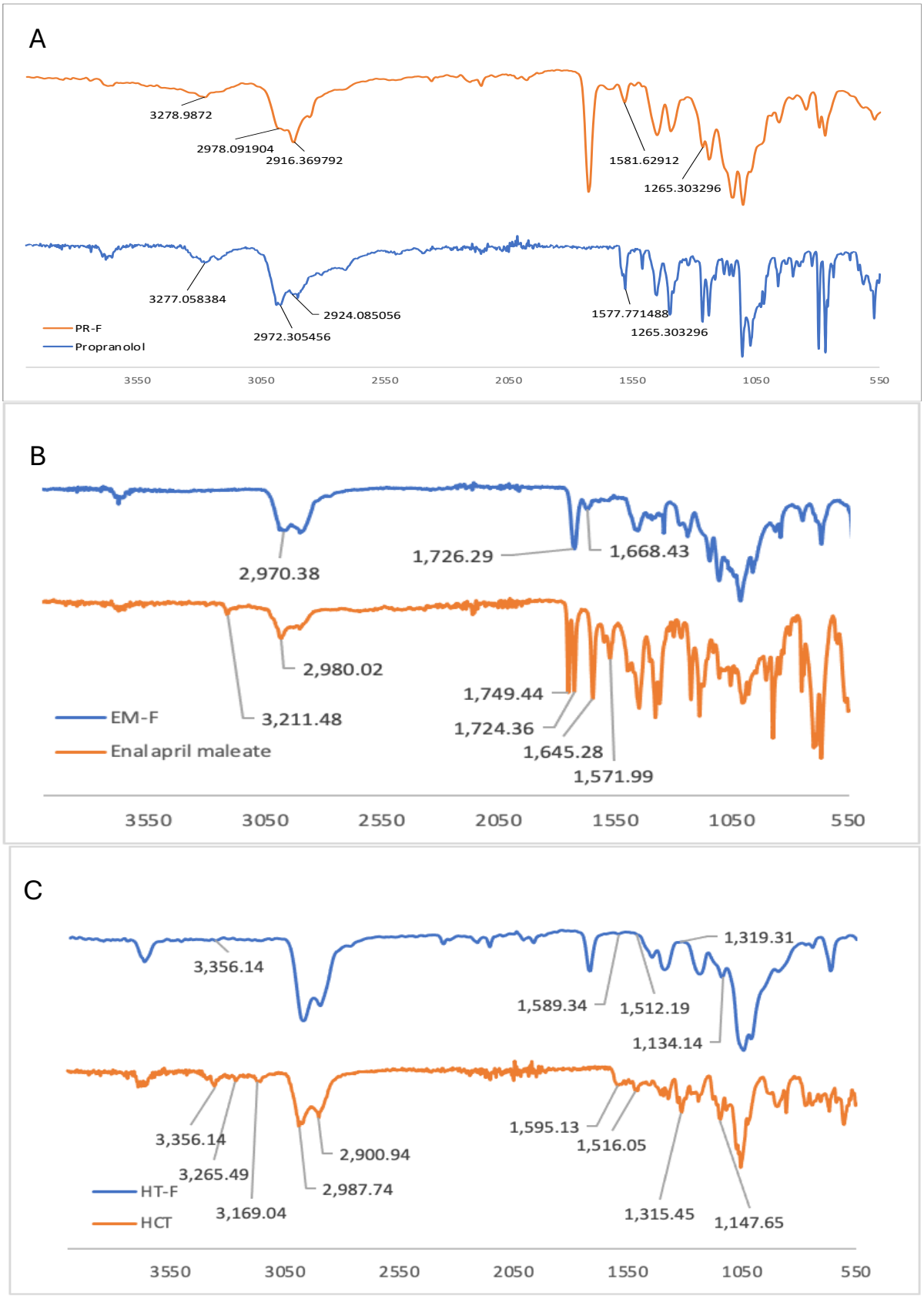

Figure 7.9 FTIR spectrum for the printed units and the pure APIs. (A) PR-F and propranolol, (B) EM-F and enalapril and (C) HCT-F and hydrochlorothiazide. EM-F= enalapril maleate formulation, HCT-F= hydrochlorothiazide formulation, PR-F= propranolol formulation.

the formulation spectrum (Sultan et al. 2017). Additionally, the C=C stretching at 1,595.13 cm^{-1} and 1,516.05 cm^{-1} decrease in intensity and shift to 1,589.34 cm^{-1} and 1,512.19 cm^{-1}, respectively, indicating potential molecular interactions. As a result, the FTIR data reveals an interaction between the HCT and the E EPO, as reported previously (Senta-Loys, Kelleher, and Jones). Figure 7.9 B compares the FTIR spectrum for the HCT printed units with the spectrum of pure HCT.

Finally, the propranolol FTIR spectrum band at 1265.3 cm^{-1}, which corresponds to the stretch of the C-O in the ether group, shows no shift in the formulation spectrum. However, the band assigned to the aromatic C-C stretching at 1577.7 cm^{-1} shifted to 1581.6 cm^{-1} in the formulation spectrum. Additionally, C-H stretching, shown as a band at 2924.1 $cm^{-1,}$ shifts to 2916.3 cm^{-1} in the PR-F spectrum (Farooqi and Aboul-Enein 1996). Moreover, the secondary amine group presence as a band at 2972.3 cm^{-1} in the propranolol spectrum shifts to 2978.1 cm^{-1}. Lastly, the band at 3277 cm^{-1} which is assigned to the hydroxyl group is broadened in the formulation spectrum due to the formation of the H-bond (C. Patra et al. 2007). All these alterations in the propranolol spectrum indicate a supramolecular interaction between it and E RLPO. Figure 7.9 C compares the FTIR spectrum for the PR printed units with the spectrum of pure PR.

7.2.7 Powder X-ray Diffraction

When analysing the Powder x-ray diffraction pattern HCT-U, the presence of a diffraction peak at 19.09º 2q in the HCT-F powder and its absence in the HCT printed unit (HCT-U) confirms the transformation of HCT crystal into an amorphous solid dispersion. Meanwhile, the other peaks corresponding to the diffraction pattern of talc are still present. On the other hand, the diffraction pattern of PR-U and the preprint powder mixture both show the presence of propranolol crystal, confirming that the DSC results of partial crystallinity are retained after processing. Finally, the diffraction pattern of the enalapril printed unit also shows only the talc diffraction peaks, confirming the formation of amorphous solid dispersion. Figure 7.10 compares the X-ray diffraction of the formulation and their physical mixture.

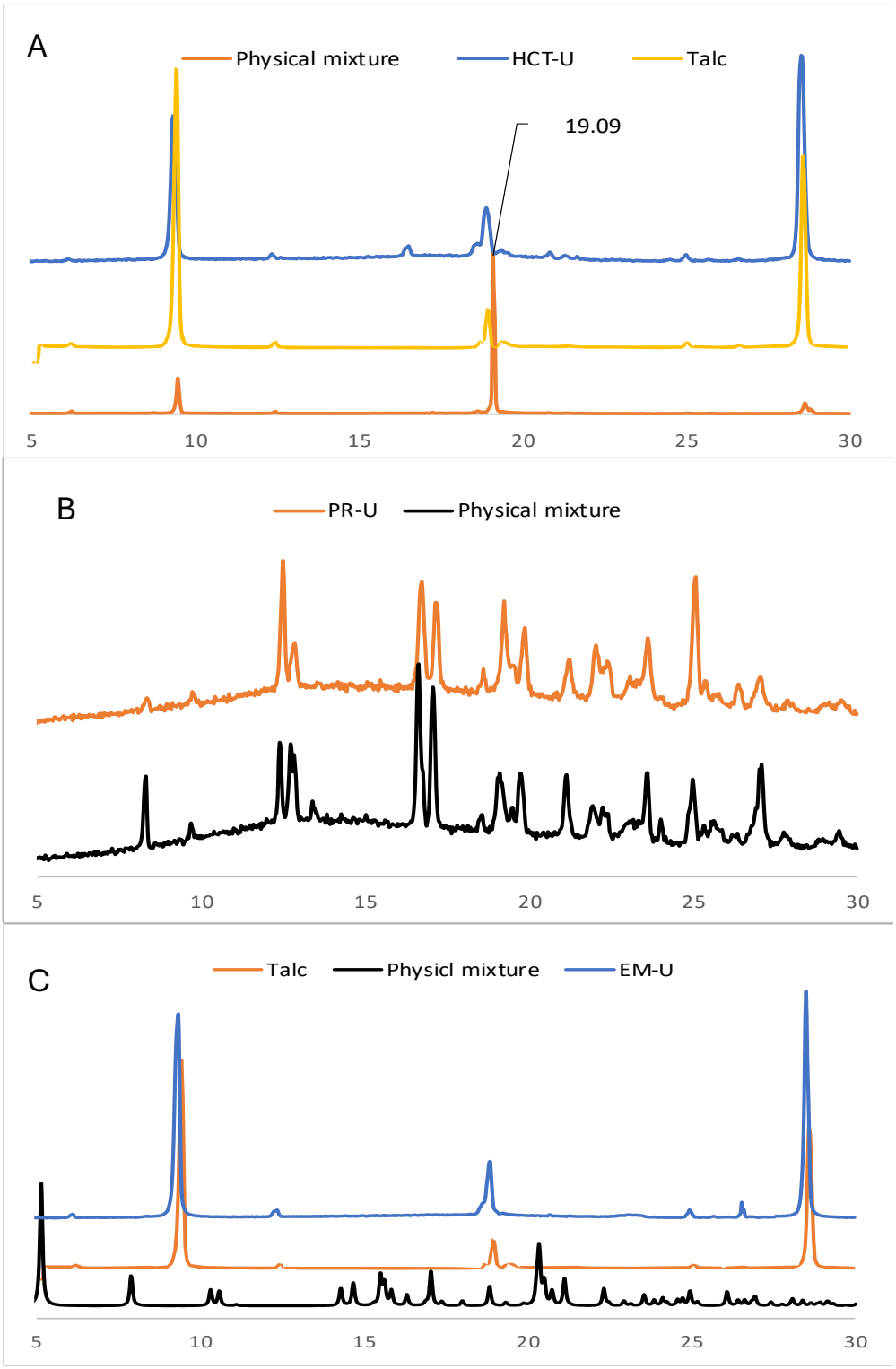

Figure 7.10 X-ray diffraction comparing the physical mixture of the combination. (A) HCT-U, (B) PR-U and (C) EM-U. EM-F= enalapril maleate formulation, HCT-F= hydrochlorothiazide formulation, PR-F= propranolol formulation.

7.2.8 Rheological Study

The FFF process depends on heating the filament to a temperature in which the thermoelastic polymer turns from an elastic to a viscous state to flow through the narrow nozzle of the printer under high shear. As a result, studying the viscoelastic behaviours of the formulation is an essential step to understanding the printing process. However, studying the rotational viscosity under steady shear is limited to low frequency due to flow disruption and sample rupture. However, according to the Cox-Merz rule, there is an empirical correlation between the viscosity under steady shear and the complex viscosity under oscillatory shear (Aho et al. 2019).

Therefore, frequency sweep with fixed strain was used to test the viscoelastic behaviour of the formulation. The strain was fixed to 1% to keep the test within the linear viscoelastic region (LVR). The temperature was set to the printing temperature for each formulation. Lastly, to determine the apparent shear rate at the printing nozzle, the volume flow rate was calculated from the pre-set printing speed and the nozzle radius which was 11 mm^3/s. Thereafter, the apparent shear rate at the printing nozzle was calculated using the equation:

$$\dot{\gamma}_{app}=4Q/\pi R^3$$

Where $\dot{\gamma}_{app}$ is the apparent shear, Q is the volumetric flow rate and R is the radius of the nozzle.

The apparent shear rate was 1,800 Sec^{-1}. As a result, high frequency was used for the comparison. The test reveals that the mean complex component of the shear *viscosity (SV)* for the PR-F, EM-F and HCT-F were 98.15, 122.6 and 341.5 Pa. S at printing temperature and frequency 100 Hz, respectively. In conclusion, the use of a high percentage of the inert filler talc in the HCT-F to improve the mechanical properties of E EPO led to higher viscosity. This is in contrast with the approach used in the EM-F, where both inert filler and polymer blends were used, hence the high printing temperature for HCT-F. Moreover, these results are in line with the value set by Qahtani et al. for printing PLA, between 1000 Pa. S to 100 Pa. S.(Qahtani et al. 2019). Additionally, the shear index, which is the parameter used to describe the flow of non-Newtonian fluids in response to applied shear forces, for both HCT-F and EM-F was less than 1. This indicates that both formulations exhibited a shear thinning, which was observed as an increase in the viscosity as the frequency decreased. However, PR-F

shows a decrease in viscosity as the frequency decreases to 25 Hz because at high frequency the behaviour of E RLPO is dominated by the elastic response due to the entanglement of the polymer chains, leading to higher complex viscosity. As the frequency decreases, these entanglements relaxes, and an increase in the viscosity with decreasing frequency can be observed. This behaviour can be observed in the relatively high shear index for PR-F. Finally, in the PR-F formulation, the loss modulus was higher than the storage modulus at low frequency but became equal to or lower than the storage modulus at high frequency. This confirms the entanglement of the polymer chain at high frequency, which can store the energy of the deformation, while at low frequency, the polymer chains are more relaxed, and energy dissipates as heat, acting like a liquid. On the other hand, the EM-F and HCT-F storage modulus is lower than the loss modulus at any frequency. Figure 7.11 presents the complex viscosity, loss and storage modulus versus frequency and the shear index.

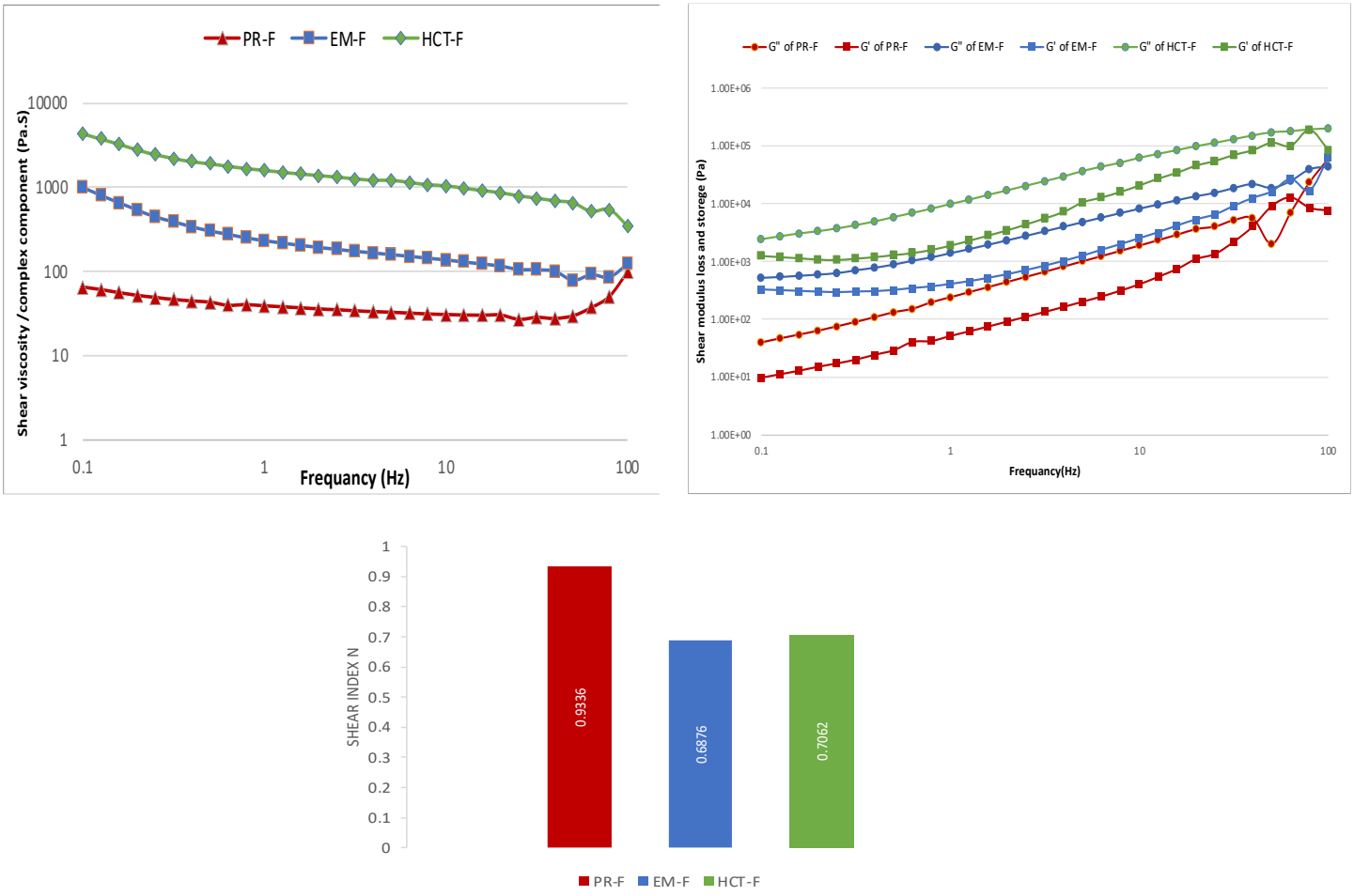

Figure 7.11 Complex viscosity versus angular frequency of the three formulations at their perspective printing temperature(left), loss and storage modulus versus frequency (right) and Shear index for the three formulations (bottom). EM-F= enalapril maleate formulation, HCT-F= hydrochlorothiazide formulation, PR-F= propranolol formulation.

7.2.9 Chromatography

One of the challenges, that stand in the way of the adaptation of polypills is finding reliable analytical methods for qualitative and quantitative analysis. The method developed for this work had an adequate separation between the maleate, HCT, propranolol and enalapril and their retention time was 1.48, 2.49, 9.42 and 10.42 minutes, respectively, and the run time was 15 minutes. However, the DAD was set to measure two signals 210 nm and 280 nm, since enalapril lambda max is at a low wavelength. Nonetheless, the baseline at these wavelengths was not ideal due to solvent interference. Therefore, a 280nm signal was used for more accurate detection of HCT and propranolol. Additionally, for the final data point in the dissolution test and drug content analysis, LC-MS was utilized to assess any degradation resulting from the dissolution medium and the processing, respectively. In both instances, the peaks exclusively corresponded to the API mass, with no detectable degradants. Figure 7.12 shows the HPLC method chromatograms with the MS peaks.

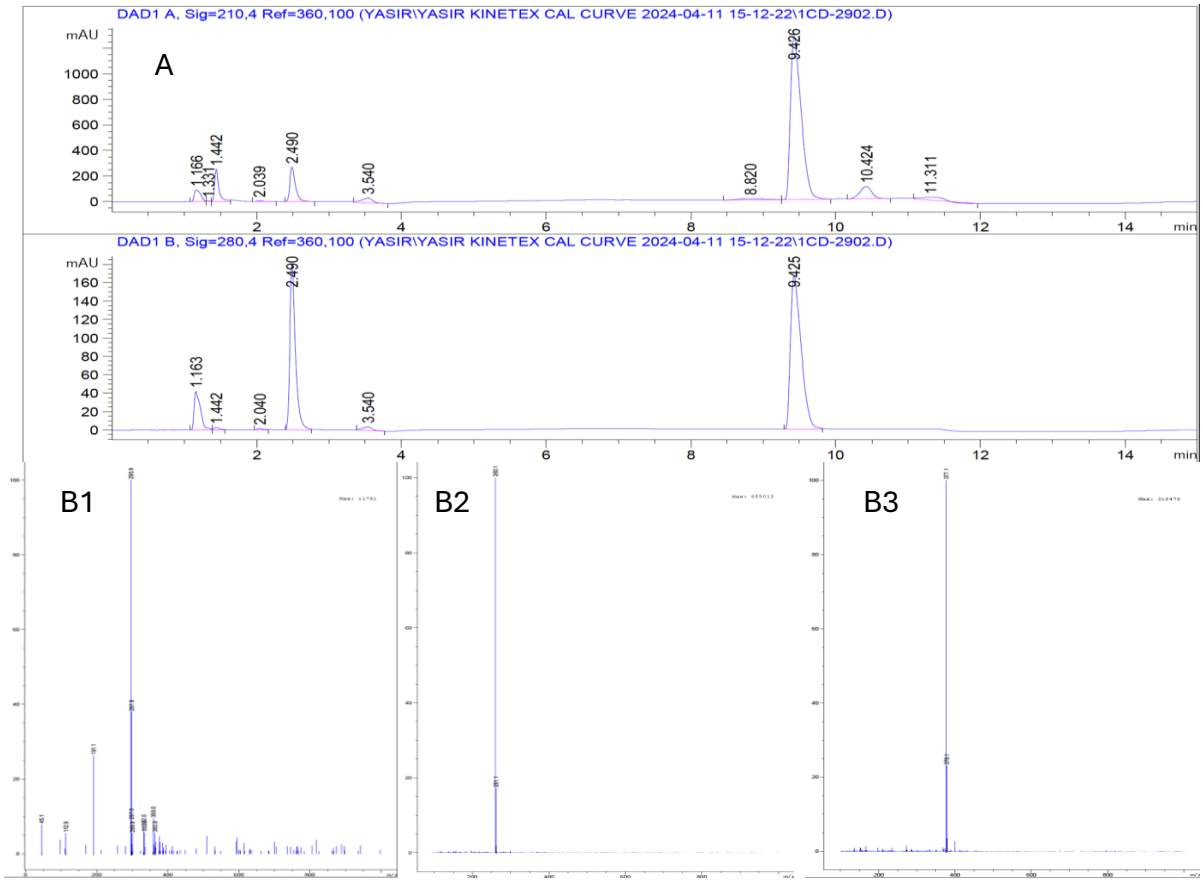

Figure 7.12 (A) Chromatogram of the HPLC method shows the retention time of the three antihypertensive. (Bs) MS spectrum of HCT (B1), PR (B2) and EM (B3). EM= enalapril maleate, HCT= hydrochlorothiazide, PR= propranolol.

7.2.10 Drug Content and Dissolution Test

Moreover, the drug content analysis demonstrates that the theoretical and experimental drug concentrations are consistent, indicating that no weight loss occurred during the processing of any formulation. In the dissolution apparatus, the rotation of the paddles was set to 100 RPM to test the floating of the tablets under vigorous conditions. Nonetheless, the tablet floated immediately after being placed in the dissolution media. After 30 minutes, the HCT-U and the EM-U disconnected from the floating PR-U, and they started to sink. Nonetheless, the dissolution test for the HCT-U and the EM-U continued in the acidic dissolution medium because the units started to erode, and it was impossible to remove them after 2-3 hours to simulate gastric emptying. The PR unit remained floating for more than 9 hours. Propranolol release from the E RLPO matrix follows first-order release kinetics. More than 75% of the drug was released within the first two hours, then the release slowed down, and a steady state was reached after 9 hours. The release model fitting shows an acceptable fit with the first-order kinetics, R^2= 0.98 and AIC= 27.46, compared to the other models.. Table 7.4 lists the fitting of the kinetic models to the release profile of the three units.

Table 7.4 Fitting a release model for the release of the three units of the FlexiPill.

	ZOM prediction correlation (R^2)	**AIC for ZOM**	**FOM prediction correlation (R^2)**	**AIC FOR FOM**	**HIG-M PREDICTION CORRELATION (R^2)**	**AIC for HIG-M**	**HOP-M PREDICTION correlation (R^2)**	**AIC FOR HOP-M**	**K-P M PREDICTION correlation (R^2)**	**AIC FOR K-P M**	**K-P M release exponent (n)**
PR-U release	0.85	42.78	**0.98**	**27.46**	0.93	49.07	0.92	46.32	0.93	37.80	0.47
EM-U release	0.78	39.80	**0.96**	**25.43**	0.86	54.66	0.91	51.70	0.90	40.45	0.29
HCT-U release (R^2)	0.79	38.77	**0.98**	**23.66**	0.88	34.95	0.98	27.31	0.90	34.43	0.37

AIC= AKAIKE Information Criterion, ZOM= ZERO-ORDER MODEL, FOM= FIRST-ORDER MODEL, HIG-M= HIGUCHI'S MODEL, HOP-M= HOPFENBERG'S MODEL, K-P M= Korsmeyer-Peppas model.

Additionally, the Korsmeyer-Peppas release exponent (n) is 0.47, falling within the range of 0.45 to 0.89, which indicates that the release follows a non-Fickian anomalous transport model (Ansary, Chaurasiya, and Huq 2016). As a result, propranolol release can be described as a non-Fickian diffusion that depend on the concentration gradient. The dissolution medium penetrates through the polymer matrix, causing it to swell and relax. While the outer part of the matrix releases the drug faster, the centre of the matrix releases the drug slower due to the longer path the drug needs to take to be eluted through the nonhomogeneous matrix (Brazel and Peppas 2000). Therefore, as time progresses, the remaining drug concentration decreases, and the release rate decreases as well. The European Medicines Agency (EMA) uses the biopharmaceutics classification system to guide immediate or sustained release oral dosage forms. The BCS classify drug molecules into four classes according to their solubility and permeability. Propranolol is classified as a class I BCS (Vogelpoel et al. 2004). According to EMA guidelines, the specification for in vitro dissolution of an oral prolonged-release product should include at least three key time points: an early time point to rule out dose dumping and/or characterise the loading or initial dose (typically 20–30% dissolved), at least one intermediate point to verify the dissolution profile's shape (around 50% dissolved), and a final point to confirm that the majority of the active substance has been released (Q = 80%) (*Guideline on quality of oral modified release products* 2014). The objective for the PR-U was to have a prolonged release, and a complete drug release occurs while the unit is still floating. In the first three points up to the 30-minute time point, there was no drug dumping the average release was 19%, 52% release was achieved at the 60-minute time point, and drug release was prolonged to 9 hours, and 96.6% was released before flotation ended. Figure 7.13 presents the accumulative release of propranolol from PR-U in the dissolution test.

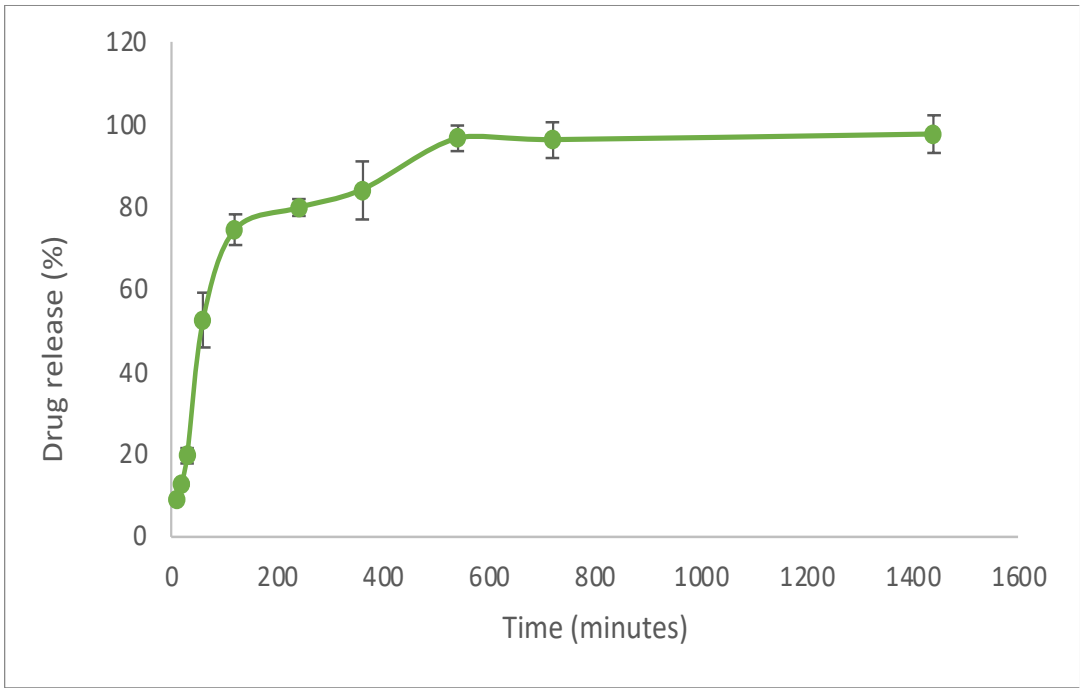

Figure 7.13 Drug release of propranolol from PR-U during dissolution test in simulated gastric medium.

On the other hand, enalapril is classified as a class III BCS with high solubility but low permeability (Verbeeck et al. 2017). Its release can be divided into two phases. Phase one, in which drug release is governed mainly by erosion of the polymer matrix, thus showing high drug release in the first 60 minutes and releasing more than 60% of the drug. In phase two, drug release is mainly through slow diffusion from the eroded unit segments. The maximum drug release that an EM-U reaches in 24 hours is 80%. The release model fitting for the release of enalapril best fits first order kinetics R^2=0.96 and AIC= 25.43. However, the release rate exponent (n) of the Korsmeyer-Peppas release model is 0.29, which is less than 0.45, indicating a Fickian diffusion. The EM-U formulation did not achieve immediate release, likely due to the presence of high molecular weight PEO. This polymer slowed the second phase of drug release, which is governed by diffusion, as enalapril must travel through extended paths within the long polymer chains. Figure 7.14 presents the accumulative release of enalapril from EM-U in the dissolution test.

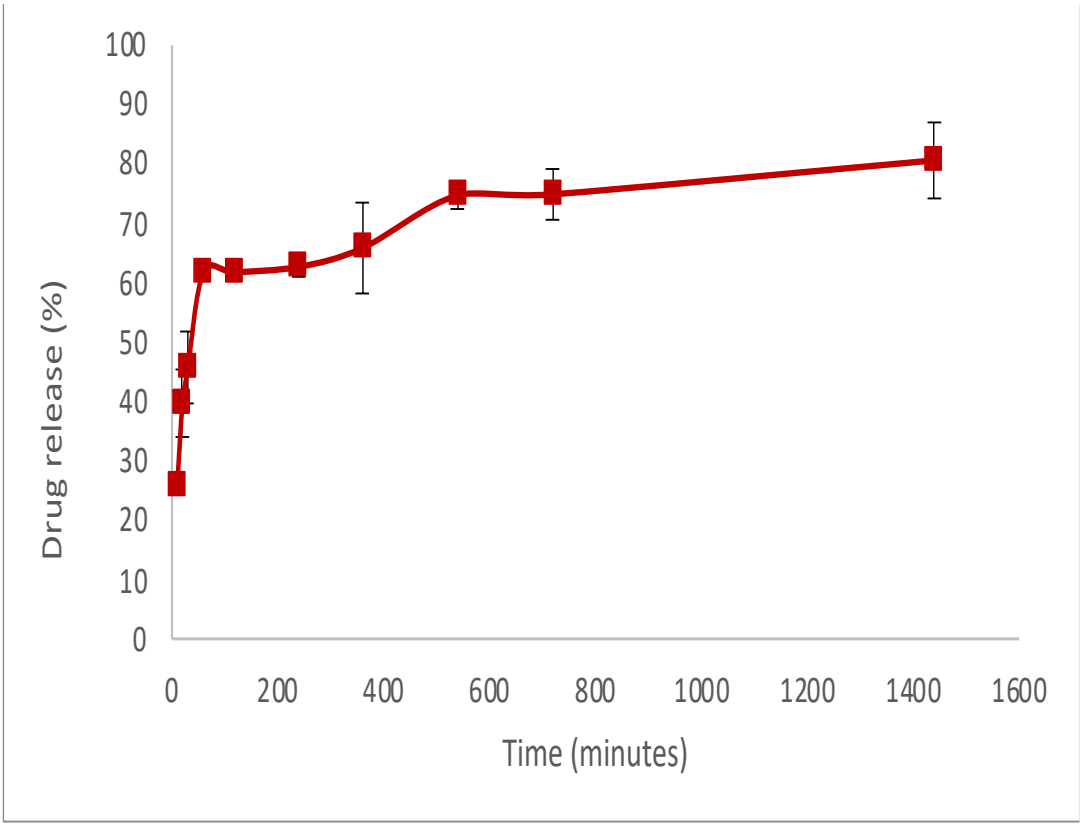

Figure 7.14 Drug release of enalapril from EM-U during dissolution test in simulated gastric medium.

Hydrochlorothiazide is classified as a class II BCS with low solubility and good permeability (Ruponen, Rusanen, and Laitinen 2020). The HCT release from its unit was relatively fast, reaching over 80% release after 60 minutes and 100% release after 6 hours. Compared to conventional tablet, only 64% is release in the first 60 minutes (Khan et al. 2015).The European Medicines Agency considers 75% drug release of the labelled drug in the first 45 minutes are the defining criteria for an immediate release formulation, according to this definition, HCT-F could be considered as such (Agency 2017). Drug release is mainly governed by the fast erosion of the cationic methacrylate copolymer in the acidic medium. There was no diffusion phase as witnessed in the EM-U since this formulation contains no PEO 200K, which slowed the release of the API in the enalapril formulation. The erosion of the matrix is homogenous, meaning that the rate of erosion depends on the amount of polymer remaining. As a result, the drug release from the HCT-U fits the first-order kinetic model R^2 = 0.98 and AIC= 23.66. Figure 7.15 presents the accumulative release of HCT from HCT-U in the dissolution test with the kinetic model fitting.

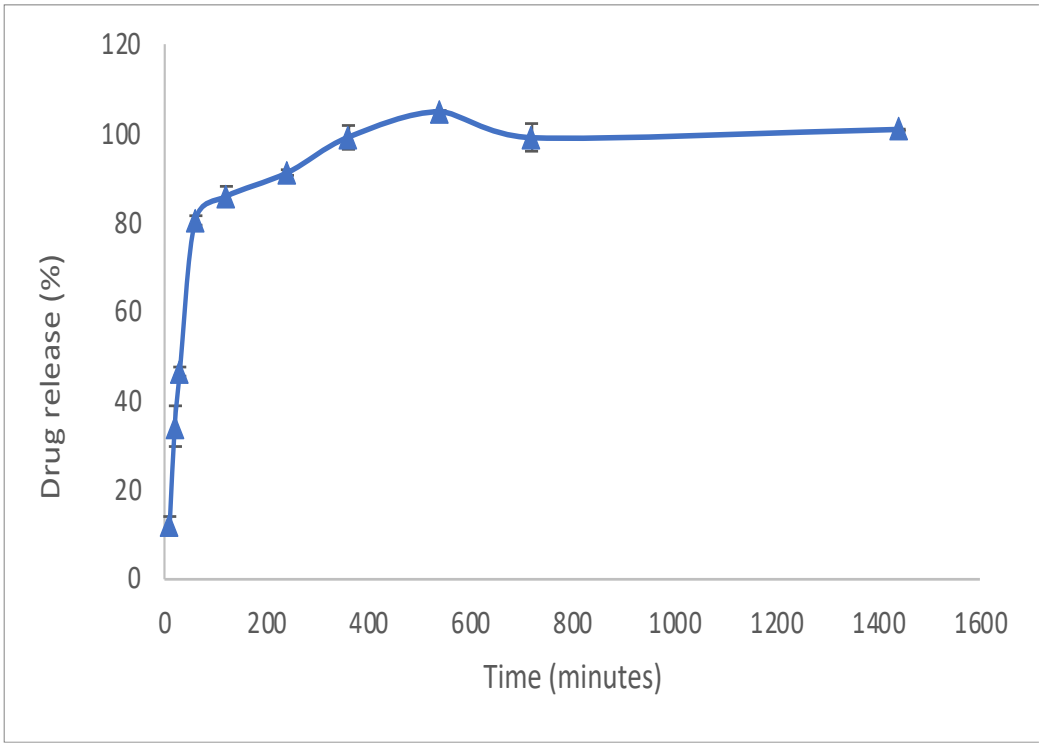

Figure 7.15 Drug release of hydrochlorothiazide from HCT-U during dissolution test in simulated gastric medium.

7.3 Conclusion

The high prevalence of hypertension worldwide causes a great burden on the healthcare system and, if not controlled, can lead to other cardiovascular complications. Hypertension is a multifactorial disease; hence, it requires treatment with multiple antihypertensive agents at the same time. As a result, the fixed-dose combination was suggested to improve patient compliance with such a high number of medications. However, due to many limitations of FDC, a Flexible dose combination that can be personalised according to patient needs has become a need for the healthcare system, especially for chronic diseases that require polypharmacy, like hypertension. Such a formulation can improve patient adherence to treatment and, as a result, ameliorate the clinical outcome of the treatment. Recent advancements in additive manufacturing can pave the way for more intricate designs and make the path to personalised medication shorter.

In this Chapter, FlexiPill, a flexible polypill for hypertension that can be assembled at the point of care according to patient needs, was designed and printed using Fused

filament fabrication. The FlexiPill contained three antihypertension medications: Propranolol was formulated as a floating unit that released the drug by diffusion with extended release, the thermolabile drug enalapril was formulated to have a low printing temperature; and hydrochlorothiazide was printed as an immediate-release unit.

Chapter 8 : Conclusion and Future Perspective

In this study, it has been established that, following recent practices, managing most chronic diseases necessitates the administration of more than one therapeutic agent. This necessity arises due to the complex pathophysiological pathways involved in these diseases, the increasing resistance observed in infectious diseases, and the adverse effects associated with high doses of a single agent. Consequently, this trend has led to a significant increase in the number of medications that patients are required to take daily, a phenomenon commonly referred to as polypharmacy. Polypharmacy has been recognized as a major factor contributing to poor patient adherence to treatment regimens, ultimately leading to treatment failure.

To address this challenge, fixed-dose combinations (FDCs) have been proposed as a solution to improve patient adherence to multidrug regimens. However, while FDCs offer the advantage of simplifying medication regimens, they also present significant limitations, such as a lack of flexibility in dose titration, which is crucial for personalising treatment according to individual patient needs. This lack of flexibility and personalisation has contributed to the reluctance of many healthcare professionals to adopt FDC formulations.

The advent of 3D printing technology, an innovative additive manufacturing approach, has revolutionized pharmaceutical research by offering unprecedented opportunities for the development of personalised medications. Researchers have explored various 3D printing techniques to produce flexible-dose combinations tailored to individual patient requirements. However, the current paradigm advocating for 3D printing at the point of care faces substantial resistance from regulatory authorities. This resistance stems from the need to regulate not only the printer and the printing materials but also the operator and the final product, ensuring compliance with stringent safety and efficacy standards.

3D printing technologies can be broadly classified based on their method of layer formation into three categories: extrusion-based printing, powder solidification, and liquid solidification. Among these, fused deposition modelling (FDM) has emerged as the most extensively studied technique due to its operational simplicity, affordability,

and the availability of cost-effective materials. Consequently, this research focuses on the application of FDM technology in pharmaceutical development.

Previous research has demonstrated the potential of FDM to achieve various pharmaceutical objectives, including controlled drug release, personalised medication, flexible-dose combinations, and gastroretentive dosage forms. Despite these advancements, FDM presents several formulation challenges, such as high printing temperatures, undefined viscosity ranges, difficulty in obtaining filaments with adequate mechanical properties, low resolution, and a limited selection of suitable polymers.

In this work, the use of a methyl acrylate polymer blend with other polymers has been investigated to enhance formulation properties, including reducing printing temperature, improving viscosity, and optimizing mechanical properties. Furthermore, this research introduces the concept of FlexiPill, a novel approach to personalised medicine in which medicated units can be printed and assembled into a polypill at the point of care according to individual patient needs.

In the first phase of this study, immediate and sustained-release units of theophylline were developed and evaluated using a quality-by-design approach. The findings demonstrated that the FlexiPill design effectively controlled drug release by adjusting the ratio of immediate-release to sustained-release units. The number of immediate-release units had a significant impact on both the level and shape of the dissolution curve, thereby offering customization of drug release profiles to meet specific patient needs. Other experimental factors included infill density, which exhibited no significant effect on drug release, and drug concentration, which significantly influenced drug release but also affected melt viscosity and print resolution. Notably, personalising infill density and concentration requires the availability of a printer at the point of care.

In the second phase, the FlexiPill design was successfully utilized to deliver three analgesic drugs in a single tablet formulation. By employing different grades of Eudragit, the release profiles of each drug were individually tailored. For instance, Eudragit EPO was utilized in the paracetamol unit to delay dissolution in alkaline oral cavity media (85% release after one hour in acidic media, but less than 30% in alkaline conditions), effectively masking the drug's bitter taste. Similarly, Eudragit E100-55 was incorporated in the ibuprofen unit to reduce its solubility in acidic gastric fluid (released less than 1% in acidic medium over 24 hours, with more than a tenfold increase in alkaline medium), mitigating gastric irritation. These findings underscore the potential

of the FlexiPill to deliver multiple therapeutic agents with distinct release profiles in a flexible and patient-specific manner.

Additionally, key formulation challenges associated with FDM, such as low drug loading and high printing temperatures, were addressed in this phase. A polymer blend of polyvinyl pyrrolidone (PVP) 40K and Eudragit EPO in a 1:1 ratio enabled the achievement of a high drug load of 55% while maintaining a lower printing temperature of 100°C.

In the final phase, an alternative FlexiPill design incorporating frustum-shaped units that can be stacked on top of each other was introduced. This design includes a floating unit capable of separating from the rest of the FlexiPill, overcoming previous design limitations. Antihypertensive agents were selected as model drugs, each presenting unique formulation challenges. Hydrochlorothiazide, a BCS class II drug with low solubility, was formulated with Eudragit EPO to enhance solubility through amorphous solid dispersion and the formulation delivered 90% release within the first hour. Enalapril, known for its thermal sensitivity, was stabilized by employing a polymer blend of Eudragit EPO, polyethylene oxide (PEO) 200K, and polyethylene glycol (PEG) 6000 to lower the required printing temperature to 150^{o}C. Propranolol hydrochloride, which degrades in alkaline media, was formulated into a floating unit (floated for 9 hours) that releases the drug via diffusion (96% released during floatation), ensuring prolonged gastric retention.

This research highlights the potential of the FlexiPill dosage form in addressing the critical balance between therapeutic personalisation and regulatory concerns. The novelty of this work has been summarized on Page 5.

Moving forward, the successful integration of 3D printing technology into mainstream pharmaceutical practice requires collaborative efforts from researchers, healthcare professionals, and regulatory authorities. Future studies should focus on developing standardized guidelines for 3D printing processes, ensuring quality assurance, reproducibility, and patient safety.

Moreover, further exploration into advanced materials and formulations could enhance the capabilities of 3D-printed pharmaceuticals, enabling the production of more complex drug delivery systems.

In conclusion, the FlexiPill concept provides a promising framework for personalised medicine by enabling flexible dosage combinations, customizable release profiles, and improved patient compliance. With continued advancements and regulatory

adaptations, this approach has the potential to bridge the existing gap between personalised therapy and current pharmaceutical manufacturing constraints.

References

Abrahams, Edward, and Mike Silver. 2010. "The history of personalized medicine." *Integrative neuroscience and personalized medicine*: 3-16.

Achorn, Peter J, and Rosalie G Ferrillo. 1994. "Comparison of thermal techniques for glass transition measurements of polystyrene and cross-linked acrylic polyurethane films." *Journal of applied polymer science* 54 (13): 2033-2043.

Agency, European Medicines. 2017. Reflection Paper on the Dissolution Specification for Generic Solid Oral Immediate Release Products with Systemic Action. European Medicines Agency Amsterdam, The Netherlands.

Ahmed, Minhaz Uddin, Ishtiaq Saaem, Pae C Wu, and April S Brown. 2014. "Personalized diagnostics and biosensors: a review of the biology and technology needed for personalized medicine." *Critical Reviews in Biotechnology* 34 (2): 180-196.

Aho, Johanna, Johan Peter Bøtker, Natalja Genina, Magnus Edinger, Lærke Arnfast, and Jukka Rantanen. 2019. "Roadmap to 3D-printed oral pharmaceutical dosage forms: feedstock filament properties and characterization for fused deposition modeling." *Journal of pharmaceutical sciences* 108 (1): 26-35.

Ai, Jia-Ruey, Fang Peng, Piljae Joo, and Bryan D Vogt. 2021. "Enhanced Dimensional Accuracy of Material Extrusion 3D-Printed Plastics through Filament Architecture." *ACS Applied Polymer Materials*.

Al-Salman, HNK, Ekhlas Qanber Jasim, Hussein H Hussein, and Falah Hassan Shari. 2021. "Theophylline Determination in Pharmaceuticals Using a Novel High-performance Liquid Chromatographic Process." *NeuroQuantology* 19 (7): 196.

Al-Zoubi, N, JE Koundourellis, and S Malamataris. 2002. "FT-IR and Raman spectroscopic methods for identification and quantitation of orthorhombic and monoclinic paracetamol in powder mixes." *Journal of pharmaceutical and biomedical analysis* 29 (3): 459-467.

Albain, Kathy S, Shona M Nag, German Calderillo-Ruiz, Johann P Jordaan, Antonio C Llombart, Anna Pluzanska, Janusz Rolski, Allen S Melemed, Jose M Reyes-Vidal, and Jagdev S Sekhon. 2008. "Gemcitabine plus paclitaxel versus paclitaxel monotherapy in patients with metastatic breast cancer and prior anthracycline treatment." *Journal of Clinical Oncology* 26 (24): 3950-3957.

Alhijjaj, Muqdad, Peter Belton, and Sheng Qi. 2016. "An investigation into the use of polymer blends to improve the printability of and regulate drug release from pharmaceutical solid dispersions prepared via fused deposition modeling (FDM) 3D printing." *European Journal of Pharmaceutics and Biopharmaceutics* 108: 111-125.

Alhijjaj, Muqdad, Jehad Nasereddin, Peter Belton, and Sheng Qi. 2019. "Impact of processing parameters on the quality of pharmaceutical solid dosage forms produced by fused deposition modeling (FDM)." *Pharmaceutics* 11 (12): 633.

Althobaiti, Abdulmajeed A, Eman A Ashour, Ahmed Almotairy, Mashan Almutairi, Mohammed AlYahya, and Michael A Repka. 2022. "Development and characterization of different dosage forms of nifedipine/indomethacin fixed-dose combinations." *Journal of Drug Delivery Science and Technology*: 104117.

Alzahrani, Abdullah, Sagar Narala, Ahmed Adel Ali Youssef, Dinesh Nyavanandi, Suresh Bandari, Preethi Mandati, Ahmed Almotairy, Mashan Almutairi, and Michael Repka. 2022. "Fabrication of a shell-core fixed-dose combination tablet using fused deposition modeling 3D printing." *European Journal of Pharmaceutics and Biopharmaceutics* 177: 211-223.

Alzoubi, Lorca, Alaa AA Aljabali, and Murtaza M Tambuwala. 2023. "Empowering precision medicine: the impact of 3D printing on personalized therapeutic." *AAPS PharmSciTech* 24 (8): 228.

Amar, Jacques, Laurent Vaur, Marc Perret, Christine Bailleau, Sylvie Etienne, Bernard Chamontin, and PRATIK Study Investigators. 2002. "Hypertension in high-risk patients: beware of the underuse of effective combination therapy (results of the PRATIK study)." *Journal of hypertension* 20 (4): 779-784.

Anaya, Brayan J., José R. Cerda, Rita Maria D'Atri, Ivan Yuste, Francis C. Luciano, Aytug Kara, Helga K. Ruiz, Maria Paloma Ballesteros, and Dolores R. Serrano. 2023. "Engineering of 3D printed personalized polypills for the treatment of the metabolic syndrome." *International Journal of Pharmaceutics* 642: 123194. https://doi.org/https://doi.org/10.1016/j.ijpharm.2023.123194. https://www.sciencedirect.com/science/article/pii/S0378517323006142.

Ansary, Johura, Amit Kumar Chaurasiya, and KM Bashirul Huq. 2016. "Formulation and evaluation of metformin HCl floating microspheres." *Asian Journal of Medical and Biological Research* 1 (3): 396-405.

Arafat, Basel, Nidal Qinna, Milena Cieszynska, Robert T Forbes, and Mohamed A Alhnan. 2018. "Tailored on demand anti-coagulant dosing: an in vitro and in vivo evaluation of 3D printed purpose-designed oral dosage forms." *European Journal of Pharmaceutics and Biopharmaceutics* 128: 282-289.

Arafat, Basel, Magdalena Wojsz, Abdullah Isreb, Robert T Forbes, Mohammad Isreb, Waqar Ahmed, Tawfiq Arafat, and Mohamed A Alhnan. 2018. "Tablet fragmentation without a disintegrant: A novel design approach for accelerating disintegration and drug release from 3D printed cellulosic tablets." *European Journal of Pharmaceutical Sciences* 118: 191-199.

Araújo, Maisa RP, Livia L Sa-Barreto, Tais Gratieri, Guilherme M Gelfuso, and Marcilio Cunha-Filho. 2019. "The digital pharmacies era: How 3D printing technology using fused deposition modeling can become a reality." *Pharmaceutics* 11 (3): 128.

Azad, Mohammad A, Deborah Olawuni, Georgia Kimbell, Abu Zayed Md Badruddoza, Md Hossain, and Tasnim Sultana. 2020. "Polymers for extrusion-based 3D printing of pharmaceuticals: A holistic materials–process perspective." *Pharmaceutics* 12 (2): 124.

Baumgartner, Ana, Katarina Drame, Stijn Geutjens, and Marja Airaksinen. 2020. "Does the polypill improve patient adherence compared to its individual formulations? A systematic review." *Pharmaceutics* 12 (2): 190.

Beer, Netta, Susanne Kaae, Natalja Genina, Sofia Kälvemark Sporrong, Teresa Leonardo Alves, Joëlle Hoebert, Marie Louise De Bruin, and Ingrid Hegger. 2023. "Magistral compounding with 3D printing: a promising way to achieve personalized medicine." *Therapeutic Innovation & Regulatory Science* 57 (1): 26-36.

Beitler, Brian G, Paul F Abraham, Alyssa R Glennon, Steven M Tommasini, Lisa L Lattanza, Jonathan M Morris, and Daniel H Wiznia. 2022. "Interpretation of regulatory factors for 3D printing at hospitals and medical centers, or at the point of care." *3D Printing in Medicine* 8 (1): 7.

Berger, Ariel, Alesia Sadosky, Ellen Dukes, John Edelsberg, and Gerry Oster. 2012. "Clinical characteristics and patterns of healthcare utilization in patients with painful neuropathic disorders in UK general practice: a retrospective cohort study." *BMC neurology* 12: 1-13.

BG, Pavan Kalyan, Sonal Mehrotra, Shirleen Miriam Marques, Lalit Kumar, and Ruchi Verma. 2023. "3D printing in personalized medicines: A focus on applications of the technology." *Materials Today Communications*: 105875.

Blagosklonny, Mikhail V. 2005. "Overcoming limitations of natural anticancer drugs by combining with artificial agents." *Trends in pharmacological sciences* 26 (2): 77-81.

Boetker, Johan, Jorrit Jeroen Water, Johanna Aho, Lærke Arnfast, Adam Bohr, and Jukka Rantanen. 2016. "Modifying release characteristics from 3D printed drug-eluting products." *European Journal of Pharmaceutical Sciences* 90: 47-52. https://doi.org/https://doi.org/10.1016/j.ejps.2016.03.013. https://www.sciencedirect.com/science/article/pii/S0928098716300665.

Borandeh, Sedigheh, Bas van Bochove, Arun Teotia, and Jukka Seppälä. 2021. "Polymeric Drug Delivery Systems by Additive Manufacturing." *Advanced Drug Delivery Reviews*.

Borujeni, Shiva Homaee, Seyedeh Zahra Mirdamadian, Jaleh Varshosaz, and Azade Taheri. 2020. "Three-dimensional (3D) printed tablets using ethyl cellulose and hydroxypropyl cellulose to achieve zero order sustained release profile." *Cellulose* 27 (3): 1573-1589.

Boshuizen, Julia, and Daniel S Peeper. 2020. "Rational cancer treatment combinations: an urgent clinical need." *Molecular cell* 78 (6): 1002-1018.

Brazel, Christopher S, and Nikolaos A Peppas. 2000. "Modeling of drug release from swellable polymers." *European journal of pharmaceutics and biopharmaceutics* 49 (1): 47-58.

Burgina, EB, VP Baltakhinov, EV Boldyreva, and TP Shakhtschneider. 2004. "IR spectra of paracetamol and phenacetin. 1. Theoretical and experimental studies." *Journal of Structural Chemistry* 45: 64-73.

Cailleaux, Sylvain, Noelia M Sanchez-Ballester, Yanis A Gueche, Bernard Bataille, and Ian Soulairol. 2020. "Fused Deposition Modeling (FDM), the new asset for the production of tailored medicines." *Journal of Controlled Release*.

Carlier, E, S Marquette, C Peerboom, K Amighi, and J Goole. 2021. "Development of mAb-loaded 3D-printed (FDM) implantable devices based on PLGA." *International Journal of Pharmaceutics* 597: 120337.

Castellano, Jose M, Robert Copeland-Halperin, and Valentin Fuster. 2013. "Aiming at strategies for a complex problem of medical nonadherence." *Global heart* 8 (3): 263-271.

Castellano, José M, Ginés Sanz, José L Peñalvo, Sameer Bansilal, Antonio Fernández-Ortiz, Luz Alvarez, Luis Guzmán, Juan Carlos Linares, Fernando García, and Fabiana D'Aniello. 2014. "A polypill strategy to improve adherence: results from the FOCUS project." *Journal of the American College of Cardiology* 64 (20): 2071-2082.

Chai, Xuyu, Hongyu Chai, Xiaoyu Wang, Jingjing Yang, Jin Li, Yan Zhao, Weimin Cai, Tao Tao, and Xiaoqiang Xiang. 2017. "Fused deposition modeling (FDM) 3D printed tablets for intragastric floating delivery of domperidone." *Scientific reports* 7 (1): 1-9.

Chapman, Richard H, Joshua S Benner, Allison A Petrilla, Jonothan C Tierce, S Robert Collins, David S Battleman, and J Sanford Schwartz. 2005. "Predictors of adherence with antihypertensive and lipid-lowering therapy." *Archives of internal medicine* 165 (10): 1147-1152.

Chaunier, Laurent, Sofiane Guessasma, Sofiane Belhabib, Guy Della Valle, Denis Lourdin, and Eric Leroy. 2018. "Material extrusion of plant biopolymers: Opportunities & challenges for 3D printing." *Additive Manufacturing* 21: 220-233. https://doi.org/https://doi.org/10.1016/j.addma.2018.03.016. https://www.sciencedirect.com/science/article/pii/S2214860417300350.

Chen, Di, Xiang-Yu Xu, Rui Li, Gen-Ao Zang, Yue Zhang, Ming-Rui Wang, Meng-Fei Xiong, Jia-Rui Xu, Ting Wang, and Hui Fu. 2020. "Preparation and in vitro evaluation of FDM 3D-printed ellipsoid-shaped gastric floating tablets with low infill percentages." *AAPS PharmSciTech* 21 (1): 1-13.

Cohen, Steven P, Lene Vase, and William M Hooten. 2021. "Chronic pain: an update on burden, best practices, and new advances." *The Lancet* 397 (10289): 2082-2097.

Cooper-DeHoff, Rhonda M, Steven T Bird, Gregory A Nichols, Joseph A Delaney, and Almut G Winterstein. 2013. "Antihypertensive drug class interactions and risk for incident diabetes: a nested case–control study." *Journal of the American Heart Association* 2 (3): e000125.

Cossé, Anne, Corinna König, Alf Lamprecht, and Karl G Wagner. 2017. "Hot melt extrusion for sustained protein release: matrix erosion and in vitro release of PLGA-based implants." *AAPS PharmSciTech* 18 (1): 15-26.

Crowley, Michael M., Zhang Feng, Repka Michael A., Thumma Sridhar, Upadhye Sampada B., Kumar Battu Sunil, McGinity James W., and Charles and Martin. 2007. "Pharmaceutical Applications of Hot-Melt Extrusion: Part I." *Drug Development and Industrial Pharmacy* 33 (9): 909-926. https://doi.org/10.1080/03639040701498759. https://doi.org/10.1080/03639040701498759.

CVD, Working Group on the Summit on Combination Therapy for. 2014. "Combination pharmacotherapy to prevent cardiovascular disease: present status and challenges." *European Heart Journal* 35 (6): 353-364.

de Cates, Angharad N, Matthew RB Farr, Nicola Wright, Morag C Jarvis, Karen Rees, Shah Ebrahim, and Mark D Huffman. 2014. "Fixed-dose combination therapy for the prevention of cardiovascular disease." *Cochrane Database of Systematic Reviews* (4).

de Souza, Steffany Manzan Marques, Pedro Ivo Brandão e Melo Franco, Maria Inês Gonçalves Leles, and Edemilson Cardoso da Conceição. 2016. "Evaluation of thermal stability of enalapril maleate tablets using thermogravimetry and differential scanning calorimetry." *Journal of Thermal Analysis and Calorimetry* 123: 1943-1949.

dos Santos, Juliana, Gabriela de Souza Balbinot, Silvio Buchner, Fabrício Mezzomo Collares, Maike Windbergs, Monique Deon, and Ruy Carlos Ruver Beck. 2023. "3D printed matrix solid forms: Can the drug solubility and dose customisation affect their controlled release behaviour?" *International Journal of Pharmaceutics: X* 5: 100153. https://doi.org/https://doi.org/10.1016/j.ijpx.2022.100153. https://www.sciencedirect.com/science/article/pii/S2590156722000445.

Dos Santos, Juliana, Guilherme Silveira da Silva, Maiara Callegaro Velho, and Ruy Carlos Ruver Beck. 2021. "Eudragit®: A versatile family of polymers for hot melt extrusion and 3D printing processes in pharmaceutics." *Pharmaceutics* 13 (9): 1424.

Dumpa, Nagireddy, Arun Butreddy, Honghe Wang, Neeraja Komanduri, Suresh Bandari, and Michael A Repka. 2021. "3D printing in personalized drug delivery:

An overview of hot-melt extrusion-based fused deposition modeling." *International Journal of Pharmaceutics*: 120501.

Economidou, Sophia N, and Dennis Douroumis. 2021. "3D printing as a transformative tool for microneedle systems: Recent advances, manufacturing considerations and market potential." *Advanced Drug Delivery Reviews*.

Egan, Mark, and Tomas J Philipson. 2014. *Health Care Adherence and Personalized Medicine.* National Bureau of Economic Research.

Ehtezazi, Touraj, Marwan Algellay, Yamir Islam, Matt Roberts, Nicola M Dempster, and Satyajit D Sarker. 2018. "The application of 3D printing in the formulation of multilayered fast dissolving oral films." *Journal of pharmaceutical sciences* 107 (4): 1076-1085.

Elbadawi, M. 2019. "Rheological and Mechanical Investigation into the Effect of Different Molecular Weight Poly(ethylene glycol)s on Polycaprolactone-Ciprofloxacin Filaments." *Acs Omega* 4 (3): 5412-5423. https://doi.org/10.1021/acsomega.8b03057. <Go to ISI>://WOS:000462921900096.

Englezos, Klaudia, Lingxin Wang, Edwin CK Tan, and Lifeng Kang. 2023. "3D printing for personalised medicines: implications for policy and practice." *International Journal of Pharmaceutics* 635: 122785.

Espinosa, James, Gabriel Meister, Mohammad Rattu, and Alan Lucerna. 2023. "The Risks of Patient Pill Splitting: A Case Report and Review." *Cureus* 15 (11).

Farooqi, Zarreen H, and Hassan Y Aboul-Enein. 1996. "IR and UV/visible spectra of propranolol and some fluorinated derivatives: Comparison of experimental and calculated values." *Biospectroscopy* 2 (2): 131-141.

FDA., U.S. 2022. Size, Shape, and Other Physical Attributes of Generic Tablets and Capsules.

Docket Number: FDA-2013-N-1434 edited by U.S. Department of Health and Human Services.: U.S. Department of Health and Human Services.

Fina, Fabrizio, Alvaro Goyanes, Martin Rowland, Simon Gaisford, and Abdul W. Basit. 2020. "3D printing of tunable zero-order release printlets." *Polymers* 12 (8): 1769.

Fisusi, Funmilola A, and Emmanuel O Akala. 2019. "Drug combinations in breast cancer therapy." *Pharmaceutical nanotechnology* 7 (1): 3-23.

Fitriani, Lili, Alianshar Haqi, and Erizal Zaini. 2016. "Preparation and characterization of solid dispersion freeze-dried efavirenz–polyvinylpyrrolidone K-30." *Journal of Advanced Pharmaceutical Technology & Research* 7 (3): 105-109.

Fu, Junhui, Hui Yin, Xiang Yu, Cong Xie, Heliu Jiang, Yiguang Jin, and Fugeng Sheng. 2018. "Combination of 3D printing technologies and compressed tablets for preparation of riboflavin floating tablet-in-device (TiD) systems." *International journal of pharmaceutics* 549 (1-2): 370-379.

Fuenmayor, Evert, Martin Forde, Andrew V Healy, Declan M Devine, John G Lyons, Christopher McConville, and Ian Major. 2018. "Material considerations for fused-filament fabrication of solid dosage forms." *Pharmaceutics* 10 (2): 44.

Fukuda, Isa Martins, Camila Francini Fidelis Pinto, Camila dos Santos Moreira, Alessandro Morais Saviano, and Felipe Rebello Lourenço. 2018. "Design of experiments (DoE) applied to pharmaceutical and analytical quality by design (QbD)." *Brazilian journal of pharmaceutical sciences* 54: e01006.

Fuster, Valentín, Francesc Gambús, Aldo Patriciello, Margaretha Hamrin, and Diederick E Grobbee. 2017. "The polypill approach–an innovative strategy to improve cardiovascular health in Europe." *BMC Pharmacology and Toxicology* 18: 1-8.

Gandhi, Rajesh T, Roger Bedimo, Jennifer F Hoy, Raphael J Landovitz, Davey M Smith, Ellen F Eaton, Clara Lehmann, Sandra A Springer, Paul E Sax, and Melanie A Thompson. 2023. "Antiretroviral drugs for treatment and prevention of HIV infection in adults: 2022 recommendations of the International Antiviral Society–USA panel." *Jama* 329 (1): 63-84.

Garjon, Javier, Luis Carlos Saiz, Ana Azparren, Idoia Gaminde, Mª José Ariz, and Juan Erviti. 2020. "First-line combination therapy versus first-line monotherapy for primary hypertension." *Cochrane Database of Systematic Reviews* (2).

Genina, Natalja, Jenny Holländer, Harri Jukarainen, Ermei Mäkilä, Jarno Salonen, and Niklas Sandler. 2016. "Ethylene vinyl acetate (EVA) as a new drug carrier for 3D printed medical drug delivery devices." *European Journal of Pharmaceutical Sciences* 90: 53-63.

Gifari, Muhammad Wildan, Pugud Samodro, and Dhadhang Wahyu Kurniawan. 2021. "Artificial intelligence toward personalized medicine." *Pharmaceut. Sci. Res* 8 (2): 1.

Gilron, Ian, Troels S Jensen, and Anthony H Dickenson. 2013. "Combination pharmacotherapy for management of chronic pain: from bench to bedside." *The Lancet Neurology* 12 (11): 1084-1095.

Gioumouxouzis, Christos I, Apostolos Baklavaridis, Orestis L Katsamenis, Catherine K Markopoulou, Nikolaos Bouropoulos, Dimitrios Tzetzis, and Dimitrios G Fatouros. 2018. "A 3D printed bilayer oral solid dosage form combining metformin for prolonged and glimepiride for immediate drug delivery." *European Journal of Pharmaceutical Sciences* 120: 40-52.

Giri, Bhupendra Raj, Eon Soo Song, Jaewook Kwon, Ju-Hyun Lee, Jun-Bom Park, and Dong Wuk Kim. 2020. "Fabrication of intragastric floating, controlled release 3D printed theophylline tablets using hot-melt extrusion and fused deposition modeling." *Pharmaceutics* 12 (1): 77.

Goh, Wei Jiang, Si Xuan Tan, Giorgia Pastorin, Paul Chi Lui Ho, Jun Hu, and Seng Han Lim. 2021. "3D printing of four-in-one oral polypill with multiple release profiles for personalized delivery of caffeine and vitamin B analogues." *International Journal of Pharmaceutics* 598: 120360.

Gorkem Buyukgoz, Guluzar, Christopher G Kossor, Shen Ji, Murat Guvendiren, and Rajesh N Davé. 2022. "Dose Titration of Solid Dosage Forms via FDM 3D-Printed Mini-Tablets." *Pharmaceutics* 14 (11): 2305.

Gottschalk, Nadine, Malte Bogdahn, Meike Harms, and Julian Quodbach. 2021. "Brittle polymers in Fused Deposition Modeling: An improved feeding approach to enable the printing of highly drug loaded filament." *International Journal of Pharmaceutics* 597: 120216.

Goyanes, Alvaro, Nour Allahham, Sarah J Trenfield, Edmont Stoyanov, Simon Gaisford, and Abdul W Basit. 2019. "Direct powder extrusion 3D printing: Fabrication of drug products using a novel single-step process." *International journal of pharmaceutics* 567: 118471.

Goyanes, Alvaro, Usanee Det-Amornrat, Jie Wang, Abdul W. Basit, and Simon Gaisford. 2016. "3D scanning and 3D printing as innovative technologies for fabricating personalized topical drug delivery systems." *Journal of Controlled Release* 234: 41-48. https://doi.org/https://doi.org/10.1016/j.jconrel.2016.05.034. https://www.sciencedirect.com/science/article/pii/S0168365916303145.

Goyanes, Alvaro, Fabrizio Fina, Annalisa Martorana, Daniel Sedough, Simon Gaisford, and Abdul W. Basit. 2017. "Development of modified release 3D printed tablets (printlets) with pharmaceutical excipients using additive manufacturing." *International Journal of Pharmaceutics* 527 (1): 21-30. https://doi.org/https://doi.org/10.1016/j.ijpharm.2017.05.021. https://www.sciencedirect.com/science/article/pii/S0378517317304313.

Goyanes, Alvaro, Masanori Kobayashi, Ramón Martínez-Pacheco, Simon Gaisford, and Abdul W Basit. 2016. "Fused-filament 3D printing of drug products: microstructure analysis and drug release characteristics of PVA-based caplets." *International journal of pharmaceutics* 514 (1): 290-295.

Goyanes, Alvaro, Pamela Robles Martinez, Asma Buanz, Abdul W Basit, and Simon Gaisford. 2015. "Effect of geometry on drug release from 3D printed tablets." *International journal of pharmaceutics* 494 (2): 657-663.

Goyanes, Alvaro, Jie Wang, Asma Buanz, Ramón Martínez-Pacheco, Richard Telford, Simon Gaisford, and Abdul W Basit. 2015. "3D printing of medicines: engineering novel oral devices with unique design and drug release characteristics." *Molecular pharmaceutics* 12 (11): 4077-4084.

Gradman, Alan H, Jan N Basile, Barry L Carter, George L Bakris, and American Society of Hypertension Writing Group. 2010. "Combination therapy in hypertension." *Journal of the American Society of Hypertension* 4 (2): 90-98.

Greenacre, Michael, Patrick JF Groenen, Trevor Hastie, Alfonso Iodice d'Enza, Angelos Markos, and Elena Tuzhilina. 2022. "Principal component analysis." *Nature Reviews Methods Primers* 2 (1): 100.

Group, PILL Collaborative. 2011. "An international randomised placebo-controlled trial of a four-component combination pill ("polypill") in people with raised cardiovascular risk." *PloS one* 6 (5): e19857.

Guideline, IHT. 2022. "Validation of analytical procedures Q2 (R2)." *ICH: Geneva, Switzerland*.

Guideline on quality of oral modified release products. 2014.

Ho, P Michael, Chris L Bryson, and John S Rumsfeld. 2009. "Medication adherence: its importance in cardiovascular outcomes." *Circulation* 119 (23): 3028-3035.

Hoffmann, Lena, Jörg Breitkreutz, and Julian Quodbach. 2022a. "Fused deposition modeling (FDM) 3D printing of the thermo-sensitive peptidomimetic drug enalapril maleate." *Pharmaceutics* 14 (11): 2411.

---. 2022b. "Hot-melt extrusion of the thermo-sensitive peptidomimetic drug enalapril maleate." *Pharmaceutics* 14 (10): 2091.

Huanbutta, Kampanart, and Tanikan Sangnim. 2019. "Design and development of zero-order drug release gastroretentive floating tablets fabricated by 3D printing technology." *Journal of Drug Delivery Science and Technology* 52: 831-837.

Hugtenburg, Jacqueline G, Lonneke Timmers, Petra JM Elders, Marcia Vervloet, and Liset van Dijk. 2013. "Definitions, variants, and causes of nonadherence with medication: a challenge for tailored interventions." *Patient preference and adherence*: 675-682.

Ilyés, Kinga, Attila Balogh, Tibor Casian, Tamás Igricz, Enikő Borbás, Balázs Démuth, Panna Vass, Lilla Menyhárt, Norbert Krisztián Kovács, and György Marosi. 2019. "3D floating tablets: Appropriate 3D design from the perspective of different in vitro dissolution testing methodologies." *International journal of pharmaceutics* 567: 118433.

Ingersoll, Karen S, and Jessye Cohen. 2008. "The impact of medication regimen factors on adherence to chronic treatment: a review of literature." *Journal of behavioral medicine* 31: 213-224.

Isreb, Abdullah, Krzysztof Baj, Magdalena Wojsz, Mohammad Isreb, Matthew Peak, and Mohamed A Alhnan. 2019. "3D printed oral theophylline doses with innovative 'radiator-like'design: Impact of polyethylene oxide (PEO) molecular weight." *International journal of pharmaceutics* 564: 98-105.

Jacob, Jules, Norman Coyle, Thomas G West, Donald C Monkhouse, Henry L Surprenant, and Nemichand B Jain. 2016. Rapid disperse dosage form containing levetiracetam. Google Patents.

Jamróz, Witold, Mateusz Kurek, Anna Czech, Joanna Szafraniec, Karolina Gawlak, and Renata Jachowicz. 2018. "3D printing of tablets containing amorphous aripiprazole by filaments co-extrusion." *European Journal of Pharmaceutics and Biopharmaceutics* 131: 44-47. https://doi.org/https://doi.org/10.1016/j.ejpb.2018.07.017. https://www.sciencedirect.com/science/article/pii/S0939641118303539.

Jamróz, Witold, Mateusz Kurek, Ewelina Łyszczarz, Joanna Szafraniec, Justyna Knapik-Kowalczuk, Karolina Syrek, Marian Paluch, and Renata Jachowicz. 2017. "3D printed orodispersible films with Aripiprazole." *International journal of pharmaceutics* 533 (2): 413-420.

Jamróz, Witold, Joanna Szafraniec, Mateusz Kurek, and Renata Jachowicz. 2018. "3D printing in pharmaceutical and medical applications–recent achievements and challenges." *Pharmaceutical research* 35 (9): 1-22.

Janczura, Magdalena, Szymon Sip, and Judyta Cielecka-Piontek. 2022. "The development of innovative dosage forms of the fixed-dose combination of active pharmaceutical ingredients." *Pharmaceutics* 14 (4): 834.

Kadry, Hossam, Taslim A. Al-Hilal, Ali Keshavarz, Farzana Alam, Changxue Xu, Abraham Joy, and Fakhrul Ahsan. 2018. "Multi-purposable filaments of HPMC for 3D printing of medications with tailored drug release and timed-absorption." *International Journal of Pharmaceutics* 544 (1): 285-296. https://doi.org/https://doi.org/10.1016/j.ijpharm.2018.04.010. https://www.sciencedirect.com/science/article/pii/S0378517318302217.

Kalaskar, Deepak M., and Tiziano Serra. 2017. *3D Printing in Medicine*. Cambridge, UNITED KINGDOM: Elsevier Science & Technology.

Kearney, Patricia M, Megan Whelton, Kristi Reynolds, Paul Muntner, Paul K Whelton, and Jiang He. 2005. "Global burden of hypertension: analysis of worldwide data." *The lancet* 365 (9455): 217-223.

Kempin, Wiebke, Vanessa Domsta, Georg Grathoff, Iris Brecht, Beatrice Semmling, Susan Tillmann, Werner Weitschies, and Anne Seidlitz. 2018. "Immediate release 3D-printed tablets produced via fused deposition modeling of a thermo-sensitive drug." *Pharmaceutical research* 35 (6): 1-12.

Khaled, Shaban A, Jonathan C Burley, Morgan R Alexander, Jing Yang, and Clive J Roberts. 2015a. "3D printing of five-in-one dose combination polypill with defined immediate and sustained release profiles." *Journal of controlled release* 217: 308-314.

---. 2015b. "3D printing of tablets containing multiple drugs with defined release profiles." *International journal of pharmaceutics* 494 (2): 643-650.

Khan, Amjad, Zafar Iqbal, Yasar Shah, Lateef Ahmad, Ismail, Zia Ullah, and Aman Ullah. 2015. "Enhancement of dissolution rate of class II drugs (Hydrochlorothiazide); a comparative study of the two novel approaches; solid dispersion and liqui-solid techniques." *Saudi Pharmaceutical Journal* 23 (6): 650-657. https://doi.org/https://doi.org/10.1016/j.jsps.2015.01.025. https://www.sciencedirect.com/science/article/pii/S1319016415000389.

Khdair, Ayman, Di Chen, Yogesh Patil, Linan Ma, Q Ping Dou, Malathy PV Shekhar, and Jayanth Panyam. 2010. "Nanoparticle-mediated combination chemotherapy and photodynamic therapy overcomes tumor drug resistance." *Journal of Controlled Release* 141 (2): 137-144.

Kimura, Shin-ichiro, Taichi Ishikawa, Yasunori Iwao, Shigeru Itai, and Hiromu Kondo. 2019. "Fabrication of zero-order sustained-release floating tablets via fused depositing modeling 3D printer." *Chemical and Pharmaceutical Bulletin* 67 (9): 992-999.

Kollamaram, Gayathri, Denise M Croker, Gavin M Walker, Alvaro Goyanes, Abdul W Basit, and Simon Gaisford. 2018. "Low temperature fused deposition modeling (FDM) 3D printing of thermolabile drugs." *International journal of pharmaceutics* 545 (1-2): 144-152.

Korte, Carolin, and Julian Quodbach. 2018. "Formulation development and process analysis of drug-loaded filaments manufactured via hot-melt extrusion for 3D-printing of medicines." *Pharmaceutical development and technology* 23 (10): 1117-1127.

Kukkonen, Juho, Tuomas Ervasti, and Riikka Laitinen. 2022. "Production and characterization of glibenclamide incorporated PLA filaments for 3D printing by fused deposition modeling." *Journal of Drug Delivery Science and Technology* 77: 103843. https://doi.org/https://doi.org/10.1016/j.jddst.2022.103843. https://www.sciencedirect.com/science/article/pii/S1773224722007547.

Lamichhane, Shrawani, Jun-Bom Park, Dong Hwan Sohn, and Sangkil Lee. 2019. "Customized novel design of 3D printed pregabalin tablets for intra-gastric floating and controlled release using fused deposition modeling." *Pharmaceutics* 11 (11): 564.

Langebeek, Nienke, Herman G Sprenger, Elisabeth H Gisolf, Peter Reiss, Mirjam AG Sprangers, Jean-Claude Legrand, Clemens Richter, and Pythia T Nieuwkerk. 2014. "A simplified combination antiretroviral therapy regimen enhances adherence, treatment satisfaction and quality of life: results of a randomized clinical trial." *HIV medicine* 15 (5): 286-290.

Li, Qijun, Haoyang Wen, Danyang Jia, Xiaoying Guan, Hao Pan, Yue Yang, Shihui Yu, Zhihong Zhu, Rongwu Xiang, and Weisan Pan. 2017. "Preparation and investigation of controlled-release glipizide novel oral device with three-dimensional printing." *International Journal of Pharmaceutics* 525 (1): 5-11.

https://doi.org/https://doi.org/10.1016/j.ijpharm.2017.03.066. https://www.sciencedirect.com/science/article/pii/S0378517317302521.

Li, Yongcheng, Huishi Pang, Zhefei Guo, Ling Lin, Yixuan Dong, Ge Li, Ming Lu, and Chuangbin Wu. 2014. "Interactions between drugs and polymers influencing hot melt extrusion." *Journal of Pharmacy and Pharmacology* 66 (2): 148-166.

Lin, Shan-Yang, Shun-Li Wang, Ting-Fang Chen, and Ting-Chou Hu. 2002. "Intramolecular cyclization of diketopiperazine formation in solid-state enalapril maleate studied by thermal FT-IR microscopic system." *European journal of pharmaceutics and biopharmaceutics* 54 (2): 249-254.

Lopez, A Pavia, S Erdine, J Zamorano, JH Kim, A Al Khadra, M Westergaard, S Sutradhar, and C Yunis. 2010. "CARDIOVASCULAR RISK FACTOR MANAGEMENT: SINGLE-PILL AMLODIPINE/ATORVASTATIN VERSUS USUAL CARE IN PATIENTS WITH HYPERTENSION AND ADDITIONAL RISK FACTORS-THE CRUCIAL TRIAL: PP. 16.96." *Journal of Hypertension* 28: e278-e279.

Luzuriaga, Michael A, Danielle R Berry, John C Reagan, Ronald A Smaldone, and Jeremiah J Gassensmith. 2018. "Biodegradable 3D printed polymer microneedles for transdermal drug delivery." *Lab on a Chip* 18 (8): 1223-1230.

Mancia, Giuseppe, and Guido Grassi. 2002. "Systolic and diastolic blood pressure control in antihypertensive drug trials." *Journal of hypertension* 20 (8): 1461-1464.

Maroni, A., A. Melocchi, F. Parietti, A. Foppoli, L. Zema, and A. Gazzaniga. 2017. "3D printed multi-compartment capsular devices for two-pulse oral drug delivery." *Journal of Controlled Release* 268: 10-18. https://doi.org/https://doi.org/10.1016/j.jconrel.2017.10.008. https://www.sciencedirect.com/science/article/pii/S0168365917308957.

Mathur, Sunil, and Joseph Sutton. 2017. "Personalized medicine could transform healthcare." *Biomedical reports* 7 (1): 3-5.

McDonagh, Thomas, Peter Belton, and Sheng Qi. 2023. "Manipulating drug release from 3D printed dual-drug loaded polypills using challenging polymer compositions." *International Journal of Pharmaceutics* 637: 122895.

Melnyk, Larissa A., and Moses O. Oyewumi. 2021. "Integration of 3D printing technology in pharmaceutical compounding: Progress, prospects, and challenges." *Annals of 3D Printed Medicine* 4: 100035.

https://doi.org/https://doi.org/10.1016/j.stlm.2021.100035. https://www.sciencedirect.com/science/article/pii/S2666964121000308.

Melocchi, Alice, Francesco Briatico-Vangosa, Marco Uboldi, Federico Parietti, Maximilian Turchi, Didier von Zeppelin, Alessandra Maroni, Lucia Zema, Andrea Gazzaniga, and Ahmed Zidan. 2021. "Quality considerations on the pharmaceutical applications of fused deposition modeling 3D printing." *International Journal of Pharmaceutics* 592: 119901.

Melocchi, Alice, Federico Parietti, Giulia Loreti, Alessandra Maroni, Andrea Gazzaniga, and Lucia Zema. 2015. "3D printing by fused deposition modeling (FDM) of a swellable/erodible capsular device for oral pulsatile release of drugs." *Journal of Drug Delivery Science and Technology* 30: 360-367. https://doi.org/https://doi.org/10.1016/j.jddst.2015.07.016. https://www.sciencedirect.com/science/article/pii/S177322471500132X.

Melocchi, Alice, Federico Parietti, Alessandra Maroni, Anastasia Foppoli, Andrea Gazzaniga, and Lucia Zema. 2016. "Hot-melt extruded filaments based on pharmaceutical grade polymers for 3D printing by fused deposition modeling." *International journal of pharmaceutics* 509 (1-2): 255-263.

Melocchi, Alice, Marco Uboldi, Matteo Cerea, Anastasia Foppoli, Alessandra Maroni, Saliha Moutaharrik, Luca Palugan, Lucia Zema, and Andrea Gazzaniga. 2020. "A graphical review on the escalation of fused deposition modeling (FDM) 3D printing in the pharmaceutical field." *Journal of Pharmaceutical Sciences* 109 (10): 2943-2957.

Melocchi, Alice, Marco Uboldi, Nicoletta Inverardi, Francesco Briatico-Vangosa, Francesco Baldi, Stefano Pandini, Giulia Scalet, Ferdinando Auricchio, Matteo Cerea, and Anastasia Foppoli. 2019. "Expandable drug delivery system for gastric retention based on shape memory polymers: Development via 4D printing and extrusion." *International journal of pharmaceutics* 571: 118700.

Melocchi, Alice, Marco Uboldi, Alessandra Maroni, Anastasia Foppoli, Luca Palugan, Lucia Zema, and Andrea Gazzaniga. 2020. "3D printing by fused deposition modeling of single-and multi-compartment hollow systems for oral delivery–A review." *International journal of pharmaceutics* 579: 119155.

Mendibil, Xabier, Gaizka Tena, Alaine Duque, Nerea Uranga, Miguel Ángel Campanero, and Jesús Alonso. 2021. "Direct Powder Extrusion of Paracetamol

Loaded Mixtures for 3D Printed Pharmaceutics for Personalized Medicine via Low Temperature Thermal Processing." *Pharmaceutics* 13 (6): 907.

Menditto, Enrica, Valentina Orlando, Giuseppe De Rosa, Paola Minghetti, Umberto Maria Musazzi, Caitriona Cahir, Marta Kurczewska-Michalak, Przemysław Kardas, Elísio Costa, and Jose Manuel Sousa Lobo. 2020. "Patient centric pharmaceutical drug product design—The impact on medication adherence." *Pharmaceutics* 12 (1): 44.

Mokhtari, Reza Bayat, Sushil Kumar, Syed S Islam, Mehrdad Yazdanpanah, Khosrow Adeli, Ernest Cutz, and Herman Yeger. 2013. "Combination of carbonic anhydrase inhibitor, acetazolamide, and sulforaphane, reduces the viability and growth of bronchial carcinoid cell lines." *BMC cancer* 13: 1-18.

Mora-Castaño, Gloria, Juan Domínguez-Robles, Achmad Himawan, Mónica Millán-Jiménez, and Isidoro Caraballo. 2024. "Current trends in 3D printed gastroretentive floating drug delivery systems: A comprehensive review." *International Journal of Pharmaceutics* 663: 124543. https://doi.org/https://doi.org/10.1016/j.ijpharm.2024.124543. https://www.sciencedirect.com/science/article/pii/S0378517324007774.

Mora-Castaño, Gloria, Mónica Millán-Jiménez, and Isidoro Caraballo. 2023. "Hydrophilic high drug-loaded 3D printed Gastroretentive system with robust release kinetics." *Pharmaceutics* 15 (3): 842.

Mora-Castaño, Gloria, Mónica Millán-Jiménez, Andreas Niederquell, Monica Schönenberger, Fatemeh Shojaie, Martin Kuentz, and Isidoro Caraballo. 2024. "Amorphous solid dispersion of a binary formulation with felodipine and HPMC for 3D printed floating tablets." *International Journal of Pharmaceutics* 658: 124215. https://doi.org/https://doi.org/10.1016/j.ijpharm.2024.124215. https://www.sciencedirect.com/science/article/pii/S0378517324004496.

Mukete, Bertrand N, and Keith C Ferdinand. 2016. "Polypharmacy in older adults with hypertension: a comprehensive review." *The Journal of Clinical Hypertension* 18 (1): 10-18.

Nafisi, Shohreh, Abolfazl Seyed Sadjadi, Sakine Shokrollah Zadeh, and Maryam Damerchelli. 2003. "Interaction of metal ions with caffeine and theophylline: stability and structural features." *Journal of Biomolecular Structure and Dynamics* 21 (2): 289-295.

Nagarajan, Neerajha, Agnes Dupret-Bories, Erdem Karabulut, Pinar Zorlutuna, and Nihal Engin Vrana. 2018. "Enabling personalized implant and controllable biosystem development through 3D printing." *Biotechnology advances* 36 (2): 521-533.

Nasereddin, Jehad M, Nikolaus Wellner, Muqdad Alhijjaj, Peter Belton, and Sheng Qi. 2018. "Development of a simple mechanical screening method for predicting the feedability of a pharmaceutical FDM 3D printing filament." *Pharmaceutical research* 35 (8): 1-13.

Nashed, Nour, Matthew Lam, and Ali Nokhodchi. 2021. "A comprehensive overview of extended release oral dosage forms manufactured through hot melt extrusion and its combination with 3D printing." *International Journal of Pharmaceutics*: 120237.

Nieuwlaat, Robby, Nancy Wilczynski, Tamara Navarro, Nicholas Hobson, Rebecca Jeffery, Arun Keepanasseril, Thomas Agoritsas, Niraj Mistry, Alfonso Iorio, and Susan Jack. 2014. "Interventions for enhancing medication adherence." *Cochrane database of systematic reviews* (11).

Nukala, Pavan Kumar, Siddhant Palekar, Manali Patki, and Ketan Patel. 2019. "Abuse Deterrent Immediate Release Egg-Shaped Tablet (Egglets)Using 3D Printing Technology: Quality by Design to Optimize Drug Release andExtraction." *AAPS PharmSciTech* 20 (2): 80. https://doi.org/10.1208/s12249-019-1298-y. https://doi.org/10.1208/s12249-019-1298-y.

Obeid, Samiha, Marijana Madžarević, and Svetlana Ibrić. 2021. "Tailoring amlodipine release from 3D printed tablets: Influence of infill patterns and wall thickness." *International Journal of Pharmaceutics* 610: 121261. https://doi.org/https://doi.org/10.1016/j.ijpharm.2021.121261. https://www.sciencedirect.com/science/article/pii/S037851732101067X.

Okwuosa, Tochukwu C, Beatriz C Pereira, Basel Arafat, Milena Cieszynska, Abdullah Isreb, and Mohamed A Alhnan. 2017. "Fabricating a shell-core delayed release tablet using dual FDM 3D printing for patient-centred therapy." *Pharmaceutical research* 34 (2): 427-437.

Okwuosa, Tochukwu C, Dominika Stefaniak, Basel Arafat, Abdullah Isreb, Ka-Wai Wan, and Mohamed A Alhnan. 2016. "A lower temperature FDM 3D printing for the manufacture of patient-specific immediate release tablets." *Pharmaceutical research* 33 (11): 2704-2712.

Oladeji, Sinmisola, Valentyn Mohylyuk, David S Jones, and Gavin P Andrews. 2022. "3D printing of pharmaceutical oral solid dosage forms by fused deposition: The enhancement of printability using plasticised HPMCAS." *International Journal of Pharmaceutics* 616: 121553.

Omari, Sundus, Eman A Ashour, Rasha Elkanayati, Mohammed Alyahya, Mashan Almutairi, and Michael A Repka. 2022. "Formulation development of loratadine immediate-release tablets using hot-melt extrusion and 3D printing technology." *Journal of Drug Delivery Science and Technology* 74: 103505.

Paarakh, M Padmaa, Preethy Ani Jose, CM Setty, and GV Peterchristoper. 2018. "Release kinetics–concepts and applications." *International Journal of Pharmacy Research & Technology (IJPRT)* 8 (1): 12-20.

Paes, Arsenio HP, Albert Bakker, and Carmen J Soe-Agnie. 1997. "Impact of dosage frequency on patient compliance." *Diabetes care* 20 (10): 1512-1517.

Palekar, Siddhant, Pavan Kumar Nukala, Saurabh M. Mishra, Thomas Kipping, and Ketan Patel. 2019. "Application of 3D printing technology and quality by design approach for development of age-appropriate pediatric formulation of baclofen." *International Journal of Pharmaceutics* 556: 106-116. https://doi.org/https://doi.org/10.1016/j.ijpharm.2018.11.062. https://www.sciencedirect.com/science/article/pii/S0378517318308883.

Paradkar, MM, and Joseph Irudayaraj. 2002. "A rapid FTIR spectroscopic method for estimation of caffeine in soft drinks and total methylxanthines in tea and coffee." *Journal of food science* 67 (7): 2507-2511.

Park, Byeong Ju, Ho Jae Choi, Sang Ji Moon, Seong Jun Kim, Rajiv Bajracharya, Jeong Youn Min, and Hyo-Kyung Han. 2019. "Pharmaceutical applications of 3D printing technology: Current understanding and future perspectives." *Journal of Pharmaceutical Investigation* 49 (6): 575-585.

Parulski, Chloé, Olivier Jennotte, Anna Lechanteur, and Brigitte Evrard. 2021. "Challenges of Fused Deposition Modeling 3D Printing in Pharmaceutical Applications: Where are we now ?" *Advanced Drug Delivery Reviews*. https://doi.org/https://doi.org/10.1016/j.addr.2021.05.020. https://www.sciencedirect.com/science/article/pii/S0169409X21001848.

Patel, Nirali G, and Abu TM Serajuddin. 2021. "Development of FDM 3D-printed tablets with rapid drug release, high drug-polymer miscibility and reduced

printing temperature by applying the acid-base supersolubilization (ABS) principle." *International Journal of Pharmaceutics* 600: 120524.

Patel, Nirali G., and Abu T. M. Serajuddin. 2023. "Improving drug release rate, drug-polymer miscibility, printability and processability of FDM 3D-printed tablets by weak acid-base interaction." *International Journal of Pharmaceutics* 632: 122542. https://doi.org/https://doi.org/10.1016/j.ijpharm.2022.122542. https://www.sciencedirect.com/science/article/pii/S0378517322010973.

Patel, Shriya K., Mouhamad Khoder, Matthew Peak, and Mohamed A. Alhnan. 2021. "Controlling drug release with additive manufacturing-based solutions." *Advanced Drug Delivery Reviews* 174: 369-386. https://doi.org/https://doi.org/10.1016/j.addr.2021.04.020. https://www.sciencedirect.com/science/article/pii/S0169409X21001484.

Patra, Ch Niranjan, Richa Priya, Suryakanta Swain, Goutam Kumar Jena, Kahnu Charan Panigrahi, and Debashish Ghose. 2017. "Pharmaceutical significance of Eudragit: A review." *Future Journal of Pharmaceutical Sciences* 3 (1): 33-45.

Patra, Chinam, Arethi Kumar, Hemant Pandit, Satya Singh, and Meduri Devi. 2007. "Design and evaluation of sustained release bilayer tablets of propranolol hydrochloride." *Acta Pharmaceutica* 57 (4): 479-489.

Pereira, Beatriz C, Abdullah Isreb, Robert T Forbes, Filipa Dores, Rober Habashy, Jean-Baptiste Petit, Mohamed A Alhnan, and Enoche F Oga. 2019. "'Temporary Plasticiser': A novel solution to fabricate 3D printed patient-centred cardiovascular 'Polypill'architectures." *European Journal of Pharmaceutics and Biopharmaceutics* 135: 94-103.

Pereira, Gabriela G, Sara Figueiredo, Ana Isabel Fernandes, and João F Pinto. 2020. "Polymer selection for hot-melt extrusion coupled to fused deposition modelling in pharmaceutics." *Pharmaceutics* 12 (9): 795.

Petropoulos, John H, Kyriaki G Papadokostaki, and Merope Sanopoulou. 2012. "Higuchi's equation and beyond: overview of the formulation and application of a generalized model of drug release from polymeric matrices." *International journal of pharmaceutics* 437 (1-2): 178-191.

Pietrzak, Katarzyna, Abdullah Isreb, and Mohamed A Alhnan. 2015. "A flexible-dose dispenser for immediate and extended release 3D printed tablets." *European journal of pharmaceutics and biopharmaceutics* 96: 380-387.

Pochan, JM, CL Beatty, and DF Pochan. 1979. "Different approach for the correlation of the Tg of mixed amorphous systems." *Polymer* 20 (7): 879-886.

Porfiryeva, Natalia N., Shamil F. Nasibullin, Svetlana G. Abdullina, Irina K. Tukhbatullina, Rouslan I. Moustafine, and Vitaliy V. Khutoryanskiy. 2019. "Acrylated Eudragit® E PO as a novel polymeric excipient with enhanced mucoadhesive properties for application in nasal drug delivery." *International Journal of Pharmaceutics* 562: 241-248. https://doi.org/https://doi.org/10.1016/j.ijpharm.2019.03.027. https://www.sciencedirect.com/science/article/pii/S0378517319302133.

Prasad, Elke, Muhammad T Islam, Daniel J Goodwin, Andrew J Megarry, Gavin W Halbert, Alastair J Florence, and John Robertson. 2019. "Development of a hot-melt extrusion (HME) process to produce drug loaded Affinisol™ 15LV filaments for fused filament fabrication (FFF) 3D printing." *Additive Manufacturing* 29: 100776.

Prasad, Leena Kumari, and Hugh Smyth. 2016. "3D Printing technologies for drug delivery: a review." *Drug development and industrial pharmacy* 42 (7): 1019-1031.

PUTTIPIPATKHACHORN, Satit, Etsuo YONEMOCHI, Toshio OGUCHI, Keiji YAMAMOTO, and Yoshinobu NAKAI. 1990. "Effect of Grinding on Dehydration of Crystal Water of Theophyline." *Chemical and pharmaceutical bulletin* 38 (8): 2233-2236.

Puttippipatkhachorn, Satit, Etsuo Yonemochi, Toshio Oguchi, Keiji Yamamoto, and Yoshinobu Nakai. 1990. "Effect of Grinding on Dehydration of Crystal Water of Theophyline." *Chemical and pharmaceutical bulletin* 38 (8): 2233-2236.

Qahtani, Mawath, Feng Wu, Manjusri Misra, Stefano Gregori, Deborah F Mielewski, and Amar K Mohanty. 2019. "Experimental design of sustainable 3D-printed poly (lactic acid)/biobased poly (butylene succinate) blends via fused deposition modeling." *ACS Sustainable Chemistry & Engineering* 7 (17): 14460-14470.

Qian, Haonan, Di Chen, Xiangyu Xu, Rui Li, Guangrong Yan, and Tianyuan Fan. 2022. "FDM 3D-printed sustained-release gastric-floating verapamil hydrochloride formulations with cylinder, capsule and hemisphere shapes, and low infill percentage." *Pharmaceutics* 14 (2): 281.

Raffa, RB. 2001. "Pharmacology of oral combination analgesics: rational therapy for pain." *Journal of clinical pharmacy and therapeutics* 26 (4): 257-264.

Rajvanshi, Nikhil, Prawin Kumar, and Jagdish Prasad Goyal. 2024. "Global initiative for asthma guidelines 2024: an update." *Indian pediatrics* 61 (8): 781-786.

Ramukutty, S, and EJCR Ramachandran. 2012. "Growth, spectral and thermal studies of ibuprofen crystals." *Crystal Research and Technology* 47 (1): 31-38.

Reddy Dumpa, Nagi, Suresh Bandari, and Michael A Repka. 2020. "Novel gastroretentive floating pulsatile drug delivery system produced via hot-melt extrusion and fused deposition modeling 3D printing." *Pharmaceutics* 12 (1): 52.

Robles-Martinez, Pamela, Xiaoyan Xu, Sarah J Trenfield, Atheer Awad, Alvaro Goyanes, Richard Telford, Abdul W Basit, and Simon Gaisford. 2019. "3D printing of a multi-layered polypill containing six drugs using a novel stereolithographic method." *Pharmaceutics* 11 (6): 274.

Rochon, Paula A, Mirko Petrovic, Antonio Cherubini, Graziano Onder, Denis O'Mahony, Shelley A Sternberg, Nathan M Stall, and Jerry H Gurwitz. 2021. "Polypharmacy, inappropriate prescribing, and deprescribing in older people: through a sex and gender lens." *The Lancet Healthy Longevity* 2 (5): e290-e300.

Rosales, José María, Cristina Cejudo, Lidia Verano, Lourdes Casas, Casimiro Mantell, and Enrique José Martínez de la Ossa. 2021. "Supercritical impregnation of pla filaments with mango leaf extract to manufacture functionalized biomedical devices by 3D printing." *Polymers* 13 (13): 2125.

Roshandel, Gholamreza, Masoud Khoshnia, Hossein Poustchi, Karla Hemming, Farin Kamangar, Abdolsamad Gharavi, Mohammad Reza Ostovaneh, Alireza Nateghi, Masoud Majed, Behrooz Navabakhsh, Shahin Merat, Akram Pourshams, Mahdi Nalini, Fatemeh Malekzadeh, Masoumeh Sadeghi, Noushin Mohammadifard, Nizal Sarrafzadegan, Mohammad Naemi-Tabiei, Abdolreza Fazel, Paul Brennan, Arash Etemadi, Paolo Boffetta, Neil Thomas, Tom Marshall, Kar Keung Cheng, and Reza Malekzadeh. 2019. "Effectiveness of polypill for primary and secondary prevention of cardiovascular diseases (PolyIran): a pragmatic, cluster-randomised trial." *The Lancet* 394 (10199): 672-683. https://doi.org/https://doi.org/10.1016/S0140-6736(19)31791-X. https://www.sciencedirect.com/science/article/pii/S014067361931791X.

Rowat, Simon J. A., Raymond L. Legge, and Christine Moresoli. 2021. "Plant Protein in Material Extrusion 3D Printing: Formation, Plasticization, Prospects, and

Challenges." *Journal of Food Engineering*: 110623. https://doi.org/https://doi.org/10.1016/j.jfoodeng.2021.110623. https://www.sciencedirect.com/science/article/pii/S0260877421001485.

Roy, Ambuj, Nitish Naik, and K Srinath Reddy. 2017. "Strengths and limitations of using the polypill in cardiovascular prevention." *Current cardiology reports* 19: 1-8.

Ruponen, Marika, Henna Rusanen, and Riikka Laitinen. 2020. "Dissolution and permeability properties of co-amorphous formulations of hydrochlorothiazide." *Journal of Pharmaceutical Sciences* 109 (7): 2252-2261.

Sadia, Muzna, Basel Arafat, Waqar Ahmed, Robert T Forbes, and Mohamed A Alhnan. 2018. "Channelled tablets: An innovative approach to accelerating drug release from 3D printed tablets." *Journal of Controlled Release* 269: 355-363.

Sadia, Muzna, Abdullah Isreb, Ibrahim Abbadi, Mohammad Isreb, David Aziz, Amjad Selo, Peter Timmins, and Mohamed A Alhnan. 2018. "From 'fixed dose combinations' to 'a dynamic dose combiner': 3D printed bi-layer antihypertensive tablets." *European Journal of Pharmaceutical Sciences* 123: 484-494.

Sadia, Muzna, Agata Sośnicka, Basel Arafat, Abdullah Isreb, Waqar Ahmed, Antonios Kelarakis, and Mohamed A Alhnan. 2016. "Adaptation of pharmaceutical excipients to FDM 3D printing for the fabrication of patient-tailored immediate release tablets." *International journal of pharmaceutics* 513 (1-2): 659-668.

Saviano, Marilena, Rita Patrizia Aquino, Pasquale Del Gaudio, Francesca Sansone, and Paola Russo. 2019. "Poly (vinyl alcohol) 3D printed tablets: The effect of polymer particle size on drug loading and process efficiency." *International journal of pharmaceutics* 561: 1-8.

Saviano, Marilena, Benjamin J Bowles, Matthew R Penny, Ahtsham Ishaq, Zaid Muwaffak, Giovanni Falcone, Paola Russo, and Stephen T Hilton. 2022. "Development and analysis of a novel loading technique for FDM 3D printed systems: Microwave-assisted impregnation of gastro-retentive PVA capsular devices." *International Journal of Pharmaceutics* 613: 121386.

Saydam, Mehtap, Selin Seda Timur, İmran Vural, and Sevgi Takka. 2022. "Cell culture and pharmacokinetic evaluation of a solid dosage formulation containing a water-insoluble orphan drug manufactured by FDM-3DP technology." *International Journal of Pharmaceutics* 628: 122307.

https://doi.org/https://doi.org/10.1016/j.ijpharm.2022.122307. https://www.sciencedirect.com/science/article/pii/S0378517322008626.

Scoutaris, Nicolaos, Steven A Ross, and Dennis Douroumis. 2018. "3D printed “Starmix” drug loaded dosage forms for paediatric applications." *Pharmaceutical research* 35 (2): 1-11.

Senta-Loys, Z, JF Kelleher, and DS Jones. "Hot-Melt Co-Extrusion Technology as a Platform for Manufacturing of Fixed-Dose Combinations with Differing Release Behaviour for the Treatment of Hypertension."

Seoane-Viaño, Iria, Sarah J Trenfield, Abdul W Basit, and Alvaro Goyanes. 2021. "Translating 3D printed pharmaceuticals: From hype to real-world clinical applications." *Advanced Drug Delivery Reviews* 174: 553-575.

Shi, Kejing, Jonathan P Salvage, Mohammed Maniruzzaman, and Ali Nokhodchi. 2021. "Role of release modifiers to modulate drug release from fused deposition modelling (FDM) 3D printed tablets." *International Journal of Pharmaceutics* 597: 120315.

Shin, Soyoung, Tae Hwan Kim, Seok Won Jeong, Seung Eun Chung, Da Young Lee, Do-Hyung Kim, and Beom Soo Shin. 2019. "Development of a gastroretentive delivery system for acyclovir by 3D printing technology and its in vivo pharmacokinetic evaluation in Beagle dogs." *PLoS One* 14 (5): e0216875.

Singh, Dev Bukhsh. 2020. "The impact of pharmacogenomics in personalized medicine." *Current Applications of Pharmaceutical Biotechnology*: 369-394.

Smith, Derrick, Yash Kapoor, Andre Hermans, Rebecca Nofsinger, Filippos Kesisoglou, Tiffany P Gustafson, and Adam Procopio. 2018. "3D printed capsules for quantitative regional absorption studies in the GI tract." *International journal of pharmaceutics* 550 (1-2): 418-428.

Smith, Dustin K, Robert P Lennon, and Peter B Carlsgaard. 2020. "Managing hypertension using combination therapy." *American family physician* 101 (6): 341-349.

Solanki, Nayan G, Md Tahsin, Ankita V Shah, and Abu TM Serajuddin. 2018. "Formulation of 3D printed tablet for rapid drug release by fused deposition modeling: screening polymers for drug release, drug-polymer miscibility and printability." *Journal of pharmaceutical sciences* 107 (1): 390-401.

Stergiou, George S. 2006. "Combination pharmacotherapy in hypertension." *International urology and nephrology* 38: 673-682.

Stergiou, GS, AK Karotsis, A Symeonidis, and VA Vassilopoulou. 2003. "Aggressive blood pressure control in general practice (ABC-GP) study: can the new targets be reached?" *Journal of human hypertension* 17 (11): 767-773.

Stevens, Ruth E, Vivian Gray, Angelica Dorantes, Lynn Gold, and Loan Pham. 2015. "Scientific and regulatory standards for assessing product performance using the similarity factor, f2." *The AAPS Journal* 17: 301-306.

Sudha, C, P Parimaladevi, and K Srinivasan. 2015. "A novel method for the separation of mono and ortho polymorphs of paracetamol in gel matrix." *Materials Science and Engineering: C* 47: 150-155.

Sultan, Amal A, Sanaa A El-Gizawy, Mohamed A Osman, and Gamal M El Maghraby. 2017. "Self dispersing mixed micelles forming systems for enhanced dissolution and intestinal permeability of hydrochlorothiazide." *Colloids and Surfaces B: Biointerfaces* 149: 206-216.

Sá, Katia Nunes, Larissa Moreira, Abrahão Fontes Baptista, Lin Tchia Yeng, Manoel Jacobsen Teixeira, Ricardo Galhardoni, and Daniel Ciampi de Andrade. 2019. "Prevalence of chronic pain in developing countries: systematic review and meta-analysis." *Pain reports* 4 (6).

Tabriz, Atabak Ghanizadeh, Md Sadeque Mithu, Milan D. Antonijevic, Lilian Vilain, Youri Derrar, Clara Grau, Anaïs Morales, Orestis L. Katsamenis, and Dennis Douroumis. 2023. "3D printing of LEGO® like designs with tailored release profiles for treatment of sleep disorder." *International Journal of Pharmaceutics* 632: 122574. https://doi.org/https://doi.org/10.1016/j.ijpharm.2022.122574. https://www.sciencedirect.com/science/article/pii/S0378517322011292.

Tabriz, Atabak Ghanizadeh, Uttom Nandi, Andrew P Hurt, Ho-Wah Hui, Shyam Karki, Yuchuan Gong, Sumit Kumar, and Dennis Douroumis. 2021. "3D printed bilayer tablet with dual controlled drug release for tuberculosis treatment." *International Journal of Pharmaceutics* 593: 120147.

Tagami, Tatsuaki, Noriko Nagata, Naomi Hayashi, Emi Ogawa, Kaori Fukushige, Norihito Sakai, and Tetsuya Ozeki. 2018. "Defined drug release from 3D-printed composite tablets consisting of drug-loaded polyvinylalcohol and a water-soluble or water-insoluble polymer filler." *International journal of pharmaceutics* 543 (1-2): 361-367.

Talevi, Alan, and María E. Ruiz. 2021. "Drug Release." In *The ADME Encyclopedia: A Comprehensive Guide on Biopharmacy and Pharmacokinetics*, 1-7. Cham: Springer International Publishing.

Tan, Deck Khong, Mohammed Maniruzzaman, and Ali Nokhodchi. 2018. "Advanced pharmaceutical applications of hot-melt extrusion coupled with fused deposition modelling (FDM) 3D printing for personalised drug delivery." *Pharmaceutics* 10 (4): 203.

---. 2020. "Development and optimisation of novel polymeric compositions for sustained release theophylline caplets (PrintCap) via FDM 3D printing." *Polymers* 12 (1): 27.

Than, Yee Mon, and Varin Titapiwatanakun. 2021. "Tailoring immediate release FDM 3D printed tablets using a quality by design (QbD) approach." *International Journal of Pharmaceutics* 599: 120402.

Thom, Simon, Neil Poulter, Jane Field, Anushka Patel, Dorairaj Prabhakaran, Alice Stanton, Diederick E Grobbee, Michiel L Bots, K Srinath Reddy, and Raghu Cidambi. 2013. "Effects of a fixed-dose combination strategy on adherence and risk factors in patients with or at high risk of CVD: the UMPIRE randomized clinical trial." *Jama* 310 (9): 918-929.

Trenfield, Sarah J, Atheer Awad, Christine M Madla, Grace B Hatton, Jack Firth, Alvaro Goyanes, Simon Gaisford, and Abdul W Basit. 2019. "Shaping the future: recent advances of 3D printing in drug delivery and healthcare." *Expert opinion on drug delivery* 16 (10): 1081-1094.

Unger, Thomas, Claudio Borghi, Fadi Charchar, Nadia A Khan, Neil R Poulter, Dorairaj Prabhakaran, Agustin Ramirez, Markus Schlaich, George S Stergiou, and Maciej Tomaszewski. 2020. "2020 International Society of Hypertension global hypertension practice guidelines." *Hypertension* 75 (6): 1334-1357.

Vaz, Vanessa Marcia, and Lalit Kumar. 2021. "3D printing as a promising tool in personalized medicine." *Aaps Pharmscitech* 22: 1-20.

Verano Naranjo, Lidia, Cristina Cejudo Bastante, Lourdes Casas Cardoso, Casimiro Mantell Serrano, and Enrique José Martínez de la Ossa Fernández. 2021. "Supercritical impregnation of ketoprofen into polylactic acid for biomedical application: Analysis and modeling of the release kinetic." *Polymers* 13 (12): 1982.

Verbeeck, Roger K, Isadore Kanfer, Raimar Löbenberg, Bertil Abrahamsson, Rodrigo Cristofoletti, DW Groot, Peter Langguth, James E Polli, Alan Parr, and Vinod P Shah. 2017. "Biowaiver monographs for immediate-release solid oral dosage forms: Enalapril." *Journal of Pharmaceutical Sciences* 106 (8): 1933-1943.

Verrue, Charlotte, Els Mehuys, Koen Boussery, Jean-Paul Remon, and Mirko Petrovic. 2011. "Tablet-splitting: a common yet not so innocent practice." *Journal of advanced nursing* 67 (1): 26-32.

Verstraete, Glenn, Aseel Samaro, Wouter Grymonpré, Valérie Vanhoorne, Bernd Van Snick, MN Boone, Tom Hellemans, Luc Van Hoorebeke, Jean Paul Remon, and Chris Vervaet. 2018. "3D printing of high drug loaded dosage forms using thermoplastic polyurethanes." *International journal of pharmaceutics* 536 (1): 318-325.

Vithani, Kapilkumar, Alvaro Goyanes, Vincent Jannin, Abdul W Basit, Simon Gaisford, and Ben J Boyd. 2019. "An overview of 3D printing technologies for soft materials and potential opportunities for lipid-based drug delivery systems." *Pharmaceutical research* 36 (1): 1-20.

Vo, Anh Q., Jiaxiang Zhang, Dinesh Nyavanandi, Suresh Bandari, and Michael A. Repka. 2020. "Hot melt extrusion paired fused deposition modeling 3D printing to develop hydroxypropyl cellulose based floating tablets of cinnarizine." *Carbohydrate Polymers* 246: 116519. https://doi.org/https://doi.org/10.1016/j.carbpol.2020.116519. https://www.sciencedirect.com/science/article/pii/S0144861720306937.

Vogelpoel, H, J Welink, GL Amidon, HE Junginger, KK Midha, H Möller, M Olling, VP Shah, and DM Barends. 2004. "Biowaiver monographs for immediate release solid oral dosage forms based on biopharmaceutics classification system (BCS) literature data: Verapamil hydrochloride, propranolol hydrochloride, and atenolol." *Journal of Pharmaceutical Sciences* 93 (8): 1945-1956.

Wald, Nicholas J, Johannes Michiel Luteijn, Joan K Morris, David Taylor, and Peter Oppenheimer. 2016. "Cost–benefit analysis of the polypill in the primary prevention of myocardial infarction and stroke." *European journal of epidemiology* 31: 415-426.

Wang, Honghe, Nagireddy Dumpa, Suresh Bandari, Thomas Durig, and Michael A Repka. 2020. "Fabrication of Taste-Masked Donut-Shaped Tablets Via Fused

Filament Fabrication 3D Printing Paired with Hot-Melt Extrusion Techniques." *AAPS PharmSciTech* 21 (7): 1-11.

Wang, Shuying, Renhe Liu, Yao Fu, and W John Kao. 2020. "Release mechanisms and applications of drug delivery systems for extended-release." *Expert Opinion on Drug Delivery* 17 (9): 1289-1304.

Wang, Xiaowen, Keyang Liu, Kokoro Shirai, Chengyao Tang, Yonghua Hu, Ying Wang, Yuantao Hao, and Jia-Yi Dong. 2023. "Prevalence and trends of polypharmacy in US adults, 1999–2018." *Global Health Research and Policy* 8 (1): 25.

Wang, Yifan, Ronald D Snee, Golshid Keyvan, and Fernando J Muzzio. 2016. "Statistical comparison of dissolution profiles." *Drug Development and Industrial Pharmacy* 42 (5): 796-807.

Webster, Ruth, Jose M Castellano, and Oyere K Onuma. 2017. "Putting polypills into practice: challenges and lessons learned." *The Lancet* 389 (10073): 1066-1074.

Webster, Ruth, Anushka Patel, Vanessa Selak, Laurent Billot, Michiel L Bots, Alex Brown, Chris Bullen, Alan Cass, Sue Crengle, and C Raina Elley. 2016. "Effectiveness of fixed dose combination medication (‘polypills’) compared with usual care in patients with cardiovascular disease or at high risk: a prospective, individual patient data meta-analysis of 3140 patients in six countries." *International journal of cardiology* 205: 147-156.

Weichseldorfer, Matthew, Marvin Reitz, and Olga S Latinovic. 2021. "Past HIV-1 medications and the current status of combined antiretroviral therapy options for HIV-1 patients." *Pharmaceutics* 13 (11): 1798.

Wilkins, Christi A, Hannlie Hamman, Josias H Hamman, and Jan H Steenekamp. 2024. "Fixed-Dose Combination Formulations in Solid Oral Drug Therapy: Advantages, Limitations, and Design Features." *Pharmaceutics* 16 (2): 178.

Williams, Bryan, Giuseppe Mancia, Wilko Spiering, Enrico Agabiti Rosei, Michel Azizi, Michel Burnier, Denis L Clement, Antonio Coca, Giovanni De Simone, and Anna Dominiczak. 2018. "2018 ESC/ESH Guidelines for the management of arterial hypertension: The Task Force for the management of arterial hypertension of the European Society of Cardiology (ESC) and the European Society of Hypertension (ESH)." *European heart journal* 39 (33): 3021-3104.

Windolf, Hellen, Rebecca Chamberlain, Jörg Breitkreutz, and Julian Quodbach. 2022. "3D Printed Mini-Floating-Polypill for Parkinson's Disease: Combination of Levodopa, Benserazide, and Pramipexole in Various Dosing for Personalized Therapy." *Pharmaceutics* 14 (5): 931. https://www.mdpi.com/1999-4923/14/5/931.

Wofford, James L. 1997. "History of fixed-dose combination therapy for hypertension." *Archives of internal medicine* 157 (9): 1044-1044.

Xie, Renxuan, Albree R. Weisen, Youngmin Lee, Melissa A. Aplan, Abigail M. Fenton, Ashley E. Masucci, Fabian Kempe, Michael Sommer, Christian W. Pester, Ralph H. Colby, and Enrique D. Gomez. 2020. "Glass transition temperature from the chemical structure of conjugated polymers." *Nature Communications* 11 (1): 893. https://doi.org/10.1038/s41467-020-14656-8. https://doi.org/10.1038/s41467-020-14656-8.

Xu, Pengchong, Jiangwei Li, Alvin Meda, Frederick Osei-Yeboah, Matthew L Peterson, Michael Repka, and Xi Zhan. 2020. "Development of a quantitative method to evaluate the printability of filaments for fused deposition modeling 3D printing." *International Journal of Pharmaceutics* 588: 119760.

Yang, Yan, Huihui Wang, Haichao Li, Zhimin Ou, and Gensheng Yang. 2018. "3D printed tablets with internal scaffold structure using ethyl cellulose to achieve sustained ibuprofen release." *European journal of pharmaceutical sciences* 115: 11-18.

Yang, Yan, Huihui Wang, Xiaocui Xu, and Gensheng Yang. 2021. "Strategies and mechanisms to improve the printability of pharmaceutical polymers Eudragit® EPO and Soluplus®." *International Journal of Pharmaceutics* 599: 120410.

Yeaw, Jason, Joshua S Benner, John G Walt, Sergey Sian, and Daniel B Smith. 2009. "Comparing adherence and persistence across 6 chronic medication classes." *Journal of Managed Care Pharmacy* 15 (9): 728-740.

Zgouro, Paola, Orestis L. Katsamenis, Thomas Moschakis, Georgios K. Eleftheriadis, Athanasios S. Kyriakidis, Konstantina Chachlioutaki, Paraskevi Kyriaki Monou, Marianna Ntorkou, Constantinos K. Zacharis, Nikolaos Bouropoulos, Dimitrios G. Fatouros, Christina Karavasili, and Christos I. Gioumouxouzis. 2024. "A floating 3D printed polypill formulation for the coadministration and sustained release of antihypertensive drugs." *International Journal of Pharmaceutics* 655:

124058. https://doi.org/https://doi.org/10.1016/j.ijpharm.2024.124058. https://www.sciencedirect.com/science/article/pii/S0378517324002928.

Zhang, Jiaxiang, Xin Feng, Hemlata Patil, Roshan V Tiwari, and Michael A Repka. 2017. "Coupling 3D printing with hot-melt extrusion to produce controlled-release tablets." *International journal of pharmaceutics* 519 (1-2): 186-197.

Zhang, Ziru, Sheng Feng, Ahmed Almotairy, Suresh Bandari, and Michael A Repka. 2023. "Development of multifunctional drug delivery system via hot-melt extrusion paired with fused deposition modeling 3D printing techniques." *European Journal of Pharmaceutics and Biopharmaceutics*.

Zimmermann, Boris, and Goran Baranović. 2011. "Thermal analysis of paracetamol polymorphs by FT-IR spectroscopies." *Journal of pharmaceutical and biomedical analysis* 54 (2): 295-302.